

KUMAMOTO, KYUSHU, JAPAN, EARTHQUAKES OF M_w 6.0 April 14, 2016 M_w 7.0 April 16, 2016 LIFELINE PERFORMANCE

By

ALEX K TANG and JOHN M EIDINGER



The Council of Lifeline Earthquake Engineering
TCLEE No. 2

and



Yokohama National University
May 7 2017

<http://www.geEngineeringSystems.com>

Table of Contents

TABLE OF CONTENTS	I
ABSTRACT.....	1
PREFACE	3
AUTHORS' AFFILIATIONS	4
ACKNOWLEDGEMENTS	5
ENDORSEMENTS.....	8
1.0 INTRODUCTION	9
1.1 LIMITATIONS.....	18
1.2 TCLEE AND ASCE	18
1.3 ABBREVIATIONS	18
1.4 UNITS.....	19
1.5 LICENSE, COPYRIGHT AND CREATE COMMONS DEED	20
1.6 ACKNOWLEDGEMENTS	20
2.0 SEISMIC HAZARDS	21
2.1 LOCATION OF THE EARTHQUAKE.....	22
2.2 SEISMICITY AND GROUND MOTIONS	28
2.3 LANDSLIDES	41
2.4 SURFACE FAULTING.....	48
2.5 LIQUEFACTION.....	53
2.6 REFERENCES	58
3.0 ELECTRIC POWER SYSTEM	59
3.1 OVERVIEW	60
3.2 THE POWER GRID	63
3.3 LANDSLIDE DAMAGE TO TRANSMISSION TOWERS	65
3.4 SUBSTATIONS.....	91
3.5 GENERATION.....	105
3.6 DISTRIBUTION.....	107
3.7 REFERENCES AND ACKNOWLEDGEMENTS	115
4.0 TELECOMMUNICATION.....	116
4.1 DESCRIPTION OF SYSTEM.....	116
4.2 OVERVIEW OF SYSTEM PERFORMANCE	117
4.3 LANDLINE NETWORK DAMAGE	117
4.4 WIRELESS SYSTEM DAMAGE	122
4.5 MAJOR OBSERVATIONS AND RECOMMENDATIONS	132
4.6 ACKNOWLEDGEMENTS	135
4.7 REFERENCES	135
5.0 WATER SYSTEM.....	136
5.1 OVERVIEW	136
5.2 PIPE INVENTORY	140
5.3 PIPE DAMAGE	142
5.4 RESTORATION OF WATER SERVICE.....	144
5.5 PIPE REPLACEMENT FOR US AND CANADIAN WATER UTILITIES.....	151
5.6 PIPE AND FACILITY PERFORMANCE	156
5.7 REFERENCES AND ACKNOWLEDGEMENTS	172

6.0 SEAPORTS	173
6.1 KUMAMOTO PORT	174
6.2 YATSUSHIRO PORT	176
6.3 BEPPU PORT	178
6.4 MAJOR OBSERVATIONS AND RECOMMENDATIONS	179
6.5 ACKNOWLEDGEMENTS	179
6.6 REFERENCES	179
7.0 AIRPORTS.....	180
7.1 PERFORMANCE OF KUMAMOTO AIRPORT	182
7.2 DOMESTIC TERMINAL	183
7.3 INTERNATIONAL TERMINAL.....	188
7.4 MAJOR OBSERVATIONS AND RECOMMENDATIONS	190
7.5 ACKNOWLEDGEMENTS	192
8.0 GAS SYSTEM.....	193
8.1 OVERVIEW OF THE GAS SYSTEM	193
8.2 GAS OUTAGES	194
8.3 GAS FACILITIES	198
8.4 GAS PIPES	199
8.5 EMERGENCY RESPONSE	204
8.6 ACKNOWLEDGEMENTS	204
9.0 TRANSPORTATION.....	206
9.1 TRANSPORTATION NETWORK OF KYUSHU.....	208
9.2 EXPRESSWAY AND BRIDGES	209
9.2.1 <i>Kanon Bashi (N32.8335°, E130.7802°)</i>	209
9.2.2 <i>Mashiki Area of Kyushu Expressway (N32.7796°, E130.7941°)</i>	213
9.2.3 <i>Kiyamagawa Bridge (N32.7654°, E130.7886°)</i>	215
9.2.4 <i>Furyo First Bridge (N32.7075°, E130.7556°)</i>	220
9.2.5 <i>Aso Ohashi</i>	222
9.2.6 <i>Oh Kirihata Ohashi (N32.8425°, E 130.9285°)</i>	227
9.2.7 <i>Kuwatsuru Ohashi (N32.8517°, E 130.9455°)</i>	231
9.2.8 <i>Tawarayama Ohashi (N32.8634°, E 130.9608°)</i>	234
9.2.9 <i>Aso Choyo Ohashi (N32.8754°, E 130.9855°)</i>	237
9.2.10 <i>Toshita Ohashi (N32.8752°, E 130.9888°)</i>	240
9.2.11 <i>Mashiki area (N32.7902°, E 130.8210°)</i>	243
9.3 ROADS	246
9.4 TAWARAYAMA TUNNEL (N32.86014°, E130.96466°)	251
9.5 SHINKANSEN AND LOCAL RAILWAYS	253
9.5.1 <i>Kyushu Shinkansen</i>	254
9.5.2 <i>JR and Local Railways</i>	259
9.6 REPAIR AND RECOVERY EFFORT	269
9.7 MAJOR OBSERVATIONS AND RECOMMENDATIONS	271
9.8 ACKNOWLEDGEMENTS	272
9.9 REFERENCES	273
10.0 LEVEES.....	274
10.1 ACKNOWLEDGEMENTS	276
10.2 REFERENCES	277

ABSTRACT

Two strong earthquakes affected the City of Kumamoto and the nearby urban centers. The two earthquakes can be characterized as the fore shock (14 April 2016) and the main shock (16 April 2016). The moment magnitudes of the fore shock was $M_w = 6.0$ ¹ and the main shock was $M_w = 7.0$. The fore shock of $M = 6.0$ occurred at 9:26 PM (local time) with the epicenter located at 32.849° N, 130.635° E at a depth of 10 km. The main shock of $M = 7.0$ occurred about 28 hours later at 1:25 AM (local time) with the epicenter located at 32.782° N, 130.726° E at a depth of 10 km. Both events occurred close to the previously-known Hinagu and Futagawa and faults. The main shock produced several recorded motions with PGA (Peak Ground Acceleration) around 0.5g to 1.0g, and PGV (Peak Ground Velocity) around 75 cm/sec. The main shock triggered many landslides, as well as permanent ground deformations (PGDs) due to fault offset (common) and liquefaction (less common). Lifelines were heavily damaged both due to high inertial shaking as well as due to PGDs.

Total fatality after the main shock was 69 dead with 1 missing, in addition to 364 seriously injured and 1,456 with minor injury, as of June 30 2016. All fatalities occurred in Kumamoto Prefecture. There were 8,044 houses totally collapsed, 24,274 houses with partial collapse, and 118,222 houses with some damage. There were a total of 1,021 evacuation shelters used among five prefectures (Kumamoto, Oita, Fukuoka, Miyazaki, and Nagasaki), with the peak number of people at shelters reaching 183,882 people as of April 17 2016, decreasing to 5,769 people by June 30 2016. 69 medical facilities within Kumamoto Prefecture were inspected, with 6 having structural problems, 23 having lifelines service problems (either power, gas and/or water) (including 3 with structural problems), and 43 were normal. Educational facilities performed reasonably well, although some had damage such as broken glasses, broken pipes, damaged exterior walls, and ceiling damage. There were 14 fire ignitions reported, but no fire spread.

Transportations system sustained serious damage due to landslides, surface fault offset, liquefaction and strong shaking. The most serious set back was around the collapsed Aso Ohashi area, including total collapse of bridges, railroads, and multi-lane highways due to landslide, and further widespread serious damage to bridges, and tunnels. Electric power, gas, water, and telecommunication suffered various set backs. Partial electric power service was restored to essentially all customers four days after the main shock. The potable water system was entirely shutdown due to a sudden increase in turbidity of the water produced by all the local wells; and then restoration proceeded to repair hundreds of broken water mains and thousands of damaged service laterals. Gas restoration took longer to recover, in part because the entire local area gas system was shutdown for fear of fire; and then waiting for the water system recovery prior to re-lighting the gas systems, for the reason of having the water system recovered first. The main set back for telecommunication was the cellular (mobile) phone network, with many cell sites having power outages, and some having suffered severed cables connecting to main exchanges, and one with a collapsed cell tower. One wastewater treatment facility out of 21 in the

¹ Various reported as M 6.1 or M 6.2

prefecture was out of service; that facility was located near the epicenter and was subjected to strong shaking and PGD issues.

Within Kumamoto Prefecture, 28 communities set up 58 temporary locations of waste/debris storage, handling and processing. Two out of 27 incinerating facilities within the prefecture stopped working after the earthquake. The total amount of waste/debris was estimated to be 1 to 1.3 million tons.

PREFACE

This report has been prepared by John Eiding and Alex Tang (collectively, "we"). For many years, we worked with our colleagues from around the world as part of the Technical Council on Lifeline Earthquake Engineering (TCLEE). TCLEE was a committee of the American Society of Civil Engineers. In 2014, ASCE ended its support of TCLEE as a stand alone committee; and now is examining lifelines under the general topic of resilience. We have independently elected to continue as The Council on Lifeline Earthquake Engineering (*TCLEE*) to maintain a sharp focus on the performance of lifelines in earthquakes. In 2015, we documented the performance of lifelines of the 2014 Napa earthquake, and in this report, we document the performance of lifelines in the 2016 Kumamoto earthquakes. Our colleagues and friends and practitioners of lifeline earthquake engineering in Japan have supported this Kumamoto investigation with tremendous support. This is a solid testament of this important task for the industry and government owning and providing lifelines services. We are sure that our friends from New Zealand, Italy, Chile, Peru, Indonesia, China, Turkey, Algeria, Portugal and other earthquake-prone areas around the world will provide us with a continuing high level of support. We acknowledge the fact that all incur a cost in the effort to document the performance of lifelines in earthquakes, with the hope that all will recognize this as an investment for resilient lifelines and our intent to achieve a long term gain in increasing our understanding of the issues.

We have worked together to undertake more than 20 field trips of post earthquake lifelines investigation. While working together in the field, we may not agree with each other all the time, but our discussions and arguments are always good.

Our intent is that this report is available at no cost to any interested person or organization, worldwide. This report is covered by the Creative Commons deed which allows you to use and re-use the information, with the provision that you provide attribution (see Section 1.5 for complete details). This report is available for free from the web at <http://www.geEngineeringSystems.com>. The authors, contributors, companies and affiliates take no responsibility of any sort for any errors or omissions, and you agree to indemnify all these parties entirely, if you use any of this information for any purpose.

John M. Eiding and Alex K. Tang, April 16 2017

AUTHORS' AFFILIATIONS

The table below lists the authors' affiliations and e-mail contact information. The authors of each chapter are listed.

Name	Affiliation	Email	Chapters
John Eidinger	G&E Engineering Systems Inc.	eidinger@geEngineering Systems.com	2, 3, 5, 8, 10
Alex Tang	L&T Consultant	alexktang@mac.com	1, 4, 6, 7, 9
Kazuo Konagai	Yokohama National University	konagai-kazuo-gh@ynu.ac.jp	Reviewer
Yoshihisa Maruyama	Chiba University	ymaruyam@faculty.chiba-u.jp	Reviewer



Field Investigation Team at Ground Zero (Aso Ohashi), behind the team was the Aso Ohashi that crossed Kurokawa (黒川).

Front row from left to right (surname capitalized): Haruka ITO, Alessandra Mayumi NAKATA KAIAMI, Yuki KAGAMI.

Standing from left to right: Masataka SHIGA, Hikaru TOMITA, John EIDINGER, Kazuo KONAGAI, Alex TANG.

ACKNOWLEDGEMENTS

The authors performed the post earthquake lifelines performance investigation and writing this report. For lifelines investigations, it takes a team with diverse knowledge and access to do such an effort. We have been very fortunate to have Professor Konagai of Yokohama National University providing us with the needed logistics support. He was also instrumental in organizing the JSCE staff and members in Tokyo to provide us a comprehensive briefing session. Many people of the Kubota Corporation provided us with tremendous support and information, with Kubota supporting more than 90 man-days in the field to collect site-by-site detailed information about the performance of buried water pipes. Professor Maruyama of Chiba University willingly took over the site guide position when Professor Konagai had to return to Yokohama to attend an important business was a blessing to us. We are also grateful to Professor Kwasinski of Pittsburg University who introduces us to Professor Fujio Kurokawa and Professor Haruhi Eto of Nagasaki University who helped us with setting up two important meetings – Kyushu Electric Power and MLIT (Kyushu). The Kumamoto City Waterworks Bureau provided us with detailed information about the performance of the water system, and provided access to sites with damaged water tanks and wells. Professor Shoji helped us organize meetings with Kumamoto Prefecture. These Professors and organizations provided valuable information and perishable data for this report, and we are indebted to their valuable insights and assistance in every manner. Their permission for us to use their photos and information in this report is extremely valuable.

As is not uncommon in post-earthquake reconnaissance, incomplete information in the weeks and months after the event can lead to omissions and misunderstandings. We apologize if the findings in this report are incomplete, and the reader is cautioned that it may take months to years of post-earthquake evaluations before a comprehensive understanding of lifeline impacts is available. The Council of Lifeline Earthquake Engineering (*TCLEE*) intends to update the lifeline performance information when more information is collected.

The findings and photos presented in this report reflect the collected input from many people and sources; all of them are credited wherever the information or the photo appears in this document. We are very thankful to them providing us with permission to use the information and photos given to us.

The following is a list of individuals and their organizations helping us to collect relevant information:

JSCE debriefing session (30 June 2016)

- Senro Kuraoka, International Activities Center, Senior Coordinator, JSCE
- Yukihiro Tsukada, Executive Director, JSCE
- Yukiko Shibuya, International Activities Center, JSCE
- Yoshihiro Katsuhama, Assistant Manager, Membership & Planning Division, JSCE

- Takanobu Suzuki (Prof), Toyo University
- Yoshohisa Maruyama (Prof), Chiba University
- Gaku Shoji (Prof), University of Tsukuba
- Takeichirou Rinkouin, NTT Kyushu
- Masato Wakatake, NTT Tsukuba
- Isamu Watanabe (Prof), Kumamoto University
- Masayuki Yoshimi, AIST, Tsukuba
- Prof Kakimoto, Kumamoto University
- Hi Tsukamoto, E-J hds, Tokyo
- Prof Konagai, Yokohama National University

JWWA debriefing session (30 June 2016)

- Osamu Kawaguchi, Assistant to Manager, JWWA
- Mr. Shibato, Deputy Director, JWWA

Kubota Corporation

- Toshio Toshima, Senior General Manager
- Osamu Kume, Deputy General Manager
- Naoto Itabashi, Senior Engineer
- Takeshi Hara, Senior Engineer
- Kohei Ikeda, Research
- Kotaro Wakahara, Manager
- Satoshi Suenaga, Engineer/Manager
- Mitsuo Hayashi, Chief Engineer

Kumamoto Prefecture Government (Kumamoto)

- Keishi Matsuda, Assistant Deputy Director, International Affairs Division
- Yuichiro Nakata, Deputy Director, Civil Engineering Technical Management Division

MILT (Fukuoka, Kyushu)

- Mr. Taku Kodaira, Director of Planning, Department of Planning
- Mr. Shojiro Sakai, Head of Disaster-prevention Division, Department of Planning
- Mr. Hiromi Kai, Head of Road Management, Road Department
- Mr. Kazuyuki Sato, Senior Specialist, Disaster-prevention Division, Department of Planning

Kyushu Electric Power (Fukuoka, Kyushu)

- Akihiko Shinkai, General Manager, Transmission & System Operation
- Kazuya Hirano, Assistant Manager, Substation
- Kengo Morita, Transmission
- Daisuke Tsurukubo, Distribution
- Takashi Nakamura, Assistant Manager, Transmission
- Hiroki Higuchi, Manager, Transmission
- Yasushi Ishimatsu, Manager, Distribution
- Hironori Koga, Manager, Substation
- Kaishi Izutsu, Group Manager, Substation
- Junichi Yoshitake, Group Manager, Distribution

- Yoshihiko Ejima, Substation

NTT West (Fukuoka)

- Chikamasa Teshima, General Manager, Kyushu Branch
- Shinichi Kunimatsu, General Manager, Disaster Countermeasure Office
- Toshinori Inoue, Assistant Manager, Operation & Maintenance Department
- Hirose Keiichi (Dr.), NTT Tokyo for establishing the above contacts

Kumamoto City Waterworks and Sewage Bureau (Kumamoto)

- Koji Nagame, General Director
- Katsuhiro Higashi, Chief Inspector
- Norichika Sakata, Deputy Director General, Operation & Maintenance
- Takeki Shiraiwa, Section Head, Operation & Maintenance
- Katsuhiro Azuma, Deputy Director General, Operation & Maintenance

We are extremely grateful to Prof. Maruyama, Prof. Shoji, and Prof. Konagai and Mr. Takeshi Hara of Kubota Corporation who accompanied us in Kumamoto and took us to important sites to investigate the failure modes and also arranging key meetings.

In addition, special thanks go to Prof. Konagai's students (figure above) who helped us overcome any language barriers and provided us insight to all matters Japanese. To these students, and the next generation of earthquake engineering practitioners around the world, we hope this report helps you to understand the world around us, and then take the needed actions to make our lifelines resilient in a cost effective manner.

Alex K. Tang and John M. Eidinger, April 16, 2017

ENDORSEMENTS

Nothing in this report should be considered as an endorsement of any particular product or company.

While we believe the information contained in this report reasonably reflects what occurred (or did not occur) in the earthquakes that affected Kumamoto Prefecture and Oita Prefecture, there is no doubt that this report does not contain all possible information, and it may contain inaccuracies.

This report makes mention of major Japan corporate and local government entities; some are listed on stock exchanges. While all of these entities shared information with us, the readers should know that none of these entities have endorsed the facts, conclusions or recommendations in this report.

1.0 Introduction

Two earthquakes occurred on the island of Kyushu in southwest Japan near Kumamoto City, Kumamoto Prefecture. The first earthquake, which was identified as the fore shock occurred on April 14, 2016 (21:26:36 local time) with a moment magnitude of 6.0 (M 6.0). Throughout this report, we use M to refer to moment magnitude, unless noted otherwise. The foreshock has been variously reported as M 6.1 or M 6.2. The following highlights the key observations for each chapter in this report.

The town of Mashiki was the community that sustained the most serious damage to houses and the regular building stock. By July 1 2016, the fatality count had reached 69 persons, with 1 person missing (presumed dead in a landslide). By July 1 2016, the count of damaged houses was: 8,044 collapsed / destroyed; 24,274 partially destroyed; 118,222 with some damage. All of the fatalities were in Kumamoto Prefecture. More than 112,000 people were displaced. This report concentrates on lifelines, and does not address these serious impacts; but clearly, this earthquake had a major impact on the build environment.

Tourism is a key industry in Kumamoto and neighboring prefectures. Damage to lifelines, and in particular the transportation network, created noticeable financial suffering in the region. It will take a year or more before the Aso Boy train service for tourists to regain its former high demand days. It may take decades for Japan to get the Kumamoto Castle completely restored, with a current cost estimate of 60 billion JPY (about US \$600 million)².

Chapter 2. Hazards

The epicenter of the fore shock was located at 32.788^o N and 130.704^o E, with a focal depth of 9 km. It is just about 3 km North of Kumamoto City, Figure 1-1. The second event identified as the main shock occurred on April 16, 2016 (01:25:06 local time) with M 7.0. The epicenter of this earthquake is located at 32.791^o N and 130.754^o E, with a focal depth of 10 km, Figure 1-2. These two earthquakes were strike slip faulting along the previously mapped Futagawa Fault system.

The fore shock coupled with the strong main shock caused significant damage to lifelines, particularly transportation systems. The strong shaking and the resulting landslides are the two main factors of lifeline damage; locally, there was additional damage due to surface faulting and liquefaction.

The town of Minami Aso was a community that suffered extensive transportation service interruption. In addition to major bridge collapses and road and railway failures and electric transmission tower damage due to landslides, this area also had substantial permanent ground deformation due to surface faulting.

² <http://www.japantimes.co.jp/news/2016/05/20/national/quake-damaged-kumamoto-castle-take-decades-restore/#.WO3BOhiZPmF>, accessed April 11 2017.

There was relatively modest amounts of liquefaction in this earthquake, much of it characterized by settlements in rice fields; a major water well field was co-located in this zone, and the settlements damaged several well structures and pipes. Slumping of levees and embankments near the various river channels resulted in damage to buried pipelines.

Again the lesson here is that pre-earthquake mitigation coupled with well planned emergency response can reduce loss of life, property and economic impact. We observed that the actual levels of ground motions often exceed those assumed by engineers during initial design, and these overloads led to failures. The potential impacts on lifelines due to landslides, surface faulting and liquefaction often remains largely overlooked. We are pleased to report that in the Kumamoto area, aggressive efforts over the past two decades (or so) to replace older fragile buried water pipes with new seismic-resistant pipes were successful. However, we need to recognize that one death is one too many, and outage durations for transportation, power, gas, water and telecommunications were still longer than could have been. Engineers, community and government still have much work to do.

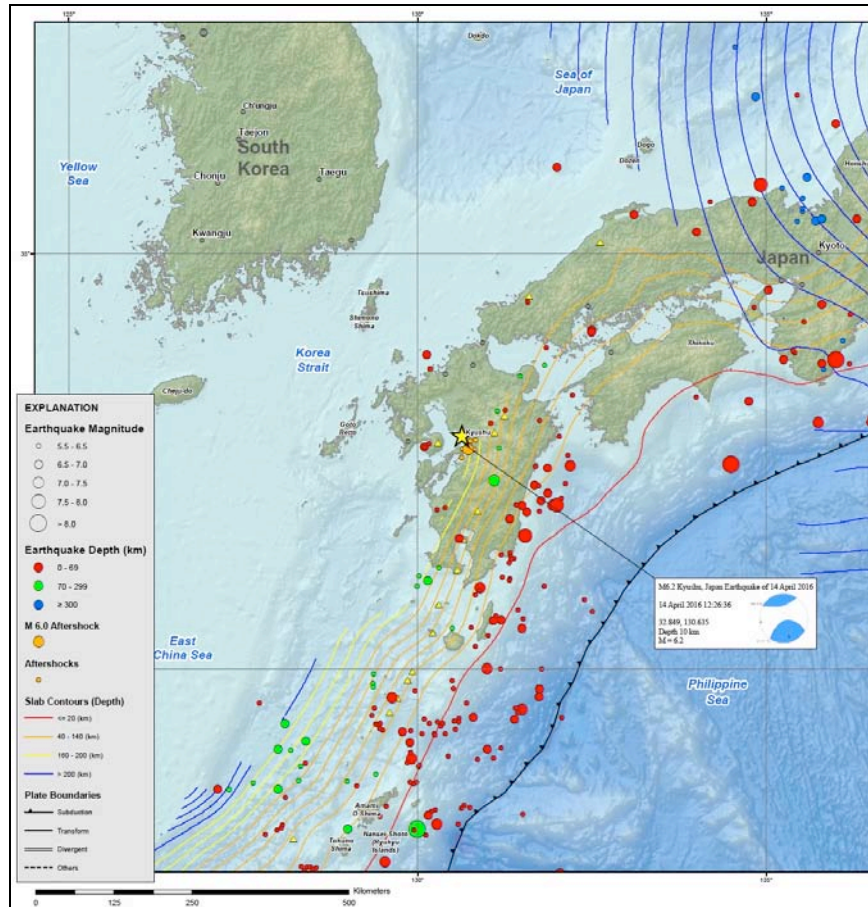


Figure 1-1. Epicenter of M=6.0 Kumamoto Earthquake (Foreshock), 14 April 2016 (USGS)

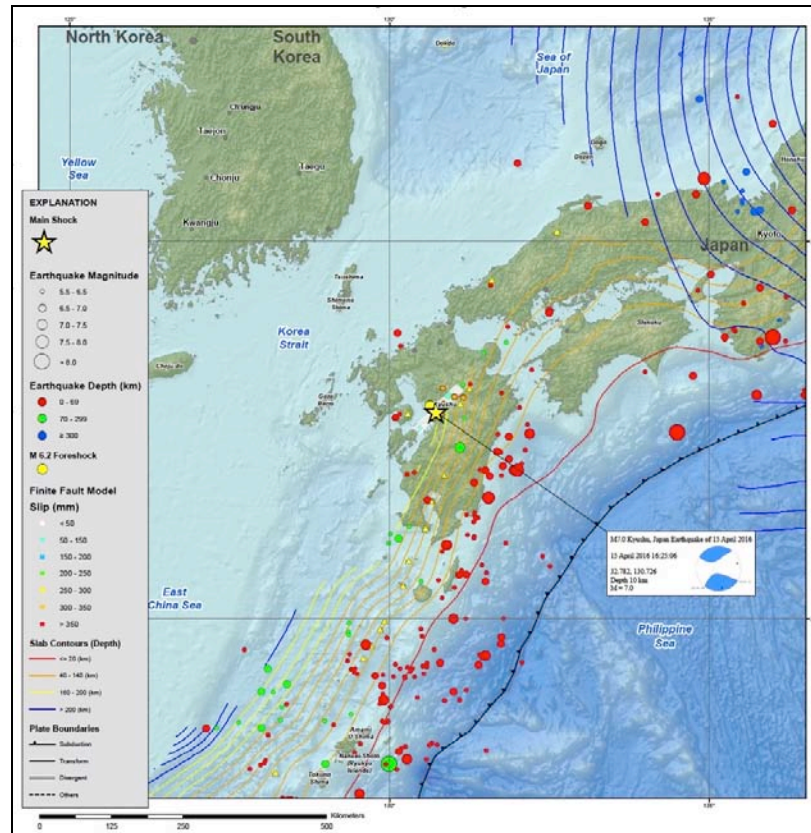


Figure 1-2. Epicenter of $M=7.0$ Kumamoto Earthquake (Main shock), 16 April 2016 (USGS)

Chapter 3. Electric Power

The electric power system for the entire area affected by the earthquakes is operated by Kyushu Electric. There was damage to equipment and bus-work in high voltage substations, transmission towers as well as to the distribution system. The hardest hit to the transmission system was in Minami Aso areas where major landslides occurred.

Damage to the high voltage substations resulted in an area-wide power outage that lasted a few hours. Damage to transmission towers and the distribution system resulted in much longer outages. Power outages were mainly in Kumamoto Prefecture. Emergency power generating trucks, being specially-built portable generators for medium voltage application (6.6 kV, Figure 1-3), greatly helped to rapidly restore limited power service in areas where the transmission towers and distribution network were damaged due to landslides or pull-downs caused by collapsed buildings.



Figure 1-3. High power generating truck provided power to circuits that were disconnected from power source (MLIT)

Chapter 4. Telecommunication

Cellular phone services were impacted by these earthquakes. Both power outage and severed cables were the main reasons of service interruption. The recovery of the cellular service was slow (99% recovered within 15 days) due to after shocks and access to sites.

The most dramatic failure was the collapse of a cell site tower. Figures 1-4 and 1-5 show the aerial picture of the before and after the earthquake, and the ground level photo of the collapsed tower.

There were no damage to Exchange Offices and the backup power systems functioned as planned.

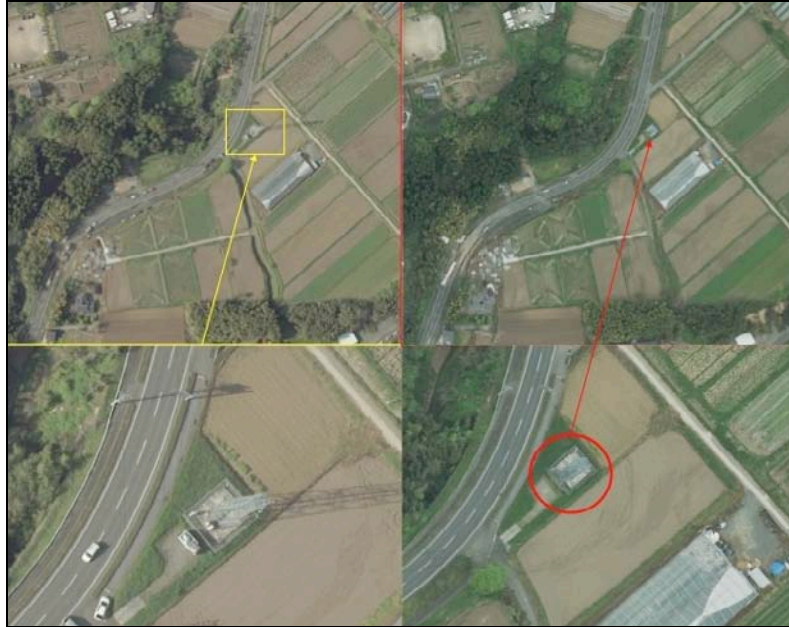


Figure 1-4. The aerial photo on the left was taken on 15 April 2016, while the one on the right was taken on 16 April 2016 after the main shock. Note the crumbled tower on the lower right, within the red circle. (Photos from Aero Asahi Corporation)



Figure 1-5. Ground level photo of the collapsed cell tower. (Courtesy: Guardian News & Media Ltd)

Chapter 5. Water and Wastewater

The City of Kumamoto and all the neighboring towns depend on ground water as the main potable water source. The strong shaking of the earthquake resulted in a sudden increase in turbidity in the well water. Automatic turbidity monitors measured this rapid

increase in turbidity, and immediately shut down all the wells. It took some time for the authorities to recognize that this temporary turbidity spike was not a real health hazard, and the resulting area-wide water interruption caused extra level of grievances to the community.

There were a few hundred potable water pipe breaks, nearly always to older styles of non-seismically-design buried pipe; thousands of repairs were needed for service lateral repairs. A few wells were damaged due to ground deformations. A couple of 2 to 5 million gallon (8 to 20 million liter) post-tensioned above-grade concrete tanks had various styles of damage, but without major leaks.

One wastewater plant (out of 21) was not functional after the earthquake.

There were 14 fire ignitions, Table 1-1, as reported by the Kumamoto Prefecture Emergency Response Department, as of April 20 2016. There was no fire spread, and the water department knew of no instance where the piped water system (failed or otherwise) was called upon to supply water for fire fighting purposes.

Kumamoto Prefecture	Number of reported Fire Ignitions
Kamimashiki	2
Kumamoto	7
Yatsushiro	2
Aso	1
Kakuchi	2
Total	14

Table 1-1. Fire Ignitions

Chapters 6 and 7. Airport and Sea Ports

Kumamoto Airport sustained some damage and was closed for 1.5 days. This airport was close to the ruptured fault, and sustained ground motions with $PGA > 0.5g$. Soils at this airport can be characterized as firm and not subject to liquefaction. There was no significant structural damage to the terminals – domestic and international, but some reinforced concrete columns showed minor cracks, as evidence of yielding of rebars within. Most of the damage was non-structural damage, such as fallen ceiling tiles, cracked dry walls, etc. Figure 1-6.



Figure 1-6. Kumamoto Airport domestic terminal the morning after the main shock in front of ANA service counter. (Courtesy Guardian News & Media Ltd)

All other airports within Kyushu island were rather distant from the zone of strong ground shaking, and were not impacted.

There were minor set backs at three seaports in Kyushu. All of these set backs involved road access to the port and ground settlement within the port.

Chapter 8. Gas

In the area affected by strong ground shaking, about half the area is supplied with natural gas by a piped system. In areas where ground shaking was recorded by instruments to have ground velocities greater than 60 cm/sec, automatic valves cut off the gas supply via the transmission pipe network. The selection of 60 cm/sec is based on Japanese observations that older non-seismic-installed gas pipes (such as galvanized steel pipe with screwed joints) tend to get damaged at or above this level. Most structures had gas meters with earthquake sensors, and these meters automatically turned off due once they sensed high levels of shaking. There was some damage to older non-seismic-designed gas mains, but more than 85% of the gas mains were constructed with seismic-resistant pipes and these had little or no damage. Most of the gas system repair effort occurred to service laterals and meters, as well as work within customer's houses. Restoration of the gas system took some time. The shut-off of the gas transmission pipes and the local shutoff at customer meters may have helped avoid gas-fed fires; there were no fire conflagrations in this earthquake sequence.

In many of the smaller communities, the majority of households use propane tanks. For the most part, these tanks are vertically-standing tanks, generally up to 1.5 meters tall by up to 0.5 meters in diameter, strapped to the adjacent building. If the buildings remained

standing, there was little damage to the propane tanks. In Mashiki town, where there were many collapsed buildings, there were no reported fires due to toppling of the propane tanks.

Chapter 9. Transportation

A high-speed rail Shinkansen, a deadhead train returning to Kumamoto service depot, derailed. There was no injury with minor damage to the track. One local rail car derailed close to the station.

A 0.5 km-long section of the rail Hoho Main Line (JR), that was close to Aso Ohashi, was destroyed by a major landslide, which also destroyed the bridge at Aso Ohashi, Figure 1-7.

There were many other bridges and roads damaged by landslides, rock falls, and permanent ground deformation.

Transportations system suffered the greatest set back in this earthquake.



Figure 1-7. Hoho JR Line destroyed by landslide

Chapter 10. Levees

There was considerable damage to levees, including slumping and lateral spreads.

Waste Management

58 temporary sites were added to collect the debris caused by the earthquake. Two out of 27 incinerators did not function after the earthquake. By 23 May 2016 all facilities were

back to normal. It was estimated to have 1 to 1.3 million tons of debris generated by the earthquake.

Social Economic Impact

Schools sustained minor damage such as broken glasses, exterior wall cladding damaged, some broken pipes, and ceiling damage.

Medical facilities sustained damage, but most of them remained functional. The following table (tabulated by the Ministry of Health, Labor and Welfare), current as of April 19 2016, highlights the types of damage that was sustained at the various hospitals and medical facilities. Out of 23 facilities that had lifelines problems, six of them also sustained structural damage (19 April).

Description	Number of medical facilities
Possible structural damage	6
Lifelines problem (power, gas, water)	23
No problem	43
Total	69

Table 1-2. Damage to Medical Facilities

Only a few stores were closed due to extensive structural damage or areas closed to access, most of them remained open – small convenience stores and major supermarkets. There are three major chains of convenience stores in the area, namely 7/11; Lawson and Family Mart. Tables 1-3 and 1-4 highlight the performance of these commercial facilities as of April 17 2016.

Name	Total	Open	Closed
7/11	287	257	30
Lawson	141	61	80
Family Mart	163	66	97
Total	591	384	207

Table 1-3. Damage to Convenience Stores in Kumamoto Prefecture (April 17)

Name	Total	Open	Close
Ion	27	11	16
Isumi	7	1	6
Sanribu	20	5	15
Seiyu Ltd	3	0	3
TOTAL	57	17	40

Table 1-4. Damage to Supermarkets in Kumamoto Prefecture (April 17)

Table 1-5 lists the number of open and closed convenience stores and supermarkets of May 31 2016 (columns 2 and 3) or May 16 2016 (right-most column).

Type	May 31 Open	May 31 Closed	May 16 open
Convenience Store	593 (99.5%)	3	74.9%
Supermarket	51 (89.5%)	6	38.6%

Table 1-5. Damage to Convenience Stores and Supermarkets in Kumamoto Prefecture

Of the 3 convenience stores still closed as of May 31, one was located in an area that remained closed to the public; one had damage to the building, and one was inside a closed shopping mall.

1.1 Limitations

The findings in this reconnaissance report was developed during the first few months after the April 2016 earthquake sequence. All findings must be considered accordingly. The data in this report may be incomplete, and the interpretations may be incorrect. The authors and contributors of this report make no warranty of any kind.

1.2 TCLEE and ASCE

Soon after the 1971 San Fernando earthquake, the Technical Council of Lifeline Earthquake Engineering (TCLEE) was formed, a committee of the American Society of Civil Engineers (ASCE). ASCE "sunsetted" TCLEE on December 31 2014. The roots of "sunset" provisions were established at the time of the Roman Republic, where the Roman senate ruled *Ad tempus concessa post tempus censetur*, translated as "what is admitted for a period will be refused after the period". Sunset provisions have been used extensively throughout legal history. Before being sunsetted, over a five decade period, TCLEE issued more than 60 monographs and reports and guidelines for the seismic performance, evaluation and design of lifelines. This large body of knowledge has formed the core for many of the guidelines and standards for lifelines used around the world. TCLEE has issued reports on lifeline performance for nearly every major destructive earthquake around the world since the 1980s, including those in the United States, Japan, China, Taiwan, Turkey, Greece, India, Philippines, Peru, Chile, Italy, as well as tsunami events, floods and major winter storms.

The authors of this report continue these efforts. The first report prepared by *TCLEE* was on the 2014 Napa, California earthquake. This report is the *TCLEE No. 2*.

1.3 Abbreviations

cm	centimeter
g	acceleration of gravity (= 32.2 feet / second / second = 981 gal)
km	kilometer
kV	kilovolts

M	Magnitude (moment magnitude unless otherwise noted)
mm	millimeter
PGA	Peak Ground Acceleration, g
PGD	Permanent Ground Displacement, (cm)
PGV	Peak Ground Velocity (cm/sec)
USGS	United States Geological Survey

1.4 Units

This report makes use of both common English and SI units of measure.

Common Conversions

1 kip = 1,000 pounds

1 foot = 12 inches

1 inch = 25.4 mm = 2.54 cm

1 mile = 1.609347 kilometers

1 pound-force = 4.448 newtons

1 pound = 0.453592 kilogram

1 psi = 6.894757 kiloPascal (kPa)

1 kPa = 0.145038 psi

1 g = 981 gal (cm/sec/sec)

1 m = 1,000 mm = 100 cm

1.5 License, Copyright and Create Commons Deed

Copyright 2017, John M. Eidinger and Alex K. Tang. The copyright remains with the authors.

Creative Commons Deed. You are welcome to use and expand on this information, provided you agree with the following Creative Commons Deed:

You are free:

- To copy, distribute, display and perform the work; and
- To make derivative works

Under the following conditions:

- Attribution. You must give the original author credit.
- Noncommercial. You may not use this work for commercial purposes.
- For any reuse or distribution, you must make clear to others the license terms of this work.

Any of these conditions can be waived if you get permission from the authors.

Your fair use and other rights are in no way affected by the above.

This is a human-readable summary of the Legal Code (the full license):

<http://creativecommons.org/licenses/by-nc/1.0/legalcode>.

Limitations. The authors and G&E Engineering Systems Inc. make no warranty or guaranty that any of the information in this report is suitable for any purpose. You are totally on your own if you use this information.

1.6 Acknowledgements

Some maps in this report use base maps derived from Google; we thank Google for their use. In each chapter, some photos were taken by the authors; and some were provided by various agencies; we thank the agencies for their use.

2.0 Seismic Hazards

Section 2 describes the seismic hazards in this earthquake.

- Section 2.1 provides maps showing the location of the fore shock and main shocks, the major population centers, regional geologic conditions, and approximate locations of the ruptures and major landslide zone.
- Section 2.2 provides data describing PGA, PGV, and Spectra Accelerations in the area.
- Section 2.3 describes some of the landslides in the areas with strong ground shaking.
- Section 2.4 examines the observed liquefaction phenomena.
- Section 2.5 examines the observed surface faulting.
- Section 2.6 provides references.

2.1 Location of the Earthquake

Figure 2-1 shows the country of Japan, highlighting the western island of Kyushu, the two largest cities (Fukuoka and Kumamoto) on the island, and locations of a few other large cities in Japan. Major destructive earthquakes have hit Kobe (1995), Niigata (2004) and Sendai (2011) over the past two decades.



Figure 2-1. Place Names

Figure 2-2 shows a satellite image that highlights Kyushu Island. Much of the island is mountainous and forested, denoted by the dark green areas. The heavily populated areas include the city of Fukuoka (metro population near 2 million people) and Kumamoto (metro population around 1.5 million people). Also highlighted is the Mount Aso region, a dormant volcanic caldera that is now populated with small towns and farming.

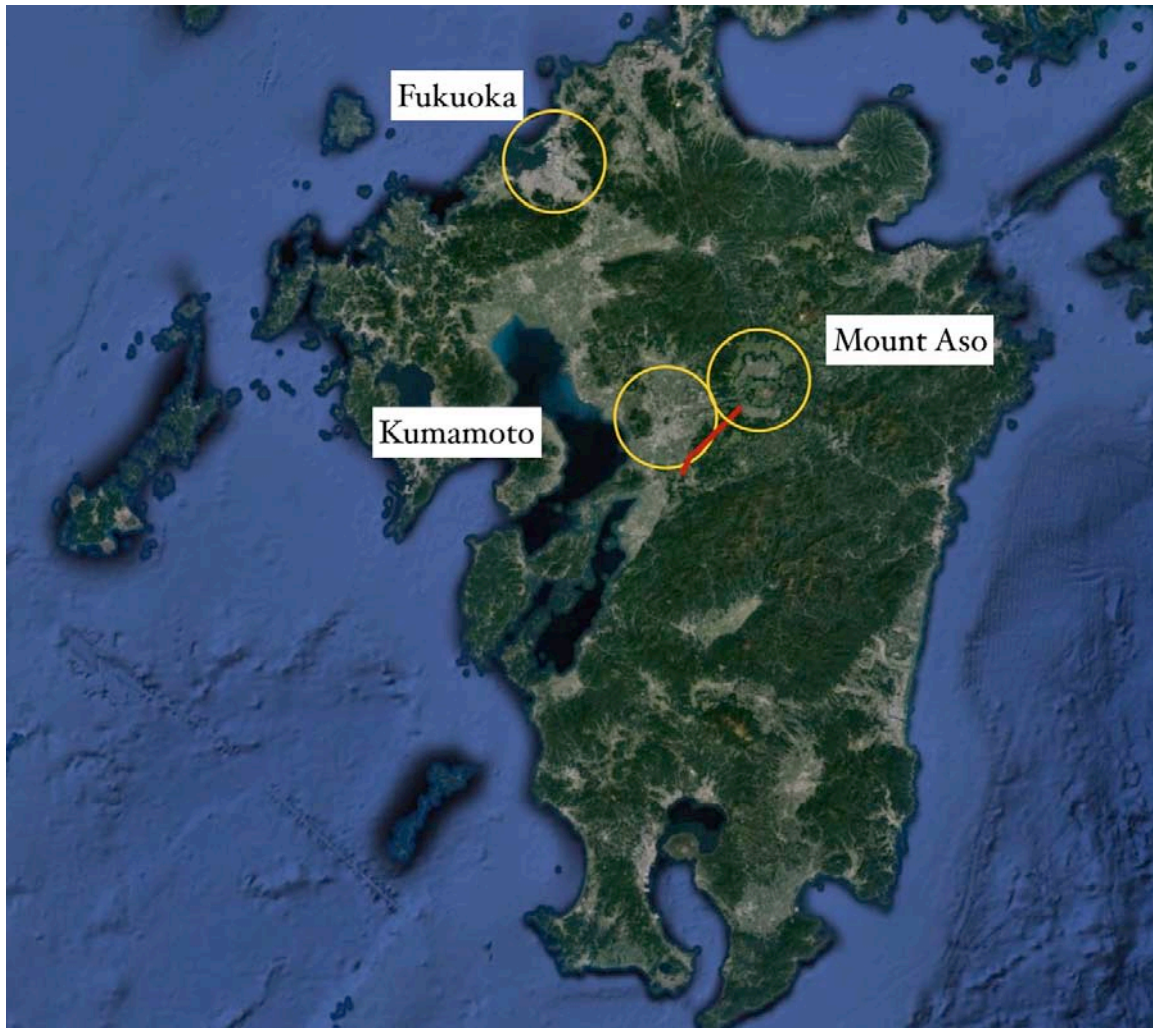


Figure 2-2. Kyushu Island

Figure 2-3 shows a topographic relief of the Kumamoto and Mount Aso region. Highlighted are the approximate ruptures of the April 14 2016 M 6.0 fore shock and the April 16 2016 M 7.0 main shock. The topographic relief of the Mount Aso caldera is clearly seen, along with the main drainage outlet to the west towards Ozu. Mashiki town is the largest urbanized area near the M 7.0 rupture.



Figure 2-3. Kumamoto and Mount Aso Area

Figure 2-4 shows a higher resolution topographic relief of the Kumamoto and Mount Aso region. Highlighted are the approximate ruptures and rupture lengths of the April 14 2016 M 6.0 fore shock and the April 16 2016 M 7.0 main shock. The boxed area labeled "Major Landslide Zone" includes most of the major landslides that are described later in this report; ground shaking in that area was commonly $PGA > 0.4g$, and hillsides were commonly rather steep, commonly 35° or so. The rail Hoho Main Line crosses through the Major Landslide Zone, and about 0.5 km of rail alignment was completely destroyed due to a major landslide in that area.



Figure 2-4. Kumamoto, Mount Aso and Landslide Area

Figure 2-5 shows a geologic map of the area. The light colors in this map are largely alluvial, and are now occupied by farming areas (including most of the Mount Aso area, and the main river that drains the caldera towards the west) or the urbanized area (the city of Kumamoto). The darker colors represent rock zones, with the various colors referring to different ages of the rock. The vast majority of the population lives in the alluvial zones.

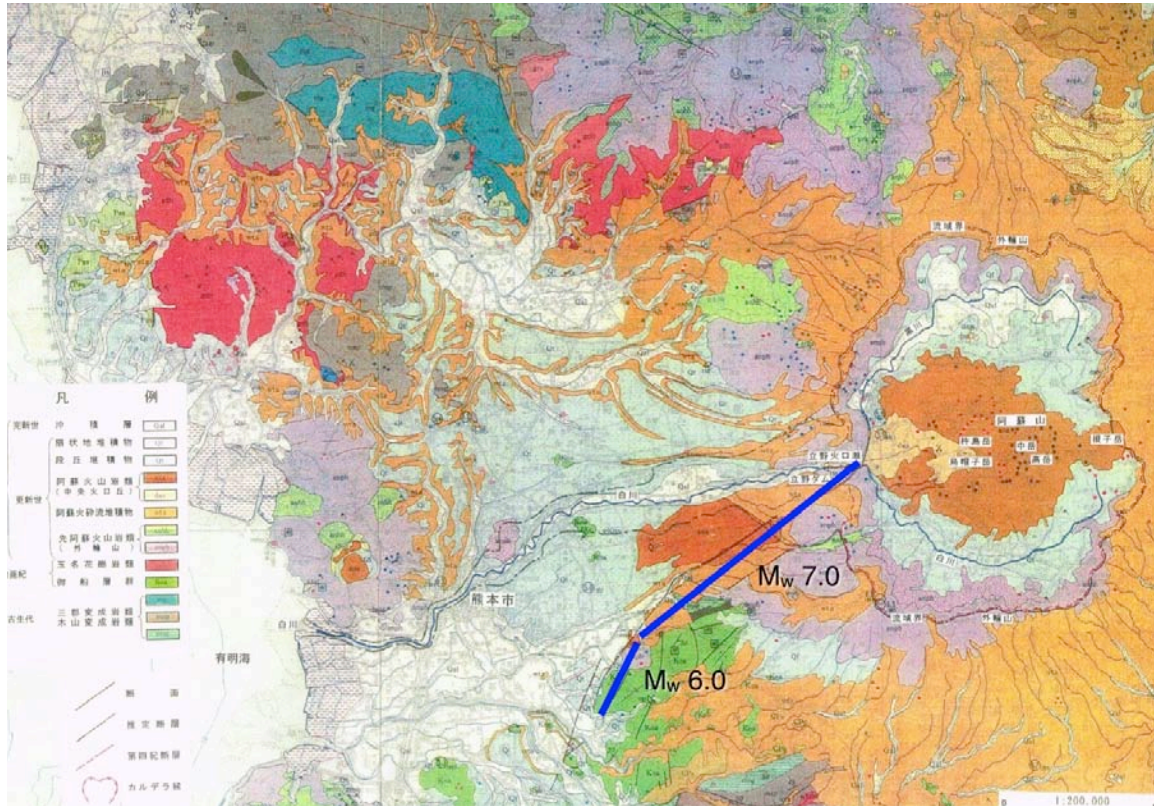


Figure 2-5. Geologic Map

Figure 2-6 shows a map of Kumamoto Prefecture, along with the various cities and municipalities within the Prefecture. The largest community in the prefecture is Kumamoto City. Mashiki Town had the most concentrated damage.



Figure 2-6. Place Names

2.2 Seismicity and Ground Motions

Figure 2-7 shows a map of a portion of Kyushu, highlighting known active crustal faults (red lines) and historic earthquake epicenters (circles, sized by magnitude). The two filled-in circles represents the epicenters of the April 14 and 16 2016 events. The dates next to the historic earthquakes

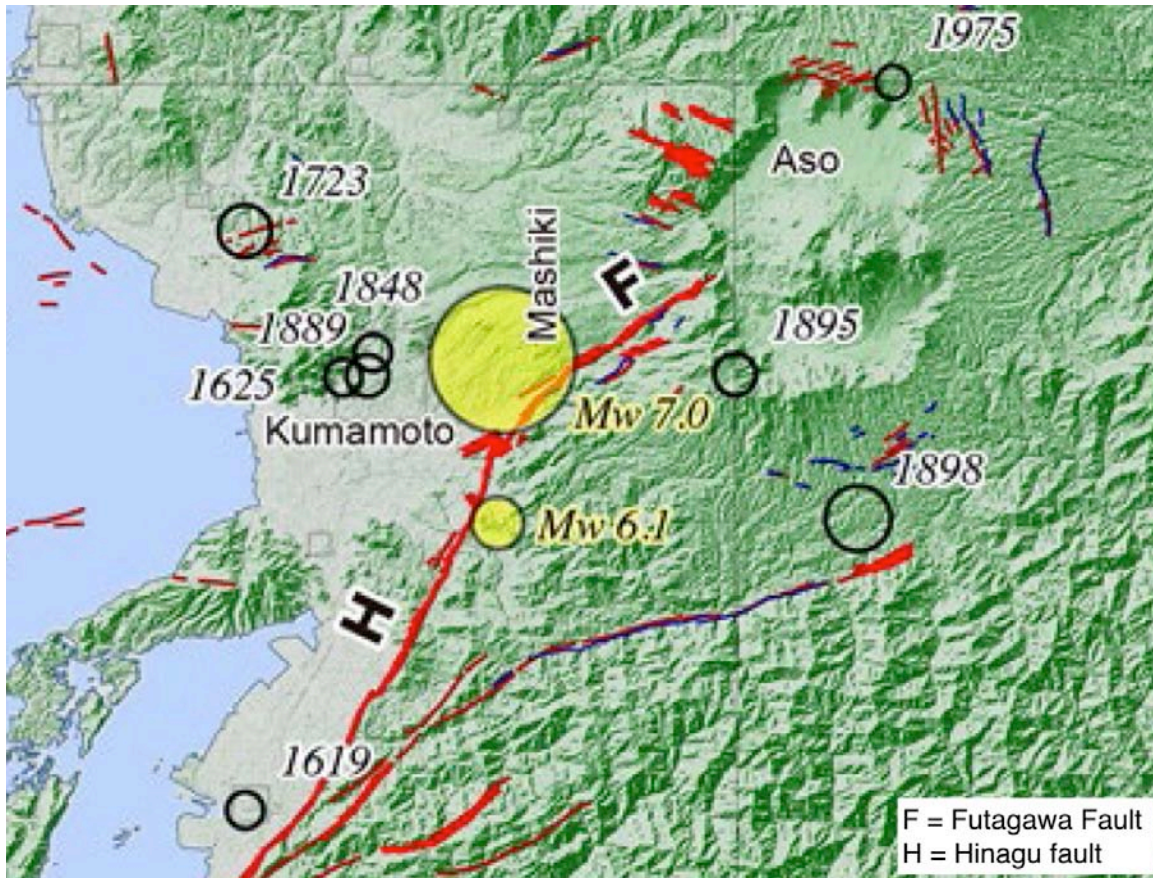


Figure 2-7. Historical Seismicity

The dates next to the historic earthquakes show that Kumamoto City has had small magnitude ($M < 5$) earthquakes under or very near the city in 1625, 1848 and 1889, and the Mount Aso region last had a close-by small magnitude earthquake in 1895. The existing infrastructure in the Kumamoto area includes a range of buildings, including the historic Kumamoto Castle (originally built 1608 as a wooden castle, largely re-built in the 1950s as a reinforced concrete structure), older Japanese-style wooden houses (similar in style of construction as those heavily damaged in the 1995 Kobe earthquake), and more modern construction, including many mid-rise and high-rise construction made of reinforced concrete and steel. There have been no recent nearby earthquakes in or near Kumamoto since the construction of the bulk of the modern lifeline systems (electricity, water, telecommunication, rail, highway, etc.)

Figure 2-8 shows the time histories and response spectra for two of the nearby strong motion instruments, called KMM006 and KMM008. Both instruments showed about 15 seconds of very strong shaking, with horizontal PGA between 0.5g and 1.0g. The heavy grey lines represent mapped faults.

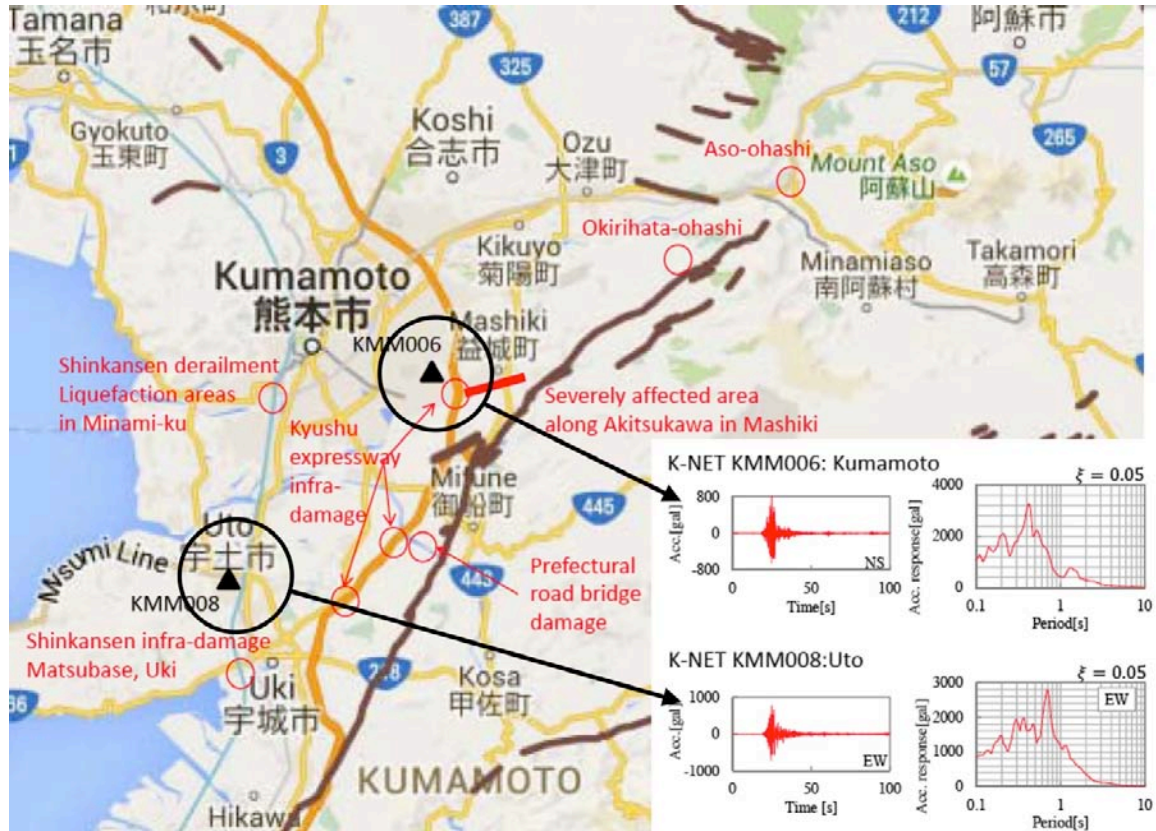


Figure 2-8. Strong Motions

Figure 2-9 shows the JMA SI map of the motions for the April 14 2016 event. The JMA Spectra Intensity scale ranges up to 7 (highest level). Up to about 2000, this scale was meant to reflect observed damage (much like MMI in the USA). Post 2000, the JMA SI map is prepared using a combination of recorded PGA and PGV, and is no longer based on observed damage. The scale units 6+ (6-upper) and 6- (6-lower) usually indicate area where heavy damage to lower seismic-capacity buildings might be expected.

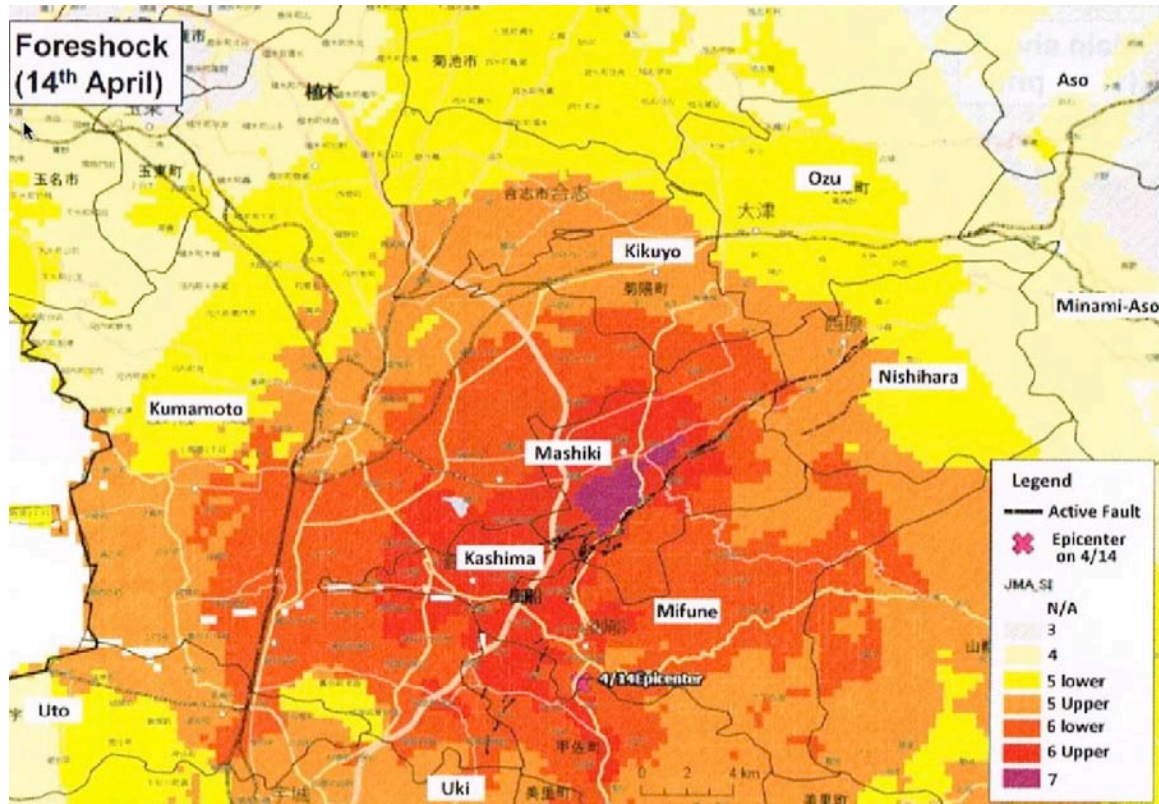


Figure 2-9. JMA SI Scale – April 14 2016 Fore Shock Earthquake

Figure 2-10 shows the JMA SI map of the motions for the April 16 2016 main shock event. As would be expected, the Mashiki town area is mapped as either 6+ or 7. The Minami-Aso area is mapped as 5+, but field observations showed that landslides and surface faulting (which are not directly captured in the JMA mapping algorithms) dominated the damage that actually occurred in that area. It must be understood that there were only about 10 strong ground motion instruments in the area mapped in Figures 2-9 and 2-10, so the accuracy of the color scheme in each of these maps can only really be attributed atop or very close to the underlying instrument; the rests is extrapolated, with the expected error of at least $\pm 50\%$ from the median at most locations.

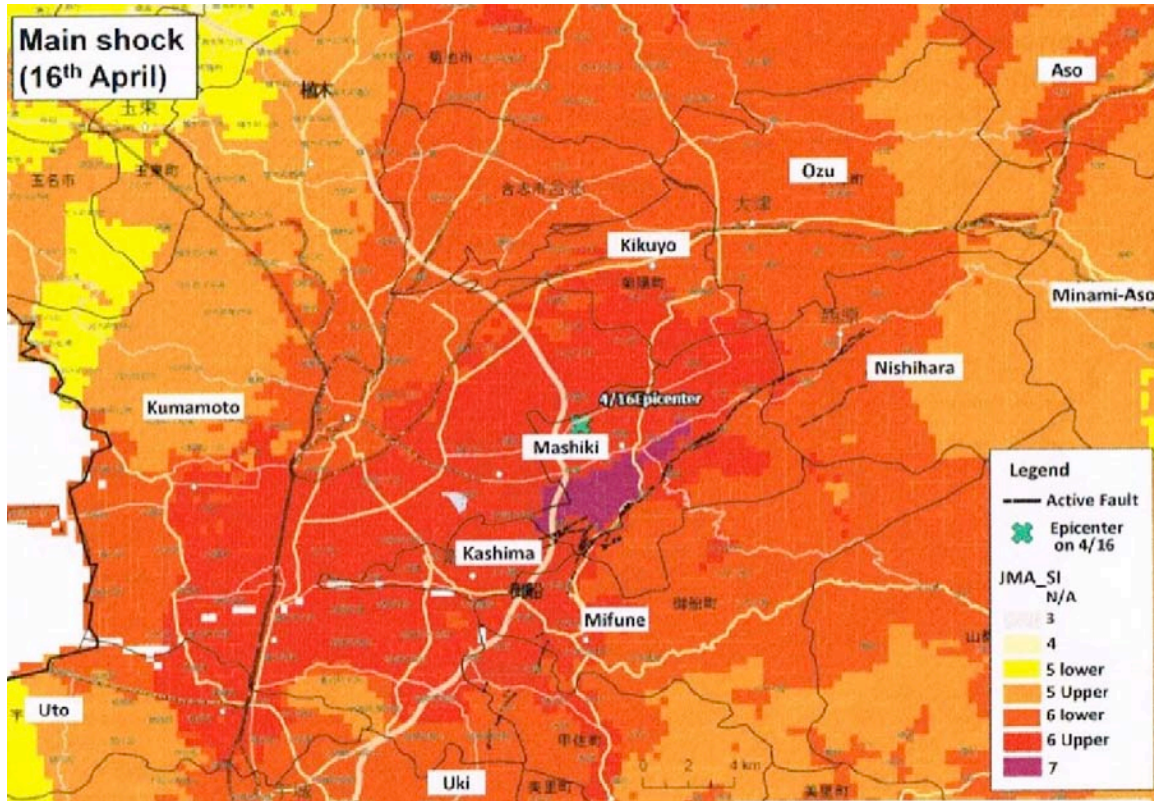


Figure 2-10. JMA SI Scale – April 16 2016 Main Shock Earthquake

It was initially reported that there was no surface faulting caused by the April 14 2016 fore shock; subsequently, there have been some reports saying that some minor offsets seem to have appeared along the northern segment of the Hinagu fault.

The Futagawa fault, source of the main shock, has been characterized as having 3 major events in the past 26,000 years, including the 2016 event. The rupture direction was from the southwest towards to east-north-east, stretching about 28 to 30 km in length. Dip of the fault was characterized as 60° to 84° west north west. This fault had previously been characterized as producing right-lateral slip; and in the main shock, observed surface rupture was mostly right lateral in sense, commonly between 0.3 meters to 1.0 meters of offset (locally as high as 2.0 meters of offset); in most places with surface faulting, there was 0 to 0.1 m of coincident vertical offset, with the "up side" varying from location to

location, but trending to be on the south side. Maximum observed vertical offsets were 0.5 meters up-on-the-south or 0.2 meters up-on-the-north (including the graben zone in the Mount Aso caldera). In the Mount Aso caldera, there was a graben formed, and it remains unclear as of the time of writing this report as to the underlying structure that formed the graben. Along the main rupture zone, the authors of this report observed little vertical offset.

Prior to the April 2016 earthquake sequence, the return period for major events on the Futagawa fault would have been "about 13,000 years", and post 2016, the long term return period might be characterized as "about 8,700" years.

In the USA, we often define the term "active fault" as those having had at least one major event in the Holocene period, or the last 11,000 years. From a "probabilistic" design point-of-view, events with either 8,700 or 13,000 year return periods produce only modestly low motions ($PGA < 0.15g$) in terms of motions commonly used for design in the USA, for designs based on either the 475 year (in vogue until 2000) or even the 2,475 year return periods (in vogue post-2000 or so). This exposes a major weakness in USA seismic design codes that ignore deterministic motions, as *if* the event occurs, PGAs are likely to exceed 0.5g in the near-fault region, or 3 to 4 times higher than would otherwise be assumed using probabilistic methods. For critical infrastructure, like many lifelines, some consideration should be made for deterministic motions for any active fault, as eventually, over the long term, these events will eventually occur. For example, some researchers in Quebec suggest that it is entirely acceptable to verify that a large reservoir impoundment dam be evaluated for $PGA = 0.06g$, whereas if a M 6 event occurs directly beneath the dam, the actual PGA may well reach 0.5g or so; with the caveat that "well, it is unlikely that the dam will see 0.5g in the next 500 years and therefore need not be made tough enough for the 0.5g event", but it is nearly sure that the dam will see 0.5g in the next 100,000 years or so... and therefore the underlying assumption is that either the dam will "magically disappear" sometime in the next 500 years or so, or that human life and economic activity is statistically "not worth enough" for the modern-day dam operator to take suitable seismic mitigation action. This is a fallacy in the thinking of many seismic-code-writers, who assume that buildings have only a 50-year (or so) lifetime.... and therefore economically do not deserve to be designed for rare but possible earthquakes.

In western San Diego County, the example from Quebec applies for the Rose Canyon fault, which is thought to have rather long return time (large events once every several thousand years), and this leads modern seismic design codes to require design for PGA of around 0.2g along the Pacific coastline of San Diego County (2/3 of the 2,475 year motion is in the range of 0.2 to 0.25g for much of the coastal zone). However, when the Rose Canyon fault does rupture, capable of events of about M 7, the ground motions near the fault will be $PGA \sim 0.5g$ (larger in some places). This means that many of SDG&E's substations and other infrastructure along the coastline will see very high motions; and if not suitable designed and installed, will suffer damage. The author of this report has previously provided SDG&E with detailed maps and data that quantify the

levels of motions at all of SDG&E's substations should a large earthquake occur on the Rose Canyon fault.

In eastern San Diego County, the level of seismic hazard is much higher, being controlled by the very active Elsinore and San Jacinto and related fault systems. The 2010 El Major - Cucapah M 7 earthquake is one such example. In this area, SDG&E has long recognized the very high seismicity, and new installations have reflected seismic designs for $PGA = 0.5g$ or so. Even so, a fair amount of damage occurred at the 500 kV yard of the SDG&E Imperial Valley substation in the 2010 earthquake, showing that more work needs to be done to make these facilities suitable resilient.

For new construction, the code design philosophy for regular buildings in Japan uses two "deterministic" events, which for this area would have $PGA \sim 0.3g$ (lower event, little damage) or $0.6g$ (upper event, more damage must still life-safety safe).

In Japan, the modern seismic design requirement for high voltage equipment is to show high reliability for 3 cycles of $PGA = 0.3g$ at the equipment's fundamental period. In the high seismic zones of the USA and Canada, the modern seismic design approach for high voltage equipment is to show high reliability for a motion with a wide-banded response spectra tied to $PGA = 0.5g$, and reasonable reliability for a motion with a wide-banded response spectra tied to $PGA = 1.0g$. But as will be discussed later in this report, neither of these approaches were adopted for the high voltage substations in the area, as they were constructed prior to 1980, before these design requirements were put into place.

Figures 2-11 to 2-14 show horizontal PGA and PGV maps based on recorded instruments for Japan (Figures 2-11 and 2-12) and Kyushu Island (Figures 2-13 and 2-14). The triangles (KNET network instruments) and squares (KIK-NET network instruments) show the locations of the actual instruments. The red star shows the epicenter of the April 16 2016 event.

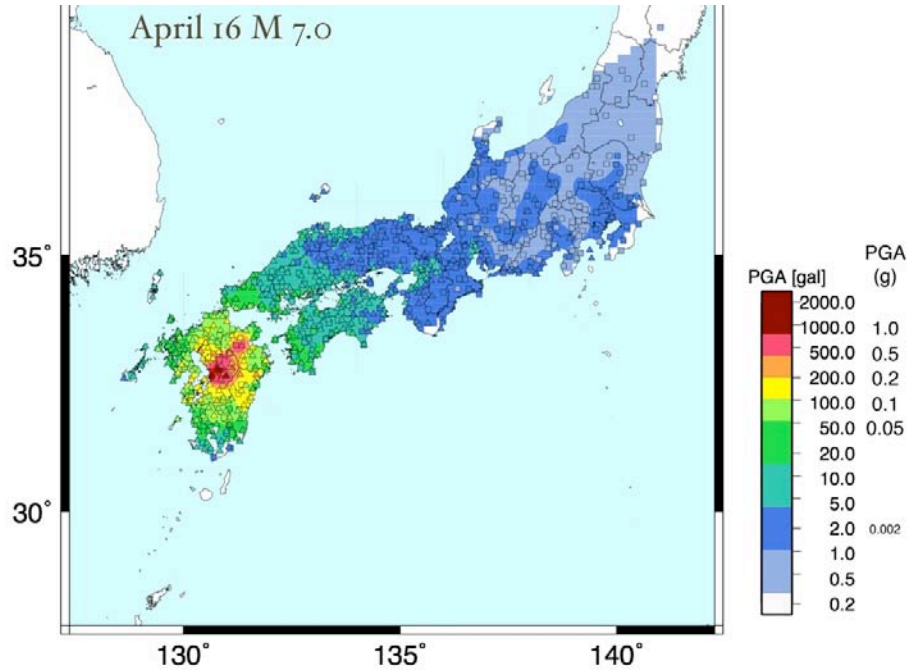


Figure 2-11. PGA Map - Japan – April 16 2016 Main Shock Earthquake

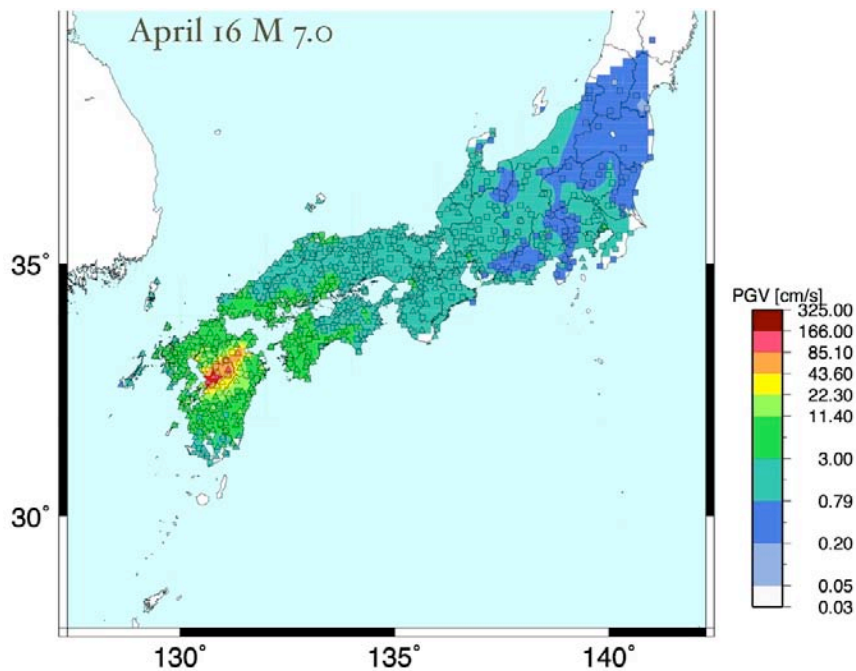


Figure 2-12. PGV Map - Japan – April 16 2016 Main Shock Earthquake

The instruments in Figure 2-13 and 2-15 show that all the instruments showed very strong motions (PGA > 0.5g) along the rupture zone.

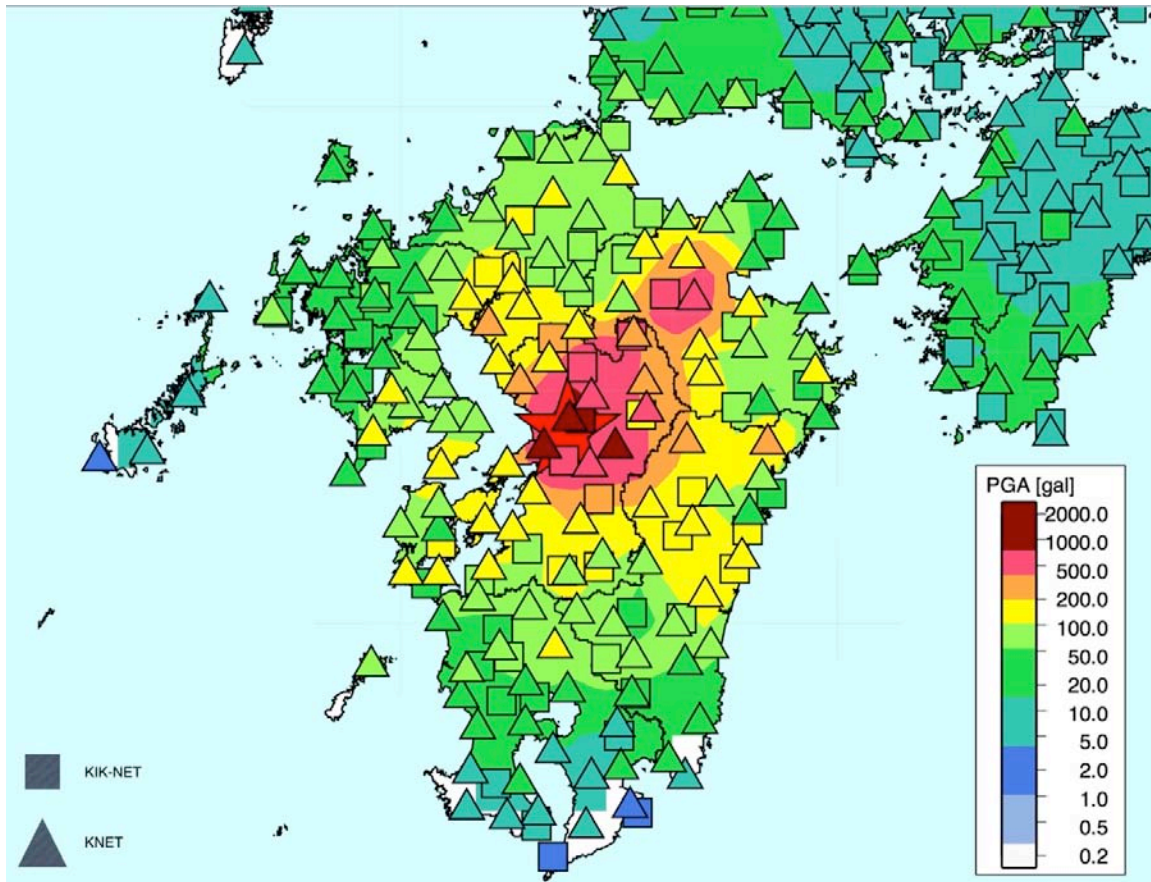


Figure 2-13. PGA Map - Kyushu – April 16 2016 Main Shock Earthquake

The instruments in Figures 2-14 and 2-16 show that the common PGV in near the fault rupture zone was between 50 and 90 cm/sec, with one locations up to about 120 cm/sec.

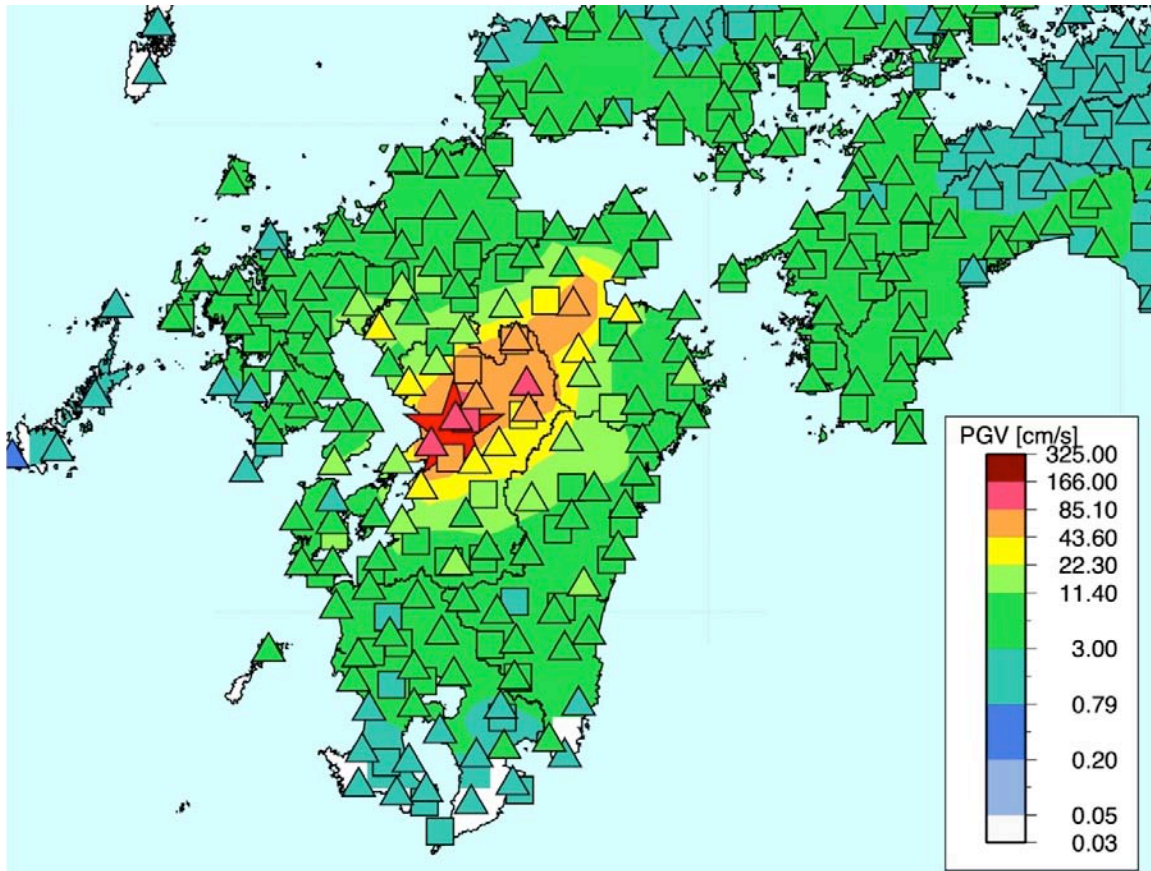


Figure 2-14. PGV Map - Kyushu – April 16 2016 Main Shock Earthquake

Figures 2-15 and 2-16 show the PGA and PGV values as a function of distance to the epicenter. Within 20 km of the epicenter, there were 7 instruments, and all recorded peak horizontal PGA between 0.5g and 1.3g. This also appears to be the case for 10 instruments within 10 km either side of the surface rupture.

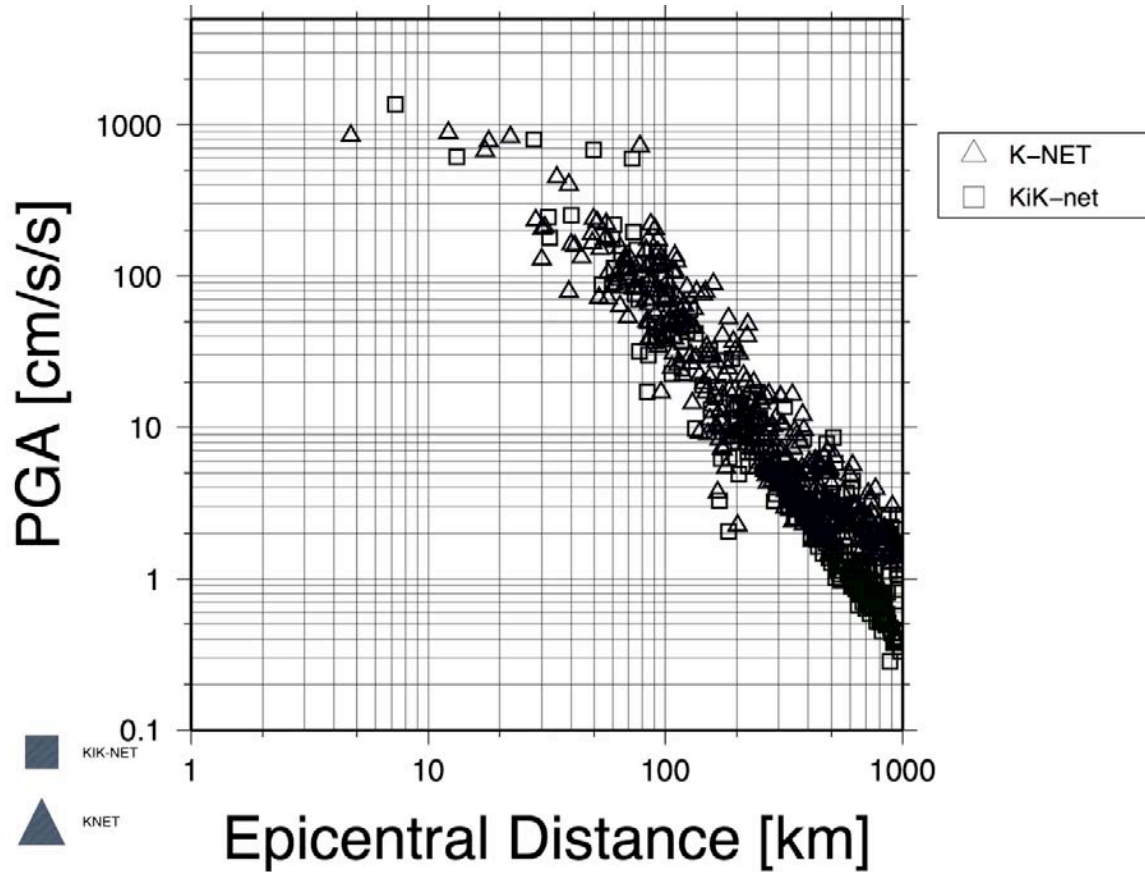


Figure 2-15. PGA versus Epicentral Distance Main Shock

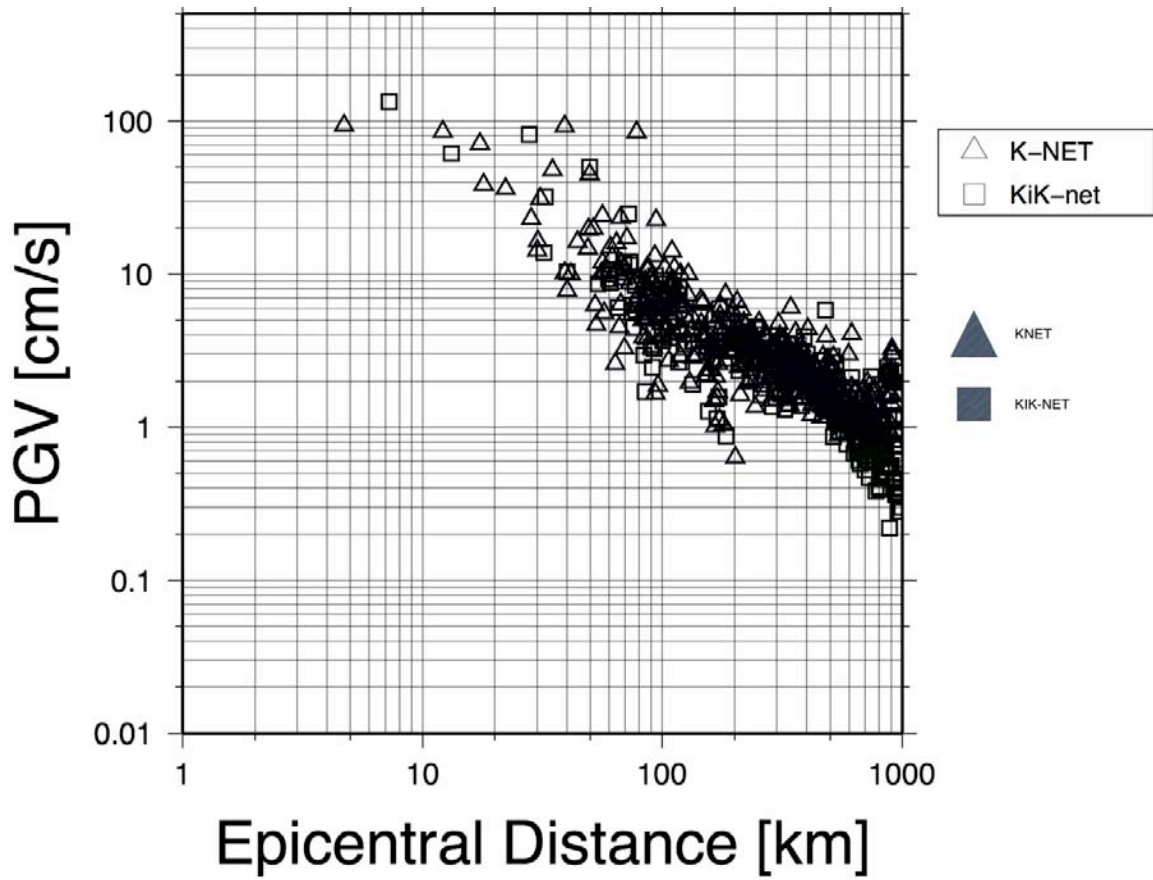


Figure 2-16. PGV versus Epicentral Distance Main Shock

Figures 2-17 and 2-18 (after EERI) show the maximum motions in three orthogonal directions for the four instruments closest to the Kumamoto airport and time histories for the two instruments shown as red triangles in Figure 2-17. The motions show about 8 seconds of very strong shaking (PGA > 0.2g).

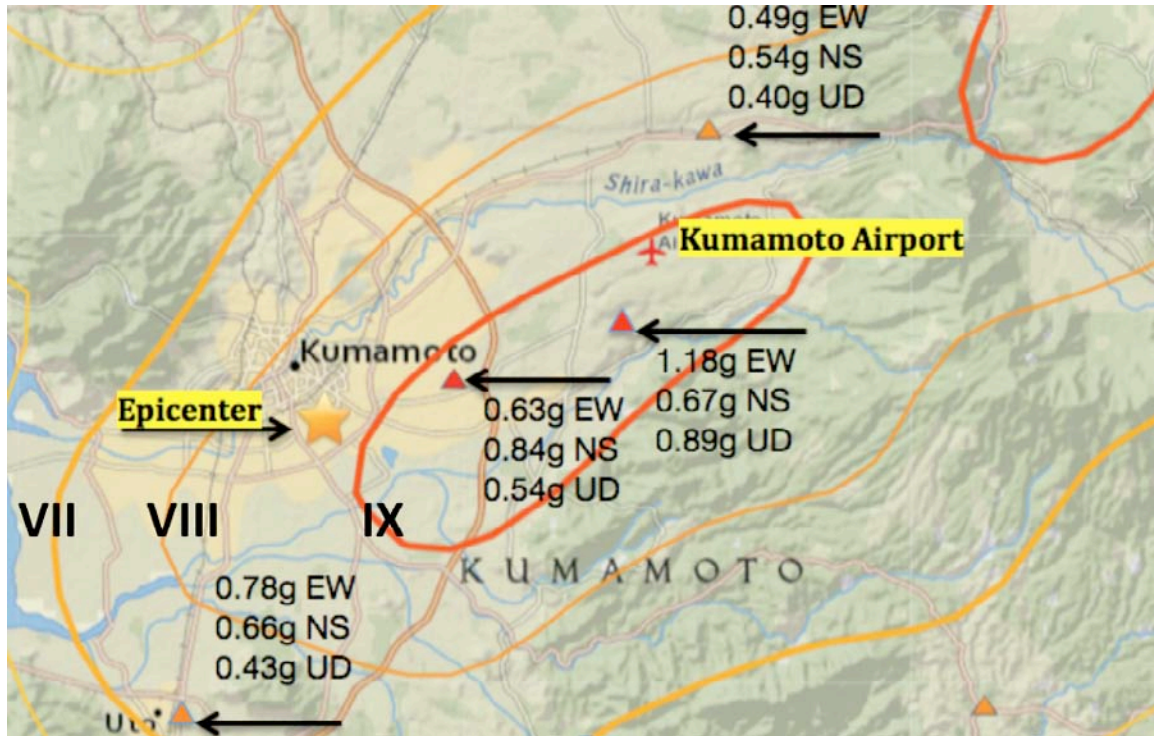


Figure 2-17. Peak Motions at Instruments near Kumamoto Airport

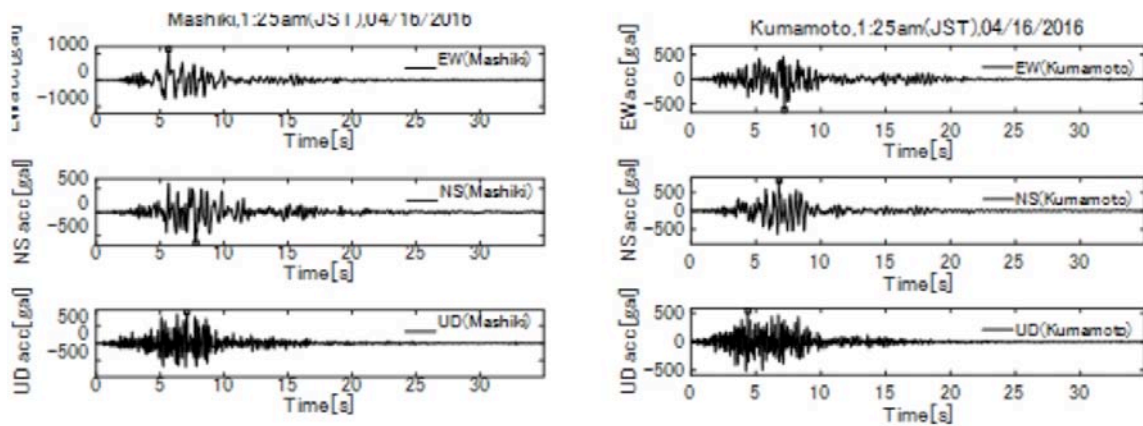


Figure 2-18. Time History Motions at Instruments near Kumamoto Airport (gal)

Figure 2-19 shows the ground motion time histories at Uto City Hall (triangle in lower left of Figure 2-17).

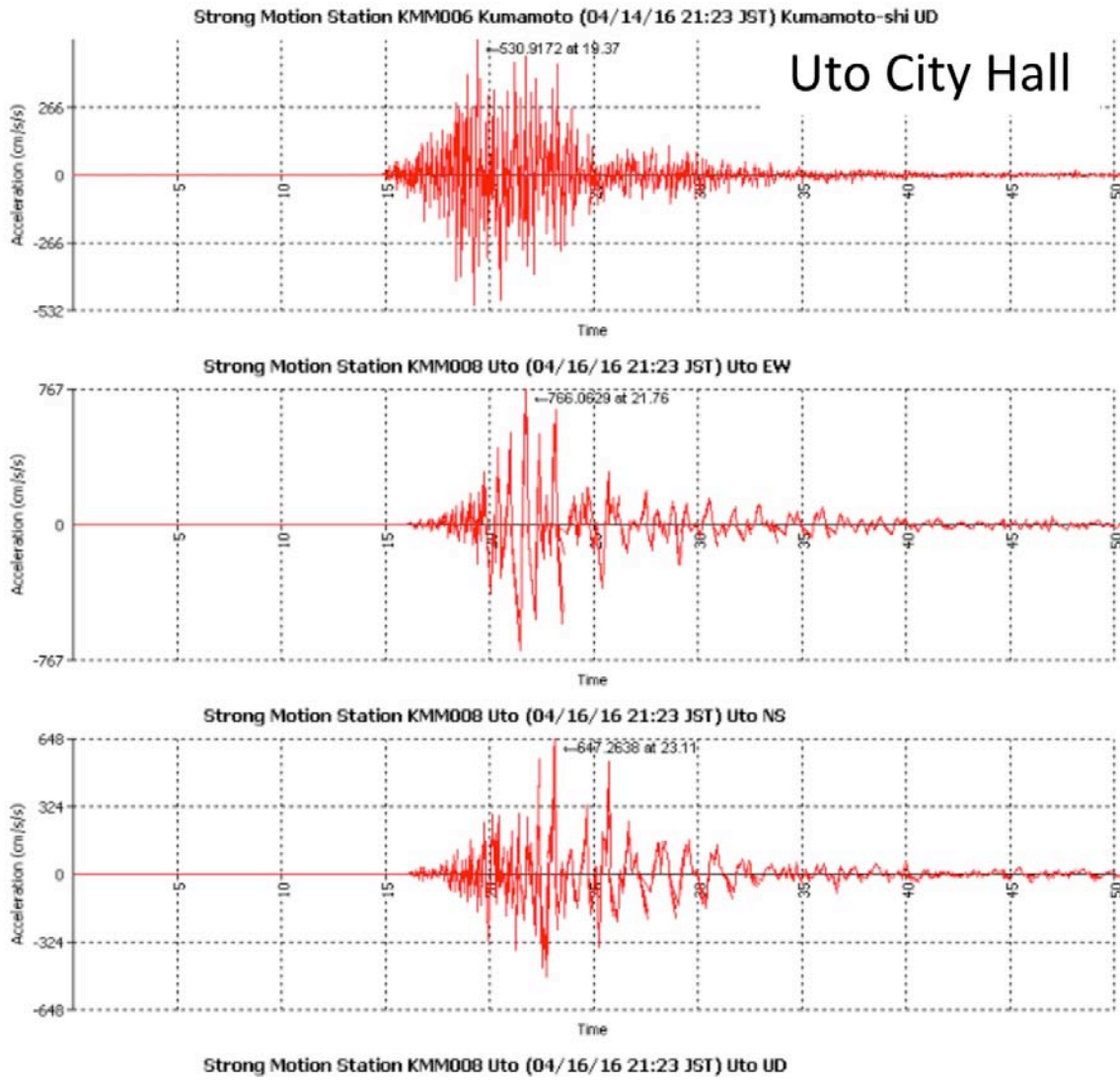


Figure 2-19. Time History Motions at Uto City Hall (gal)

2.3 Landslides

Figure 2-20 shows the north facing slopes in the mountains on the south side of the area marked as "Major Landslide Zone" in Figure 2-4. The mountainside seen in this photo has common slope of about 35°. About 10% of the slopes are denuded of trees, and these are the areas with deep seated slides from the April 16 2016 earthquake. About 10% of the surface area has slid. For the most part, there is little to no infrastructure along this slope. The landslide zones seen are primarily along drainages, but that is not always the case. In the lower and more gentle slopes seen in Figure 2-20, it is not obvious from this photo that landslides occurred; but we did some reconnaissance by foot in those areas, and there were occasional (perhaps 1% to 2% of that area) that did have sufficient debris flows or deep seated slides as to force closure of graded dirt access roads. PGAs in this area were likely 0.4g or higher.



Figure 2-20. Landslides – North Facing Slope

Figure 2-21 shows a major landslide on the east-facing slopes for the mountainside directly opposite to that in Figure 2-20. In the GEER report, this landslide is called the "Great Aso Landslide". PGAs in this area were likely 0.4g or higher. This deep-seated slide destroyed a water flume, a railroad, a 4-lane highway, and undermined a long span bridge causing that bridge to completely collapse. LiDAR imagery of this slope, and adjacent slopes that did not slide in this earthquake, indicate that slides of this nature on nearby slopes have taken place before. The height of this landslide is on the order of 350 meters, the width near the base is on the order of 700 meters across, and the depth of the slide (original ground surface to bare ground observed in the photo) is commonly on the order of 3 to 10 meters. The buildings in the foreground are more than a km from the base of the slide, and while they were exposed to high levels of shaking, they are not severely damaged.



Figure 2-21. Great Aso Landslide – East Facing Slope

Figure 2-22 shows the same landslide seen in Figure 2-21, with the photo taken at about 8:30 an April 16 2016, the day of the earthquake, from a helicopter (courtesy Kyushu Electric).



Figure 2-22. Great Aso Landslide

Figure 2-23 shows the same Great Aso landslide as seen in Figures 2-21 and 2-22, looking northwesterly, from the south side of the bridge that was destroyed.



Figure 2-23. Landslide and Failed Infrastructure – East Facing Slope

In Figure 2-23, we show yellow double-headed lines to indicate the approximate locations of water, rail and highway infrastructure that were destroyed by this landslide. This photo was taken July 2 2016, 10 weeks after the earthquake. Between the "JR railway" and "water flume" yellow lines can be seen a remotely-operated excavator, which is attempting to establish a foothold in the landslide zone in which suitable protection can be constructed, to allow eventual re-building of the railway and highway below. This approach raised some questions, recognizing that at elevations several hundred feet higher, the head scarps of the slide zone appeared to remain subject to further failures; and perhaps that is why the work was being done solely by remote-controlled excavators.

Figure 2-24 shows a failed embankment that formed an at-grade asphalt parking lot for the buildings in the background. The height of this minor man-made slope was perhaps on the order of 15 feet, likely formed by filling a pad without much attention to slope design for earthquake shaking. This slope is located about a hundred feet away from surface faulting, so ground shaking at this site might have been $PGA \sim 0.6g$; the yellow building in the right background was subjected to fault offset.



Figure 2-24. Embankment Slope Failure

Figure 2-25 shows a landslide that undermined a distribution power pole. The level of shaking at this site was likely PGA $\sim 0.6g$. The crest of the slope, prior to the earthquake, was flat, with the pole set back several feet from the steep edge of the slope. The depth of pole embedment was about 6 feet, and the remaining distribution wires on the pole's cross arms prevented the pole from sliding down the slope to the river below.



Figure 2-25. Slope Failure with Distribution Pole

In addition to the deep-seated landslides shown above, there were debris flows. Figure 2-26 shows a mud flow that covered several farming fields.



Figure 2-26. Mud Flow (32.8644° 131.0232°) Courtesy Geospatial Institute of Japan

There were no rock avalanches that we observed. Sections 3 (Electric Power) and 9 (Transportation) provide more photos and discussion of the various landslides that affected the region. The GEER report (see references) provides additional information about landslides.

2.4 Surface Faulting

There were about 28 km of surface faulting along the Futagawa fault. Surface faulting went through the Ohkiriata dam (no release); many roads (with rupture of the asphalt road surface very common) and some highway bridges (with various types of serious damage). In Section 2.4, we do not show all these impacts, which are addressed elsewhere in this report, as well as in the GEER report (2016). Herein, we show a few impacts of surface faulting for the less widely-studied lifelines.

Figure 2-27 shows one of the areas with surface faulting along the Futagawa fault. The heavy red dashed line shows the approximate strike of right lateral faulting, mostly through farmland. The highlighted yellow circle shows an area where surface faulting was close to buildings and other infrastructure.

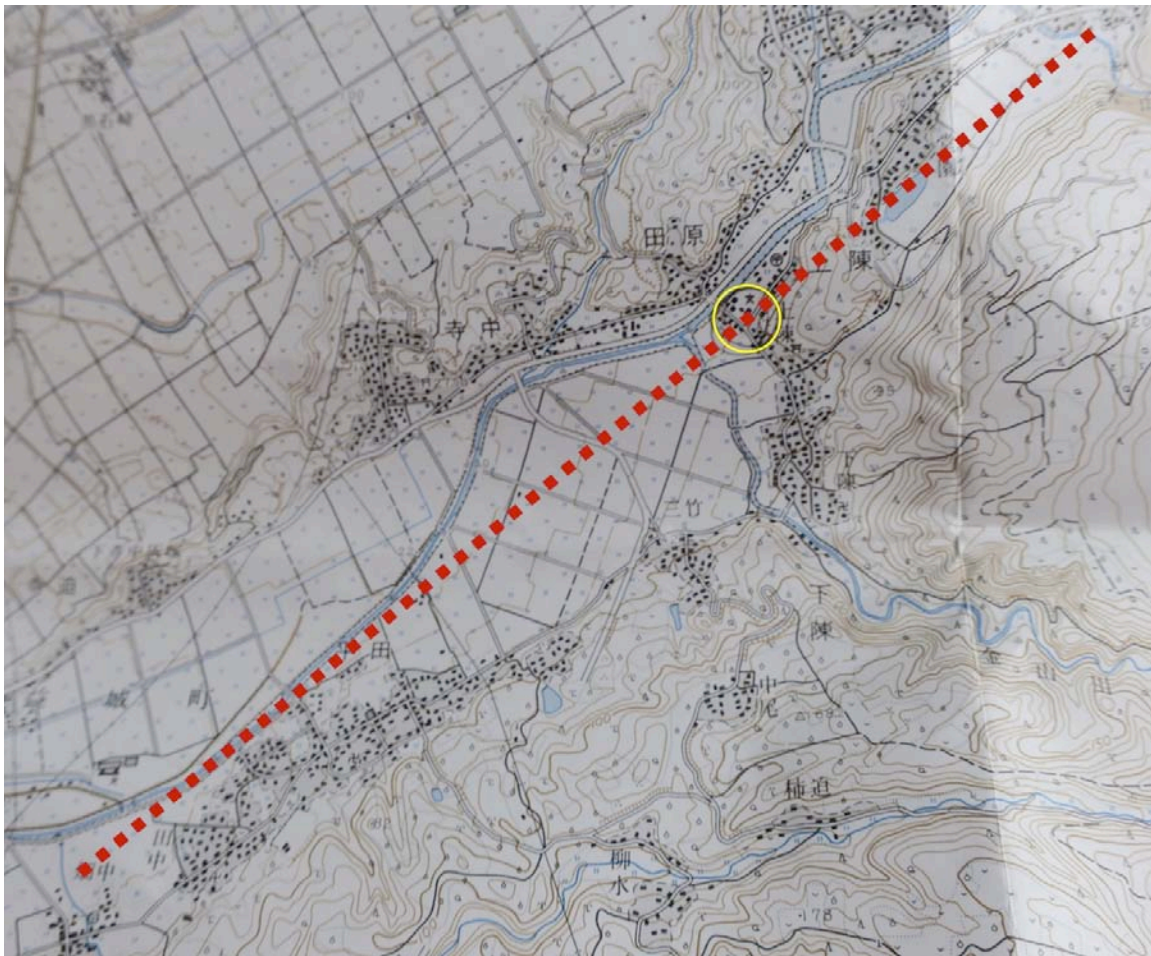


Figure 2-27. Location of Surface Faulting in Farming Area

Figure 2-28 shows where the fault (yellow dashed line) went through a msonary-lined channel used for agriculture.



Figure 2-28. Surface faulting through concrete-lined irrigation channel

Figure 2-29 shows where right lateral surface faulting of about 1 to 2 meters (yellow dashed line, continuing into background along the mole-track towards an open trench where the fault offset was being studied in detail) traversed between two concrete poles. Both poles had been installed in 2013. The pole on the left supports telephone wires; the pole on the right supports distribution voltage (6.6 kV) electric power primary feeder. Figures 2-30 and 2-31 show these same two poles. The base of the telephone pole was in the shear zone of surface faulting, and the pole tilted somewhat as it was attached to the adjacent power pole. As can be seen in Figure 2-31, the two lower level "cross arms" rotated about the poles to accommodate the imposed relative movements between the poles.

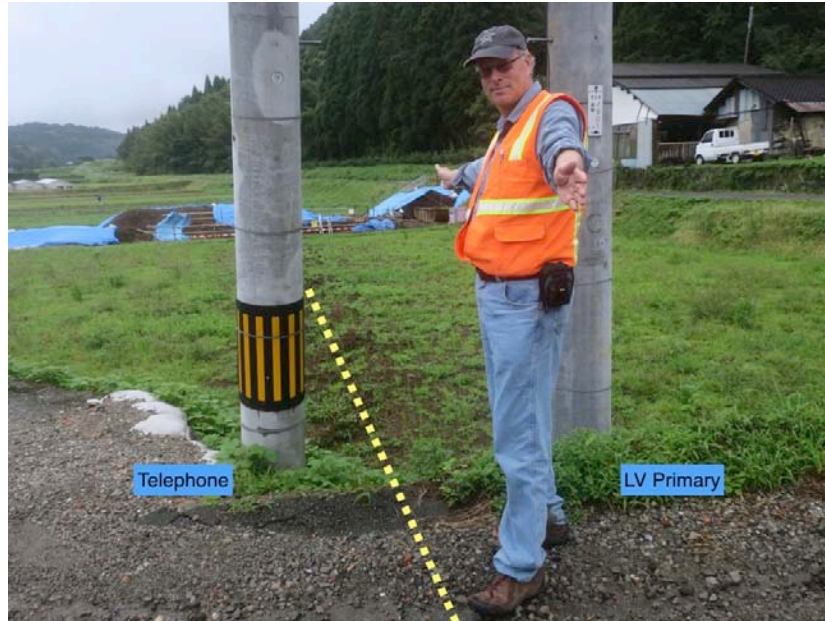


Figure 2-29. Surface faulting near power poles (John Eidinger). Photo taken July 4 2016.

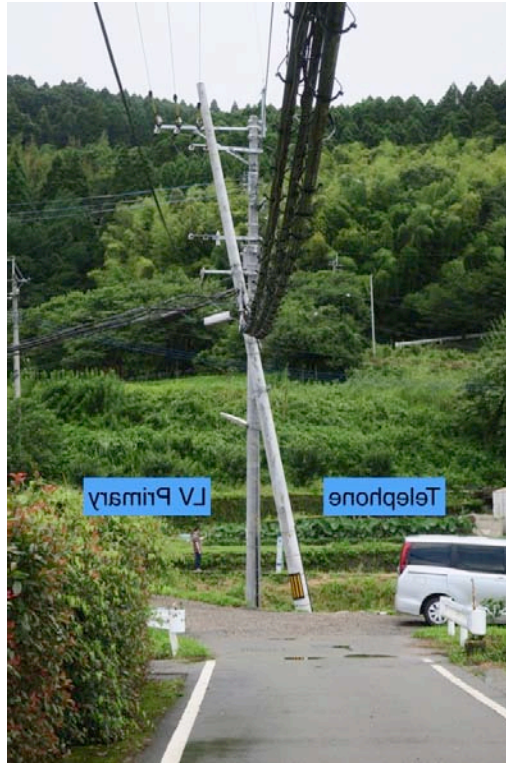


Figure 2-30. Surface faulting near poles



Figure 2-31. Surface faulting impact for telephone and power poles

Figure 2-32 shows the mole track of the surface faulting highlighted by the dashed yellow line in the distance of Figure 2-29. There was about 10 weeks between the time these two photos were taken; this area receives a lot of rain, and the obliteration of the mole track does not take a lot of time.



Figure 2-32. Surface faulting (photo taken ~April 20 2016) (Courtesy Prof. Maruyama)

Figure 2-33 shows a vertical offset of a roadway in Aso Town. This area was subjected to a formation of a graben (see Section 3 for aerial photos of the surface deformations next to some transmission towers). In the GEER report, this zone is characterized as a "Depression Zone". In this report, we use the term "graben". This is not "surface faulting". In the GEER report, it is suggested that this area was over a magma chamber, and possibly the strong ground shaking allow a block of land to sink downwards. Perhaps future examination of the region will be able to further describe the cause(s) of this ground deformation.



Figure 2-33. Graben formation (surface faulting) in Aso Town (Courtesy MLIT)

2.5 Liquefaction

In general, there was not a lot of liquefaction-related ground failures in this earthquake. This was surprising, as much of the area has a high ground water table, and the level of shaking was commonly high enough to trigger liquefaction (PGA commonly over 0.3g).

We speculate that the lack of widespread liquefaction (especially with large permanent ground deformations, PGDs, such as those from lateral spreads) reflects the relatively short duration of strong shaking (under 10 seconds or so), and the geographic layout that put much of the alluvial-style soils in areas where $PGA < 0.2g$ or so. Also, along the main river outlet of the Aso caldera, it is felt that the flat farmland is underlain by layers of soil and volcanic flows, possibly with relatively thin layers of liquefiable materials. In the immediate vicinity of the Caldera, liquefaction phenomena, such as sand boils, were not observed.

Further to the west, and along and within the floodplains, liquefaction phenomena did occur. This was evident in one of the water well fields southeast of Kumamoto City, where pile-supported tanks and wells and buildings did not settle, but the adjacent lands did settle several inches.

A developed land tract surrounded on two sides by rivers was protected by levees, Figure 2-34. This area had many instances of liquefaction that damaged perhaps 25% of all the houses in this area, as outlined in Figures 2-35 to 2-38.



Figure 2-34. Island Subjected to Liquefaction (Photo Taken Prior to Earthquake)

Figure 2-35 shows the levee on the north side of this area, with the photo taken looking westwards from the northeast corner of the area. The plastic bags on the right side of the photo have been placed, post-earthquake, at the high level of the levee, to provide protection from rising flood waters; the top of the levees have displaced vertically downwards by liquefaction.

The houses in this area do not appear to have suffered much direct damage, as they are on piles. However, there is considerable damage in the transition zones between the houses and the native soils, such as to driveways, Figure 2-36. Houses in this area obtain gas using small propane tanks attached to the outside walls of houses, Figure 2-37; in this photo, the twin tanks appear to have had no damage, and they are supported on a small concrete pad extension off the main house, also on piles.



Figure 2-35. Levee Protection, North Side of Island



Figure 2-36. Driveway damaged by liquefaction



Figure 2-37. Differential settlement between pile supported house and propane tank pad and driveway (Prof. Shoji)

Figure 2-38 shows a house in this liquefied region. The power pole in the foreground is tilted, and remains in service as of the day this photo was taken (July 4 2016), with the small yellow notice on the pole stating: "this pole will be repaired". Several other power poles were similarly tilted (typically up to 5°) in this area, but none collapsed; excessive tilt did result in some slack issues, and the authors presume these had already been repaired as most houses were then occupied and had power.



Figure 2-38. Tilted Power Pole

2.6 References

GEER, Geotechnical Aspects of the 2016 Mw 6.2, Mw 6.0 and Mw 7.0 Kumamoto Earthquakes, Version 1.0, July 2016 (available at www.geerassociation.org).

3.0 Electric Power System

Section 3 describes the performance of the electric power system.

- Section 3.1 provides an overview of the performance.
- Section 3.2 provides an overview of the power grid serving the Kumamoto area.
- Section 3.3 describes the damage to transmission towers.
- Section 3.4 describes the damage to high voltage substations.
- Section 3.5 examines the damage to low voltage distribution.
- Section 3.6 describes emergency response and recovery of the power system.

3.1 Overview

The Kyushu Electric Company provides generation, transmission and distribution electric power service for the entire Kyushu Island, including the entire area affected by both the fore shock and main shock earthquakes.

Kyushu is the fourth largest electric company in Japan. Kyushu Electric serves an area of 42,200 square kilometers. Kyushu's system includes about 942 km of 500 kV and 1,708 km of 220 kV transmission lines. Annual power sales between 2011 and 2015 has varied between 79 to 85 terawatt hours. Peak demand in Kyushu is about 16.5 gigawatts.

Kyushu owns and operates two nuclear power plant sites, both situated far from the epicenters. The Sendai nuclear generating station was operating at the time of the earthquakes. The Genkai nuclear power generating station was not operating at the time of the earthquakes. The highest recorded ground motions at these nuclear power plants was PGA = 0.03g (Sendai) or PGA = 0.02g (Genkai). Neither station suffered any damage.

Figure 3-1 shows the power outage and restoration curve.

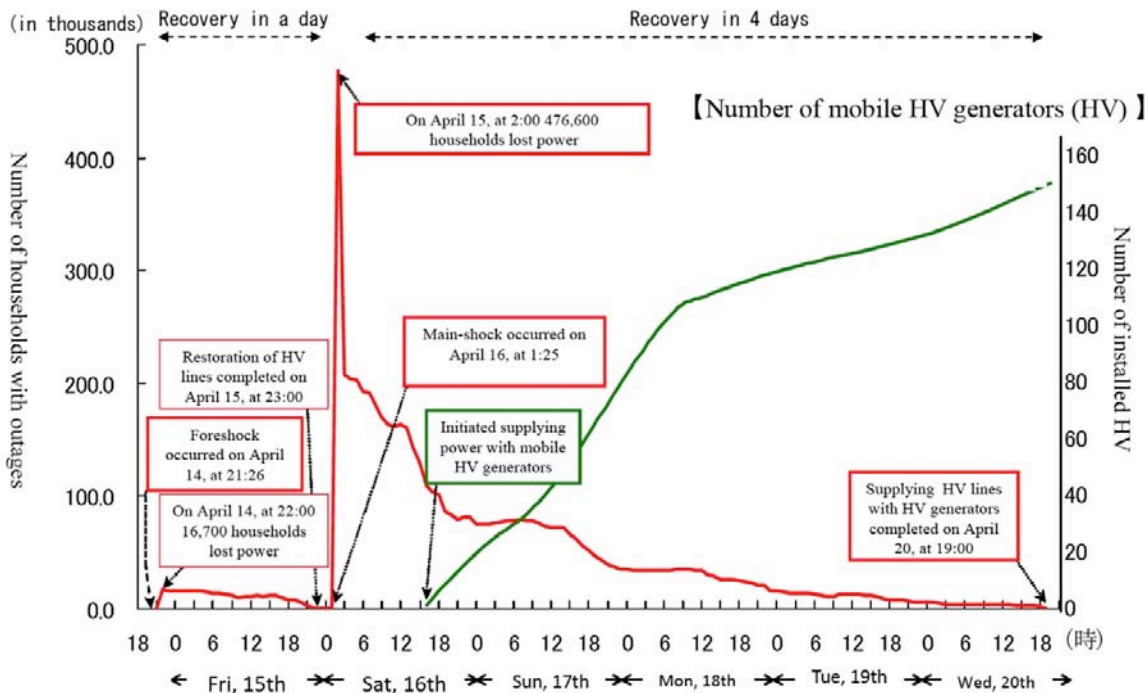


Figure 3-1. Electric Power Restoration

On Thursday April 14 2016 at 9:26 pm local time, the fore shock occurred near Mashiki Town. This led to power outages that affected, at its peak, 16,700 households (1 household = 1 billing account).

On Saturday April 16 2016 at 1:25 am local time, the main shock occurred. This resulted in loss of power to as many as 476,000 households, the greatest single power outage that had ever occurred to Kyushu Electric.

The restoration effort by Kyushu Electric involved more than 4,000 personnel, including 2,185 personnel from Kyushu Electric Company, 1,424 personnel from contractors and 629 personnel from other Japanese electric power companies. The work provided to be very challenging due to factors such as landslides and damaged roads.

A variety of damage occurred to the electric power system, including damage to high voltage equipment at substations; damaged transmission towers due to landslides, damaged distribution poles primarily due to building pull-downs, landslides, damaged water flumes, penstocks and hydroelectric power plants. In areas that lost transmission capability totally, as well as in towns that had a lot of distribution feeder damage due to pull downs, medium-sized portable emergency generator sets were brought in to re-energized distribution circuits that were able to receive power; at its peak during the restoration process, 169 emergency generators were in use. It took until Tuesday April 20 (4 days post earthquake) to install these emergency generators throughout the service area, and thus restore power to all customers able to receive power on distribution feeders that were not otherwise damaged.

Kyushu Electric has the following count of damaged facilities:

- 9 hydro electric power plants. Includes damage to headrace channels (flumes) due to landslides.
- 27 transmission lines. Includes damage to two four-legged towers due to landslide, damage to other towers due to the formation of grabens, permanent offset of insulators leading to faults of phase-to-ground due to changes in conductor slack due to tilted towers due to landslide; damage to string insulators.
- 10 substations. Includes damage to transformers, disconnect switches, and other equipment at 220 kV yards.
- 259 distribution feeders. Includes damaged, collapsed or tilted distribution poles, breakage and twisting of cross arms, wire entanglements.

A total of 31 transmission towers and transmission poles were installed after the earthquake, in order to bypass towers that had been damaged in the earthquake. Two transmission towers were tilted due to landslides that undermined their foundations. Several other towers were exposed to ground deformations due to surface faulting / formation of grabens in the Aso crater area. Two new tall transmission towers (4 –legged steel lattice type) were installed by April 27 (11 days post-earthquake) to allow bypass of the towers affected by the landslides, and the remaining smaller towers were later installed.

As of writing this report, the final count of replaced distribution poles remains uncertain, but likely on the order of several hundred. Of these, the largest majority were replaced or repaired due to pull down actions caused by partial or full collapse of adjacent buildings; a few were replaced due to landslides or surface faulting effects. Poles in liquefaction zones were tilted or dropped, and likely could be repaired to vertical orientation as part of long term restoration of these areas.

In the area with strong shaking ($PGA > 0.1g$ or so), Kyushu operates essentially no buried high voltage power cables (60 kV or higher) except for a few cables within substations.

In the area with strong shaking ($PGA > 0.1g$ or so), Kyushu operates no buried low voltage power cables (commonly 6.6 kV to 25 kV). Essentially all distribution is done via primary and secondaries that are supported by concrete poles.

The power restoration curve in Figure 3-1 shows all households with restored power by Wednesday April 20, 4 days after the main shock. The time needed by Kyushu Electric to restore the entire electric system to its pre-earthquake condition and reliability was much longer. By 2.5 months post-earthquake, the following significant efforts remained ongoing:

- About 29 to the 31 replacement transmission poles has been permanently installed, but it was planned to further reconstruct the two largest replacement lattice-type towers with permanent foundations.
- Hundreds of distribution poles (and related overhead equipment) needed to be replaced, with the timing to coincide with the reconstruction of the damaged adjacent buildings. This was particularly true in the lower elevations of Mashiki Town, where ground failures (small slope slips and lateral spreads into the lower area farming region) and strong shaking seriously damaged or collapsed many buildings. The time frame to complete this effort might be a year or longer.
- Water flumes, and penstocks bringing water to small hydro power plants remained to be repaired. The time frame to complete this effort might be a year or longer.

3.2 The Power Grid

Figures 3-2 and 3-3 show the main transmission lines serving the Kumamoto and Mount Aso region. The heavy black lines denote 500 kV transmission lines (all transmission is AC in this area). The medium-thickness black lines denote 230 kV transmission lines. The thin black lines denote 66 kV sub-transmission lines. Small open circles are substations. Small open rectangles are generation power plants (all hydro electric in the Mount Aso area). Small rectangles with black-and-white triangles are thermal (fossil fuel) generation power plants. The background colors are the JMA intensities for the foreshock.

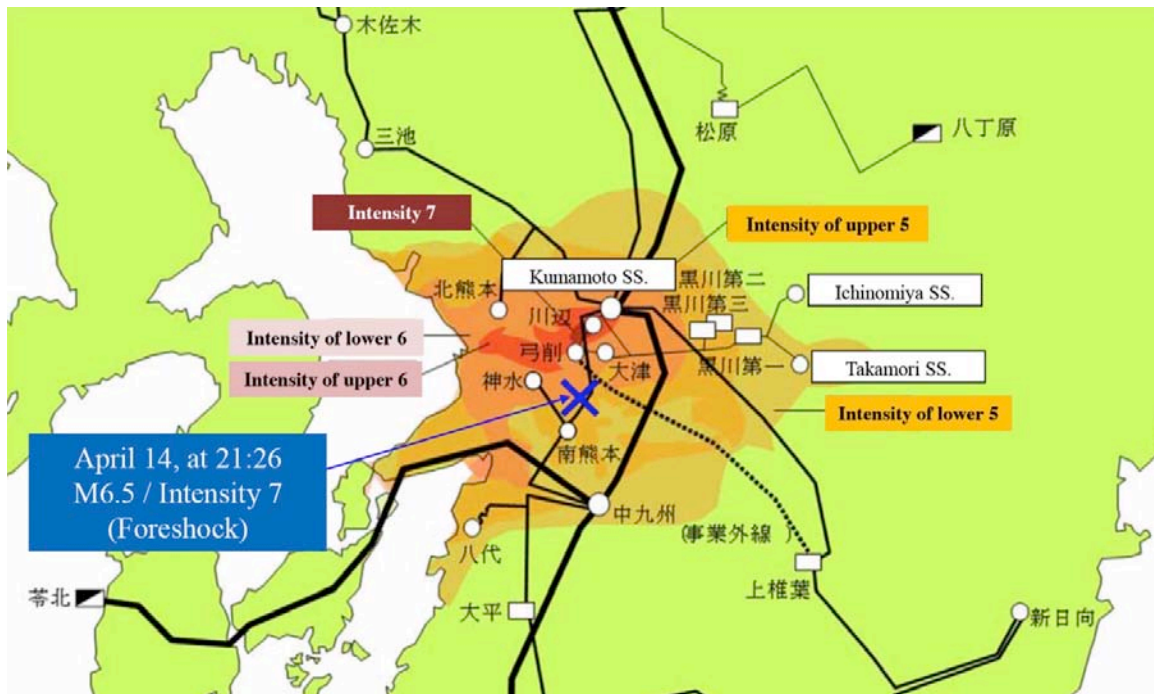


Figure 3-2. Power Grid in Kumamoto and Mount Aso Region, Fore Shock

Power to the Mount Aso region is supplied via 66 kV transmissions along a west-to-east corridor, and then split into two 66 kV alignments, one ending at the Ichinomiya 66 kV substation, and the other ending at the Takamori substation.

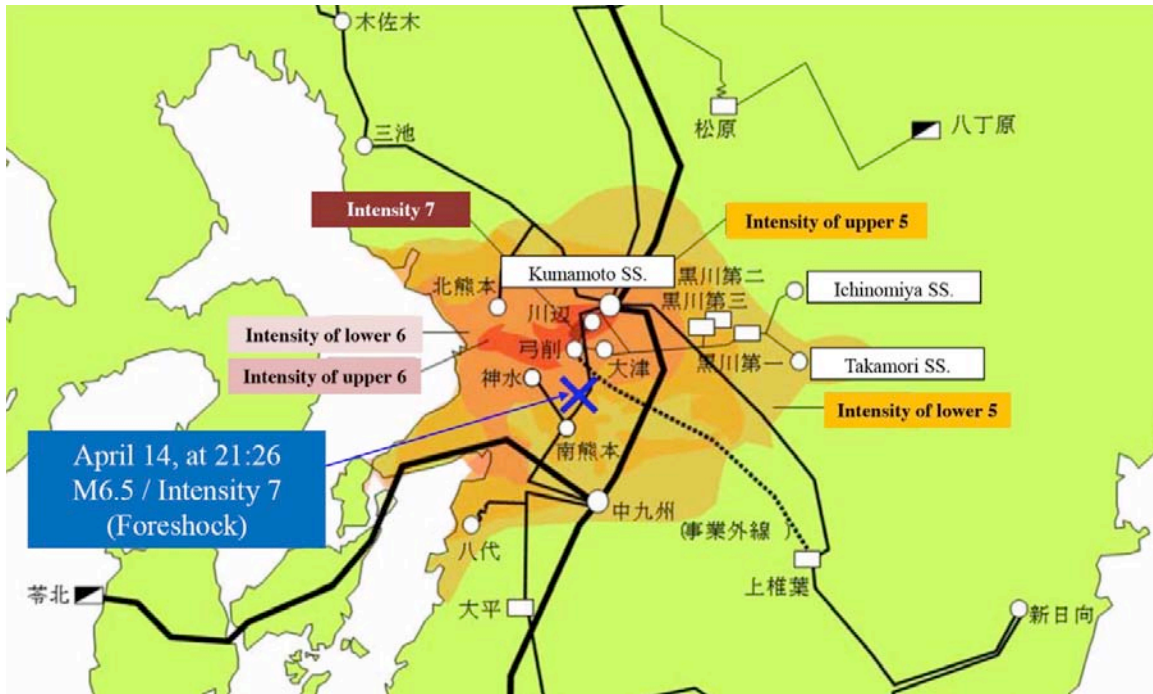


Figure 3-3. Power Grid in Kumamoto and Mount Aso Region, Main Shock

3.3 Landslide Damage to Transmission Towers

Figure 3-4 shows an aerial photo of the large landslide near the Mount Aso caldera (center rear of the image), along with the towers (small black icons) and 66 kV transmission lines (white lines) of the affected transmission lines. The numbers (No. 5, No. 6, etc.) shown in Figure 3-4 are used in this section to identify individual towers.

In this section, we describe the landslide impacts for Towers No. 7 and No. 2, both of which were tilted due to landslide deformations at the base of the towers. We also examine the damage to Towers No. 5, 6, 8, 9 and 10, as well as some other towers affected by ground deformations.

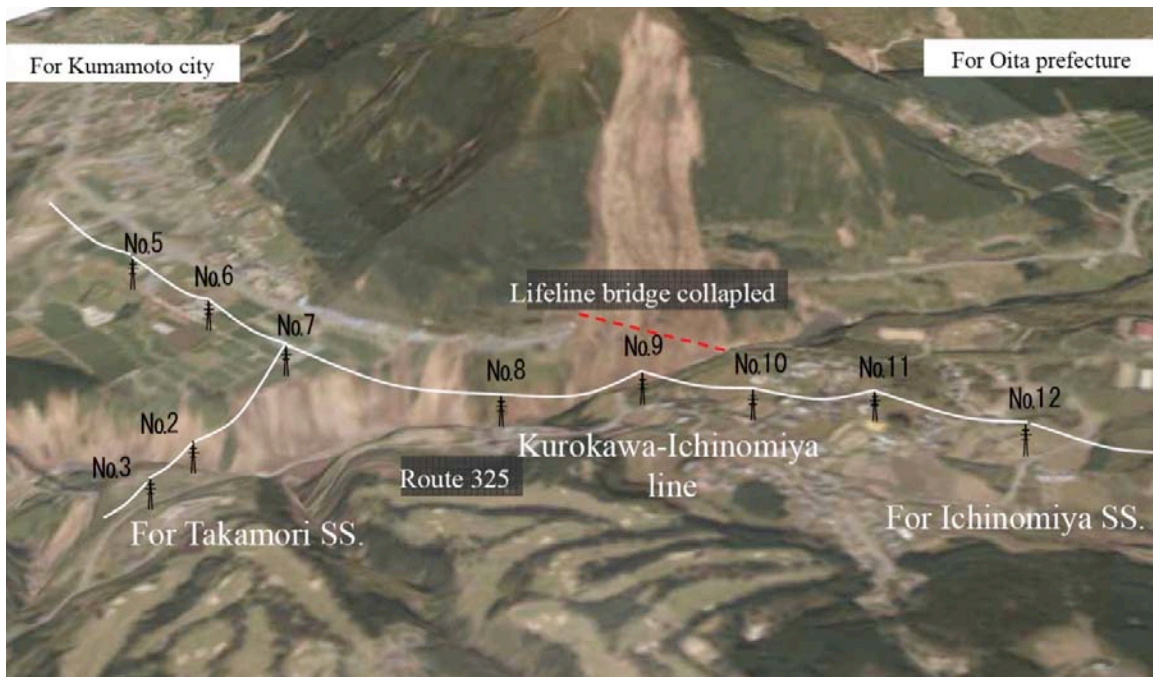


Figure 3-4. 66 kV Transmission Lines Near Major Landslide

Figure 3-5 shows a higher resolution photo of this area, looking north. The light grey coloring along the river embankments show that perhaps 75% to 90% of the all these slopes along the river edges in this area suffered landslides. The triple green lines schematically indicate the conductors between the towers; in fact, each tower supports two circuits, or six phases total, plus two static wires.

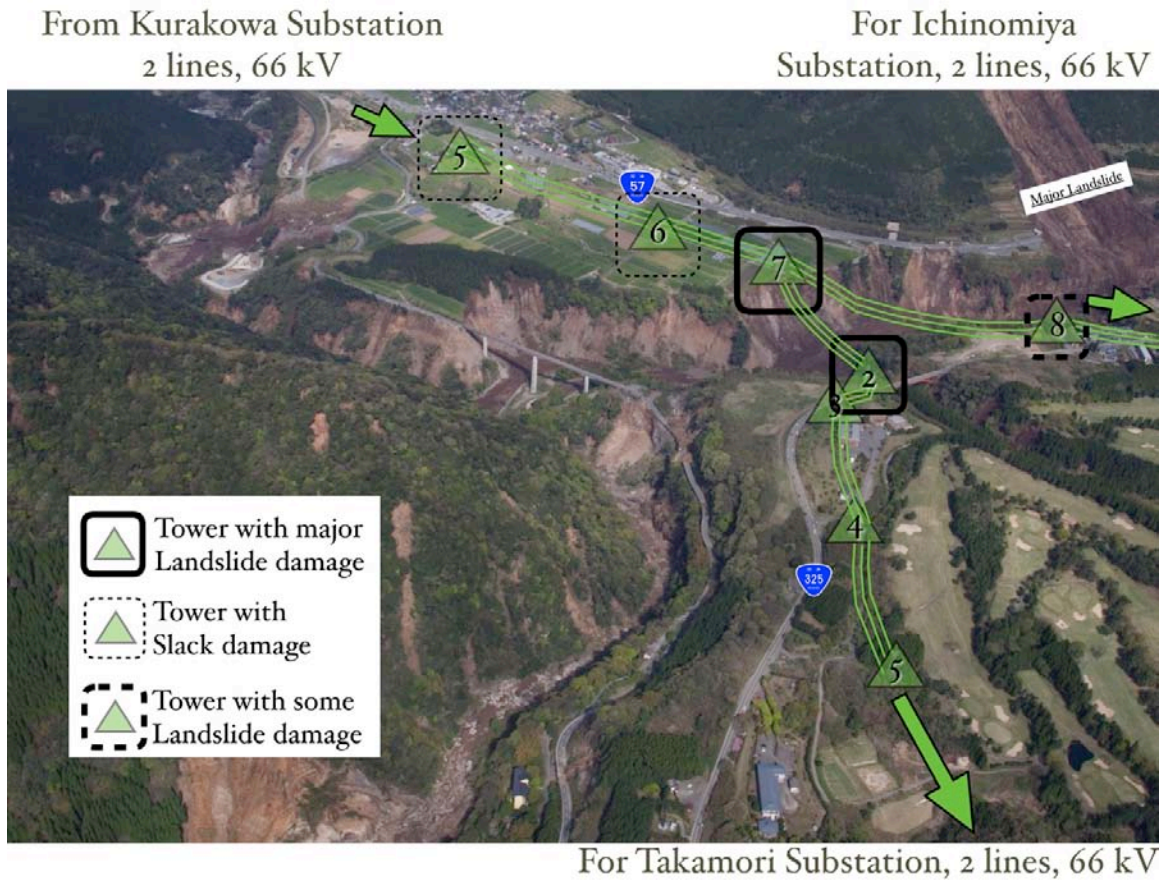


Figure 3-5. 66 kV Transmission Lines Near Major Landslide

Figure 3-6 shows Towers 7 and 6, with the photo taken at 8:21 am local time on April 16 2016 (as soon as the sun came up the day of the earthquake), looking west. The landslide head scarp is clearly seen at the base of Tower 7. The four lane expressway to the right has no cars on it as the road has failed at the Major Landslide location, just to the right (east) of this photo.

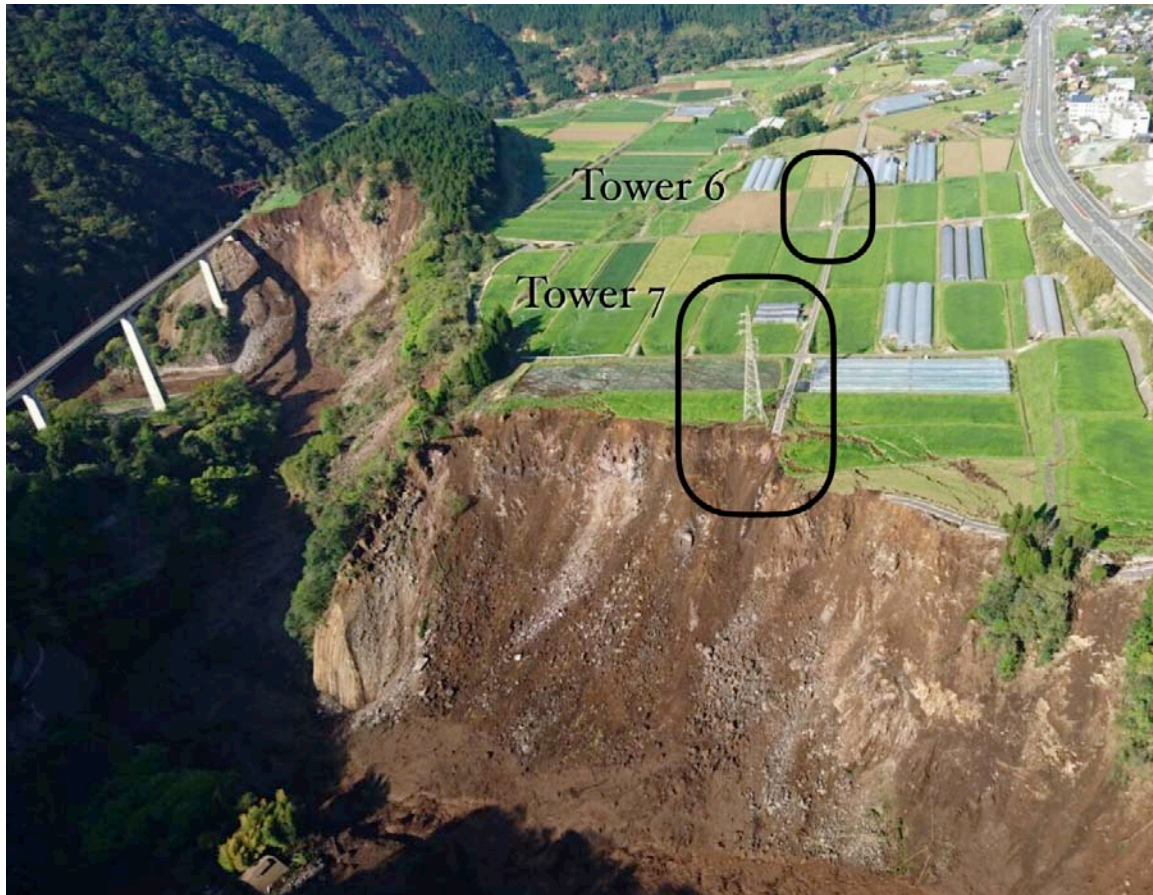


Figure 3-6. Towers No. 6 and No. 7

None of the towers in Figures 3-4, 3-5 or 3-6 collapsed outright. However, several were damaged due to landslide movements, due to changes in cable slack, or due to strong inertial shaking, and the following text describes what happened.

The Major Landslide seen in Figures 3-4 and 3-5 was on the north side of the river channel, and the debris from that landslide did not directly impact any transmission tower. Towers No. 2 and No. 7 were located in flat ground, and before the earthquake they were within 30 feet or so of the steep slopes of the river channel. Landslide motions of these steep slopes that affected these two towers, with the result that both Towers 2 and 7 tilted towards the river.

Figure 3-7 shows the "temporary" realignment and new "temporary" towers that were constructed in the weeks after the earthquake. The 8 replacement towers in this area are

numbered Towers 1-1, 1-2, 2 (new), 3-1, 6-1, 4-1, 5-1 and 5-2. These are called "temporary", in that their foundations were installed as rapidly as possible, in order to restore power as quickly as possible; it is Kyushu Electric's intention to later replace these structures with permanent installation.

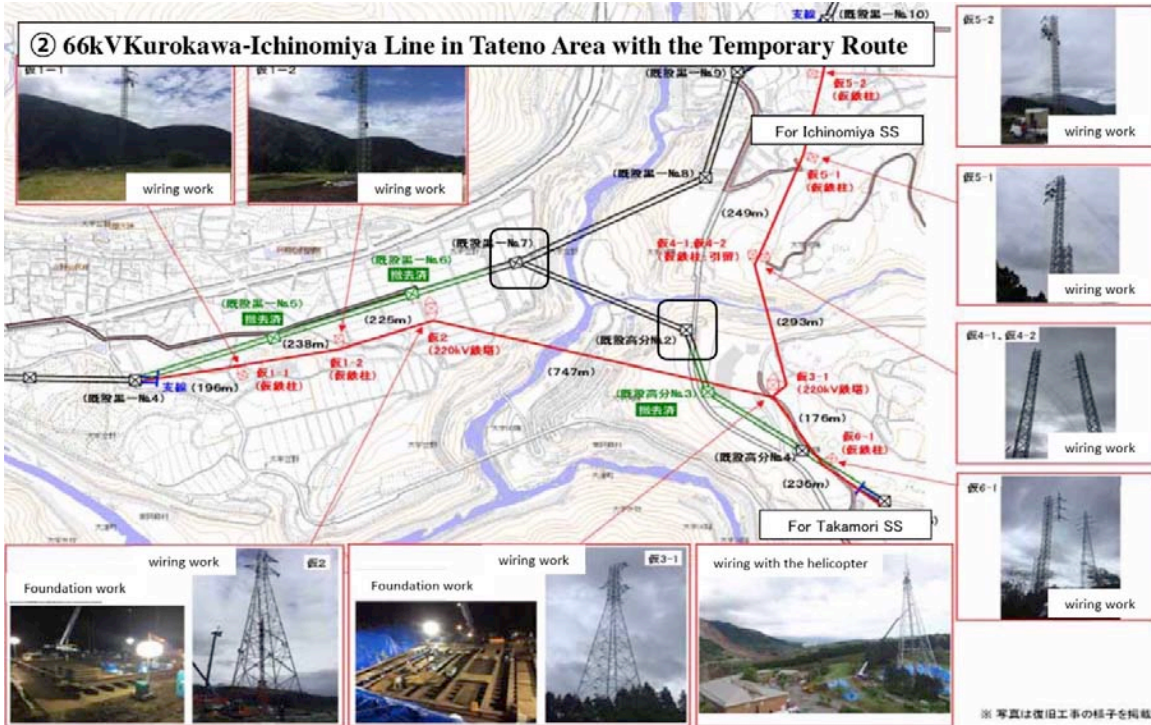


Figure 3-7. Replacement Towers

Towers No. 5 and No. 6 were four-legged suspension towers. When Tower No. 7 tilted towards the river, the tilt "used up" the slack in the conductors, and the suspension string insulators on Towers 5 and 6 tilted severely towards tower 7. The severe tilt of these string insulators resulted in the initial phase-to-ground fault that was the apparent electrical reason why power was lost to the Ichinomiya and Takamori substations.

Figure 3-8 provides further detail as to damage of transmission towers in the Mount Aso region. The data in Figure 3-8 total 16 temporary towers were used to bypass the damage; the final count, according to Kyushu Electric, was 31 towers. Near Matoishi, the text "extensive cracks" refers to the ground failures in the graben zone,

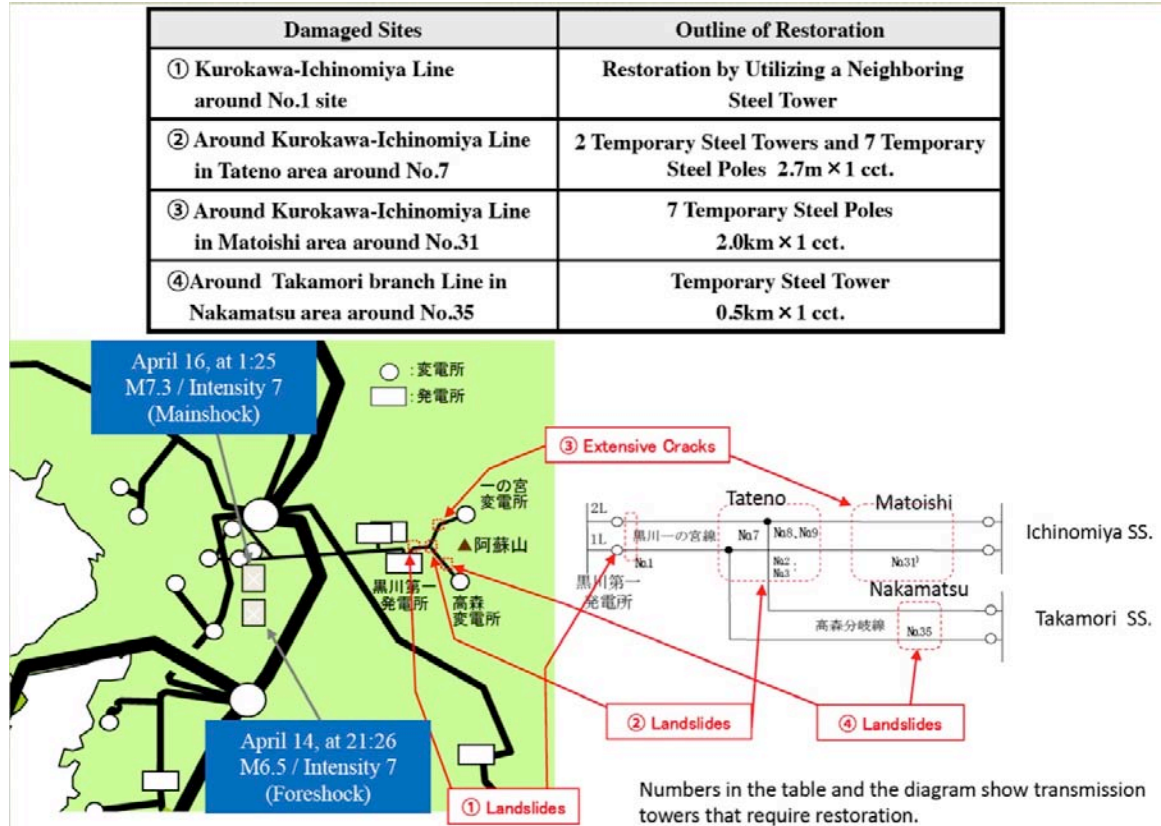


Figure 3-8. 66 kV Transmission Lines Affected by Ground Deformations

Figure 3-9 shows the original Tower No. 7 (in black box in foreground) along with the temporary replacement "New Tower 2" and two New Poles 1-2 and 1-1. This photo was taken 10 weeks post-earthquake. In the background, original Tower No. 4 remains in service. In the foreground, as further highlighted in Figure 3-6, the landslide into the river is clearly observed. To the right (north) of the old Tower 7, the remnants of a narrow asphalt road can be seen, with much of that road having slipped into the river below. The Old Tower 7 remains standing, with two legs still in "somewhat stable" ground, and the two legs closest to the river in precarious condition. This tower was originally situated some 30 feet or so away from the steep embankment. Other than perhaps this prudent setback, Kyushu Electric engineers reported that no special precaution was taken for landslide hazards in the design of their towers. While the four main legs (heavy angles, common 7x7x0.625 inch used for strain towers in this area) remain intact, the river-side foundations appear to have dropped about 2 to 4 feet, and the landward-side foundations have displaced about a foot. Due to ongoing access restrictions to this area, the author was not able to get to the base of Tower No. 7. In this photo, the old Towers 5 and 6 have already been removed.

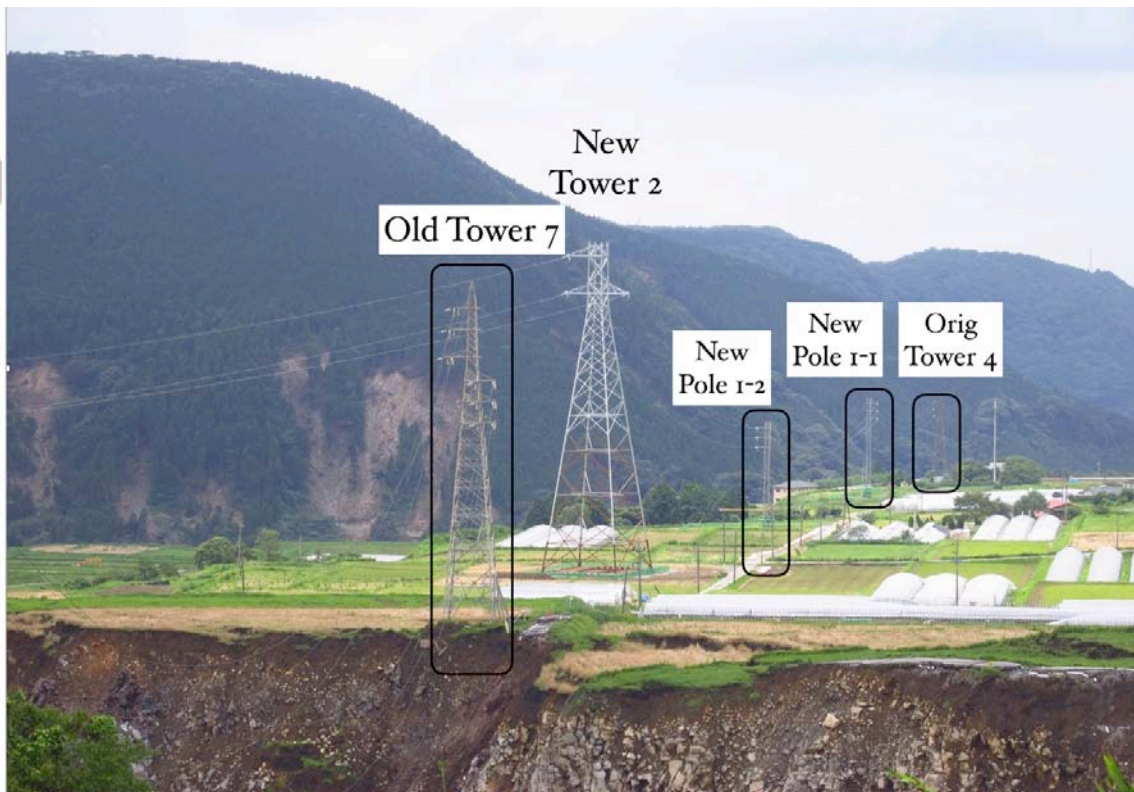


Figure 3-9. Towers 4, 5, 6, 7

The "New Tower 2" was constructed in emergency mode. This New Tower 2 is a standard 220 kV tower used elsewhere in the Kyushu system, with heavy tubular-type legs. The need to rapidly construct the New Tower 2 required Kyushu to use a steel grillage-type foundation, and no new concrete foundations were installed in order to shorten the post-earthquake installation time. It is Kyushu's intent to eventually replace

this New Tower 2 with a permanent tower. Note that for the replacement towers, the double circuit was modified into a single circuit, also to shorten the installation time.

Figure 3-10 shows the tilt on the suspension insulators of Tower 5. New Poles 1-1 and 1-2 were installed in part to make the transition from a double circuit at Tower 4 to the single circuit at Tower 2, and part due to the swinging of the insulators on both Towers 5 and 6.



Figure 3-10. Tower 5 with Suspension Strings Displaced due to Tilt of Tower 7

For moderate amounts of ground deformations due to landslides, 4-legged towers have some capability to remain in service. If the landslide deformations are on the order of up

to 1 foot, most such towers will remain standing and remain quite serviceable, although with some reduced margin against high winds or ice loads. If the landslide deformations are on the order of 2 to 4 feet, many such towers will remain standing and possibly remain serviceable, although there can be major damage to secondary members. In landslide zones, it would be rare to have a four legged tower have each leg "tied together" at the foundation level, and it is unclear if this type of mitigation would help rather than hinder, as it would depend on the actual PGD pattern in the specific landslide, which is generally very hard to predict.

Figure 3-11 shows Tower No. 8, on the opposite side of the river from Tower No. 7, for the lines to Ichinomiya.



Figure 3-11. Old Tower 8

Tower 8 is a strain tower, with two 66 kV circuits. This photo was taken 10 weeks after the earthquake, and the conductors between Towers 7 and 8, and 8 and 9, remain strung, but no longer in use. The two conductors in the left foreground are not guy wires attached

to Tower 8, but are conductors for low voltage distribution and coaxial cables supported on distribution poles that are located outside the view in this image. Old Tower 7 and New Tower 7 are seen in the background.

Figure 3-12 shows the superstructure for Tower 8, and visibly, it remains in good condition with no obvious deformations.



Figure 3-12. Old Tower 8

Tower 8 was exposed to some landslide deformations at its foundation. Figure 3-13 shows the ground deformations for the two legs closest to the river. The ground deformations were on the order of a foot. The primary legs are steel angles, attached to another steel angle that is embedded in a circular concrete pier-type footing. The cracked concrete pads around the circular pier, as well as the concrete pad under the tower, are often used to provide a clean area and avoid vegetation growth directly beneath the tower, and in of themselves, are not part of the structural system; the imposed PGDs have cracked these unreinforced concrete slabs. Tower 8 exhibited no buckled primary or secondary members, even though the PGDs imposed on the foundations have imposed a high level of force within the tower steel superstructure. Kyushu elected to abandon this

tower post-earthquake, owing to its location in a landslide zone; it would seem that this tower could be eventually removed and re-used at some other location.



Figure 3-13. Old Tower 8 Foundation

Figure 3-14 highlights the precarious situation for Tower 2, with the photo taken 9:30 am April 16 2016. The landslide has damaged Tower 2 as well as displaced the abutment for the adjacent arch bridge,



Figure 3-14. Old Tower 2 (foreground) and Old Tower 3 (background right)

Figure 3-15 shows Tower 2, with the downed conductors (left side of photo) being those that spanned the river chasm from old Tower 7. Tower 2 is located on the south side of the river. This photo was taken 10 weeks after the earthquake. This is a strain angle tower.



Figure 3-15. Old Tower 2

Figure 3-16 shows the base of the Tower 2, highlighting the direction of landslide movement. One can see that the main compression leg angle member in the left foreground is "kinked" out of alignment below the first bracing level. Like Tower 8, the foundations are circular concrete piers; unlike Tower 8, there is no concrete slab at the base of this tower. The PGDs are on the order of 1 foot down and 2 feet sideways, with the soil between the 4 legs moving towards the river, and the concrete footings at the four legs serving to quasi-reinforce the soils locally. The tower, in its post-earthquake condition, has undergone major internal stress redistribution, and the dead weight of the tower is no longer nearly-equally supported by the four legs.

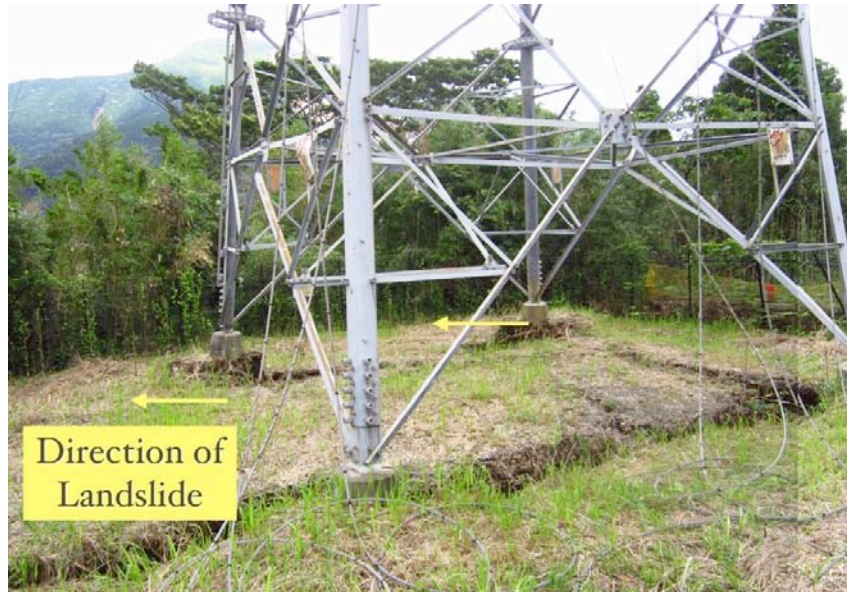


Figure 3-16. Old Tower 2 Foundation Level

Figure 3-17 shows a close-up of the tower leg in the background of Figure 3-16. The internal framing of the tower is apparently acting to resist the lateral movement of the pier foundation. This results in high tensions in some of the diagonal elements, which have to be resisted elsewhere by compression, as evidenced by the buckle in the secondary member seen in Figure 3-18.



Figure 3-17. Old Tower 2 Ground Deformation



Figure 3-18. Old Tower 2 Buckle in Secondary Member

Figure 3-19 highlights a disconnected connection at the first panel point for Tower 2. It is possible that this bolt failed due to the severe leg distortion, and this was the condition of the connection at 850 am April 16, 2016, when crews first approached the tower from the ground. There were two other connections in the secondary bracing for the lower panel that were similarly disconnected. The missing bolts (there were several missing bolts connecting the secondary members for this tower) were not observed when the tower was inspected 10 weeks after the earthquake.



Figure 3-19. Old Tower 2 Unbolted Connection

Figure 3-20 shows an aerial view of Towers 8, 9 and 10, looking towards the east. The major landslide that undermined the railway and freeway is on the lower left of this photo, and the collapsed bridge was previously located near Tower 9 (the bridge debris fell into the river below and is not visible in this photo).

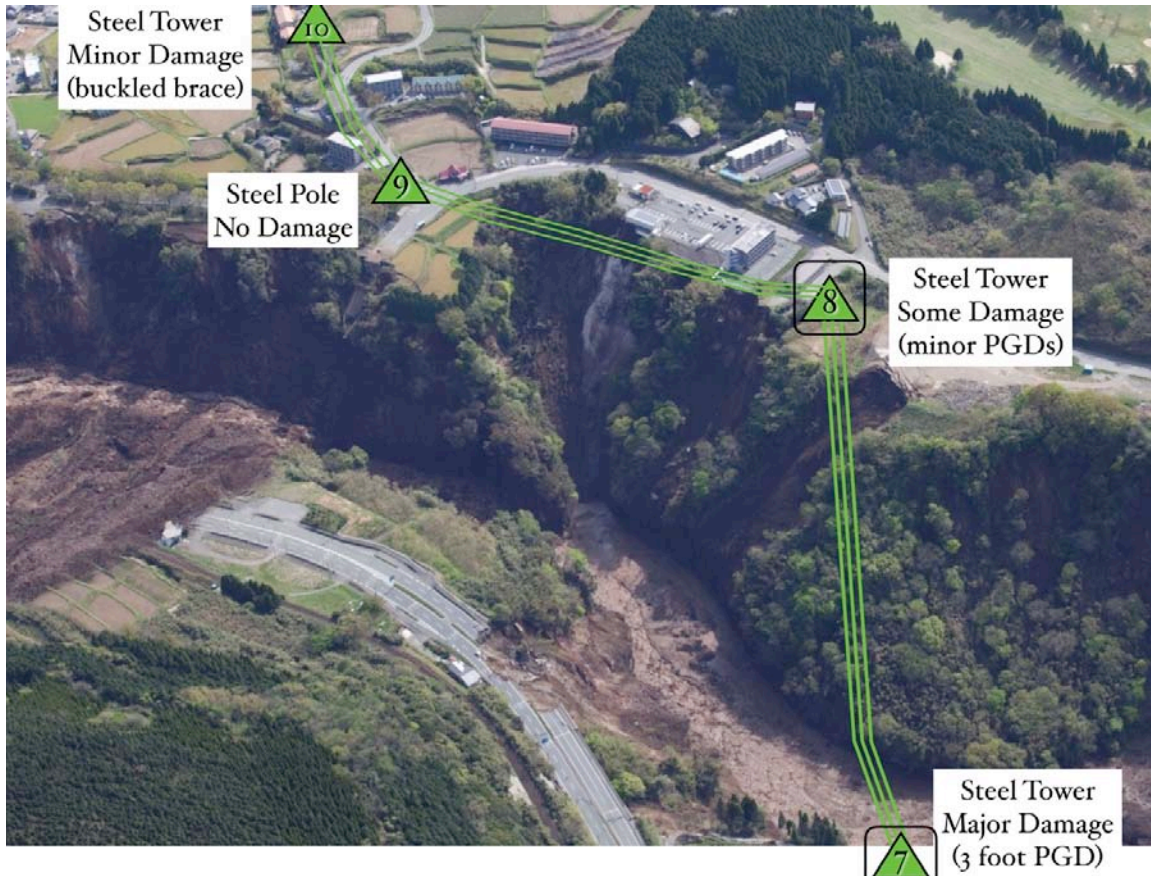


Figure 3-20. Old Towers 9 and 10

Figure 3-21 shows the steel pole, Tower 9. This pole was exposed to very high levels of ground shaking, likely in the range of PGA ~ 0.5g to 0.6g. We examined this pole carefully, and could see no sign of steel yielding, buckling or joint slippage. This pole did not appear to have been exposed to any PGDs.



Steel Pole 9
No apparent yielding

Figure 3-21. Tower 9 (Steel Pole)

Figure 3-22 shows Tower 10, a four-legged lattice steel strain tower. As with Tower 9, it was exposed to very strong shaking. We observed no obvious evidence of PGDs at the tower base. A secondary member in the lower panel was buckled, but the tower was otherwise without obvious permanent deformations.



Steel Tower 10
Buckled Brace



Figure 3-22. Tower 10 (Buckled Secondary Brace)

Figures 3-23 and 3-24 show Towers 30 and 31 (see Figure 3-8 for location within the network). These photos were taken at about 9:30 am April 16 2016.

These towers are located a few km to the east of Tower 10. In this area, a graben formed, and evidenced by the ground cracks and pooling of water at the lowest elevation of the newly formed graben. Professor Kaz Konagai has written a detailed report on the ground deformations for this graben, and it is his initial observation that this ground failure is not surface faulting, but rather caused by some underlying feature in the volcanic caldera that was moved by the strong shaking at this location, possibly on the order of $PGA = 0.3g$ to $0.4g$. The tower legs for Tower 30 were exposed to PGDs of about 1 to 2 feet, and the tower remained structural sound. As a precaution, Kyushu Electric ultimately constructed new towers to bypass this zone of ground deformation.



Figure 3-23. Tower 30



Figure 3-24. Tower 31

Figure 3-25 shows Tower 35 along the Takamori Branch line (see Figure 3-8 for location within the network). The landslide has destroyed the road below the tower, but the tower, located about 100 feet up hill from the landslide scarp, remains structurally sound.

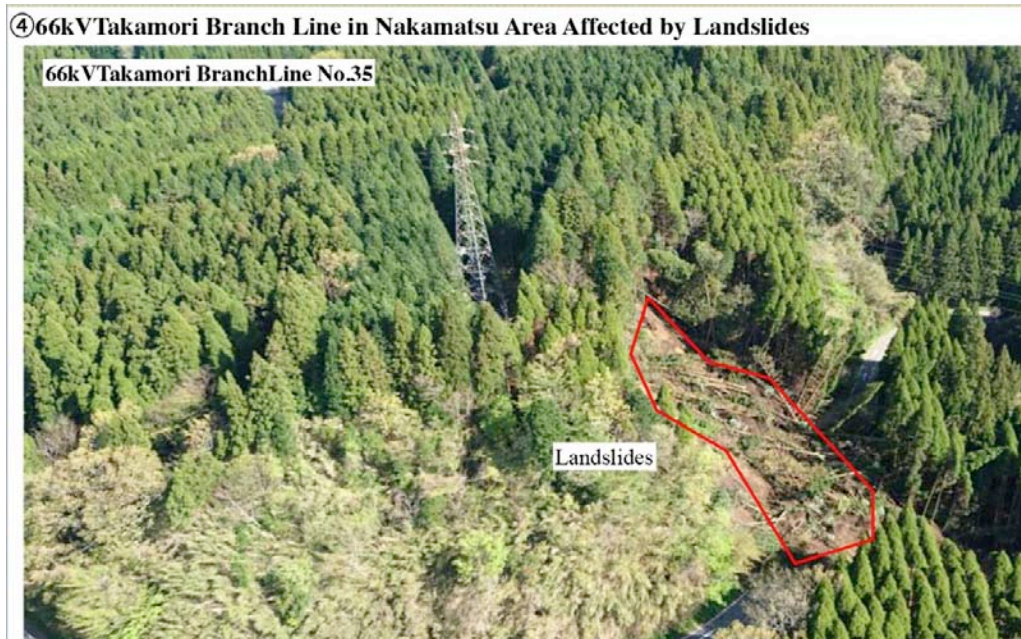


Figure 3-25. Tower 35

Figure 3-26 shows a typical 500 kV double circuit angle (strain) tower in the Kumamoto region. This tower was exposed to $PGA \sim 0.4g$, near the town of Ozu. None of the 500 kV towers were structurally damaged, but several suffered damage to their string insulators. Kyushu Electric reported that they have no specific seismic design requirements for their towers, but all towers are designed to remain elastic under strong winds, with a minimum wind speed used for design of 40 meters / second (90 miles per hour). Knowledgeable engineers from Kyushu Electric expressed disbelief that the common design practice in California is 8 psf (56 miles per hour) for high voltage transmission towers, a practice that is embedded in California General Order 95, and largely considered "too low" by some cognizant practicing engineers in California. The topic of seismic design for towers, to which this report tries to make some headway, suggests that for PGA up to $0.7g$, towers designed for wind loads at 70 mph to a initial yield (or buckling) state, and kept in good maintenance, should perform reliably (fewer than 1 failure in 1,000 towers); but towers that are concurrently exposed to PGDs can suffer serious damage or collapse.

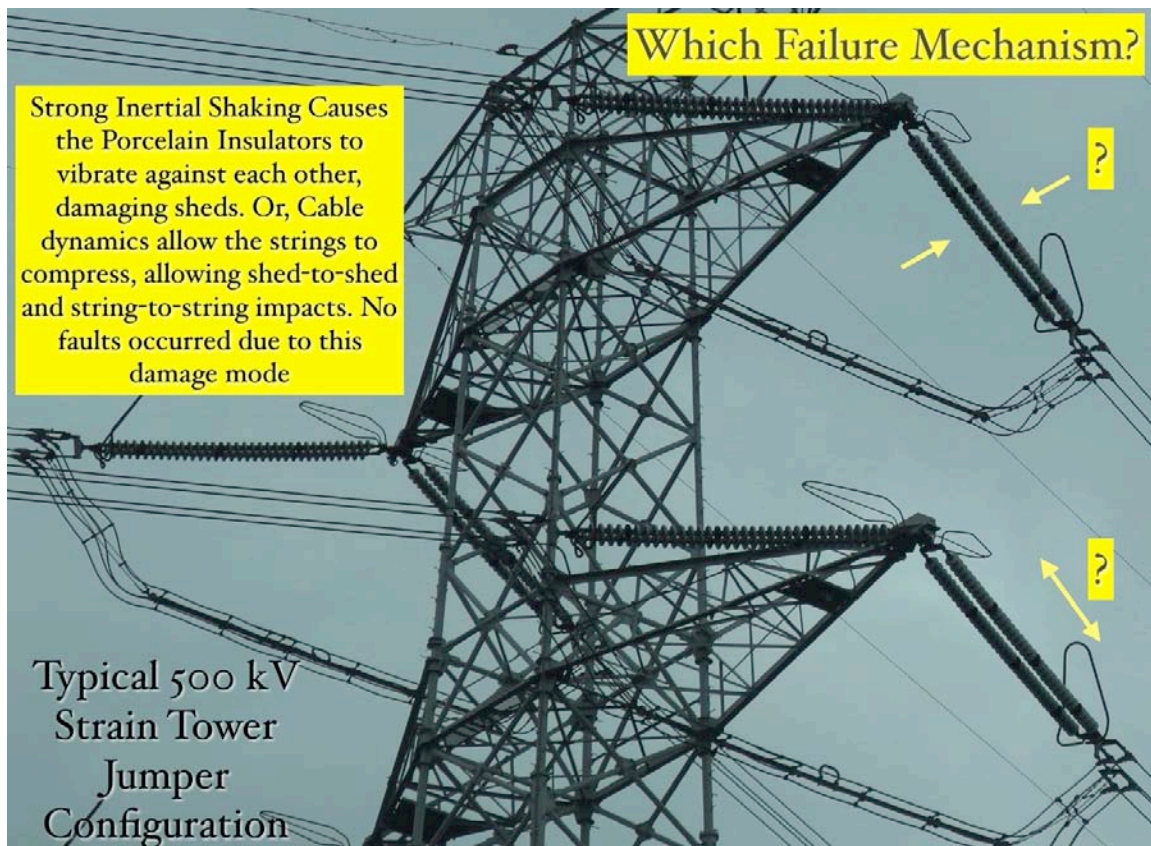


Figure 3-26. Typical 500 kV Tower Jumper Configuration, Angle Tower

Figure 3-26 shows a close-up of the typical jumper configuration used on this angle 500 kV angle tower. As can be seen, double tension strings are used to connect each 4-bundle conductor phase to the tower cross arms. The yellow arrows indicate two of the possible failure mechanisms during strong shaking, whereby the strings vibrate laterally and impact each other, or cable dynamics that temporarily allow the strings to unload in tension, temporarily allowing high rotations along the cap-and-pins; both mechanisms led to damaged porcelain sheds, Figures 3-27, 3-28, 3-29 and 3-30, both for angle and suspension towers. No faults occurred due to this failure mode.



Figure 3-27. Typical 500 kV Tower Jumper Configuration, Suspension Tower

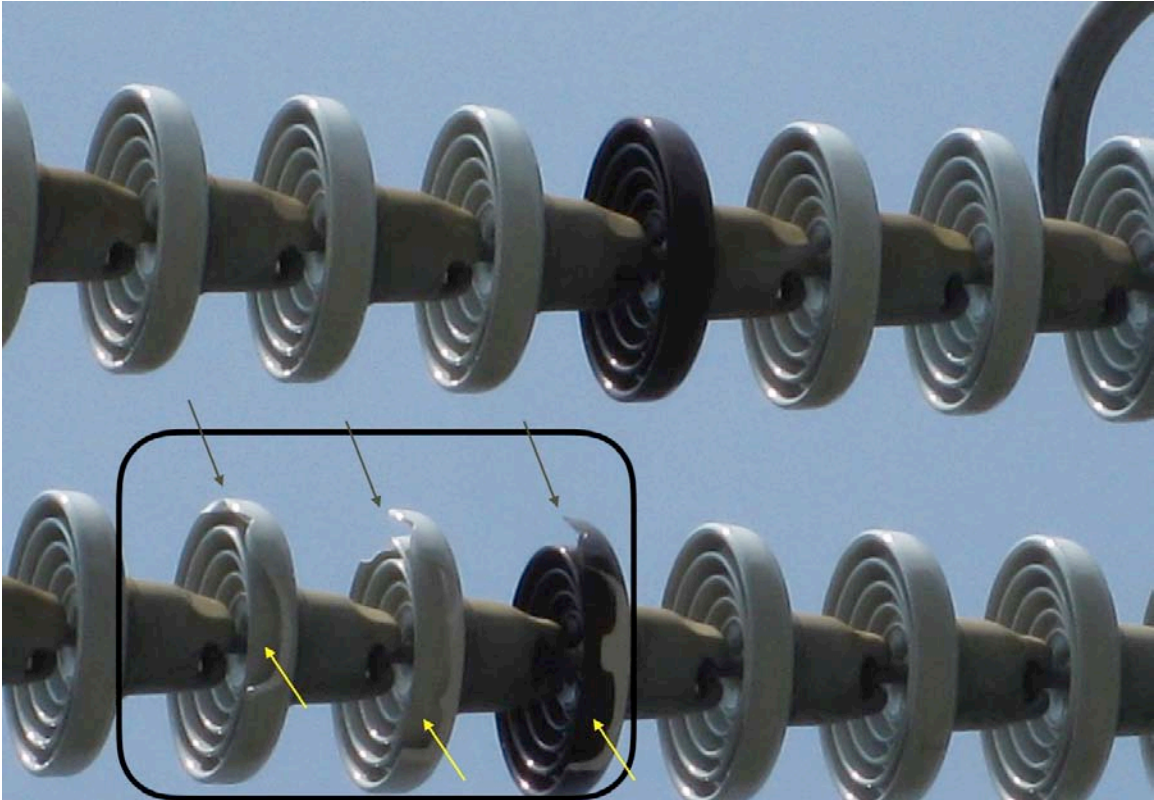


Figure 3-28. Damaged Porcelain Sheds on 500 kV Kumamoto Transmission Line 1, Angle Tower

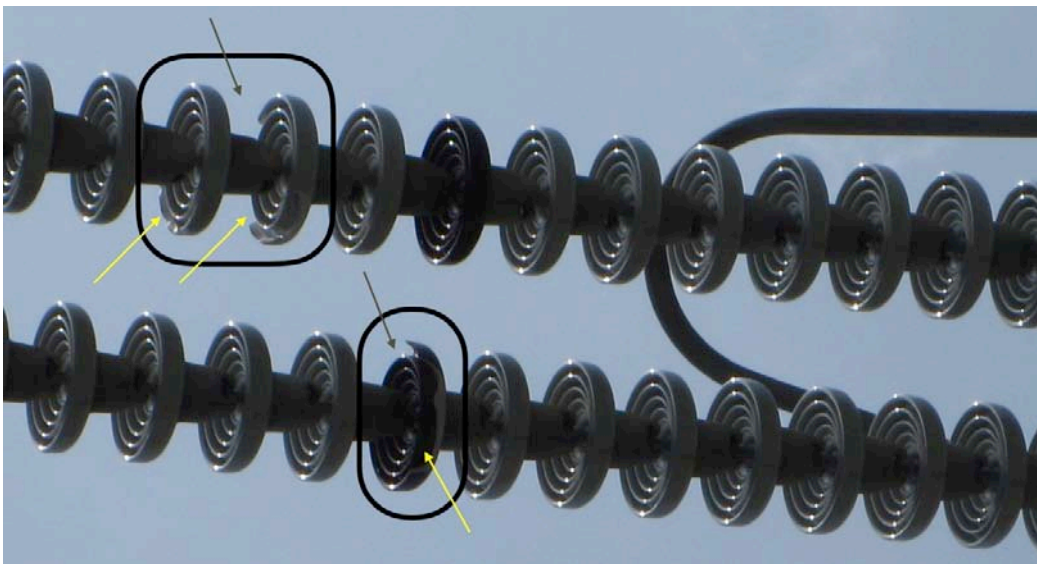


Figure 3-29. Damaged Porcelain Sheds on 500 kV Kumamoto Transmission Line 2, Angle Tower

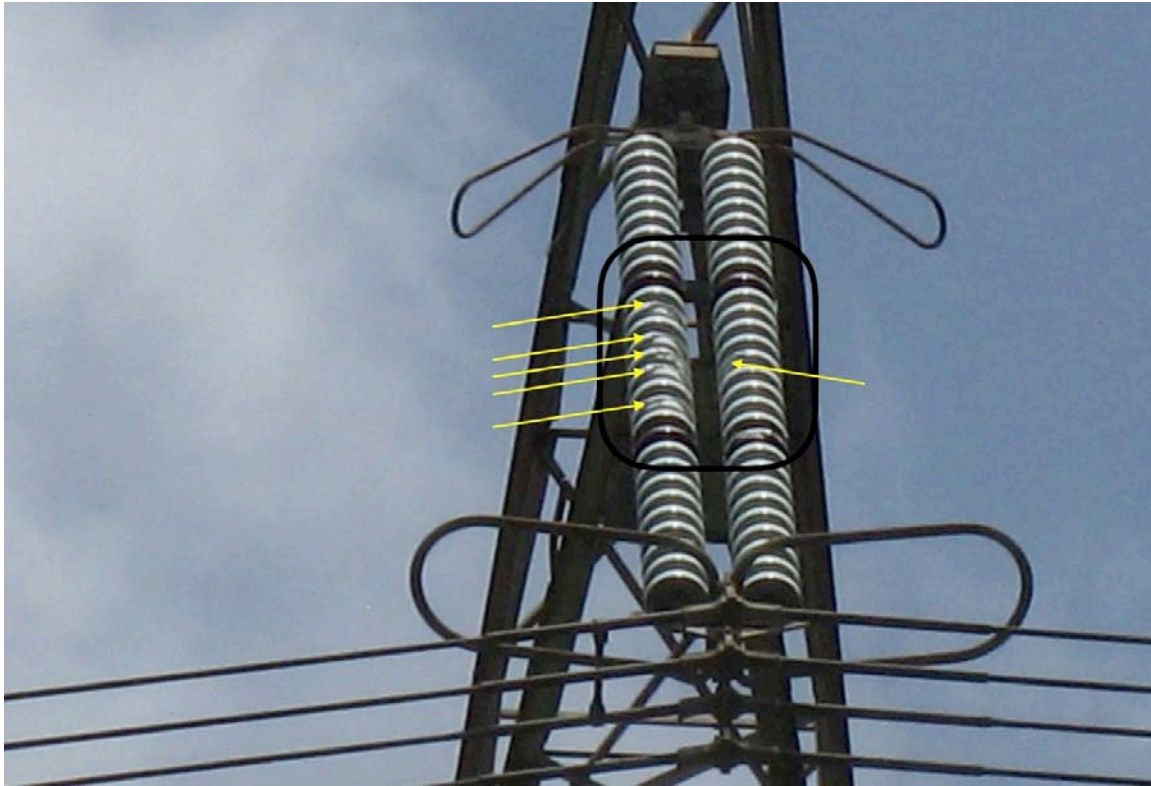


Figure 3-30. Damaged Porcelain Sheds on 500 kV Reihoku Transmission Line, Suspension Tower

3.4 Substations

Figure 3-31 shows an aerial view of the Kumamoto substation; the image is dated 2015. This yard includes 4 500 kV and 10 220 kV circuits. The 500 kV yard uses gas insulated switchgear (GIS). The 220 kV yard includes two 220 kV rigid busses, with each circuit connected to the busses via one SF6 dead-tank circuit breaker and two sets of pantograph switches. The yard includes one 3-phase 500 kV to 220 kV transformer and one 3-phase 220 kV to 66 kV transformer, and one 66 kV reactor.

There was no recording instrument near this substation, which is located well north of the rupture. The area near this substation is forested or used as farmland, and the few structures in the vicinity showed little or no damage; except those structures immediately adjacent to drainages. The estimated level of shaking might have been about PGA \sim 0.3g.

Both power transformers performed well.

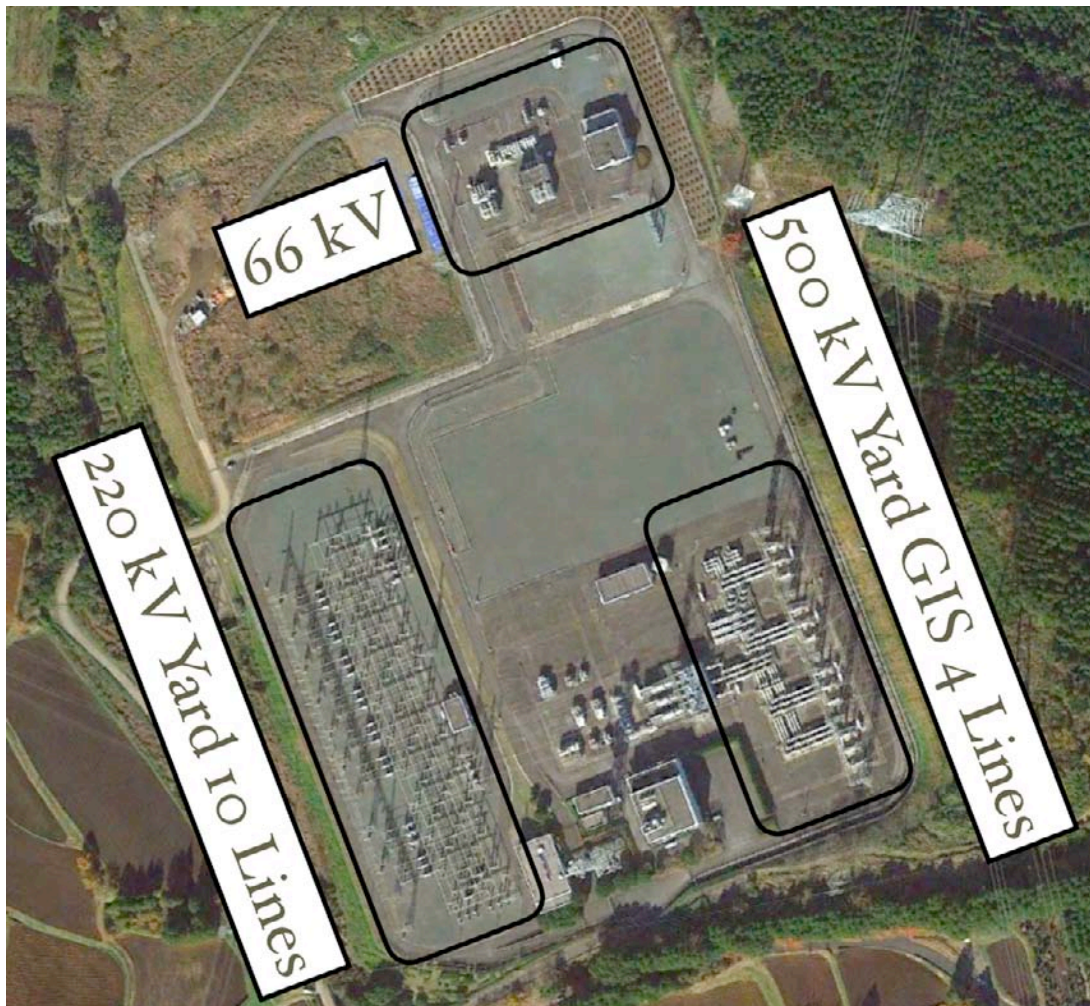


Figure 3-31. Kumamoto Substation

Figure 3-32 shows a slipped bushing on the 66 kV Neutral.



Figure 3-32. Slipped Bushing

Figure 3-33 shows an aerial view of the 220 kV yard. The circles show locations of damaged disconnect switches (DS) and voltage transformers (VT). The numbers indicate the 220 kV line numbers from north to south (1 through 6).

Two types of disconnect switches are used in the 220 kV yard: two horizontal break (sometimes also called two post center break), and pantograph. One set of horizontal break switches are used to provide isolation for each 220 kV line. Two sets of pantograph switches are used to connect each line to the primary and secondary 220 kV overhead rigid buses.

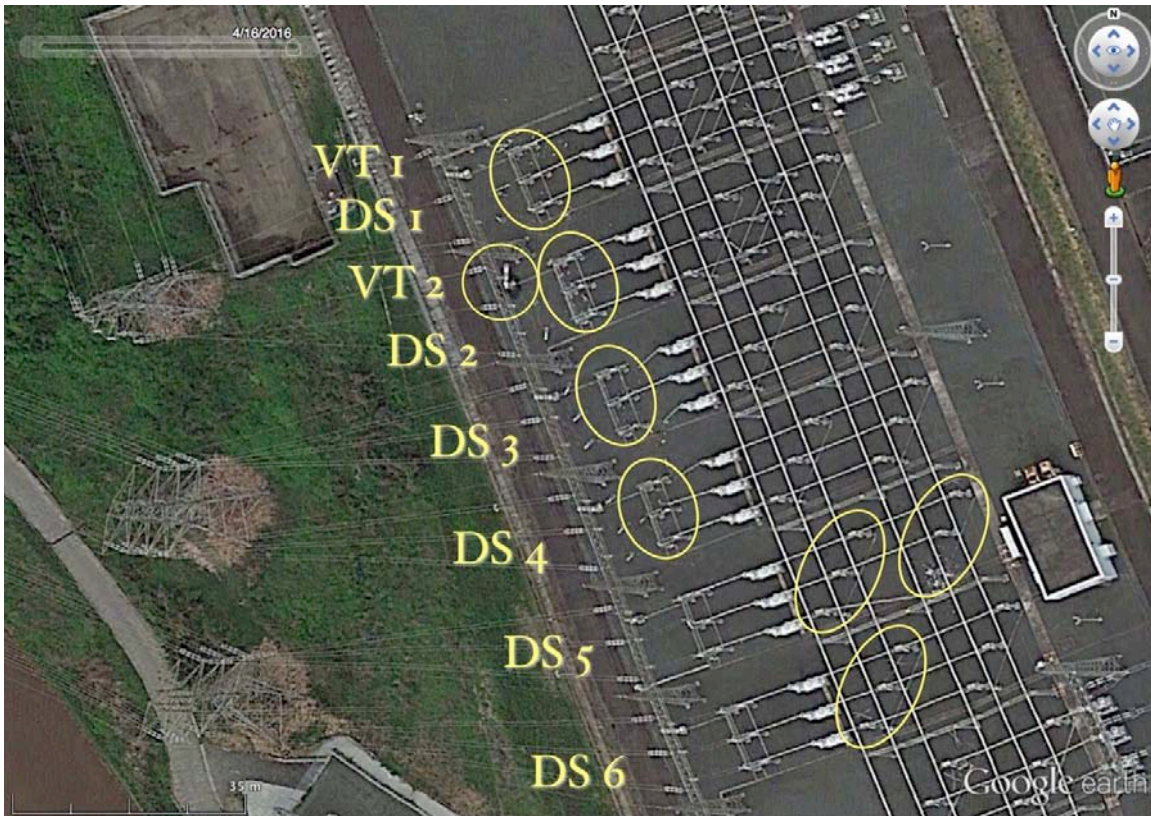


Figure 3-33. Damaged Equipment in 220 kV Yard

Figure 3-34 shows a damaged voltage transformer VT 2 and two positions of damaged center break disconnect switches. This photo is taken looking north, in the northwest corner of the 220 kV yard, showing VT1 (background) and VT 2 (foreground) and DS1 (background) and DS2 (partially seen in the right foreground) as located in Figure 3-33. The same model of VT also failed at a 220 kV yard in the 2011 Tohoku earthquake, at a substation in Sendai.



Figure 3-34. Damaged VT and DS 1 and DS2 in 220 kV Yard

The VT in the background (Figure 3-35) also suffered some damaged sheds, but did not collapse. There is evidence of ground cracking in Figures 3-34 and 3-36, suggesting incipient ground failure of the built-up pad at the western edge of the yard. There appears to be at least several inches of slack between the VT and the underhung rigid posts under the dead-end frame. Up-and-down motions of the 220 kV line may have imposed impact forces via the conductor onto the VT. High levels of twisting of the underhung posts (see discussion for Figure 3-39) on the frames may have also resulted in cable slack impact forces. The damage to the switches may have been caused by the imposed bending moments into the porcelain posts caused by the rigid bus connections to the right of the photo. The DS are supported on light steel horizontal members atop square steel posts, composed of four small steel angles, stitched together in a moment-truss-type configuration. While this support structure is certainly very strong for vertical loads, it might not provide very high lateral stiffness for the DS, and the racking of the structure in the earthquake would have induced bending moments into the porcelain posts, leading to incompatible deformations when factoring in the rigid bus connections.



Figure 3-35. Damaged VT and DS 1 in 220 kV Yard

Figure 3-36 highlights the broken DS 4 switches in the foreground, with DS 3 switches in the background. The damage pattern seen in Figure 3-34 for DS 1 and DS 2 and Figure 3-36 for DS 3 and DS 4 shows that all (12 / 12) of the line-side porcelain posts are broken, but 3/6 of the bus-side posts remain essentially intact. Ground cracks in the switchrock (3 cracks seen in the foreground of Figure 3-36) suggest that the pad in this part of the yard underwent incipient ground failure. Throughout the yard, only DS 1 and DS 2 suffered damage, while the same type of switches at all the other line positions remains undamaged. It is plausible that the temporary softening of the soils near DS 1 and DS 2 resulted in a lower fundamental period for these components, as well as VT 1, leading to increased tip displacements at the top of these components, which may have resulted in high cable impact forces if the conductors became tight. Another explanation of the damage to these DS is that the rigid bus in the background between the DS and the CB tried to displace laterally (transverse to the switches), leading to high and unintended moments in the DS posts, leading to failure; this failure mechanism is suggested by the lateral offset of the still-standing DS on the right of Figure 3-36.



Figure 3-36. Damaged DS 4 in 220 kV Yard

Figure 3-37 shows pantograph DS, with all three phases being broken. On the left phase, the "scissor" part of the switch is severely tilted to the left; on the center and right phases, the scissors part of the switch is entirely broken off. The cause of these failures is incompatible displacements between the scissor switch (with flexible steel post and bolted-base plates beneath the porcelain posts) and the north-to-south movement of the rigid bus atop the steel frames. Had the "grabber" part of the bus below the rigid bus been designed as a flexible system, capable of absorbing the relative displacements between the bus and the frame, then likely there would have been no damage to the switches.



Figure 3-37. Damaged Pantograph Switch DS 5 in 220 kV Yard

Figure 3-38 shows another damaged pantograph switch, with the failure mode in this instance being in the porcelain posts beneath the operating mechanism. As with the switches in Figure 3-37, the root cause leading to the damage is incompatible motions between the rigid bus and the switch, with the switch attempting to provide lateral support for the bus.



Figure 3-38. Damaged Pantograph Switch DS 5 in 220 kV Yard

Figure 3-39 shows another view of DS 1. In this view, the attachment of the under hung posts to the dead end frame suggests that the stiff posts are attached to a rather flexible steel plate, which in turn is attached to the relatively flexible frame. These posts can weigh on the order of several hundred pounds, and the base plate may have yielding, allowing a lock of rocking of the posts, and possibly leading to cable clack interactions below.



Figure 3-39. Damaged Switch DS 1 in 220 kV Yard

Figure 3-40 shows the damaged 220 kV busses at the South Kumamoto 220 kV substation. This yard may have experienced PGA $\sim 0.4g$ to $0.5g$ or so. This yard has 10 positions, 3 from generating plants, 6 to transmission lines, and 1 cross-over. There are two rigid busses that connect all these positions. The porcelain posts supporting the busses were damaged at ten different locations; and there was also some damage to pantograph switches.



Figure 3-40. Damaged 220 kV Rigid Bus End Posts

At the left side of Figure 3-40, the 6 porcelain posts at the end bay have all failed. The structures supporting these porcelain posts are steel tubes, possibly with lower lateral stiffness than the square tube-type structures used at the previously-described substation, as seen in Figures 3-37 and 3-38.

Figure 3-41 shows the typical damage at the connections between the rigid bus and porcelain posts. The rate of damage throughout this yard to the center post "B" phase was higher than for the "A" or "C" phases, suggesting that the extra flexibility allowed by the truss frame between the two steel posts resulted in even higher bus-to-post differential displacement and thus higher forces leading to higher damage rates. This type of vulnerability could likely be easily quantified by considering a structural 3D space frame for the entire system, and thus properly quantifying the forces and thus allowing suitable mitigation by either increasing stiffness and strength, or introducing more flexibility between different components of the overall system.



Figure 3-41. Damaged 220 kV Rigid Bus Post

Figure 3-42 shows damaged porcelain posts supporting 66 kV static condensers at this yard. The use of diagonal porcelain posts as diagonals to resist seismic forces should be carefully considered, as in order for the diagonals to take significant forces, the columns must also take bending moments at their connections, and simple truss-type computations will often ignore these secondary actions. As porcelain posts are very stiff, even small deflections / rotations can lead to high bending moments in the post, leading to high tensions and splitting of the porcelain. In some more modern installations, formal "pinned" joints are included in the designs for the columns, allowing them to take small rotations allowing the diagonals to suitably take the lateral forces; the flexibility of the base pad should also be considered if one is to arrange lateral resisting porcelain elements in this fashion.



Figure 3-42. Damaged Post Supports for 66 kV Static Condensers

Three of four 66 kV shunt reactors suffered slipped or broken bushings at this yard. Each reactor was three phase. The damage including slipped bushings, extruded rubber gaskets, and blown-out porcelain. Reactor 4 is shown in Figure 3-43. Bushing R is fractured entirely.



Figure 3-43. Damaged Bushings for 66 kV Shunt Reactor

Figure 3-44 shows the slipped bushing "S" with an extruded gasket. Figure 3-45 shows the slipped bushing "T" with an extruded gasket; once the bushing has excessive slip, continued rocking of the porcelain on the metal flange leads to high contact stresses, resulting in rupture of the porcelain.



Figure 3-44. Damaged S Bushing for 66 kV Shunt Reactor in Figure 3-43



Figure 3-45. Damaged T Bushing for 66 kV Shunt Reactor in Figure 3-43

IEEE 693 does not require seismic qualification of 66 kV equipment (including bushings). This reflects that until the 2011 Christchurch earthquake, and this 2016 Kumamoto earthquake, damage to 66 kV class equipment has been rarely, if ever, observed. A discussion with the authors of IEEE 693, after examining this observed damaged, suggests that this assumption might have to be revisited.

3.5 Generation

In the epicentral area, exposed to $PGA > 0.4g$, there are a few hydroelectric power stations, each having some form of damage. Distant from the epicentral area, and exposed to $PGA < 0.1g$, are a variety of thermal (coal, oil, gas) and nuclear power plants, none of which had any known damage.

Figure 3-46 shows an overview of the 45 MW Kurokawa hydroelectric facility. This facility is owned by Kyushu Electric. This plant takes source water from the Kurokawa river within the Aso Caldera, moves it southwesterly via two water flumes (channels), and then drops it down via several penstocks to a turbine building, and then releases the water back into the Shirakawa river.

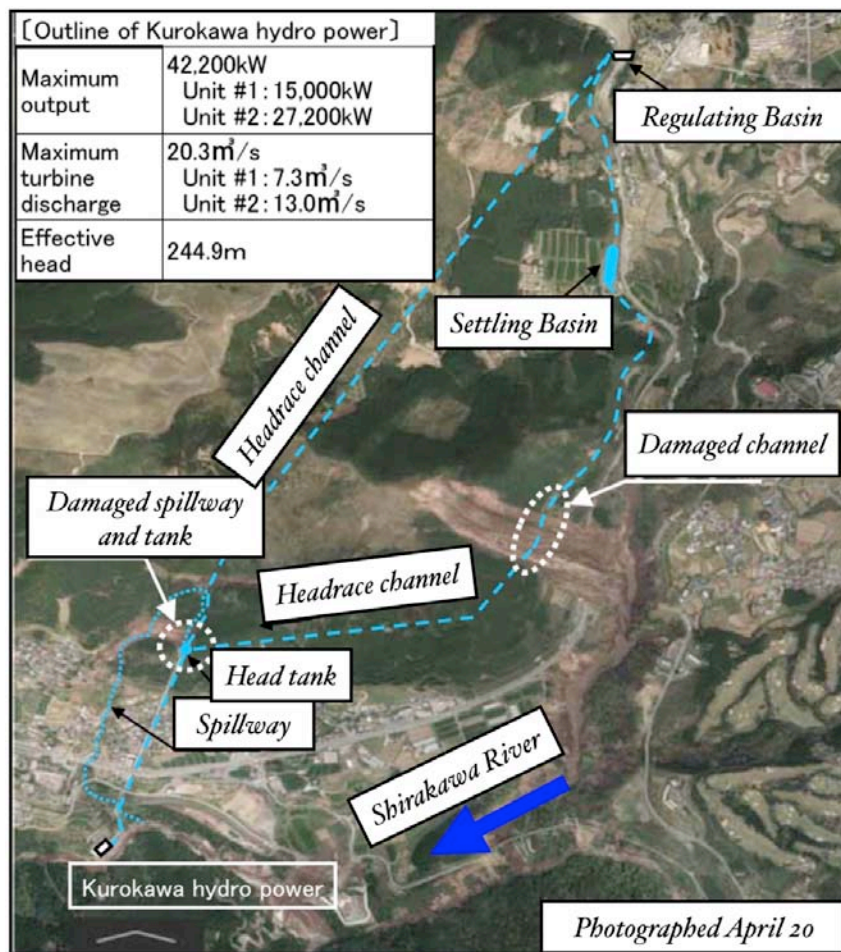


Figure 3-46. Kurokawa Hydroelectric Generation Facility

One of the two flumes delivering water to the penstock traversed the major landslide, and was entirely destroyed, Figure 3-47. Figure 3-48 shows another location with damage at the top of a spillway.

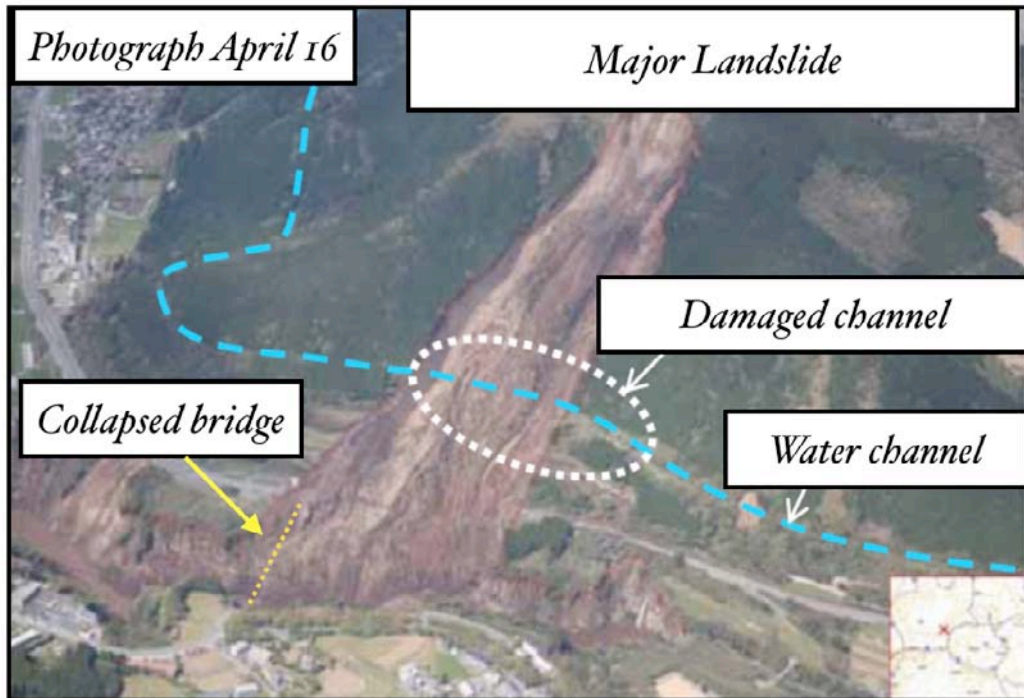


Figure 3-47. Damaged Headrace Channel

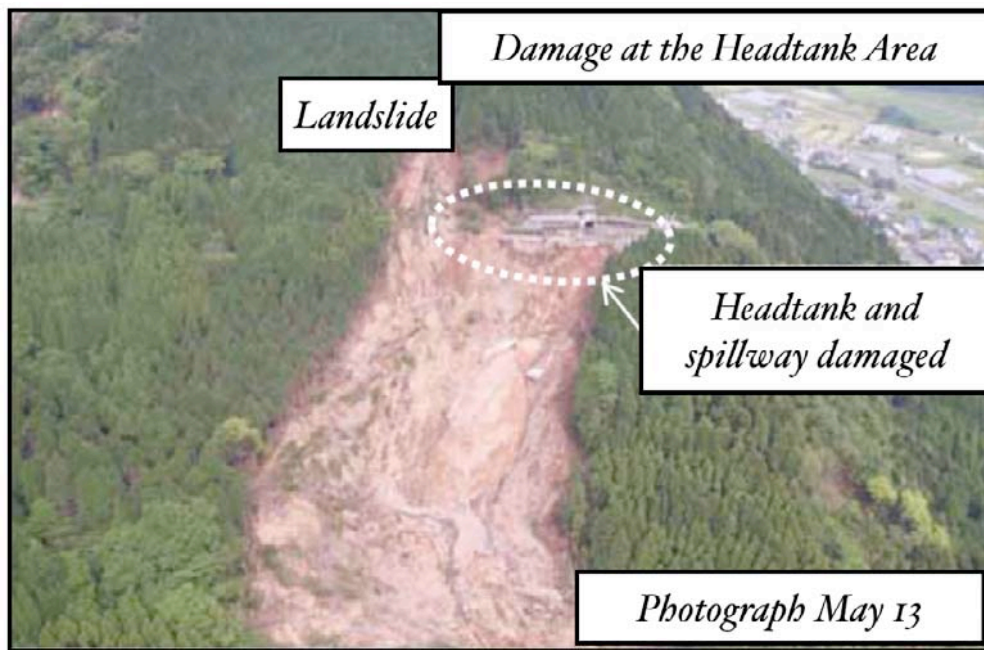


Figure 3-48. Damage at the Headtank Area

Figure 3-49 shows the unreinforced brick masonry turbine building for a small hydroelectric power plant owned by a private company, JNC. This facility was located on the south side of the Shirokawa River, and was likely exposed to $PGA \sim 0.5g$. The photo was taken 77 days after the earthquake, and repairs to the building have not yet started, as the only access road to the building was damaged by a landslide; that road was being repaired, with the presumed strategy of fixing the building once heavy equipment could be brought in. The 66 kV step-up transformer is located within the building, the wall bushings and SF 6 dead tank circuit breaker (on the backside of this photo) appeared to be undamaged.



Figure 3-49. Damage at the JNC Hydroelectric Plant

3.6 Distribution

The electric power restoration plot in Figure 3-1 shows an area-wide power outage lasting a few hours; this area-wide outage was primarily caused by damage at the high voltage substations. Once the damage at these yards was worked around, power to the major commercial and residential areas of Kumamoto City were restored. However, there were lingering outages in Mashiki town and the Mount Aso area, primarily caused by damage to transmission towers and the 66 kV circuits, as well as widespread damage to the distribution feeder lines.

Figure 3-50 shows a typical (undamaged) distribution pole in the area. The primary distribution feeder is commonly operated at about 6.6 kV. The secondary circuit takes power from the primary, drops it down to final voltage (commonly 100 to 200 V), and then has wires to take the power to nearby customers. The poles are commonly reinforced

concrete tubular poles. The cross arms (Figure 3-51) are commonly steel, attached to the concrete pole using friction clamps. There are almost no buried distribution cables in the area.

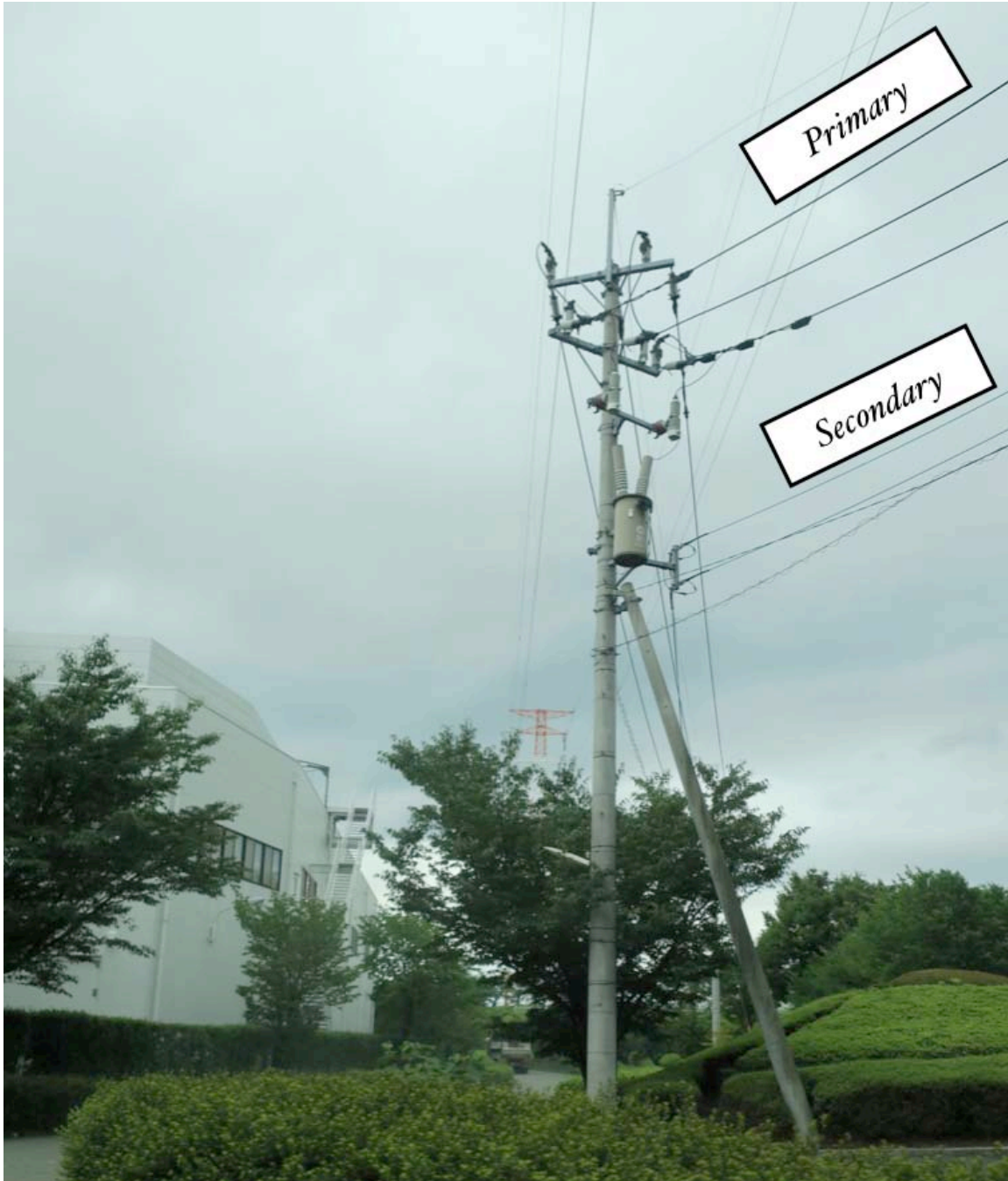


Figure 3-50. Common Distribution Pole

There were three common styles of damage to the distribution poles:

- The pole collapses as it was founded in a landslide or exposed to PGDs due to fault offset or liquefaction. For example, see Figure 2-25. This occurred at perhaps a dozen (or so) locations.
- The pole is "pulled down" (or severely tilted) due to collapse of an adjacent building. This happened at dozens of locations, primarily in places like Mashiki Town where there were widespread building collapses.
- The cross arms are rotated severely, due to pull down forces from collapses adjacent buildings, or tilted adjacent poles.

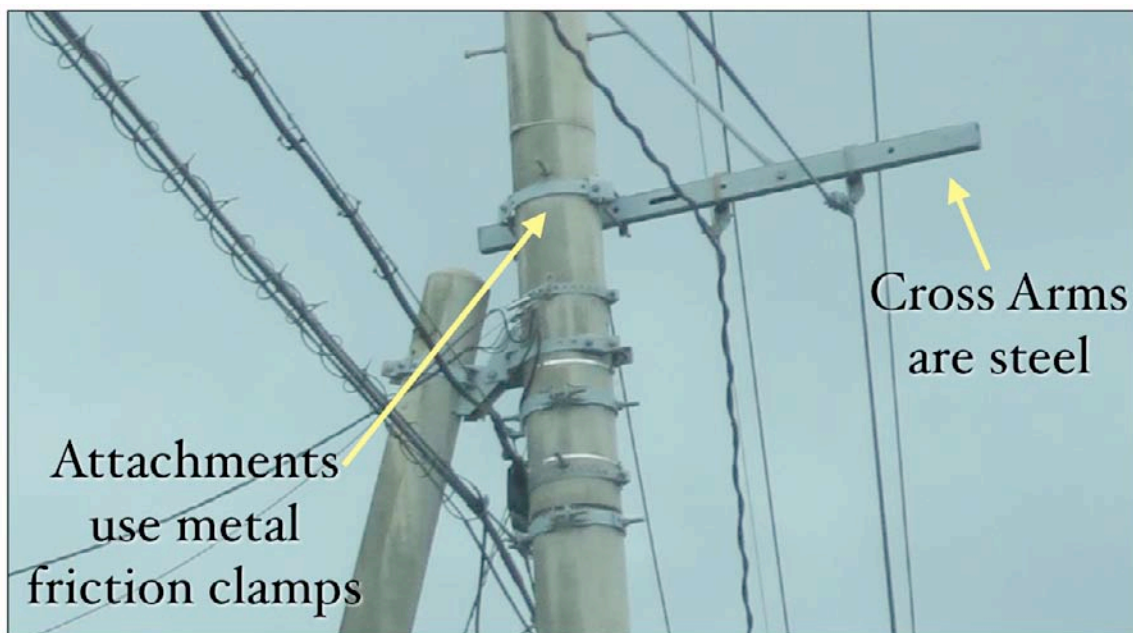


Figure 3-51. Common Cross Arm on Distribution Pole

Figure 3-52 shows a distribution pole that was exposed to surface fault offset. The surface faulting in this area is about 3 to 5 feet, with some up-and down movement. The pole is likely founded about 1.75 meters. The pole is tilted about 15 degrees to the right, leading to excessive conductor sags on the adjacent span. A kicker pole (for the angle forces) has also tilted to the right. A third pole in this photo supported telecommunication cables.



Figure 3-52. Distribution Pole Exposed to Surface Faulting

Pole collapses of the type in Figures 3-53 to 3-57 were due to pull down forces due to slope failures, avalanche / rockfall impacts, or collapsed or distorted adjacent structures.



Figure 3-53. Distribution Pole Collapse



Figure 3-54. Distribution Pole Collapse



Figure 3-55. Distribution Pole Collapse



Figure 3-56. Distribution Pole Collapse



Figure 3-57. Distribution Pole Collapse

Figure 3-58 shows the hookup of a 500 kVA emergency generator to an undamaged distribution primary feeder, commonly at 6.6 kV. A total of 169 emergency generator trucks were used to restore power to distribution feeders that has been cutoff from the grid either due to the collapse of transmission towers, or damage elsewhere along the feeder circuit.



Figure 3-58. Hooking up an Emergency Generator to a Distribution Primary



Figure 3-59. Hooking up an Emergency Generator to a Distribution Primary

3.7 References and Acknowledgements

Konagai, K., et al (2016). "Ground fissures that appeared in Aso Caldera Basin in the 2016 Kumamoto Earthquake, Japan." *J SCE Disaster Fact Sheet, FS2016-E-0003*.

Kyushu Electric provided several images and information about the performance of their electric system. In Chapter 3, Figures 1-8, 14, 20, 23-30, 32, 34-48, 53-59 are courtesy Kyushu Electric.

4.0 Telecommunication

Among the three key service providers in the region, NTT West (including DoCoMo), KDDI, and SoftBank, there was minor service interruption mostly due to power failure. The majority of the service interruption was in cellular service. The main reason for many cell sites losing signal connectivity was due to the short duration of reserve power capability at cell sites when commercial power from Kyushu Electric failed. A few cell sites also had interconnecting cables (both metallic and optical fiber) severed due to ground deformation.

There was no reported damage to Exchange facilities, except again some circuits suffered from broken connections due to ground deformation.

The recovery of the cell sites was a little bit slower than due to previous earthquakes of similar magnitude in Japan. About 85% of the cell sites were restored within 4 days after the main shock. It took 12 days to recover to 99% of normal operation. The main reason of the delayed recovery was due to difficult access to areas within Minami Aso and the Aso Mountain area; although there remains a need to collect more information to fully understand the slowdown during the last part of recovery.

All three major service providers provided free both telecom service and hardware to evacuation centers. The services included both landline and wireless connections. Routers, smart phones, tablets, and satellite phone handsets were loaned by the service providers to the various evacuation centers.

Both radio and television services had a short duration service interruption after the main shock. All of them recovered the next day.

4.1 Description of System

NTT West (including DoCoMo), KDDI, and SoftBank provide both landline and wireless services in the earthquake impacted area. Their services include voice and data. All of them use copper cables, optical fiber cables and microwave as the interconnecting media.

The voice services have not changed for a couple of decades, while data services evolve at lightning speed. The demand of bandwidth and speed of processing various data services creates the growth of optical fiber cable of the telecommunication network.

With the growth of smart phones in cellular service, the associated applications within these smart phones created demand of cell site capacity as well as number of cell sites to handle the increasing subscribers.

In addition, the wireless network will need to embrace the Internet of Things (IoT), which is increasing at an alarming speed, both tools and customers.

4.2 Overview of System Performance

As NTT West was the only service provider willing to meet with us and provide us with their system performance information and also answering our questions relating to service interruption and recovery, this report contains only NTT West (including DoCoMo) data. The tower failure was not part of NTT data. The owner of the tower was not known. We really appreciate their willingness and time to meet us during the busy post earthquake period to handle customer services.

From previous post earthquake investigations, such as for the Tohoku 2011 earthquake, this team learned a lot about NTT Corporation philosophy dealing with earthquake protection and network resilience. The key is that whenever there is a network growth implementation within a region, NTT will create a mesh topology instead of the former practice of loop or star topology. This investment did help the network to be more resilient.

In this earthquake, although a few circuits at one Exchange in Kumamoto City were damaged, the overall network performance was not affected.

The performance of wireless network needs improvement in this region. The need to focus on power supply to reduce future service interruptions is urgent. Developing micro-grid³ power supply will be a promising effort to maintain power to cell sites and Exchange Offices.

This section also includes telecom performance information provided by the emergency service office of Kumamoto Prefecture.

4.3 Landline Network Damage

Overall the landline network performed very well. There was no damage to any Exchange Office buildings and the backup power worked as designed.

In one NTT Kumamoto Exchange Office, about 300 circuits were damaged due to ground failure. SoftBank had 10 dedicated circuits and 734 ADSL (Asymmetric Digital Subscriber Line) circuits failed. ADSL is basically broadband service using the copper cable technology; this technology provides a faster download than upload. All damaged circuits were back to normal on 20 April 2016, four days after the main shock, which inflicted the failures.

While 21 NTT Exchange Office buildings within Kyushu were on backup power for four days after the main shock.

Both underground and aerial cables sustained damage due to permanent ground failures (PGDs) including landslides. Figure 4-1 (32.8829°N, 130.9905°E) shows one of the many

ground failures with buried cables and other lifelines, which were damaged. Figures 4-2 to 4-5 show aerial cable failures. Figure 4-2 (32.8044⁰N, 130.8587⁰E) shows ground failure resulted in a tilted pole. To the left of this pole was where surface faulting occurred. Note also that the pole sank into the ground. Figure 4-3 (32.8819⁰N, 130.99⁰E) shows a damaged telecom cable due to landslide and the pole fell. Figures 4-4 and 4-5 display the aerial damage within Mashiki town.



Figure 4-1. Buried cable with flexible conduit severed (Minami Aso)



Figure 4-2. The utility pole carrying the telecom aerial cable bundles sustained ground failure damage. The top part of the pole was resting on the power cable isolator



Figure 4-3. The telecom pole fell and resting on the side of the building



*Figure 4-4. Many telecom and power cable poles were damaged in Mashiki Town
(32.7901°N, 130.8209°E)*



Figure 4-5. In Mashiki town these aerial cables (power and telecom) dropped almost to the ground and they were touching one another at the lowest point ($32.7888^{\circ}N$, $130.8205^{\circ}E$).

Some landlines that are co-located with bridges failed due to bridge collapse. The most prominent case was the collapse of Aso Ohashi in Minami Aso. Figure 4-6 shows the co-located optical fiber cable severed by the massive landslide at Aso Ohashi, which was collapsed by the same landslide.

Drop wires to houses were damaged due to pole failures, this is usually a cascading effect when one pole pulled the others tight or caused the pole to lean at a large angle. There were many cases of severed drop wires due to house collapses. Figure 4-7 shows a case of pulled drop wire to a house, which was partially damaged. In this case it looked like the wire terminations were not disconnected, therefore the phone would work in this house if the phone still functioned.

The silver lining of collapsed houses was telecom service was not needed. However, the cable bundle on the same circuit might be impacted. With new switching technology, most errors can be corrected at the control center of the service provider. There is no need to send repair crew out to the field, except for physical damage to the cable bundle.



Figure 4-6. The two ends of the buried optical fiber cable bundles were severed by landslide (32.885°N , 130.9866°E). The distance was about 500 meters. (Courtesy: MLIT Kyushu)



Figure 4-7. The drop wire connection was pulled from the exterior wall of this house in Mashiki town (32.7884°N , 130.8184°E). Note the proximity of the power drop wire.

4.4 Wireless System Damage

When compared with the landline network, wireless network did not perform as well. Although most of the failures were electric power related, this type of failure has been known for a long time. There is a need to re-visit the power supply part of the cell sites to ensure better performance in future earthquakes.

Official record from Kumamoto Emergency Disaster Response Headquarters indicated 12 days of cell sites recovery in the impacted area. The total number of cell sites was over 250. Figure 4.8 is the recovery chart of the three major wireless service providers. As

there was no data on 29 April 2016, the chart record was zero. From 30 April 2016 the record of cell sites not recovered remained the same until 11 May 2016, when one service provider kept two cell sites off air. There was no information whether this service provider will ever restore these two sites.

Close to 85% of the failed cell sites were restored within 5 days after the main shock of 16 April 2016. The remaining cell sites took longer than usual to get back to service. The main reason was access to these cell sites, which are in Minami Aso where the huge landslide occurred and in the Aso Mountain area.

In Mashiki area, there was a cell tower collapsed, the owner of this tower was not known. The location of this tower is close to a road surface damage area. Satellite photos of before and after the main shock indicated the tower failure. Figure 4-9 shows the before and after image of this tower. The information was provided by Aero Asahi Corporation with the assistance of Prof. Konagai of Yokohama National University. Figure 4-10 shows the area with significant damage near the collapsed tower site. Figure 4-11 is the failed tower at ground level.

NTT West provided us with a couple of examples of cell site failures, which will be detailed in the following section. We also visited on cell site, which is very close to the surface faulting area.

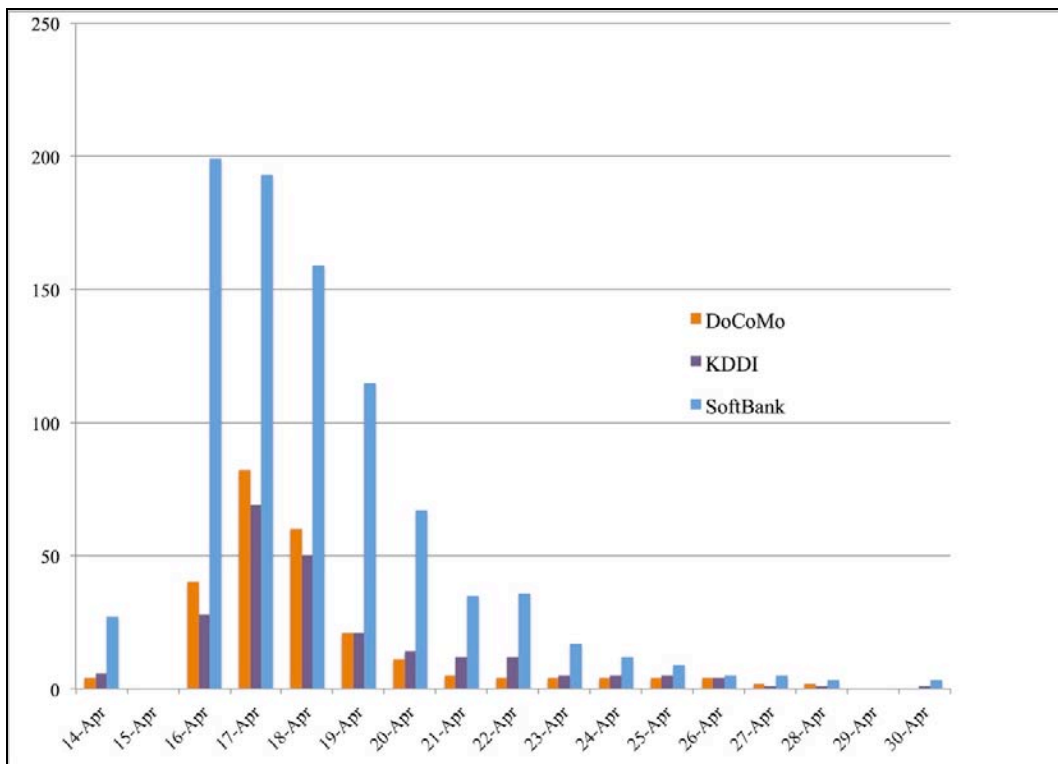


Figure 4-8. Cell site recovery progress after the earthquakes

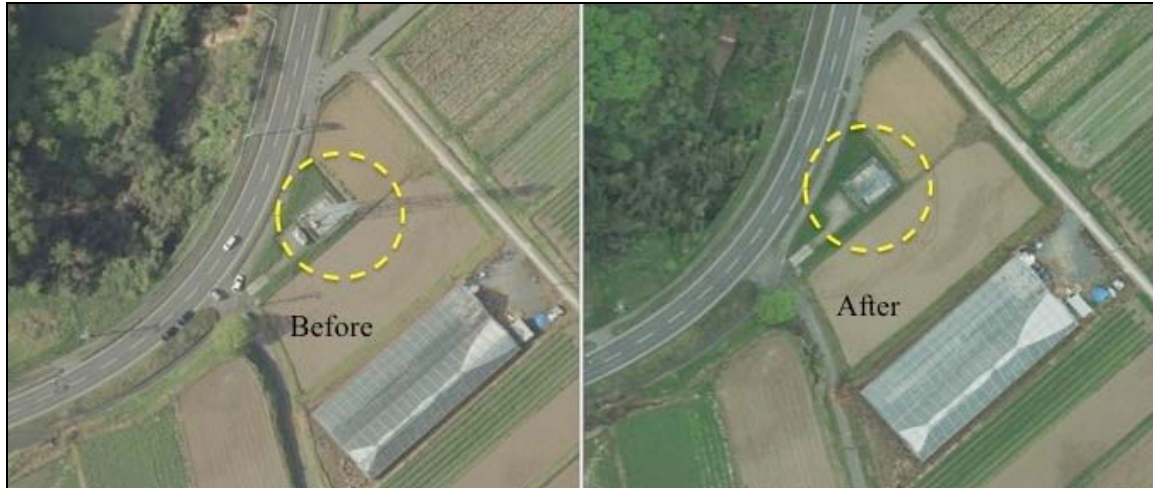


Figure 4-9. The unknown cell site with the collapsed tower was photographed by satellite (32.7928°N , 130.8235°E). Courtesy: Aero Asahi Corporation).

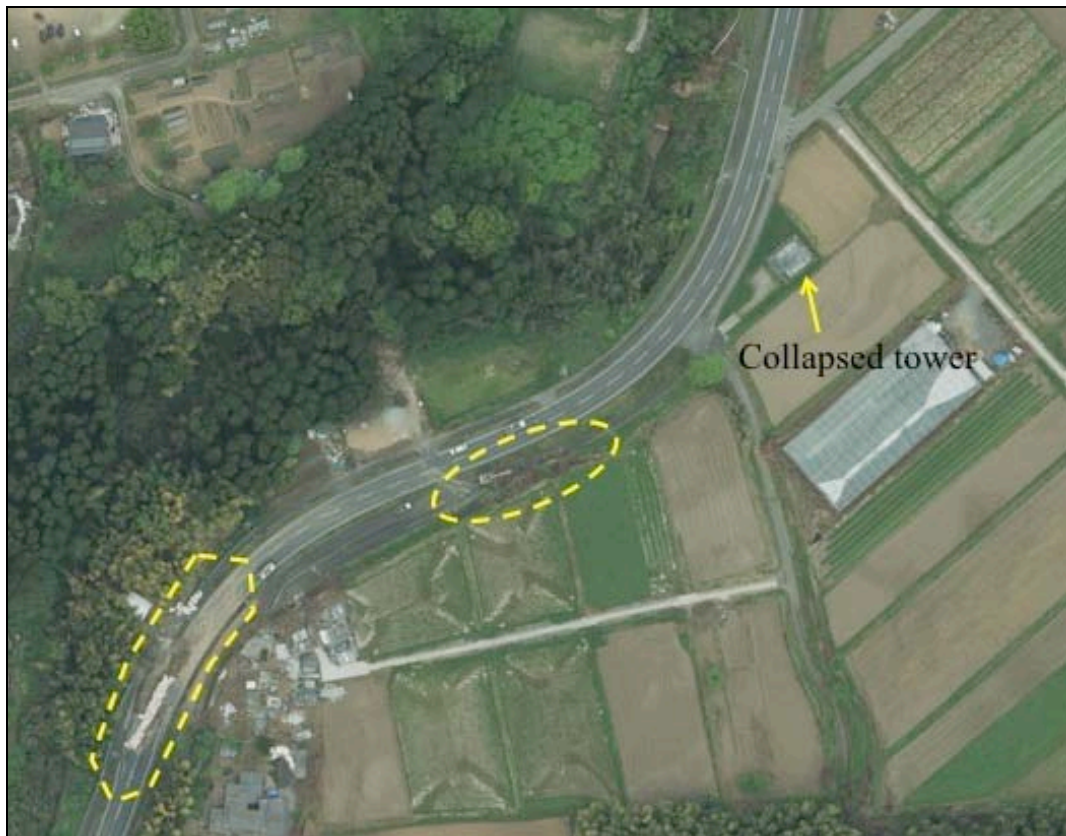


Figure 4-10. Aerial view of the area where the tower collapsed, Note the road damage (Auxiliary National Road 443) within the circled areas. (Courtesy: Aero Asahi Corporation)



Figure 4-11. Collapsed cell tower (Courtesy: Guardian News & Media Ltd)

NTT West provided us with the two reasons of cell site off air after the earthquake. The first one was electric power outage at cell sites. Cell sites have limited power reserve, so when power does not resume before the reserve power is exhausted, the cell site goes down. The second reason of cell site outage was the transmission cable to Exchange was damaged due to permanent ground deformation.

At this mid-zone base station (Figure 4-12) in Aso City the commercial power went out and power generator had to be delivered to site to provide power to sustain the cell site. At this cell site (Figure 4-13) also in Aso City, the transmission cable was damaged due to ground deformation. In some cases a mobile satellite truck was used to provide transmission link before the cable could be fixed. Mobile satellite trucks were used to provide transmission links wherever needed. Figure 4-14 show a satellite truck outside of the Aso City Gymnastic Hall.

Mid-zone base stations are critical after an earthquake, as they are use to cover smaller cell sites (small in terms of channel capacity) when they fail. Figure 4-15 shows the concept of mid-zone base station to provide wireless coverage when it is needed.

In addition, NTT DoCoMo also stretches battery holding time to provide power to critical stations from Exchanges. However in this case, the cell sites that are in the mountainous regions do not have the battery connection to Exchanges. In terms of transmission link damage, multiple links are also used for important cell sites; usually the cell sites that cover a densely populated area.



Figure 4-12. This DoCoMo Mid-zone Base Station had a power generator brought in to provide power to operate the base station. (Courtesy: NTT West)



Figure 4-13. The transmission link at this cell site was damaged by the ground subsidence. (Courtesy: NTT West)



Figure 4-14. DoCoMo satellite truck outside of the Aso City Gymnastic Hall providing transmission link for damaged underground cable at cell sites

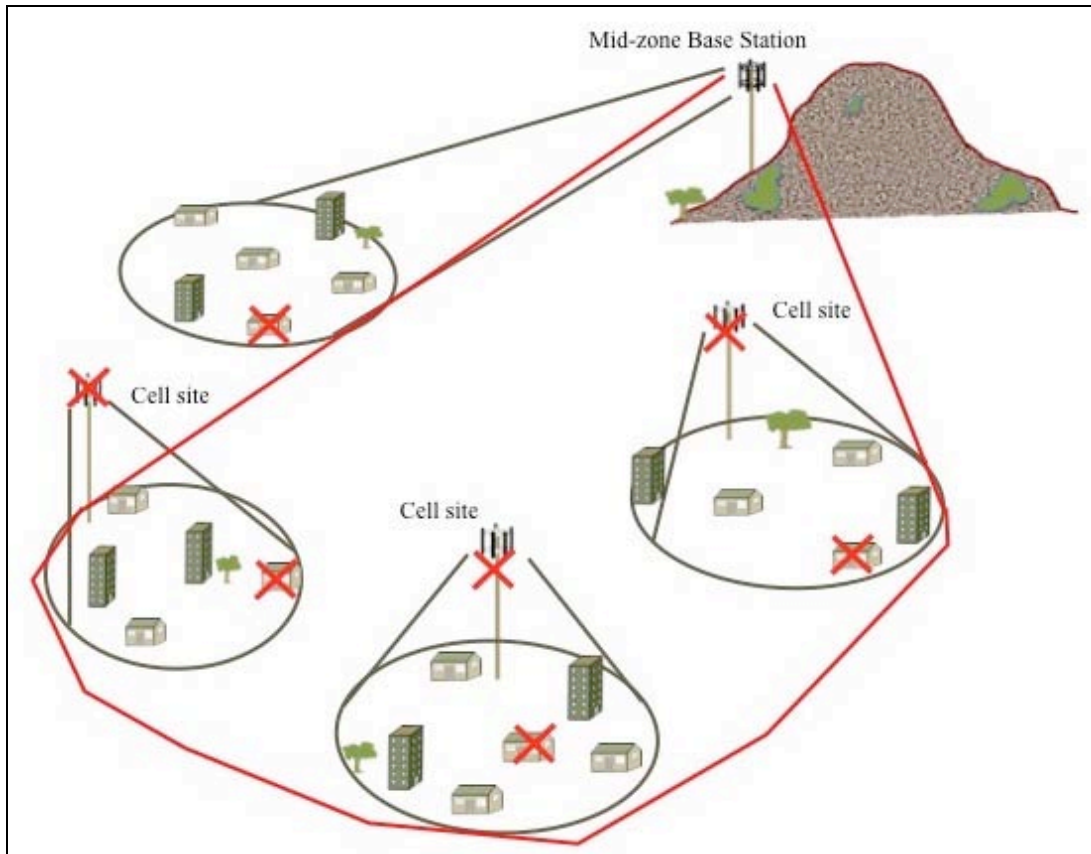


Figure 4-15. A graphical representation of a mid-zone base station (cell site) covering smaller cell sites that are off air due to any type of damage.

We visited a DoCoMo cell site, which is located at the end of the surface fault line to investigate the site condition and the facility. This site is located at 32.8041°N , 130.8566°E and is about 10 to 12 meters above the main road. Figure 4-16 provides an aerial view of the site with respect to the surface faulting. The path leading to the cell site was covered with small rock and vegetation debris indicating a very small scratch due to strong shaking as well as rain fall creating mud slide after the earthquake, Figure 4-17. The concrete slabs in front of the gate were cracked due to ground movement, Figure 4-18. The two huts housing the wireless equipment did not show any signs of damage. The concrete platform and blocks that the housing footings were anchored did not show any sign of movement. The tower was in good shape. Figures 4-19 to 4-22 provide a record of the structural components of this site and the earthquake impact to close by structure to provide a testament of the strong shaking.



Figure 4-16. A landscape view of the location of NTT cell site with respect to the surface faulting. Figure 4.2 was taken at the end of the red line at the Y-intersection



Figure 4-17. The insert on the top left corner shows the debris on the path leading up to the cell site (Investigation team photo). The road surface crack was most likely the end of the surface faulting (Courtesy: Geospatial Information Authority of Japan)



Figure 4-18. Two cracks were visible just in front of the cell site gate.



Figure 4-19. This aerial view of the cell site shows no visible damage on the outside of the huts and the tower footings



Figure 4-20. The equipment hut anchoring does not show any stress or deformation. The concrete pad was in good shape



Figure 4-21. The cable entry points was not stressed and there was no signs of deformation



Figure 4-22. This concrete path with step to the small shrine sustained damage due to ground deformation. This shrine is about 10 meters above the cell site. The cell site aerial photo was taken from this point

4.5 Major Observations and Recommendations

Hardening of wireless network against large magnitude earthquake needs to be improved in addition to dealing with loss of power.

With recent success of the micro-grid power by NTT in Sendai during the Great East Japan Earthquake and Tsunami of 2011, deploying this concept to major cities and towns seem to be the best approach to handle power. Increasing backup power to cell sites is a good practice. Using solar panels to recharge batteries will reduce the consumption of commercial power.

The failure of a cell tower, which folded at half height, was the first ever observed. There was no information of the owner of the tower. A study of the failure is recommended to improve future design to avoid similar failure.

Cables that are co-located with bridges are recommended to have redundant routes to ensure connectivity.

Kumamoto prefecture has a lot of rice fields. There are many cell sites that are located within the rice fields. Figure 4-23 shows one of the many cell sites installed in the middle of a large rice field. This area is susceptible to flood; this cell site was not engineered to

prevent flood damage. The levee height is notably higher than the footing of the equipment, Figure 4-24. However, this cell site, which is situated on the edge of the rice field is installed on a platform. This cell site was engineered to prevent flood damage, Figure 4-25. From a network resilience point of view, consideration of all hazard must be included in preparedness and mitigation planning.



Figure 4-23. This cell site is in the middle of a large rice field. Note the height of the levee on the left of the cell site



Figure 4-24. Close up view of the cell site in Figure 4-23 shows that the equipment is only about 0.5 meter above the field level



Figure 4-25. This cell site on the edge of the rice field is installed on a high steel platform. The equipment is installed with flood as one of the hazards

Network cable management is a critical item in ensuring good network resilience. Figure 4-26 shows the congestion of cable bundles, most likely a few service providers sharing a single pole. If this pole is damaged then a large number of customers will be out of service. Disperse redundancy is necessary to maintain a high degree of resilience.

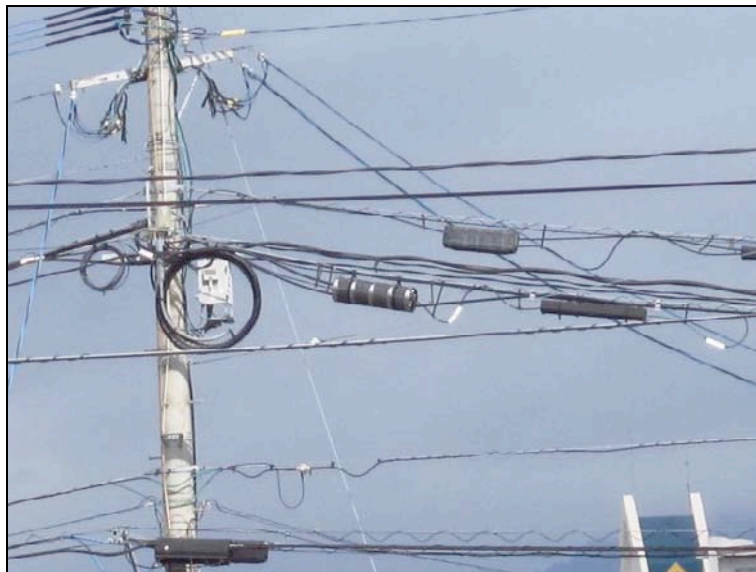


Figure 4-26. Aerial cable congestion on one pole

4.6 Acknowledgements

Dr. Keiichi Hirose of NTT East was instrumental in establishing a high level management support from NTT West in Fukuoka. Mr. Chikamasa Teshima, Mr. Shinichi Kunimatsu, and Mr. Toshinori Inoue of NTT West were very helpful providing us with a valuable presentation of their investigation result and provided us with location of cell sites within the disaster area to inspect the impact.

With the guidance of both Professor Maruyama and Professor Konagai and our assistants (Mr. Yuki Kagami, Professor Konagai's student) we were able to gain access at many sites and we are extremely grateful of their kind support.

4.7 References

Tang, A. and Eiding, J. Seismic Performance of Lifelines in the Great Eastern Japan Tohoku Earthquake of 2011 (in press).

5.0 Water System

5.1 Overview

Each city and town in Kumamoto Prefecture has a potable water distribution system. In total, 445,000 households lost water supply, as follows:

- 432,000 in Kumamoto Prefecture
 - 327,000 in Kumamoto City
 - 31,000 in Ozu Town
 - 11,000 in Mashiki Town
 - 10,000 in Aso Town
 - 50,000 in smaller communities
- 10,000 in Oita Prefecture
- 2,800 in Kiyazaki Prefecture

The City of Kumamoto water department (the City) has long recognized the threat of earthquakes. For the period between 2010 and 2028, the City had budgeted \$US 410 million, with focus on integration of smaller nearby water systems into the larger City-wide water system. In addition, for the period between 2009 and 2021, the City had budgeted \$US 310 million, with focus on integration of seismic improvements to the existing City-wide water system.

The following summarizes the inventory of facilities in Kumamoto City:

- 113 wells (of which 96 were in operation at the time of the earthquake). In the main shock earthquake, 5 had various types of structural damage and all had water quality issues.
- 19 pump stations.
- 61 distribution tanks, with total storage of 58 million gallons. The largest tank has capacity of 6 million gallons.
- 3,366 km of pipe, ranging from 3 to 60-inch diameter. Of this total pipe inventory, the types include:

- 577 km of earthquake resistant ductile iron pipe (ERDIP)
 - 1,882 km of ductile iron pipe (DIP)
 - 73 km of welded steel pipe
 - 424 km of PVC pipe
 - 136 km of High Density Polyethylene Pipe (HDPE)
 - 81 km of Cast Iron Pipe (CIP) or other
- Total water supply capacity of 84 MGD (316,116 m³ / day)
 - Average Day Demand 58 MGD (218,171 m³ / day)
 - Population served: 740,000 people

Since 2005, all water pipe installed in the system has been "seismic-resistant" pipe. The earliest "seismic resistant" pipe installed in the City was in 1979. As of 2014, 75% of all pipe 14-inch diameter and larger (trunk lines) are "seismic" pipe; 22% of all pipe are "seismic" pipe.

In the major soft ground / liquefaction zones, all trunk pipes are welded steel pipes. Within these liquefaction zones, there were no known failures of these welded steel pipes, but at the edge of the major liquefaction zone, where the welded steel pipes transition from liquefied to non-liquefied soil conditions, there were failures in the adjacent liquefied and non-liquefied soil zones.

By June 1 2016, the repair statistics in the City were:

- 125 trunk pipe repairs
- 107 distribution pipe repairs
- 1,574 service line repairs (generally up to the customer's meter)
- 1,638 "customer side" investigations (repairs, if needed, generally made by contractors)
- 17 wells with damage, including: pipes 5; buildings 12; electrical instrumentation 2; pump 1; fences 2; ground settlements 12.

- 1 reservoir with damage.
- 2 pump stations with damage, including: pipes 3; building 1; ground settlement 2.
- 7 tanks with damage, including: pipes 3; instrumentation 1; fence 1; ground settlements 3.



Figure 5-1. Kumamoto City Water System Service Area

Figure 5-2 shows a schematic representation of the geologic layers of the Kumamoto Region. The region is formed by pyroclastic sediments laid over base rock that came from Mount Aso. Mount Aso has erupted many times in the last 300,000 years (last time about 90,000 years ago). Four large-scale eruptions were responsible for creating the huge caldera. The pyroclastic sediments are a porous layer with many cracks and is highly permeable.

The source water is derived from the Mount Aso caldera watershed, which feeds a river and aquifers that flow westward to the ocean. The water supply for Kumamoto City is derived from well water, via 96 wells. The well water comes from the second Togawa lava layer, are commonly 100 to 200 meters deep.

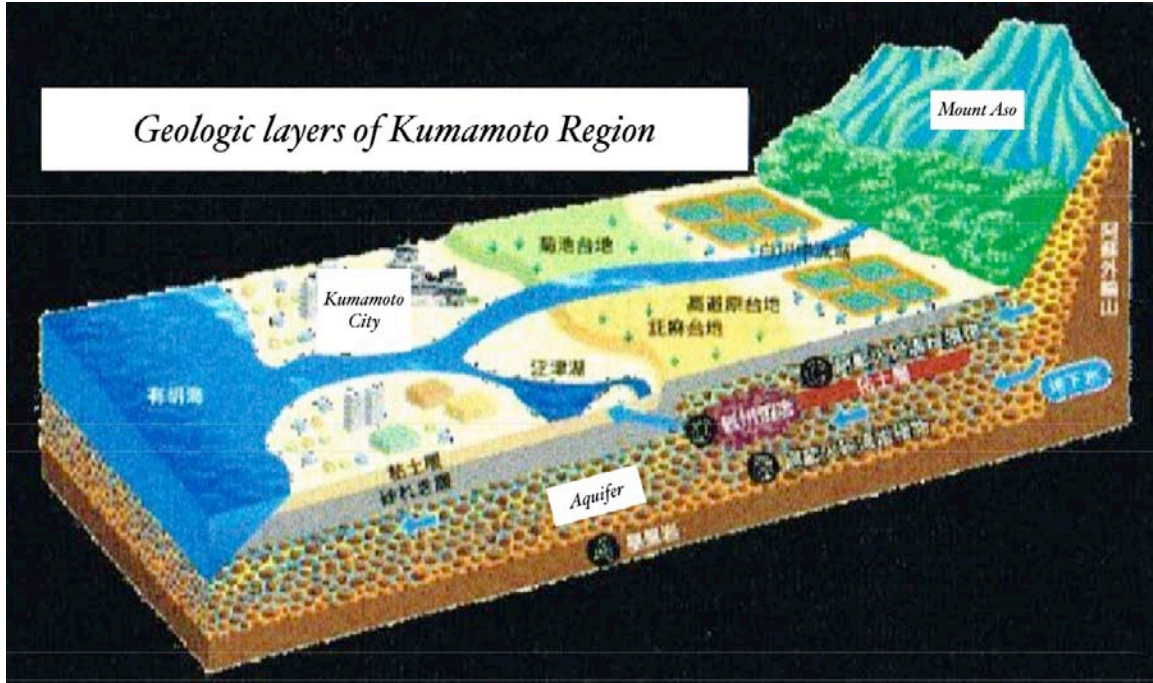


Figure 5-2. Kumamoto Region Geology



Figure 5-3. Flow of Groundwater

5.2 Pipe Inventory

Figure 5-4 shows the length breakdown of the 3,366 km of pipe, by diameter. The most common diameters are 3 and 4 inches; in comparison, the most common diameter for distribution pipe in major United States cities is either 6 or 8 inches, with few (if any) pipes 4 inch diameter or smaller. In the U.S., pipe diameter is commonly controlled by hydraulics required to deliver a minimum flow of 1,000 gpm to any hydrant in residential areas (resulting in 6- or 8- inch diameter commonly); or 4,000 to 8,000 gpm flows in commercial and major industrial zones (resulting in 12- to 16-inch diameter commonly). Kumamoto City's largest diameter transmission pipes (600 to 1350 mm diameter) are used to deliver water from major well fields to the smaller pipes that are used in the distribution system.

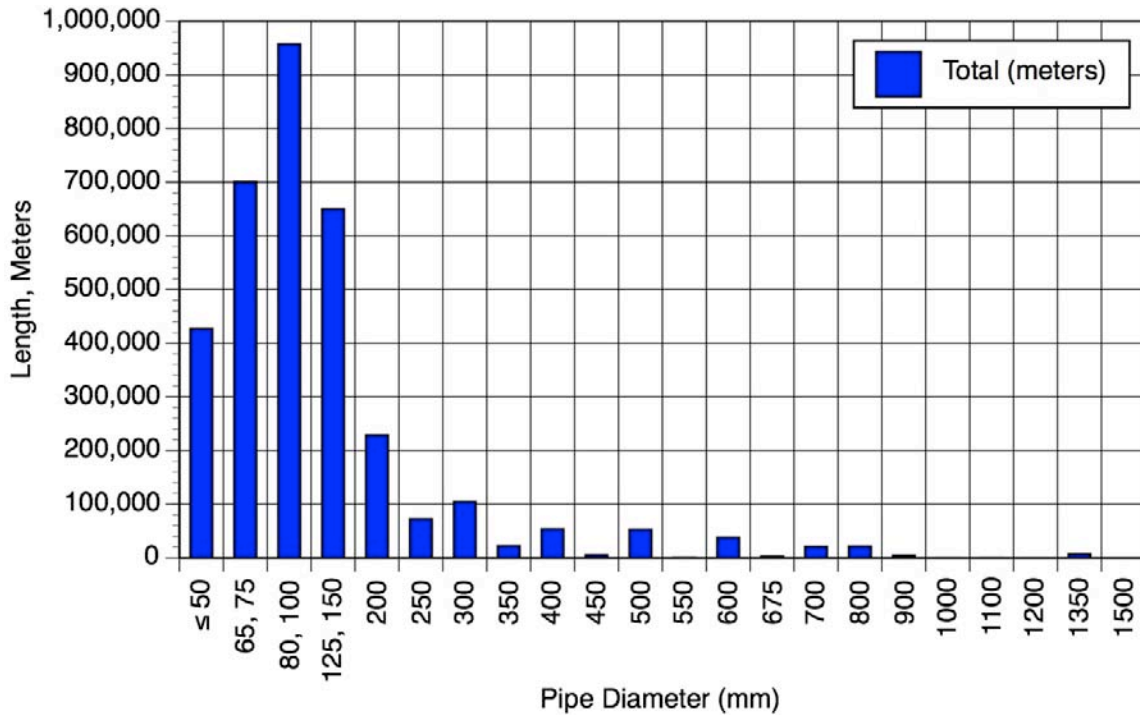


Figure 5-4. Pipe Length, by Diameter (Kumamoto City)

Figures 5-5 and 5-6 provide a further breakdown of the type of pipe materials used. The most common pipe is DIP (non-seismic design), followed by ER DIP (the bulk of which had been installed in the last decade). HDPE has been used for small diameter (2 inch and smaller) pipe.

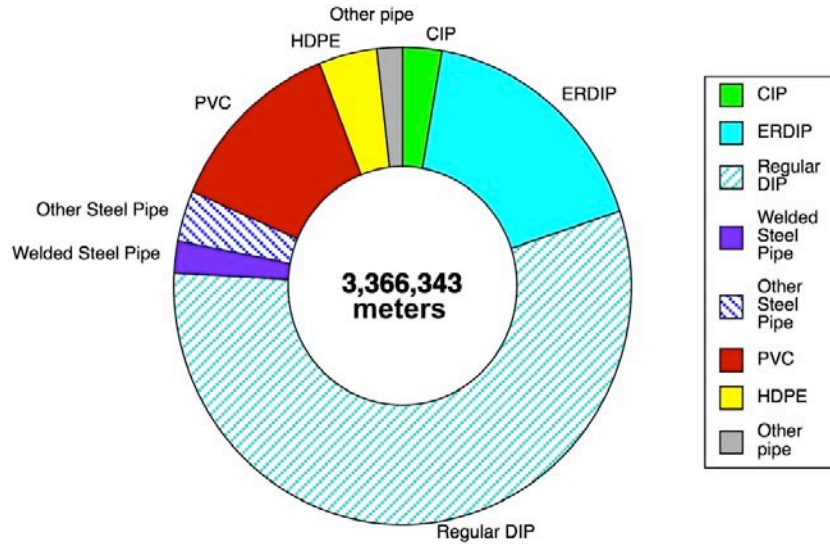


Figure 5-5. Pipe Length, by Material (Kumamoto City)

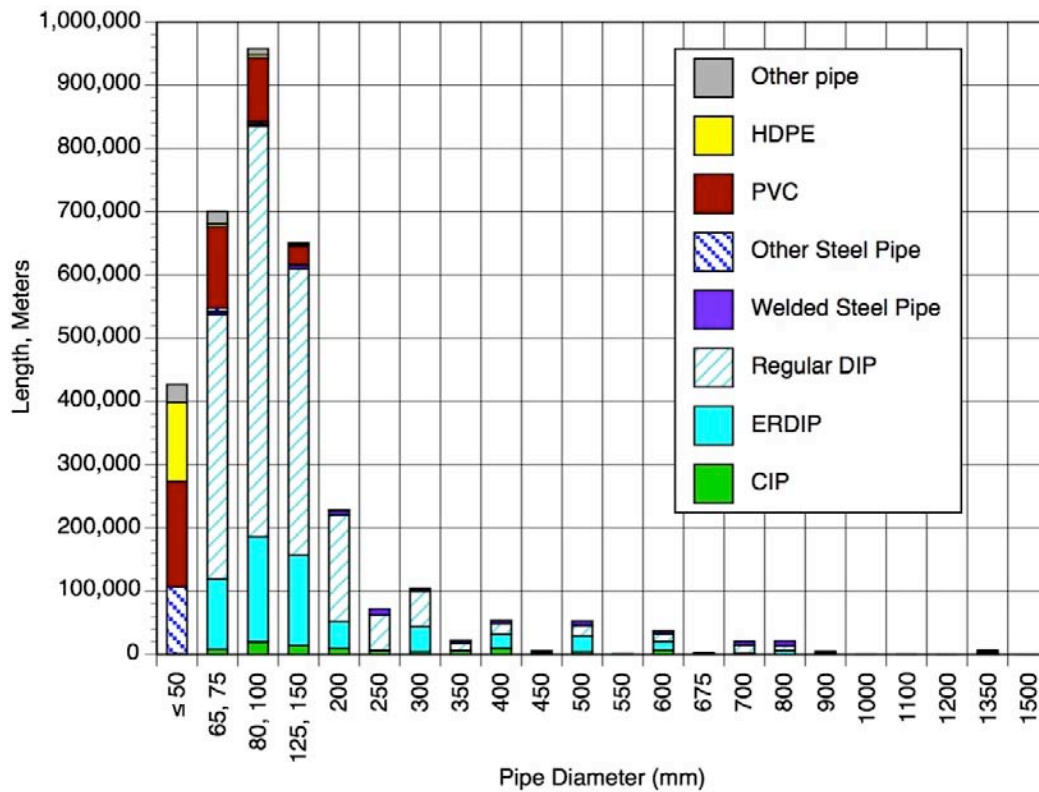


Figure 5-6. Pipe Length, by Material and Diameter (Kumamoto City)

5.3 Pipe Damage

Table 5-1 lists the repairs made to trunk pipes, as of June 1 2016.

#	District	Pipeline	Installation	Bridge	Location	Material	Size	Damage
1	East	Transmission	Buried		秋津町沼山津(送水場内)	Steel pipe	800	Crack
2	East	Transmission	Buried		秋津町沼山津(送水場内)①	Steel pipe	700	Crack
3	East	Transmission	Buried		秋津町沼山津(送水場内)②	Steel pipe	250	Crack
4	East	Transmission	Buried		秋津町沼山津(送水場内)	Steel pipe		Crack
5	East	Transmission	Buried		秋津町沼山津(送水場内)	Steel pipe		Crack
6	East	Transmission	Buried		秋津町沼山津(送水場1井戸建屋敷内)	Steel pipe		Leak of flange
7	East	Transmission	Buried		秋津町秋田(秋田配水場内)	Steel pipe		Split
8	East	Transmission	Buried		秋津町沼山津(沼山津7井)①	Steel pipe		Crack
9	East	Transmission	Buried		秋津町沼山津(沼山津8井)②	Steel pipe		Crack
10	East	Transmission	Buried		徳軍4丁目(庄口公園内)	Steel pipe		Leak of flange
11	West	Transmission	Buried		池上町(池上4井)	Cast iron pipe		Transverse crack
12	East	Trunk	Buried		秋津町沼山津	Steel pipe		Crack on bend
13	East	Trunk	Buried		秋津町沼山津	Steel pipe		Crack
14	East	Trunk	Buried		沼山津4丁目	Steel pipe		Crack on valve
15	East	Trunk	Buried		大瀬1丁目(徳軍水源地内)	Steel pipe		Crack
16	East	Distribution	Buried		新町町大字下舞田	Steel pipe	1350	Ruptured flange gasket
17	East	Distribution	Buried		沼山津3丁目	Cast iron pipe	300	Leak of flange
18	West	Distribution	Buried		池島町	Cast iron pipe	300	Crack on bend
19	West	Distribution	Buried		池島町	Cast iron pipe	250	Slip out
20	West	Distribution	Buried		上藤本3丁目	Steel pipe		Transverse crack
21	East	Trunk	Bridge attached	上沼山津橋	秋津町沼山津	Steel pipe		Overexpanded
22	East	Distribution	Bridge attached	青藤橋左岸	徳軍5丁目	Steel pipe	500	Crack
23	West	Distribution	Bridge attached	山王橋①	花園5丁目	Steel pipe	500	Overexpanded
24	West	Distribution	Bridge attached	山王橋②	花園5丁目	Steel pipe	500	Overexpanded
25	South	Transmission	Bridge attached	第2橋	八幡5丁目	Steel pipe	250	Transverse crack

Table 5-1. Trunk Line(14-inch and larger) Repairs (Kumamoto City)

Table 5-2 lists the repairs made to distribution and trunk pipes, as of June 1 2016. Table 5-3 highlights that about two-thirds to 80% of the damage is to appurtenances (air release and gates valves), with this percentage exceeding 80% on the largest diameter pipes (24-inch and larger)

Pipe Size and materials	50 mm	75 mm	100 mm	125-150 mm	200 mm	250 mm	300 mm	350-500 mm	600-700 mm	800 mm	Unknown	Total	Note
DI (ER Joint)							1					1	a
DI (general joint)			7	6	10	2	4	1				30	
Cast Iron pipe				3	4			1	3			11	
Steel pipe (not specified)				1	4	1	5	10	7	4	6	38	b
Hard PVC (PR long joint)												0	
Hard PVC (PR joint)												0	
Hard PVC (TS joint)			4	3								7	
Hard PVC (not specified)												0	
ACP												0	
HDPE (fusion bonded joint)												0	
HDPE (cold short joint)												0	
Joint coupling and Leak mended portion												0	
Material unknown												0	
Equipment: air valves and gate valves			6	7	11	10	1	2	33	21	46	8	145
Total	0	17	20	29	13	10	15	43	25	52	8	232	
Notes													
a. Damage was caused by incorrect installation													
b. Expansion pipe and expansion flexible pipe are included													

Table 5-2. Trunk and Distribution Repairs (Kumamoto City)

Category	14"+	3" - 12"	Total
Pipe body or joint	20	46	66
Air valve, gate valve, hydrants	100	45	145
Aqueduct on bridge	5	16	21
Total	125	107	232

Table 5-3. Trunk and Distribution Repairs (Kumamoto City)

Table 5-4 provides the pipe repair rates (for mains only).

Material	Repairs	Length (km)	Repair rate per km
ERDIP	1 (Note)	518	0.002
DIP	30	1887	0.016
CIP	11	98	0.112
Steel	38	186	0.204
ACP		0.2	0
PVC	7	432	0.016
HDPE	0	120	0
Stainless steel	0	5	0
Others	0	63	0
Subtotal	87	3,310	0.026
Appurtenances	145		
Total	232		0.07

Table 5-4. Trunk and Distribution Pipe Repair Rate (Kumamoto City)

Note . In Table 5-4, the single failure to a 300 mm ERDIP was investigate and found to have been caused due to incorrect installation. No ERDIP was located at locations that underwent fault offset.

In Table 5-4, we have separated out the repairs for appurtenances. In many past earthquake investigations, the damage to appurtenances have often been tabulated and attributed to the type of material used for the pipe main. This attribution little sense from a mechanical point-of-view, and in this report, we have enough data to be able to de-aggregate these failures. From the data for Kumamoto City, about two-thirds of the 232 repair locations for damage to pipe mains (generally requiring digging up the street) can be attributed to the appurtenances. The level of effort needed to make repairs to a 6-inch main, or an air-release valve on a 12-inch main, might be on the same order of magnitude, so from the perspective of manpower and equipment needed to make the repairs, the distinction in the style damage is not too important. However, from a seismic design perspective, the distinction of the style of damage can be very important, both in terms of planning for spare parts, as well as developing improved initial designs for appurtenances, both in terms of corrosion protection, as well as in terms of mechanical protection due to high PGVs or modest to high PGDs.

The relatively high rate of damage to large diameter steel pipes near the well field can be attributed to 10 to 50 cm of settlements that occurred in that area. Within the center of the liquefaction zone, where there are a lot of medium-to-large diameter steel pipe moving water from the wells, there were no reported pipe failures. However, where these larger pipes merge into an even larger transmission welded steel pipe that traverses from the liquefaction zone to an area without liquefaction, the steel pipe, along with appurtenances and branch pipes, had a high rate of damage.

In examining the data, the total repairs to mains (and their appurtenances) was 232, a figure that is "not too severe". Clearly, the replacement of older non-seismic pipe made for some improvement, given that the newly installed ERDIP faired essentially perfectly (a repair rate of 0.002 / km is considered as "nearly perfect". There were no failures of small diameter HDPE. Has ERDIP, HDPE (or similar) been used for 100% of the pipe inventory, and had proper seismic design been adopted for larger diameter steel pipes in / near liquefaction zones, the total repair quantity might have dropped to under 10 or so, a much easier problem to address, being only somewhat worse than the common pipe damage rate on any given cold day. It is evident that the strategy of pipe replacement with newer pipe materials with seismic design features (generally able to take 1% ground strain without damage) can be very effective; the cost effectiveness of this type of pipe replacement program must always be addressed, as for a median sized city (population on the order of 1 million), this cost might easily surpass \$1 billion, and certainly this will have an affect on water rates.

Prior to the 2016 earthquake, Kumamoto City had developed planning-level scenarios for possible damage to the pipeline system in future earthquakes. For their "worst case" type of earthquake, with fault rupture that extended through the city, the forecast was for over 1,000 pipe repairs. In the actual April 2016 earthquake, the fault rupture did not extend into the city, and little or no liquefaction occurred near the port area.

5.4 Restoration of Water Service

By far the largest level of effort to restore the water system in Kumamoto City was due to leakage of the pipe mains and service laterals. The following statistics highlight the repair effort:

- Between April 16 (1:25 am local time) and April 19, the City of Kumamoto had essentially a complete water outage, reflecting the shutdown of the wells due to water quality concerns. All wells reported an increase in turbidity (NTU), and by legislative rule, the system turns off these wells. Managers of the water utility reported that this led to "thousands" of complains by customers, overwhelming switchboards and personnel in the first few days post-earthquake; they suggested that "perhaps this rule was not wise" as it caused a lot of possibly non-important outages. No water borne disease issues were reported at any time during the recovery process from the earthquake. No "boil water alerts" were issued, an action that might be taken by some US regulatory agencies. No sewer backups were known to the water agency staff we interviewed (that is not to say that none

occurred). No locations were known to water utility managers to have required water for fire flows.

- During this time frame, up to 34 emergency water stations were set up (potable water delivered by tanker truck, peaking at 89 tanker trucks) so that people could get potable water from these trucks using bottles and containers. Figure 5-11 shows the equipment and manpower (peaking at 420 people) used for emergency water delivery by tanker truck.

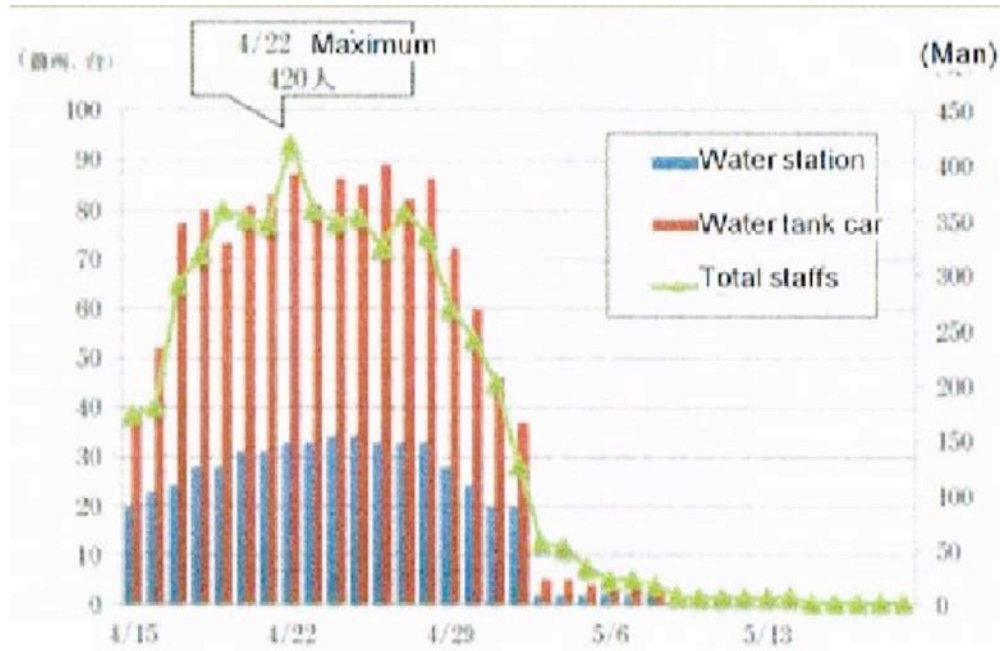


Figure 5-7. Emergency Water Delivery (Kumamoto City)

Figure 5-8 shows the quantity of tanker trucks in use in Kumamoto City and beyond.

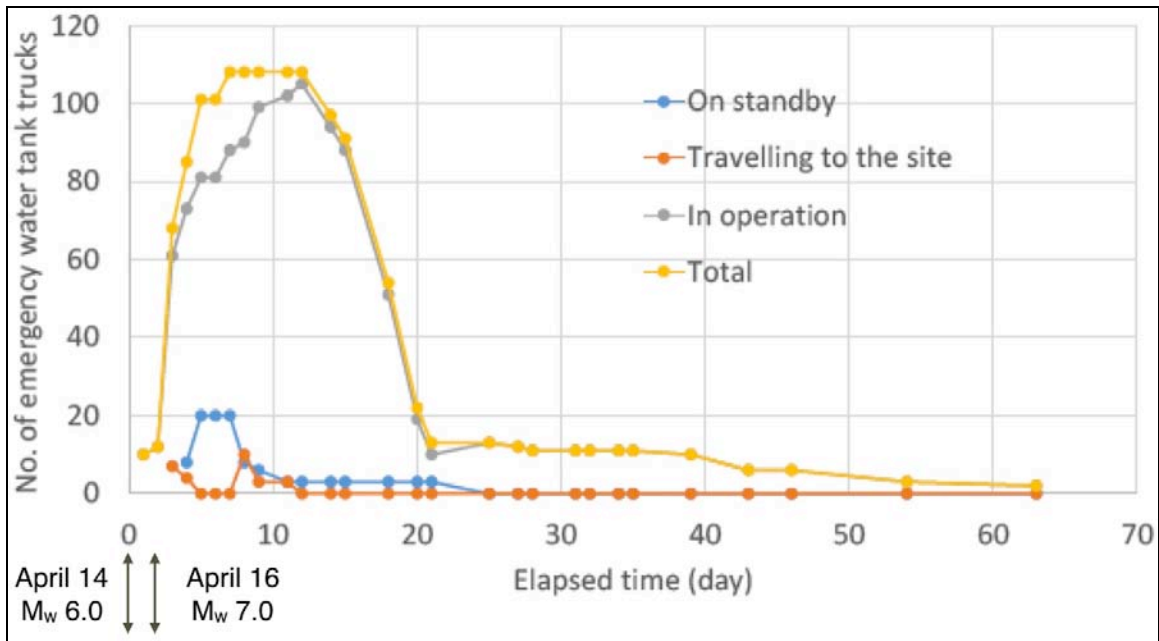


Figure 5-8. Emergency Water Tanker Trucks (Kumamoto City)

Figure 5-9 shows the number of households without water in Kumamoto City and beyond. The lower plot concentrates on the smaller towns outside of Kumamoto City.

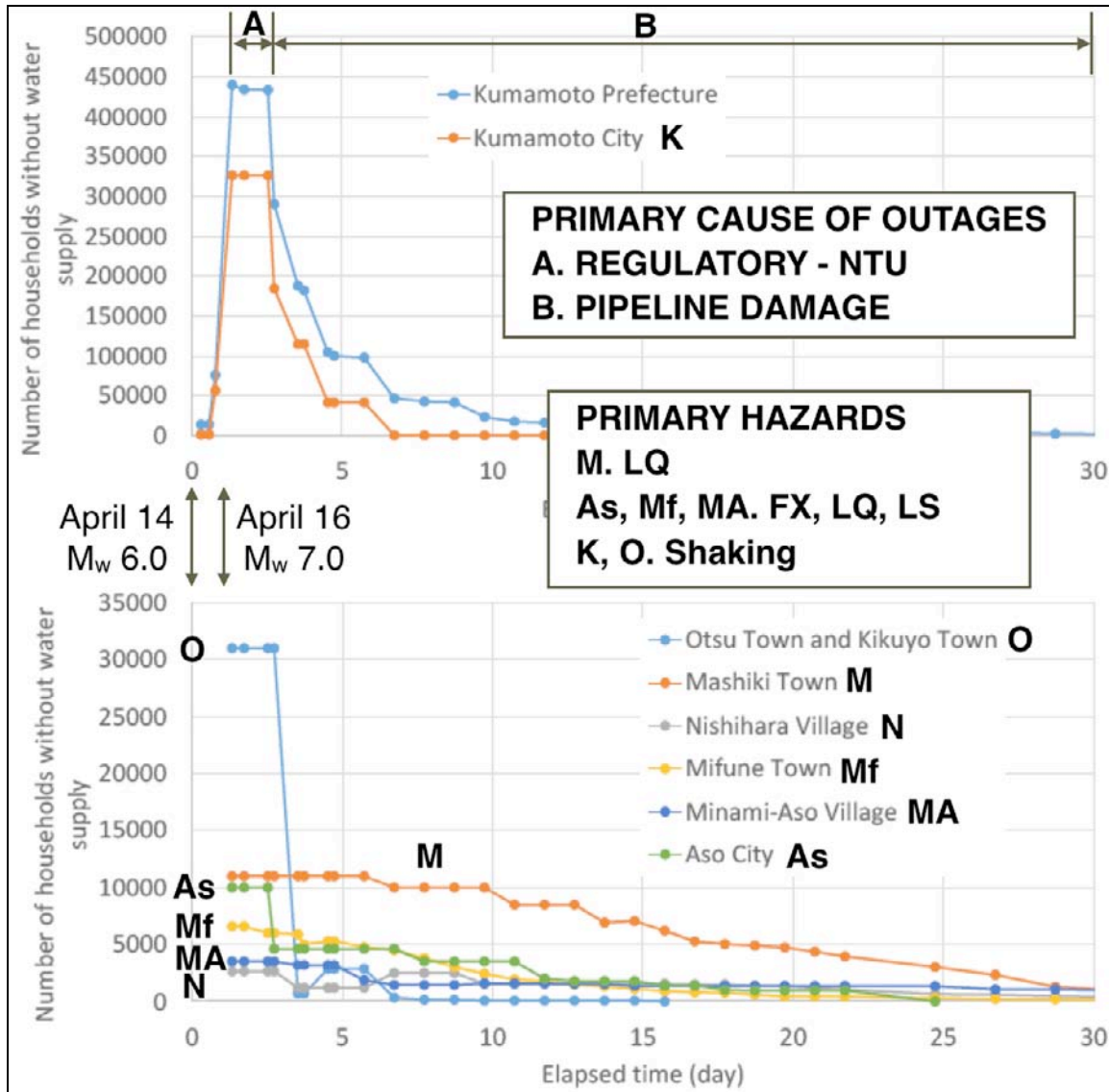


Figure 5-9. Water Outages (courtesy Maruyama)

The bulk of the water outages in the first three days was regulatory-driven, owing to the turbidity effects in the well supply. Over the longer term, damage to pipelines was the primary issue. In the lower plot, we highlight the primary hazards affecting each community are listed. While Kumamoto City is listed as "shaking", liquefaction did play an important part in pipe damage near one of the primary well fields.

- Between April 19 and April 25, 251 people were involved in identifying and isolating locations of leaks. These people came from 19 different municipalities, 2 authorities and JWWA. During this time frame, water supplied into the water system peaked at 287,000 m³ / day, or about 33% higher than the then average day demand, with the supply gradually being reduced to about 20% higher than the average day demand as leaks were identified and isolated / repaired, coupled with water conservation efforts.
- Between April 26 and May 17, 5,166 people were involved in identifying locations of leaks and making repairs. These people were organized in 58 groups (crews), with the people supplied from 75 different companies other than the city of Kumamoto.
- Between April 26 and May 31, 1,379 people from the City of Kumamoto were involved in identifying locations of leaks and making repairs.
- By May 31, the quantity of water being supplied was nearly normal, and the bulk of the repair effort was completed. By May 29, some 3,644 leak investigations had been done, and 3,444 repairs had been completed.

Figure 5-10 plots the outages in terms of the percentage of households receiving water. The longest duration for restoration of water service is shown as Minami-Aso village, a small community that had suffered major PGDs due to fault offset, and had many damaged buildings, some of which were occupied, and some of which were not occupied. Restoration of customer service to the "last customer" in areas with many collapsed or partially collapsed buildings is often problematic, reflecting "chicken-and-the-egg" issues, factoring in that the households who would normally need water are gone / displaced, so why restore water service quickly to those customers? And also, if the is no water service restored, why re-building the damaged buildings?

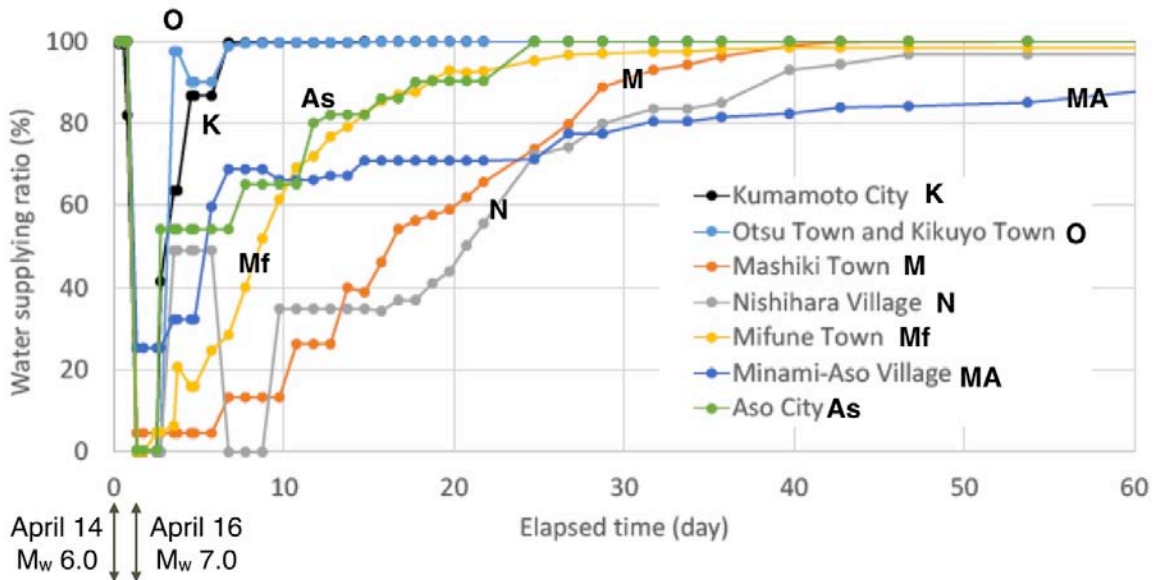


Figure 5-10. Percentage of Households with Water. Smaller towns had a much higher ratio of PGDs as compared to Kumamoto City (courtesy Maruyama)

Figure 5-11 shows a map of Kumamoto Prefecture and surrounding communities that were affected by the earthquake. This map was prepared by Profs. Nojima of Gifu University and Prof. Maruyama of Chiba University, using the underlying data in Figures 5-9 and 5-10.

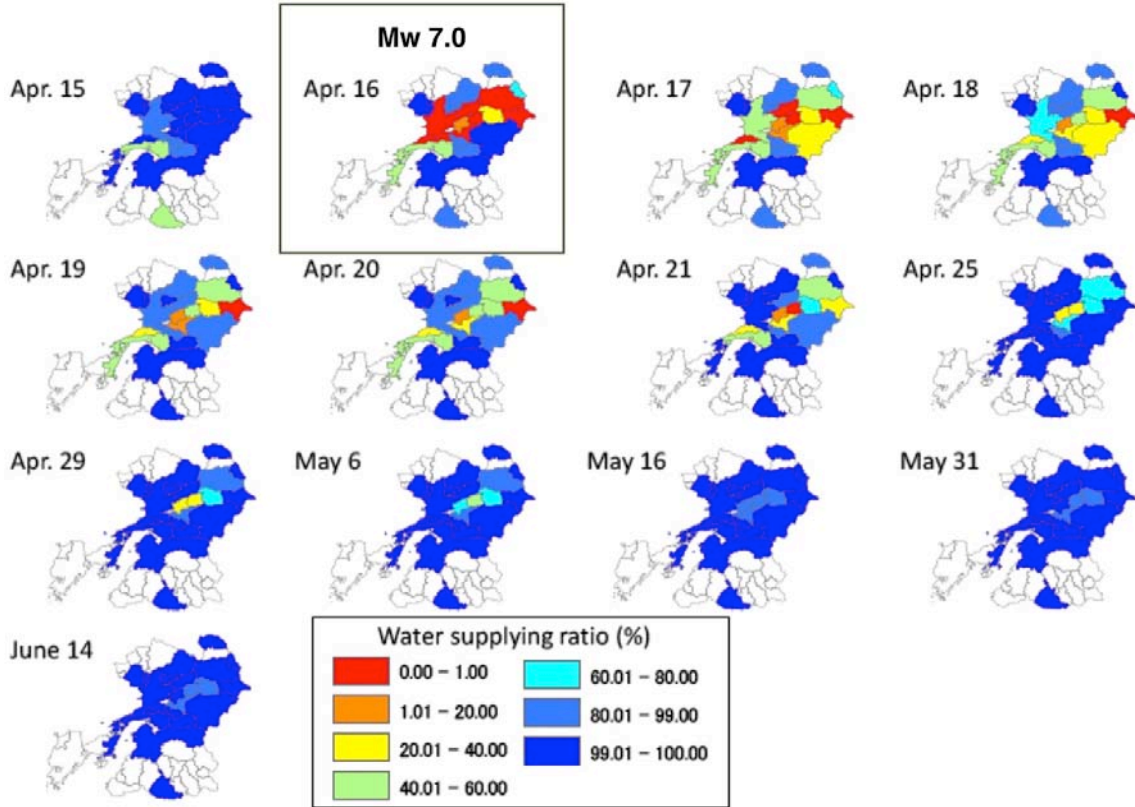


Figure 5-11. Map of Percentage of Households with Water (courtesy Maruyama)

Figure 5-12 shows a water tank car with hose bibs set up to allow local residents in Mashiki Town to obtain potable water, still in use as of July 5 2016. There were many partial and complete collapsed buildings in this area.



Figure 5-12. Water tank car in Mashiki Town, July 4 2016

5.5 Pipe Replacement for US and Canadian Water Utilities

This earthquake, and many other earthquakes worldwide, exposed the primary vulnerability of water utilities: damage to buried pipes. In the US and Canada, the vast majority (>99%) of buried water pipes have been installed without any seismic requirements. This "Achilles heel" of water systems remains a serious weakness.

One brute-force way to solve this weakness is to replace these vulnerable non-seismic pipes with new, seismic-resistant pipes. In the USA, the major "code writing" organizations, namely AWWA and ASCE, have been nearly silent on this topic. Neither AWWA or ASCE have code-style "standards" for seismic design of water pipes; in fact, the AWWA manual for the design of steel pipes (M11 2004) ignores seismic loads; for example, the details for welding girth joints for steel pipes as outlined in AWWA M11 are deficient and lead to joints much less capacity than the main barrel of the steel pipe, thereby undermining much of the potential ductility of steel pipes; so the continuing use of M11 for design of steel pipes is propagating the installation of more badly-designed pipe from a seismic perspective.

TCLEE has published dozens of reports over the past five decades that document problems and weaknesses of buried water pipes in earthquakes.

Reflecting these issues, a task group was organized in 2004 under the auspices of the American Lifelines Alliance. That task group developed and issued a report called the "Guidelines for Seismic design of Water Pipes" (ALA 2005). Today (2017), these Guidelines remain the single core document in the USA that gives comprehensive guidance as to how to approach the design of new or replacement water pipes for seismic issues. In 2004, this task group made a conscious decision to call the document "Guidelines" rather than a "Standard", meaning that the task group intended the Guidelines to be entirely voluntary. Why were they made voluntary?

The task group, being composed of engineers from water utilities, consultancies and universities, were especially worried about the cost effectiveness of pipeline replacement strictly for seismic reasons. The task group's concern was that while there are definitely newer water pipe materials and designs (for example, Kubota's seismic resistant "chained" ductile iron pipe Figure 5-16, HDPE Figure 5-17, etc.) that can be extremely reliable to accommodate high levels of ground shaking and moderate to large permanent ground deformations, the installation of these pipes will be expensive and capital intensive. The incremental benefits these seismic-resistant pipes bring derive from avoiding earthquake-induced water outages for earthquakes with rather long return intervals. For new subdivisions, the incremental cost of seismic-resistant pipes versus "standard non-seismic-resistant" pipes might be very small (or nil), and it makes good economic sense to use them in seismic prone areas. For replacement of older existing pipes, the cost of the seismic-resistant pipes might not often be cost effective, when considered on a full life cycle basis, with the alternative of the "do-nothing" alternative coupled with a reasonably well thought out emergency response plan to deal with broken pipes after a rare earthquake.

It is this author's observations that essentially no US water utility serving a moderate-to-large community (say about 1,000,000 people or more) is truly prepared to ramp up to several thousand people to take care of all the pipe damage and its ancillary effects that an earthquake can cause. Most water utilities serving a population of 1,000,000 people are easily able to manage repair for one or two pipe breaks per day using its regular manpower and equipment and spare part resources; with few economic impacts and few customer complaints; but few (if any) water utility can manage a situation where several thousand pipe repairs must be dealt with simultaneously. This will lead to long restoration times for water service. Even "industry leader" water utilities like EBMUD still face, as of 2017, the potential for several thousand pipe repairs in a single future earthquake, and with manpower limitations, restoration times to reach nearly 100% restoration of water service might take many weeks (or months). For the customers without water for weeks to months, the economic impacts will be large, and customer anger at the water utility might become unbridled. If one ignores the political issues of public versus private ownership of water utilities, the public's perception of incompetence on the part of the affected water utility's management will become poor if widespread outages last much longer than a few days; if unchecked fires turn into conflagrations, one

could easily imagine public outcry that water utility management should be "hung from the yard arm" or its modern day equivalent; and untold numbers of lawsuits. Whether any post-disaster use of the court system will much good (other than trying to line the lawyers' pockets with gold at the expense of the public), remains a topic open to debate; and hopefully that topic will never arise.

It would seem prudent that to avoid being called negligent, that modern-day water utility managers should inform and quantify for themselves of their earthquake exposure, and then make informed decisions as to how to proceed. If one takes a prudent long term course of action, one could be inoculated from the charge that the modern-day water utility has "lined its pockets" at the expense of its customers. In some fashion, the water utility manager can quantify whether the "no pipe replacement / rely on post-earthquake response" approach (lower initial capital cost for customers, but larger post-earthquake economic losses) is a more cost effective long term strategy than a "do some pipe replacement / have a good emergency response plan to deal with residual weaknesses" approach.

What the public does not easily grasp is that the economics of pipeline replacement with seismic resistant pipe is a costly business. And yet it is up to today's water utility managers to understand these economic issues, and then make an informed decision as to whether, or not, to replace old and seismically-weak pipe with new seismic-resistant pipe. This type of program, for a community of 1,000,000 people in California, will cost around \$7.6 billion dollars. For example, if the average pipe diameter is 8 inches and a City of 1,000,000 people has 3,000 miles of pipe to be replaced, and the average cost of replaced pipe is \$60 per inch-foot, then a full pipe replacement program will take about \$7.6 billion dollars (in constant 2017 dollars). This translates to a capital cost per capita of about \$7,600. If one amortizes this capital cost over 15 years (reflecting a rather rapid time duration to accomplish the work), the capital cost per capita per month is about \$42. For an average household of 2.5 people, this translates to a capital cost on the order of \$100 per month, or perhaps doubling the average water utility bill per household. Most likely, the rate-paying public will not happily embrace a doubling of the water rates.

Clearly, a smarter approach for pipe replacement is needed than a simple "brute force, replace it all" strategy.

Excluding seismic issues, there are three other reasons for water utilities to replace pipe. These include:

- Water pipes continue to age, and with time, water pipes will deteriorate due to the effects of external and internal corrosive attack, erosion and damage to internal liners, tuberculation. When this accumulated damage becomes severe enough, resulting in a pipe repair rate much in excess of about 0.3 to 0.5 repairs per mile per year, it will clearly become cost effective to replace these old pipes. There is no single "replacement time cycle" applicable to all pipes; in passive soils, a well-constructed cast iron pipe installed in 1910 might remain economically viable for

200 years or longer, whereas the same pipe installed in aggressive soils might remain economically viable for only 30 years or less. Water utilities who replace older cast iron pipe that have been experiencing relatively low repair rates (much under 0.10 repairs per mile per year) are probably replacing pipes too quickly / in a non cost-effective manner, if one ignores concurrent seismic issues.

- Water pipes also need to occasionally be replaced due to changes in water demand (peak demand or fire flow demands).
- When new highways are built or streets re-routed, older pipes often need to be replaced or rerouted.

It is beyond the scope of this report to examine these all these pipe replacement issues. The author has written extensively on the economics of replacing pipe due to a combination of seismic and aging-related issues, as for example (Eidinger 2010, 2015, 2016). Many water utilities replace about 0.2% to 0.4% of their pipe inventory, per year, based on non-seismic issues, and the capital costs for such replacement are already "baked in" to ongoing water rates. What is often apparent in these ongoing pipe replacement programs, is that most (but not all) of water utilities continue to replace the older pipes with newer non-seismic pipes. Thus, these water utilities are making the potentially costly mistake that they are making little or no improvement for seismic issues, even if the differential capital cost is tiny or nil.

The failure by water utilities to adopt ALA 2005 as part of their ongoing work when pipes are being replaced for non-seismic issues is only "punting" the problem down the road, and is likely a non cost effective strategy in seismic-prone regions. Water utilities in high seismic regions (including much of California, Oregon, Washington, Alaska, Utah, New Madrid Zone, Charleston Zone, all of Vancouver Island, the Lower Mainland of British Columbia (including communities from Vancouver to Abbotsford) should be encouraged to adopt ALA 2005, or possibly its successors "manuals of practice" or "standards", as being an example of sound economic and management practice. If a water utility develops a capital budget to replace between 0.5% to 1% of its pipe inventory per year, then over a 30 to 75 year time frame, the majority of the seismic weaknesses of buried pipes can be eliminated, with the residual vulnerabilities addressed though an aggressive and well thought out emergency response plan.



Figure 5-13. Kubota Chained Seismic Resistant Ductile Iron Pipe



Figure 5-14. Seismic Resistant High Density Polyethylene Pipe Using Electric-Fusion Joint Coupling System

5.6 Pipe and Facility Performance

Figure 5-15 highlights a part of the water system in southern Kumamoto City that experienced PGDs, enclosed in the yellow dashed line. Common settlements in this zone were on the order of 10 to 50 cm. Some lateral spreads or the levees likely occurred in this area at the river embankments, possibly under water, as the top of some of the levees surrounding the rivers were settled.

Most of the large diameter steel pipe damage occurred at or within 100 pipe diameters of the transitions from this zone to the non-liquefied zones to the immediate north.

We visited several of the water wells and the two facility locations highlighted with circled "P" in this area. At the easternmost "P" location there are two pile-supported prestressed concrete storage tanks (about 2,400,000 gallons each), plus a chlorination facility plus a pump station. At the southernmost "P" location there are two pile-supported prestressed concrete tanks (about 5,300,000 gallons each), plus several pile-supported buildings with pumps, and various water quality equipment.

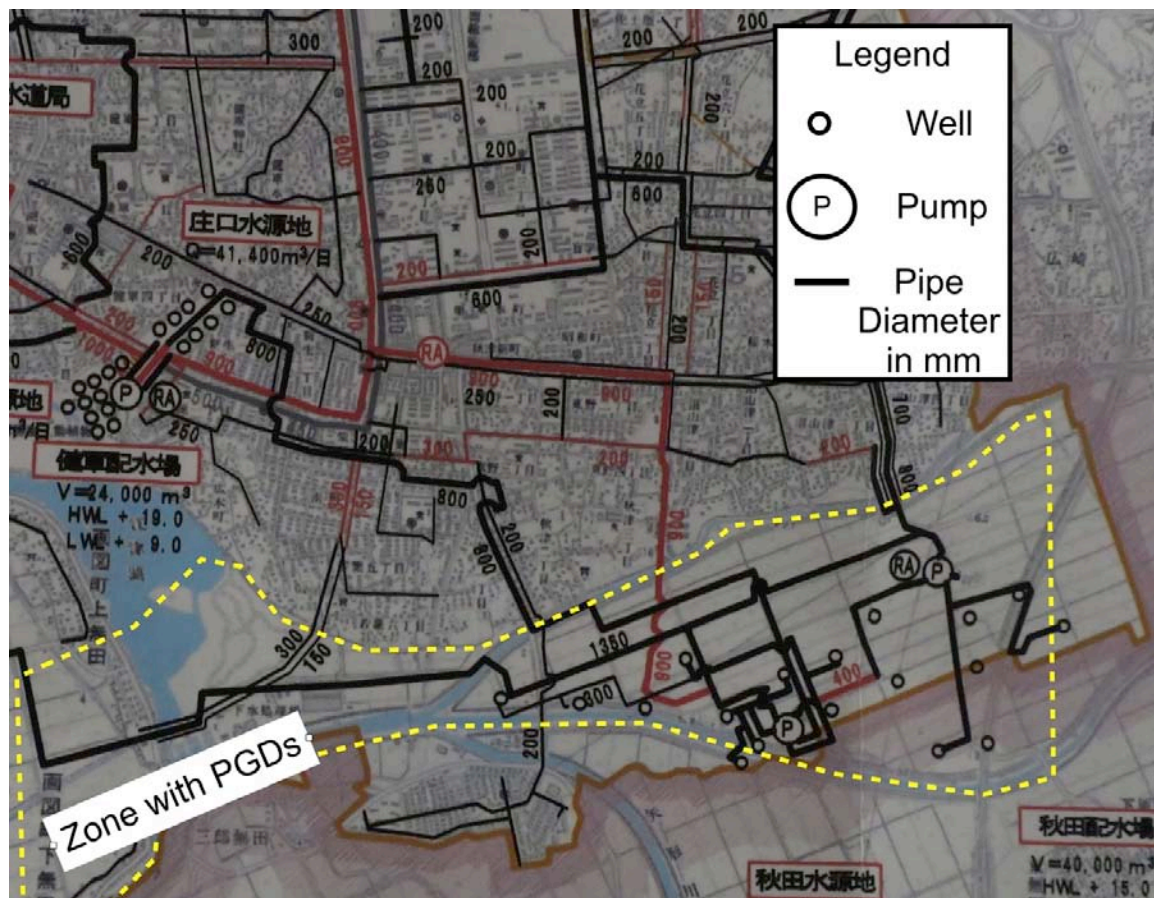


Figure 5-15. PGD Zone in southern Kumamoto City water system

Figures 5-16 to 5-29 show the pipe damage in the area highlighted in Figure 5-15.



Figure 5-16. Leak of 3-inch High Impact PVC (HIVP) Pipe, near Nichome Akitsu

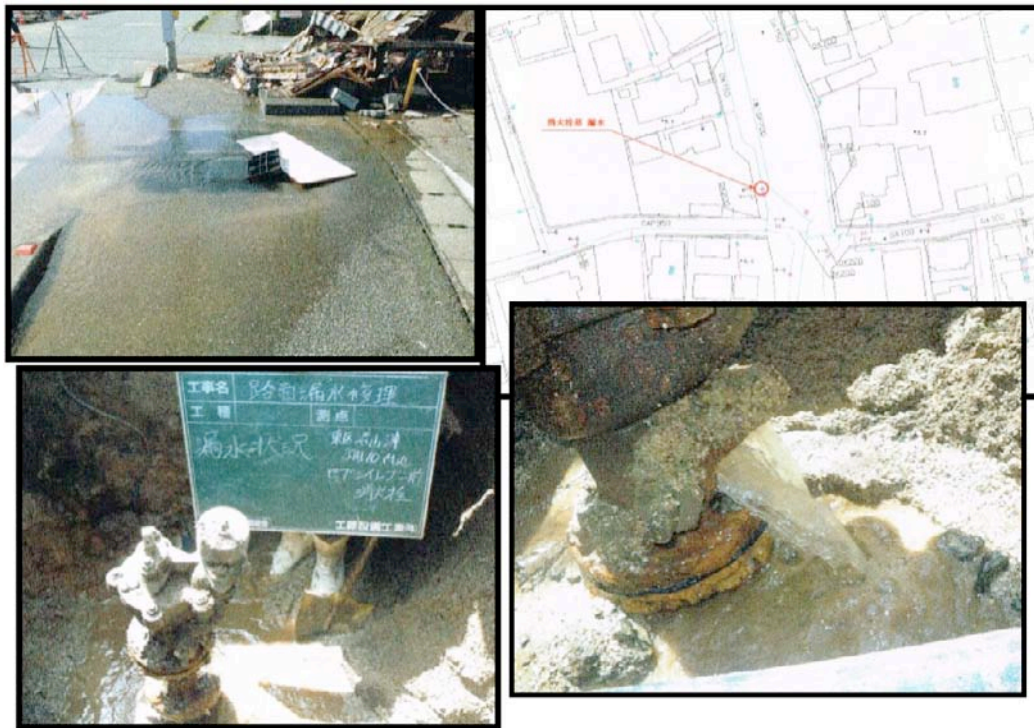


Figure 5-17. Leak of 150 X 75 mm (6x3-inch) fire hydrant, near Sanchome Numayamazu



Figure 5-18. Leak of 350 mm (14-inch) cast iron pipe, near Sanchome Numayamazu

Figure 5-19 shows an aerial view of the westernmost portion of Figure 5-15. The 1350 mm steel pipe in the zone in the large black circle was damaged. Figures 5-20 to 5-22 show the leak and the equipment used during the repair of this pipe. Just to the east of this location is one of the wastewater treatment plants for Kumamoto City, at the confluence of two rivers; this plant suffered various types of damage to pile supported structures.



Figure 5-19. Location of 1350 mm Steel Pipe Repair near Ezumachishimomuta

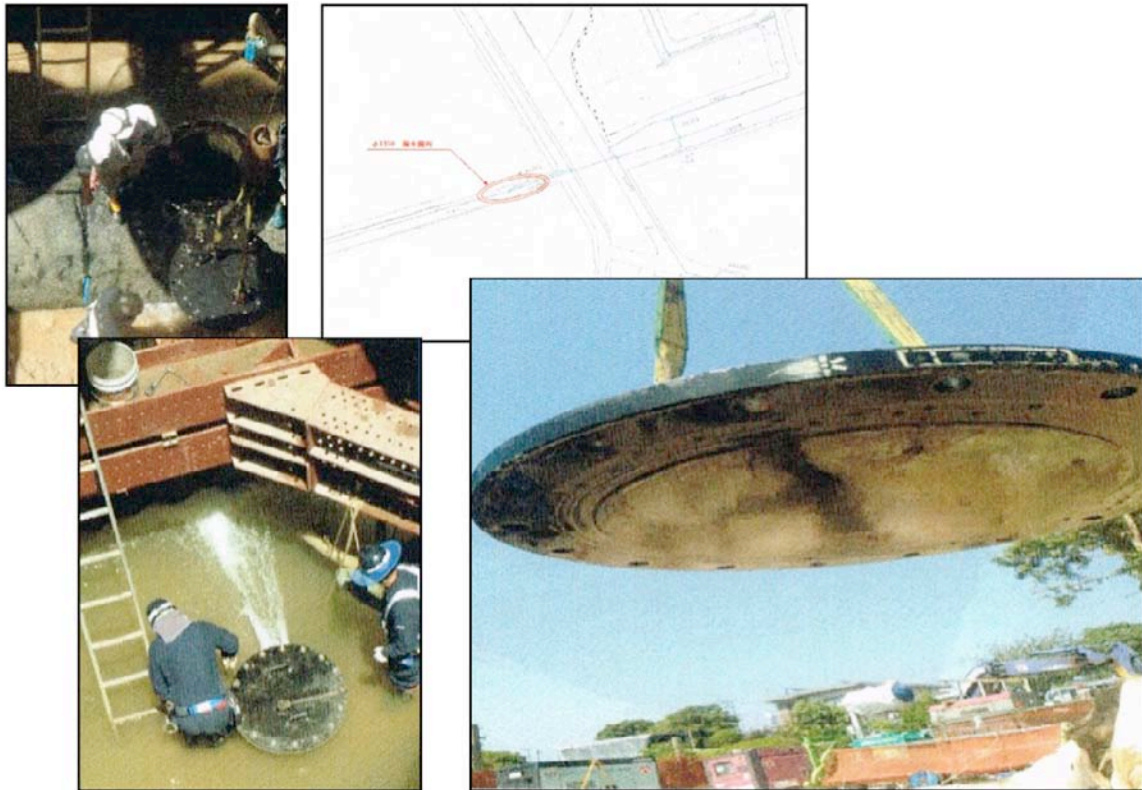


Figure 5-20. Excavation of 1350 mm Steel Pipe. Flange is bent and leaking

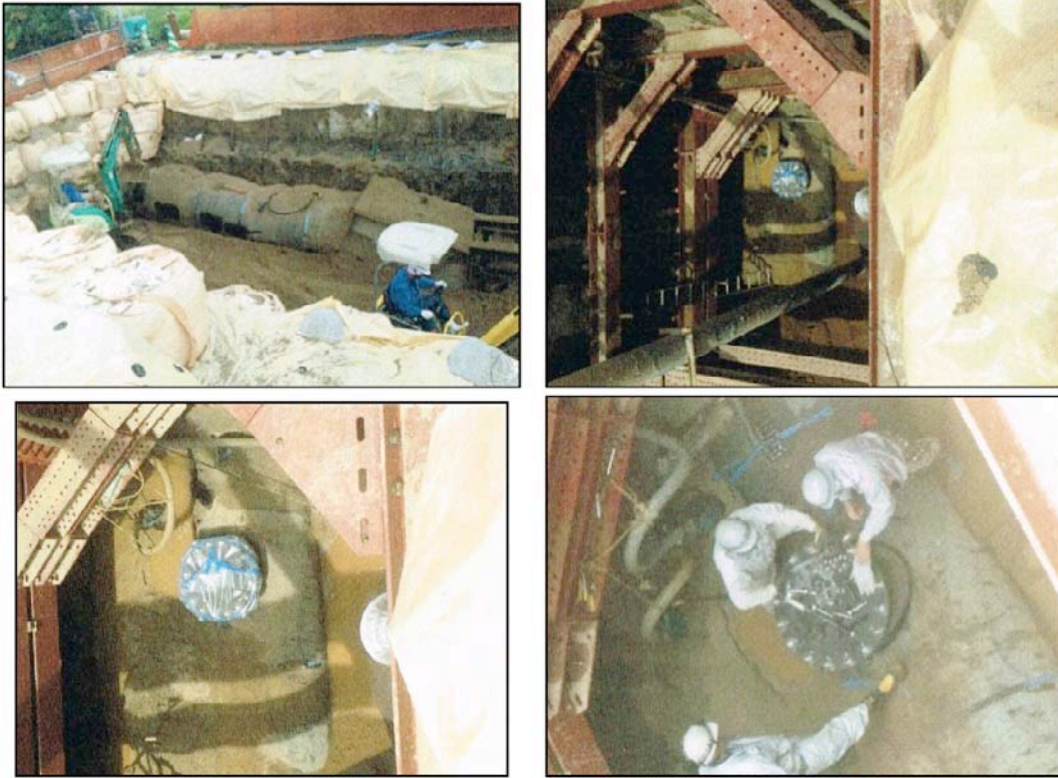


Figure 5-21. Repair of 1350 mm Steel Pipe



Figure 5-22. Completing Repair of 1350 mm Steel Pipe

Figure 5-23 shows a map of a location with 7 pipe repairs near the Kaminumayamazu bridge. In Figure 5-23, the red dot shows the location of the 32-inch steel pipe, on the bridge, that was leaking. Figure 5-24 shows the location and repair of a 150 mm pipe (DI with mechanical K-type joint).

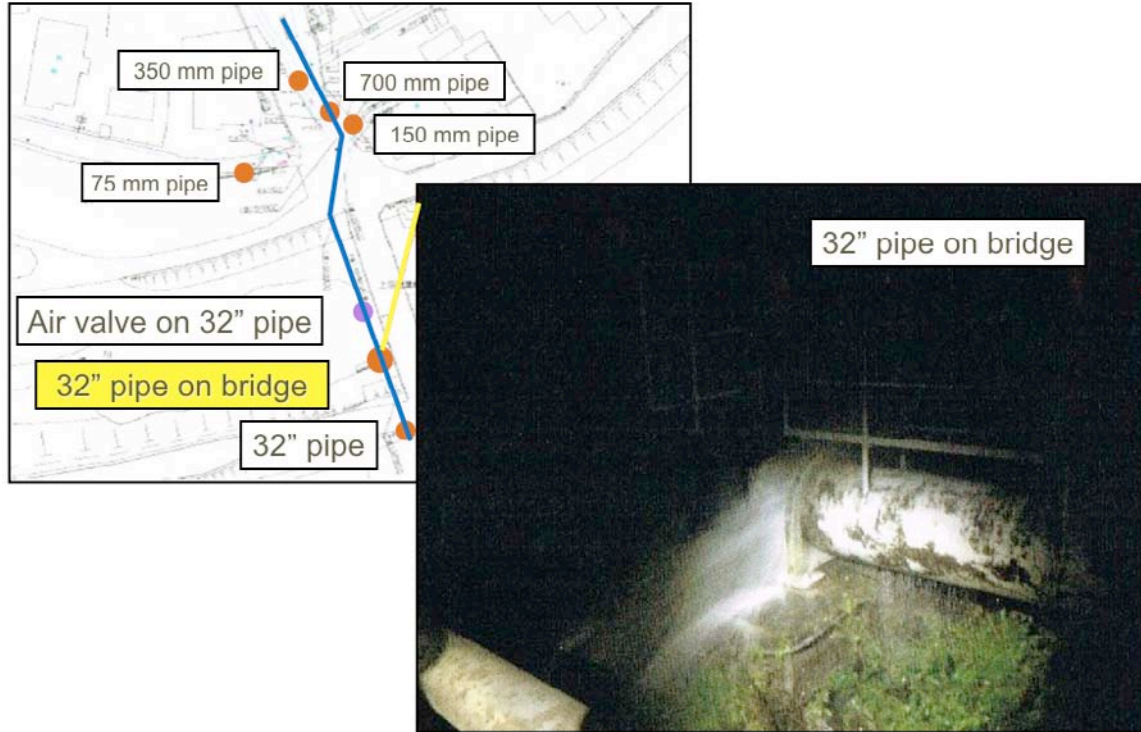


Figure 5-23. Repair of 32-inch steel pipe on bridge

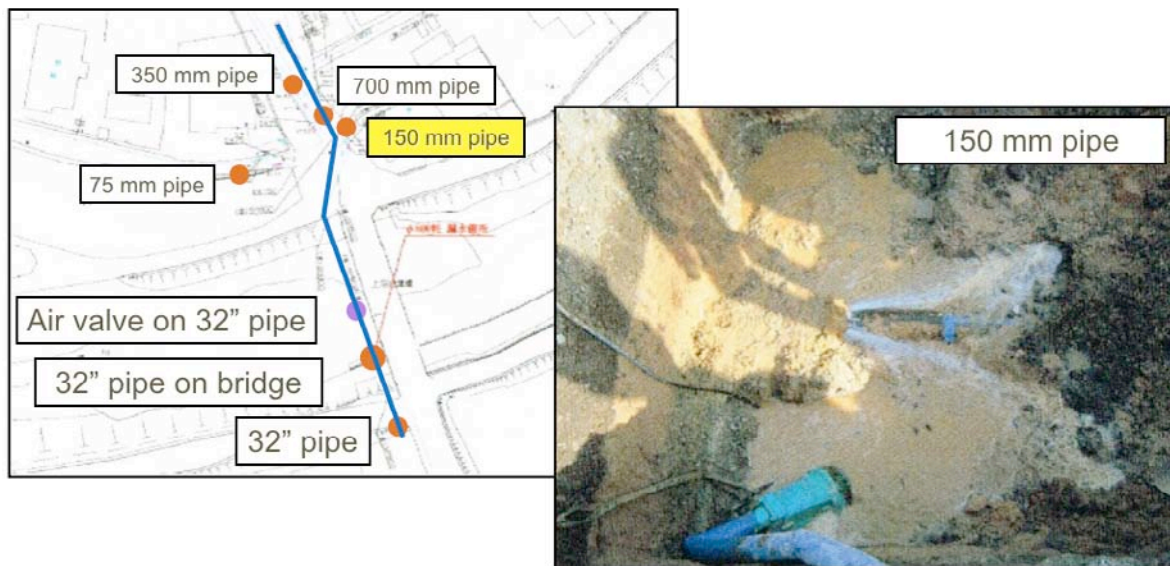


Figure 5-24. Repair of 150-mm ductile iron pipe (K-type joint)

Figures 5-25 and 5-26 show the location and repair of a 800 mm (32-inch) steel pipe just south of the bridge. The failure is likely due to PGDs at the river / levee location.



Figure 5-25. Repair of 800-mm steel pipe south of the bridge

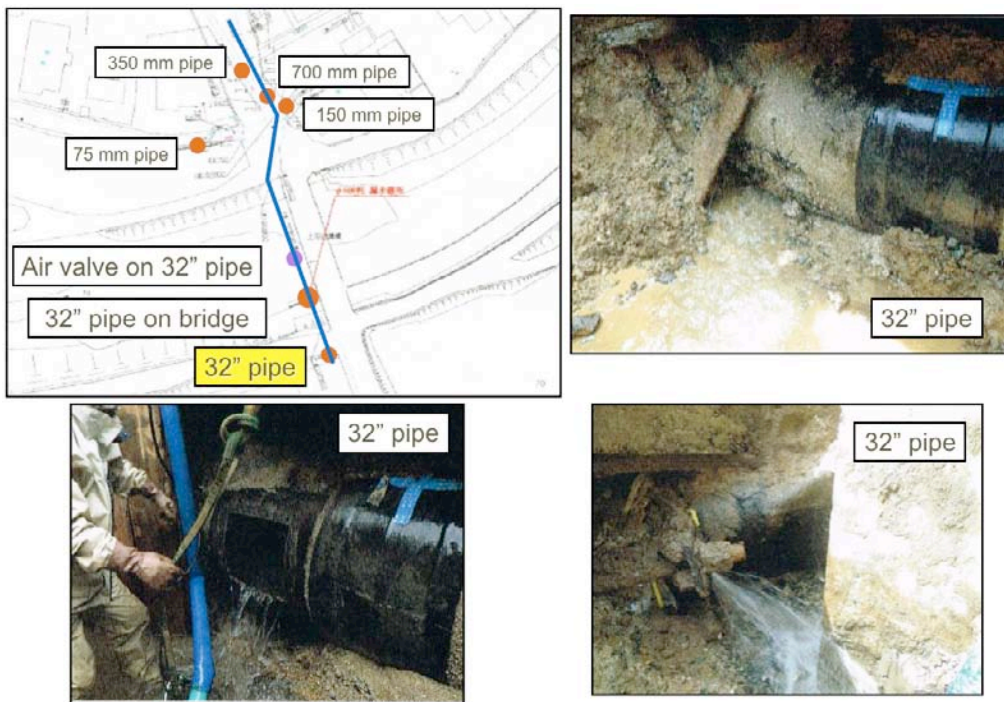


Figure 5-26. Repair of 800-mm steel pipe south of the bridge

Figures 5-27 and 5-28 show the repair of a 700 mm pipe just north of the bridge.

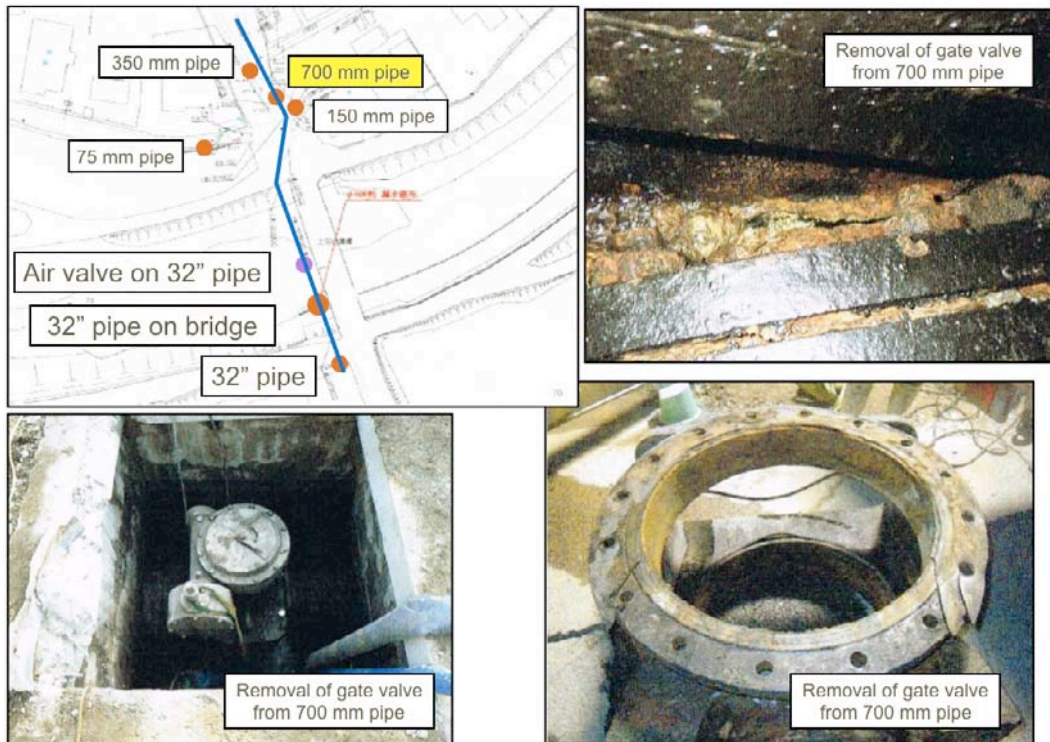


Figure 5-27. Repair of 700-mm steel pipe north of the bridge

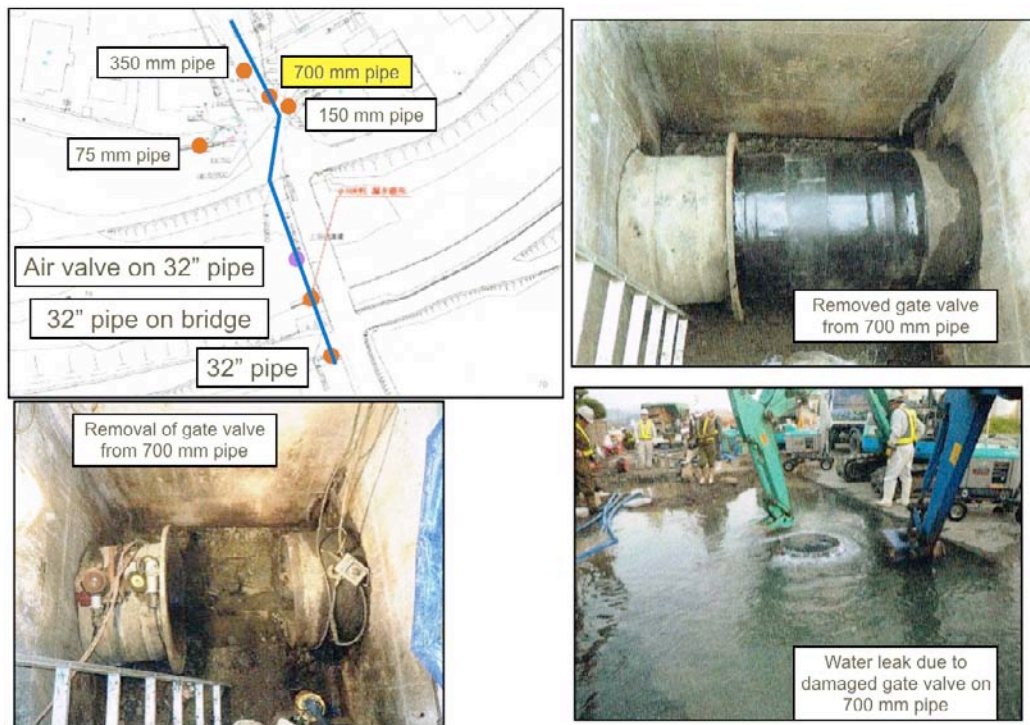


Figure 5-28. Repair of 700-mm steel pipe north of the bridge

Figure 5-29 shows the repair of a 75 mm DI pipe near the bridge.

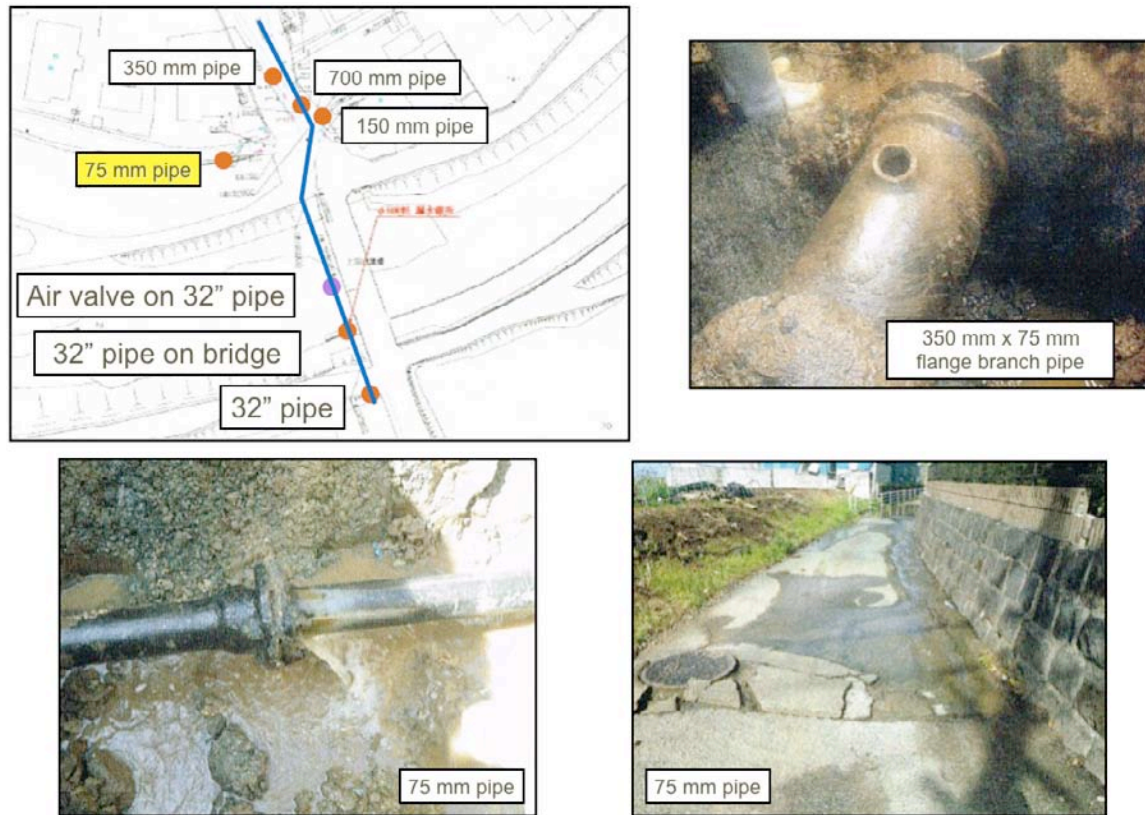


Figure 5-29. Repair of 75-mm DI pipe north of the bridge

Figure 5-30 shows the two 2.4 MG (9,000 m³ x 34 meter diameter x 10 m height) pile-supported concrete tanks. The blue tarps on the left tank were placed as part of ongoing repair efforts for earthquake-related damage, as of July 2 2016. Both of these tanks had been seismically upgrade prior to the earthquake, using a system of externally-added drilled piers, Figure 5-31. It appears that the external piers were added by doweling into the original foundation, with the intent that the seismic base shears form the tank be partially resisted by the new external piers. The intent of this type of upgrade would be to reduce the base shear resisted by the original vertical-load carrying piles, and hence reduce the ductility demands on the piles and reinforced concrete floor-to-pile connections. There was damage to the tanks in the earthquakes, as follows:

- The thickened-portion of the circular walls that serve as tendon anchor points for the circumferential post-tensioning cables. At the base on one of these thickened wall sections, the concrete as spalled and blow out. The cause(s) for this damage might include high compressive forces due to local wall bending (this seismic load pattern is commonly ignored in US design following AWWA D110). With the damage comes a loosening of the tendon anchorage points, and thus a loss of prestress load around the lowest elevation of the tank.

- The water utility staff noted that they did not think the tank was leaking, but they were removing all the top concrete of the exterior basemat (original plus extension of the exterior piers), to visually examine for damage. We observed the progress they were making in this effort, and observed no gross damage to the exposed rebar. We inquired if the water utility was further planning to expose the condition of (at least some) of the buried piles, and they reported that "at this time, we are not, in part because that would be expensive).



Figure 5-30. Two Pile-Supported Concrete Tanks

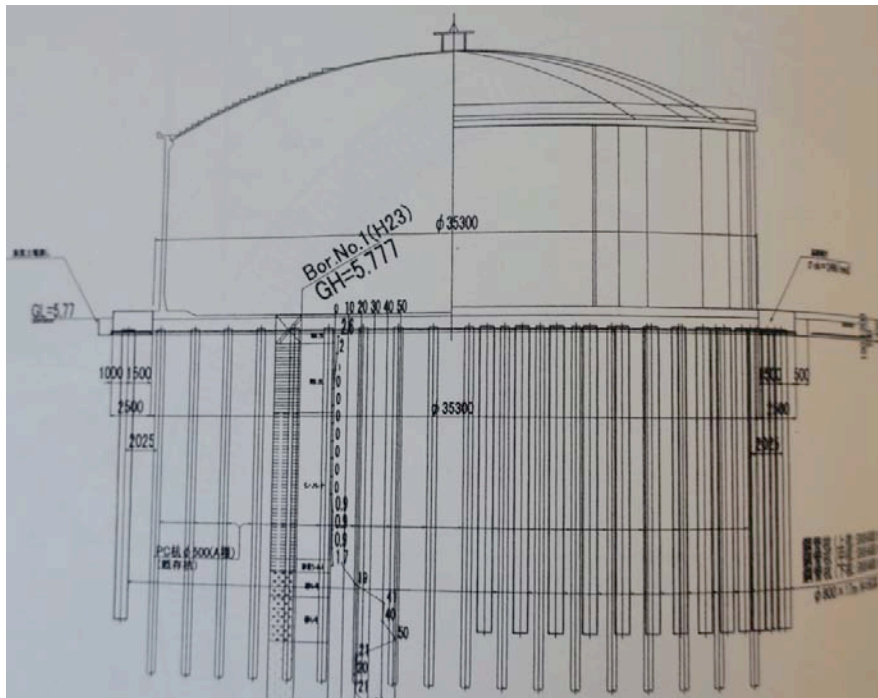


Figure 5-31. Piers and External Seismic Piers for Tanks in Figure 5-30

In considering the style of observed damage, we think that the tanks were likely exposed to PGA about 0.3g to 0.5g, coupled with local soil settlements on the order of a few cm. The settlements would not have seriously harmed the tanks, as they were pile supported, and attached pipes were installed with flexible fittings able to absorb these modest differential movements. The efficacy of the external driller piers might have been useful to relieve some of the lateral seismic base shears off the piles, thus reducing their level of damage / yield due to high bending moments.

Figures 5-32 and 5-33 show two of the tendon anchor points. The inset in Figure 5-32 shows the damage observed the day of the earthquake, and the main image in Figure 5-32 shows the condition 10 weeks after the earthquake, after the spalled concrete has been removed. In these photos, the plastic pipes are roof drains from the tank's roof, and have no bearing on the performance of the concrete. The exposed rebar in the main photo in Figure 5-32 and the blue tarp in Figure 5-33 reflects that the utility was in the process of chipping away the concrete cover of the basemat at the time these photos were taken (July 2 2016).



Figure 5-32. Damaged Tendon Anchor Point, with Gross Spalling



Figure 5-33. Damaged Tendon Anchor Point, with Incipient Spalling

The use of thickened walls as in Figures 5-32 and 5-33 to provide tendon-anchor points for "fixed base" type concrete tanks looks to be an inherent weakness, as those locations must attract locally high bending forces as the tank wall bends. The vertical tank walls in these photos were constructed monolithically with the tank foundation, a so-called "fixed foundation" system for prestressed concrete tanks, still allowed in modern USA AWWA D110 codes. Possibly this type of design should require $R < 1.5$ or so, or perhaps "ductility" should not be allowed at all ($R = 1$), or otherwise be detailed to ensure that the concrete can never spall due to the high compressive forces it will attract, in any fashion that might allow deterioration of the tendon anchorages. If further investigation shows that the tendon anchorage might have been impaired, leading to a loss of prestress, then the tank will not be leak-tight. For designers, it must be cautioned that the hoop stress provided by the steel wires / tendon system should ideally be designed to remain elastic under the highest seismic loads; no yielding in these wires should ever be contemplated in design, as yielding implies permanent lengthening of the wires, and thus reliance on hoop tension in the concrete, which will generally not be reliable. Modest hoop direction yielding will result in leakage of the water; major yielding (much over 3% or so) can lead to wire rupture, and gross failure of the tank wall and rapid release of the water contents. Prestress wires can have degraded strength or ductility due to corrosion or other forms of embrittlement, and the sudden increase in forces in the wires due to horizontal and vertical seismic loading can find any weaknesses. Prestressed concrete tank damage

modes and of these kinds have been observed in the 1989 Loma Prieta and 2011 Christchurch earthquakes.

Figure 5-34 shows a reinforced concrete pump station at the southern-most "P" in Figure 5-15. This building is on piles. The "open first floor" type design reflects that the nearby rice farm area has been prone to flooding.



Figure 5-34. Pump Station Building

Figure 5-35 shows a close-up of the ground level beneath the building in Figure 5-34, showing a nearly uniform soil settlement of about 6 to 10 cm everywhere except at the grade beams connecting between the pile-supported columns. The building and its interior equipment were reported to have performed well.



Figure 5-35. Pump Station Building Soil Settlement

Figure 5-36 shows about 10 to 15 cm of differential settlement adjacent to the roof of a buried reinforced concrete vault at this site. Sand ejecta is seen at the edges of the vault. No pipe damage appears to have occurred, demonstrating the importance of installing flexible pipe connections (or otherwise ductile) at the interface boundaries between buried vaults, pile supported structures and pipes supported on native soils.



Figure 5-36. Buried Vault Soil Settlement

Figures 5-37, 5-38 and 5-39 show wells No. 1, 2, 3, 8 and 9 in this area. As with the pump station building in Figure 5-34, all wells in this area are "two story" structures, with an open first floor, to accommodate annual flooding of the adjacent rice fields. The casing pipe for the well 8 can be seen in the smaller of the two openings in Figure 5-36. The field observations indicated differential settlements all around these wells, but no (or very little) evidence of lateral spread. The well buildings are commonly supported on piles that are 22 meters deep. It appears that some of the piles lost vertical load-bearing capacity, at least temporarily during the earthquake, leading to the well casing pipe trying to act as a vertical support system for the well building. This led to high forces to the well pipe, and in some buildings, obvious tilting of the building. The punching shear failure seen for Wells 1 and 2 (photos taken within the building) indicate that the building was trying to settle, and the well casing pipe was then forced to act as a vertical "support", and the well casing-to-concrete-to-floor connection was grossly unable to accommodate the punching shear. The sharp offset of the ball-jointed connection for Well 1 clearly highlights the effects of differential settlement, and perhaps suggest that the

distance between the two ball joints could have been increased. In total, 5 of 18 wells in this area suffered pipe failures of various sorts, reflecting the variability of the PGDs.



Figure 5-37. Numayamazu Well No. 8

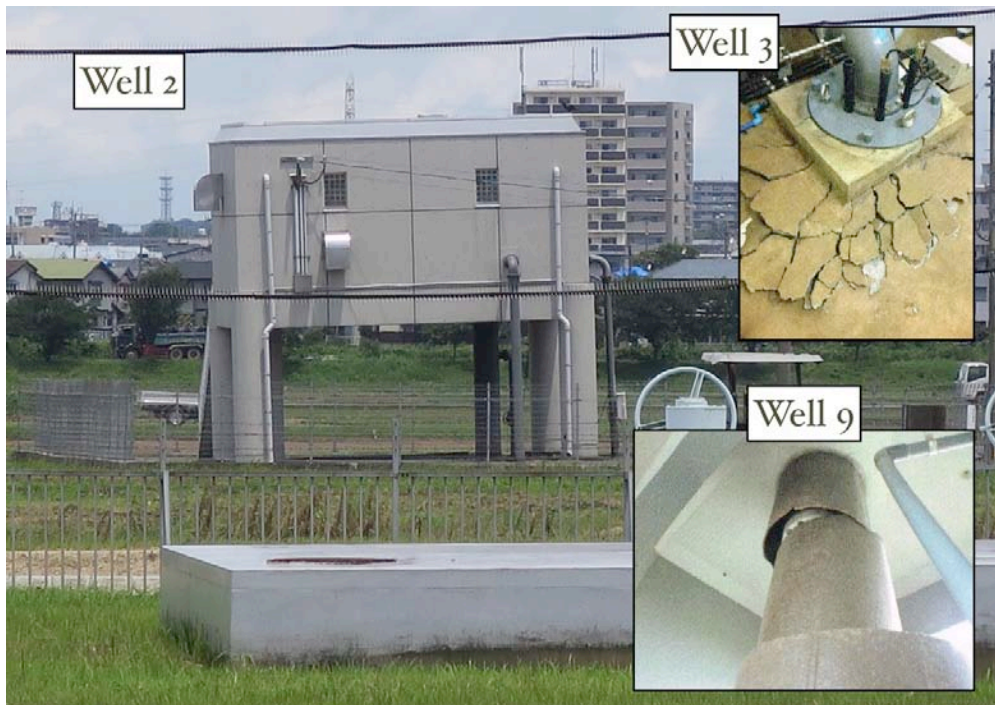


Figure 5-38. Akita Wells No. 2, 3, 9

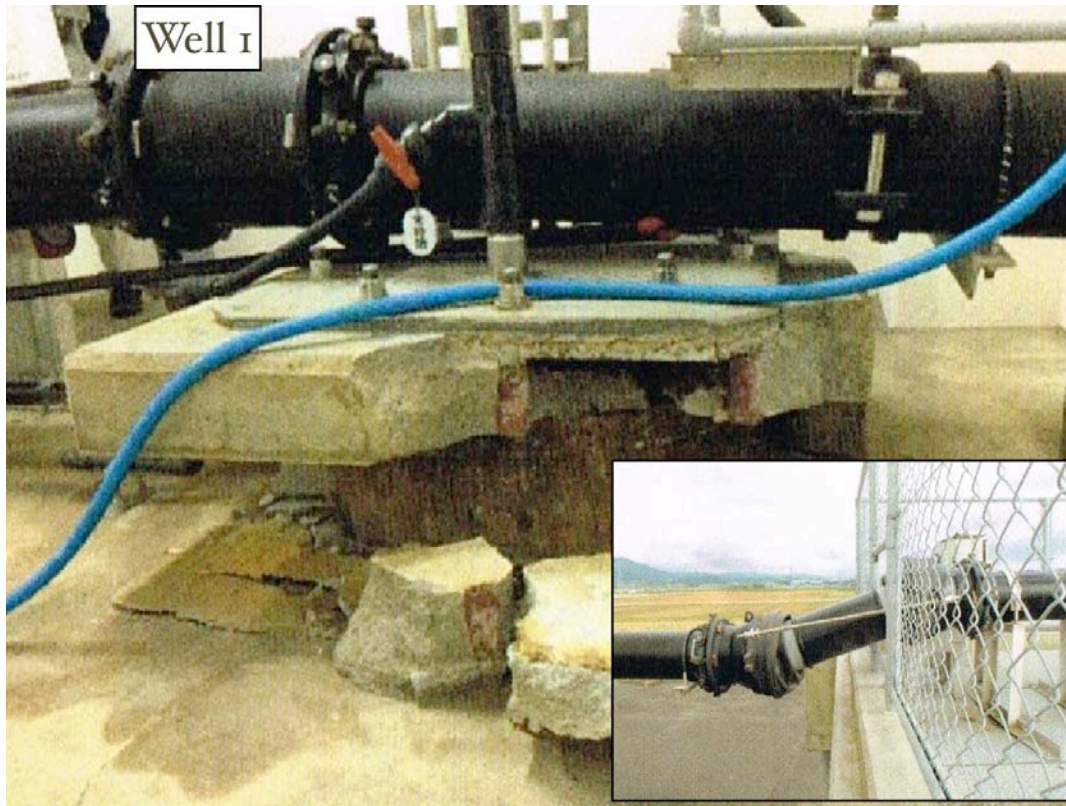


Figure 5-39. Well No. 1

5.7 References and Acknowledgements

Prof Maruyama developed the charts that show the restoration water water service.

AWWA, American Water Works Association, M11 Steel Pipe, A Guide for Design and Installation, 4th Edition, 2004.

ALA, Seismic Guidelines for Water Pipelines, American Lifelines Alliance, www.americanLifeinesAlliance.org, www.geEngineeringSystems.com, March 2005.

Eidinger, J., Replacing Seismically-weak and aging water pipes, <http://www.geEngineeringSystems.com>, 2010.

Eidinger, J., Water Pipe Replacement, Pipeline Users Group, Berkeley, <http://www.geEngineeringSystems.com>, February 2015.

Eidinger, J., Cioffi, J., Pipe Replacement Strategies for Aging and Seismic Issues, ASCE Pipelines Conference, Kansas City, <http://www.geEngineeringSystems.com>, June 2016.

6.0 Seaports

There are 15 ports in main island of Kyushu, Figure 6-1. The major ports (Kumamoto Port, Yatsushiro Port, and Beppu Port) are classified as important. Both Kumamoto Port and Yatsushiro Port are in Kumamoto Prefecture, while Beppu Port is in Oita Prefecture. The facilities serve as container berths, ferry terminals, fishing ports and cruise ship terminals.

Kumamoto Port is the closest to the epicenters, while Yatsushiro Port is not that far from the epicenters either. Both port sustained some damage. Although Beppu Port is much further north of the epicenters, it also sustained minor damage due to the earthquake. All ports were open two days after the main shock.

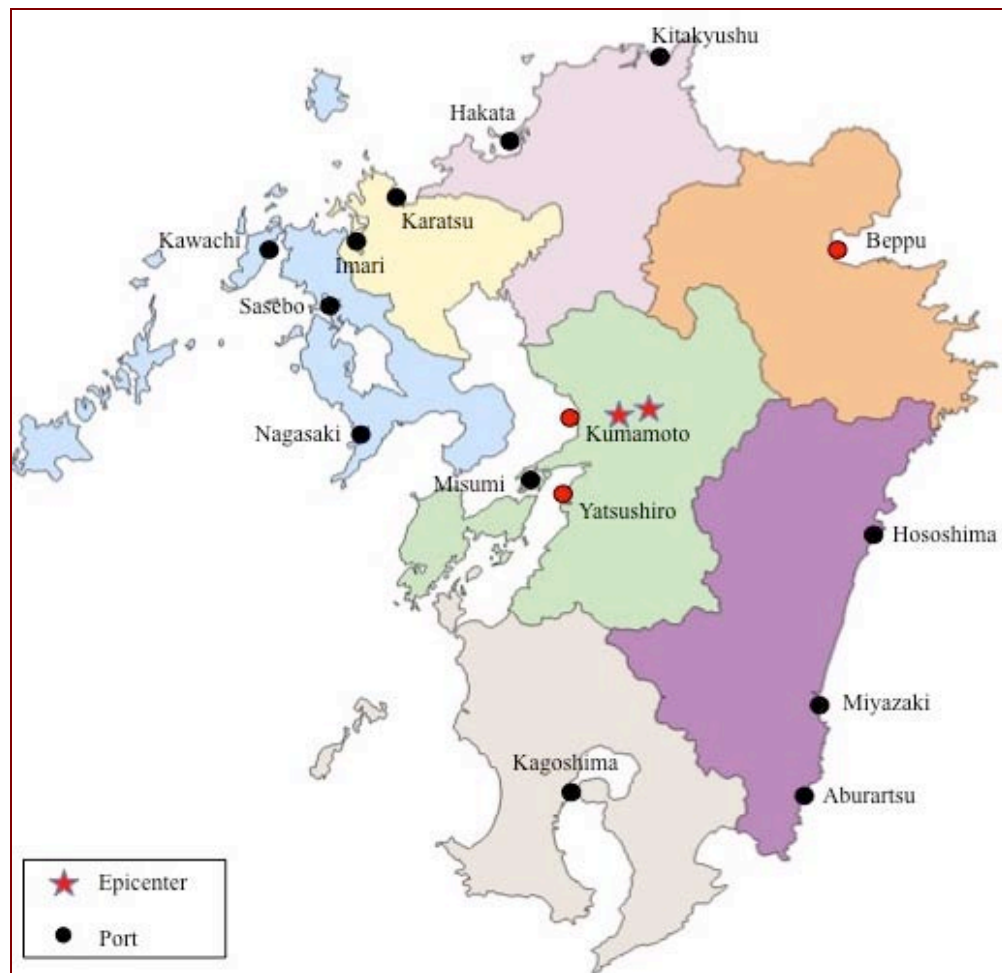


Figure 6-1. Location of Kyushu Ports, the Red Dots are the ports sustained minor earthquake damage to access roads.

All the ports shown in Figure 6-1 are cruise ship ports, as tourism is the main industry of Kyushu. Cruise passengers are mostly Japanese; there are also international cruise ships docking at some of these ports.

6.1 Kumamoto Port

Kumamoto Port (32.7629° N, 130.5858° E) is located east of Kumamoto City. It is built on reclaimed land. There is only one access road from main land to the port. Figure 6-2 shows an aerial view of the port. The PGA of the area is about 0.2g and the PGV is about 22 cm/sec (USGS data of the April 16 main event).



Figure 6-2. Aerial view of the Kumamoto Port (Source: Google Earth)

As the port is a land filled site, some liquefaction is expected. The circled area in Figure 6-2 sustained minor liquefaction and ground settlement failures.

Inspection by the Civil Engineering Department of Kumamoto Prefecture reported the following occurrence at the Kumamoto harbor (Kumamoto City):

- Bridge misaligned at the joint in both ends (Figure 6-3)
- The movable bridge for getting car on and off to the ferry inoperative
- Cracks in the road behind the quay (Figure 6-4), caused by liquefaction
- Gantry crane of the container terminal inoperative

- Pile damage at the joint of the floating bridge for Fishing Boats and Government ships⁴.

All the above issues were either fixed or temporary measures were in place to allow the port to function within two days.



Figure 6-3. Bridge misaligned – Kumamoto Port (Source: Kumamoto Prefecture, Civil Engineering Department)

⁴ Reported on 22 April 2016.



Figure 6-4. Road surface cracked and ground settlement – Kumamoto Port (Source: Kumamoto Prefecture, Civil Engineering Department)

6.2 Yatsushiro Port

Yatsushiro Port (32.5121⁰N, 130.5585⁰E) is the second port of Kumamoto Prefecture that is located south of Kumamoto Port. Figure 6-5 shows an aerial view of the port. This is also a land filled site. It is further away from the epicenters. There was no damage to the port. The setback was cracks on road and ground settlement of road shoulder, Figure 6-6.



Figure 6-5. Aerial view of Yatsushiro Port



Figure 6-6. Ground settlement - Yatsushiro Port (Source: Kumamoto Prefecture, Civil Engineering Department)

Yatsushiro Port serves as a wharf for handling mainly foreign cargo, and it is the largest port in Kumamoto Prefecture, as it has a 10-meter deep quay with 4 berths, a 12-meter deep quay with 1 berth, and a 14-meter deep quay with 1 berth. In addition, a land and sea transportation network has been set up, as roads connect the Yatsushiro Port with the

Kyushu Expressway, the Minami-Kyushu Expressway, National Route 3, Kyushu Shinkansen have been built.

6.3 Beppu Port

Beppu Port (33.3034°N, 131.5031°E) is one of the ports (Figure 6-7) reported by Civil Engineering Department of Kumamoto Prefecture sustained setbacks. This port is in Oita Prefecture. However, there was no service interruption due to the failures.



Figure 6-7. Aerial view of Beppu Port. (Source: Google Earth)

The damage reported is as follows:

- Sinking of the quay, liquefaction behind, water spouting due to rupture of the water pipe,
- The ground was depressed in two sites, about 10 cm diameter by 30 cm deep, along the coastal area.
- These damages were fixed within two days.
- Since March 2011 with the wharf open for 140,000 tons class ships, it became one of the key cruise ship port to Kyushu.

6.4 Major Observations and Recommendations

Liquefaction and ground settlement resulting in access to the ports were the major set back noted in this earthquake. Kumamoto Port is basically a land filled port and some ground failure is expected. Kumamoto Port is close to the epicenter.

The quickness to repair the roads for access to the port was the reason for the brief interruption. Therefore speed of damage restoration is a key factor to resilience.

6.5 Acknowledgements

The authors are indebted to MLIT and Kumamoto Prefecture officials providing us with many photographs and relevant information of site damage, which make this chapter more complete.

6.6 References

Presentation by Civil Engineering Department of Kumamoto Prefecture.

Report of 22 April 2016 by Emergency Response Department of Kumamoto Prefecture.

7.0 Airports

There are 9 airports within Kyushu main island and four regional airports in the neighboring islands, Figure 7-1. The airports on the main island are all connected to major cities within Japan and also direct or connect flights to international destinations. Kumamoto Airport (also known as Aso Kumamoto Airport) is one of the major airports within Kyushu. The airport code is KMJ.

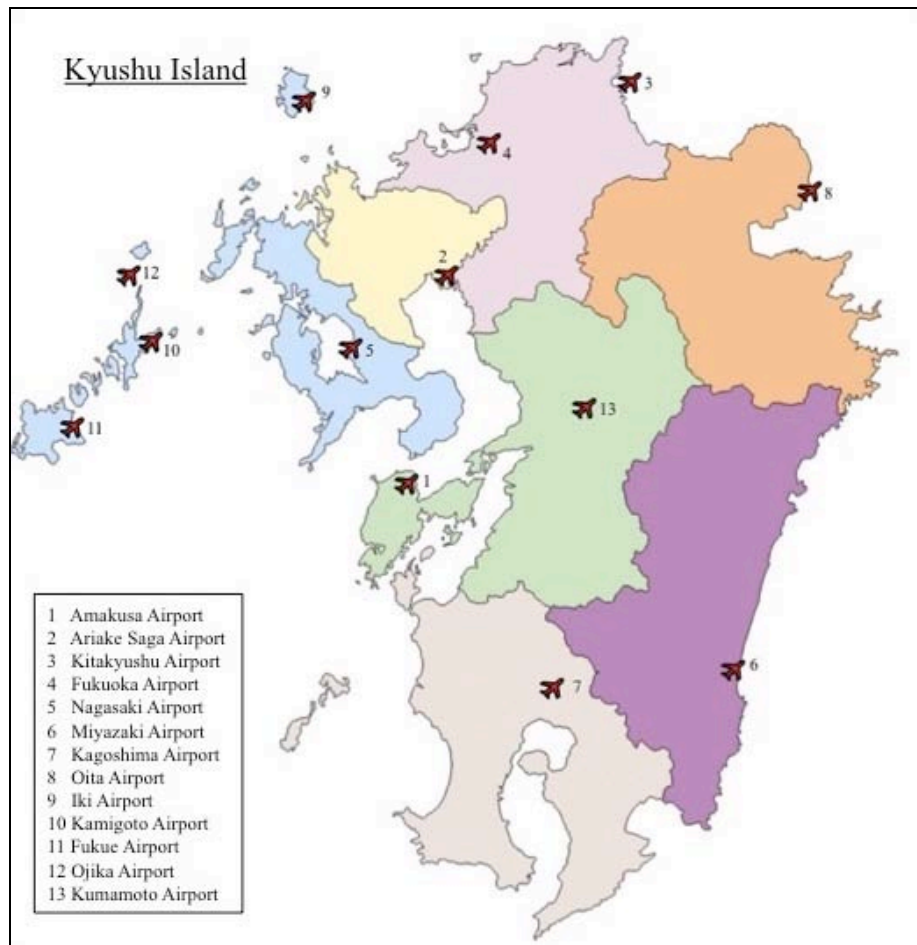


Figure 7-1. Location of Kyushu airports

Kumamoto Airport consists of two terminals, a domestic terminal and an international terminal. The domestic terminal has four gateways, while the international terminal has only one. Major airlines such as JAL⁵ and ANA⁶, as well as regional airlines (such as Skynet) serve this airport. The annual passenger volume is just over a million. The majority of the passengers are tourists and vacationers.

⁵ JAL = Japan Air Line

⁶ ANA = All Nippon Airway

The airport is located in Mashiki, Kumamoto Prefecture and about 10 km west of the epicenter of the main shock, Figure 7-2. The airport was closed for two days after the main shock on 16 April 2016. The reasons of closure were road access to the airport and non-structural damage in the domestic terminal. The international terminal sustained very light non-structural damage.

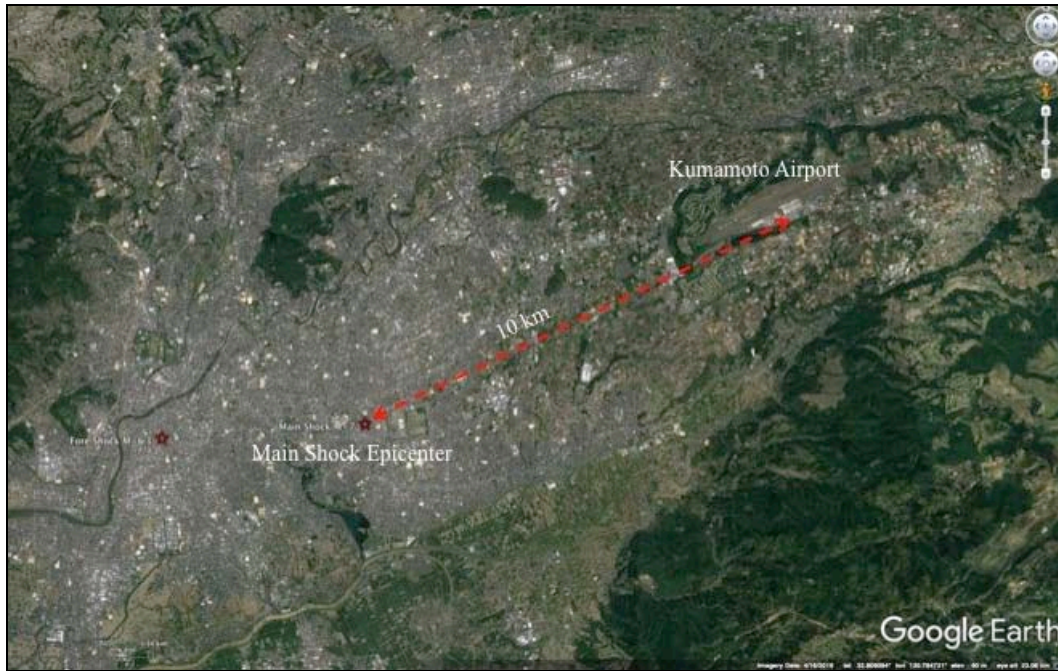


Figure 7-2. Location of Aso Kumamoto Airport with respect to epicenter of the 16 April 2016 M= 7.0 Main Shock.

Figure 7-3 is a satellite photo of Kumamoto Airport; this airport handles more domestic flights than international flights. The international terminal is about 1/3 the size of the domestic terminal.



Figure 7-3. Satellite view of Kumamoto Airport, the Control Tower is to the left of the Domestic Terminal. (Source: Google Earth)

7.1 Performance of Kumamoto Airport

On the 15 April 2016, after the M=6.3 earthquake, ANA cancelled 2 flights with 6 flights delayed, SNA⁷ has 2 flights cancelled and 2 flights delayed, while JAL has 3 flights delayed. All other airports in Kyushu had normal operation.

After the main shock on 16 April 2016, controllers at Kumamoto Airport were evacuated to the Meteorological Office from the Control Tower. Commercial electric power failed and back up power was on to provide power to Control Tower. The Runway guide light went out due to power failure. The Runway was not damaged. The terminals had ceiling parts damaged and fell on the floor. Many objects on the floor not anchored toppled. There was also water leak in the terminal. There were many pillars and walls cracked, both in the waiting areas and security areas. Both ANA and JAL stopped landing any flights at Kumamoto Airport. The airport was announced closed at 4:45 AM local time on 16 April 2016.

The following provides a chronological order of events at the airport after the April 16 main shock.

The airport authority announced all flights cancelled for 17 April 2016.

On 18 April 2016, all security operations were in place 24 hours to support relief flights only. The controllers evacuated to the Meteorological Office used small wireless devices to provide necessary information to relief aircrafts. All traffic lights of roads to the airport

⁷ SNA = Skynet Airline

were back to normal and some road surfaces were repaired for slow traffic only. Clean up and repairs were on going in the domestic terminal and passengers paths and guides were set up. All passenger flights were cancelled for 18 April 2016.

On 19 April 2016, at 7:30 AM the Control Tower was reopened for operation. The domestic terminal was still closed for repairs. Limited passenger flights were allowed with 19 arrival flights and 6 departure flights.

On 20 April 2016, at 3 PM the domestic terminal resumed operation, only three of the four gates were opened. There were 50 passengers flights scheduled for 20 April and that was about 70% of normal operation.

On 23 April 2016 in the morning, the fourth gate was opened for passenger flights.

On 28 April 2016 about 80% of passengers flights were back to normal.

Roads and Highway access to the airport were the other key factor in closing the airport. It took MLIT⁸ Kyushu about three days to establish detours and temporary repairs of the roads and Highway to Kumamoto Airport. For details of transportation damage, refer to Chapter 6 of this report.

7.2 Domestic Terminal

This terminal sustained lots of non-structural elements damage, such as ceiling falling, wall and column cracks, water pipe broken, and power outage.

We had the opportunity to investigate this terminal during our field visit. The parking lot was reasonably full when we visited on 03 July 2016 just before noon. We had time to walk around to check what happened after the main shock.

Although there were many strong shaking damage within the domestic terminal, the vast majority of the exterior of the domestic terminal did not show any sign of shaking damage; even the glass panels performed well, Figures 7-4 and 7-5.

On 3 July 2016, there were areas within the terminal that were closed to public access as repair was still in progress. Some superficial damage such as cracks on wall panels, which were exposed and not repaired yet. Figure 7-6 shows an area closed to public access. This area most likely was used as rest area for relatives and friends waiting for either arrival or departure passengers. The ceiling was covered with a sheet of plastic to catch any fallen objects.

⁸ MLIT = Ministry of Land Infrastructure and Transportation (Tourism) of Japan Government

Figures 7-7 to 7-9 provide an idea of the damage to drywall. The elevator close to the damage wall did not sustain any damage and it was operational when the power was restored.

Figure 7-10 shows the walk way from the elevator to the second floor level was covered with plastic sheet in order to avoid dust, and fallen objects during repair.

Figure 7-11 shows the only off set of the cladding at the column joint inside the terminal.

Figure 7-12 shows the mural of Aso Volcano, a tourist attraction in Kumamoto, did not have any crack or loosen pieces. Aso Volcano is the orange cone behind John Eiding.



Figure 7-4. Exterior of Kumamoto Airport Domestic Terminal, the whole front wall is glass panel. There was signs of stress or displacement of the gasket around the glass panel.



Figure 7-5. Another view of the front glass wall of the domestic terminal



Figure 7-6. Ceiling damaged in the concession area, which was closed on July 3 2016



Figure 7-7. Cracks along the upper part of this dry wall



Figure 7-8. Cracked dry wall joints in the waiting area



Figure 7-9. Cracks along the dry wall joints; the ceiling tiles were no damaged. The elevator was not damaged

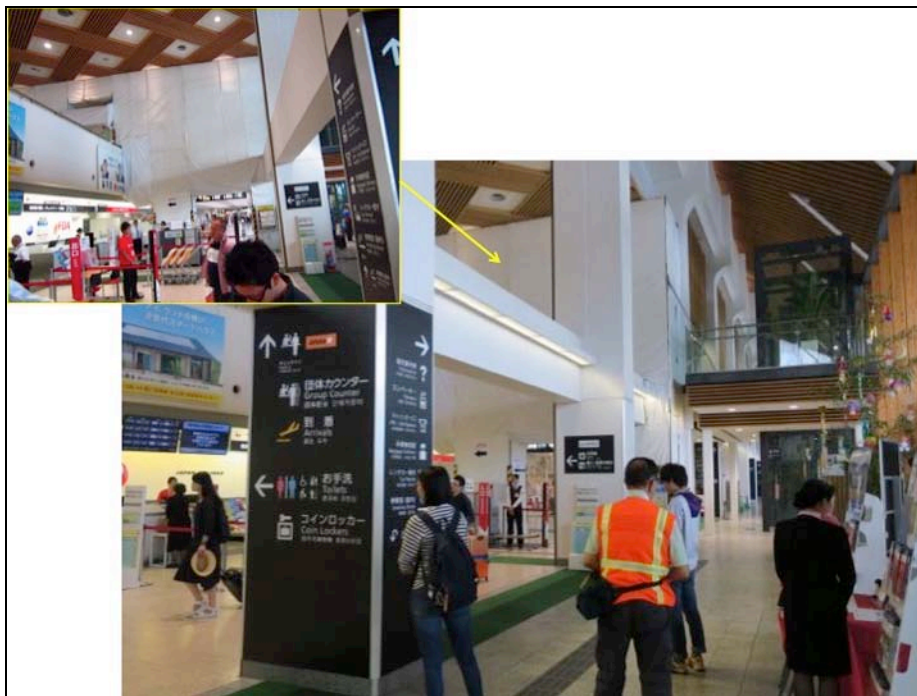


Figure 7-10. Inside Domestic Terminal with airline check-in counters on the left. The insert shows the covered walk way on the second floor, the departure level



Figure 7-11. The column joint cover separated, no damage to the column.



Figure 7-12. John Eidinger was standing in front of the mural, which had no sign of any strong shaking. Note also that the floor tiles had no cracks at all

7.3 International Terminal

The International Terminal performed better than the Domestic Terminal, Figure 7-13 shows the exterior of this terminal. The inside of the terminal did not have any damage

like that in the domestic terminal. There might be a problem with the Internet service during the power outage period. Two pairs of telecommunication cables were noted hanging from the open window, Figure 7-14. It looked like a temporary solution to keep communication operational.

The terminal did not have any departure flight or arrival flight during on July 3 2016. The security area was very empty at that time, Figure 7-15.



Figure 7-13. Exterior of the International Terminal



Figure 7-14. Two sets of telecommunication cables were installed to provide Internet service



Figure 7-15. International Terminal security checkpoint of departing passengers

7.4 Major Observations and Recommendations

Non-structural damage can cause lots of operational problems. In order to reduce service impact, it is worth the investment to mitigate probable damage to non-structural elements in airport terminals.

The Control Tower (Figure 9.16) did not have any structural damage (not even the glass panels); with the controllers having to move to the Meteorological Office and using small wireless device to guide relief flights, the speculation of the interval required to allow the controllers back to the tower was:

- Power outage (short duration),
- Personal safety (after shocks),
- Equipment problem (not functional), and
- Access to the observation part of the tower (impaired).

Further understanding will be needed to provide a complete picture of the airport's performance.

Airport is critical lifeline in the post earthquake emergency support. It provides a gateway for quick delivery of relief materials to the victims. It is prudent to ensure airports having a higher standard to prevent service interruption.



Figure 7-16. Exterior view of the Kumamoto Airport Control Tower.

7.5 Acknowledgements

We extend our sincere appreciation of Professor Maruyama flying in from Tokyo to help us performing this field investigation on lifelines in Kumamoto. We also would like to thank Mr. Yuki Kagami and Ms. Haruka Ito who assisted us with interpretation service.

8.0 Gas System

8.1 Overview of the Gas System

The primary natural gas supplier in Kyushu Island is Saibu Gas Co., Ltd. Throughout Kyushu, Saibu supplies gas to about 1,104,800 customers. In the Kumamoto area, Saibu provides gas to about 112,100 customers (statistics current as of March 31 2016).

Saibu Gas was established in 1930, incorporating several smaller gas companies in Kyushu that has initiated operations as early as 1902. In the early years, natural gas was created using the coal gasification process, in a manner similar to that done in California at the time of the 1906 Great San Francisco earthquake. By 1971, Saibu had closed all the coal gas facilities, and the modern Saibu system largely relies on imported liquefied natural gas (LNG), some of it imported from Malaysia. Large scale importation of natural gas into the Kumamoto area began in 1976, with the construction of a gas transmission main.

This was not the first major earthquake to impact the Saibu Gas system in modern times. In 2005, an earthquake hit offshore, west of Fukuoka Prefecture, and about 600 Saibu Gas staff were then involved with the restoration of the affected gas system.

Over time, Saibu Gas has taken precautions for seismic design. Most of the buried pipeline system in the Kumamoto area had been installed with "earthquake resistant" pipelines, and this played an important role in limiting the impacts to the gas system in the 2016 earthquakes. As will be described later in Chapter 8, the April 16 2016 earthquake showed that the bulk of the repair effort in the gas system was to service laterals and customer-side issues; a similar issue occurred to Pacific Gas and Electric's gas system in the 2014 Napa California earthquake.

Overall, this earthquake demonstrates that to achieve a highly resilient gas system, the facilities (terminals, gas holders) need to be seismic resistant; the gas transmission and distribution pipes need to be earthquake resistant; and the service laterals and customer-side appliances need to be earthquake resistant.

The use of seismic gas shut-off valves requires careful planning for the subsequent manpower intensive labor effort needed for gas re-lights. More study of this earthquake is needed to assess whether (or not) "automatic seismic shut-off valves" on transmission pipes, as well as at household customer connections, remain entirely satisfactory or cost effective. Certainly, closure of these valves resulted in large manpower-intensive efforts after the earthquake, as needed to check for leaks before re-lights of pilot lights. As highlighted elsewhere in this report, fire spread never occurred in this earthquake, but it remains unclear if the shut-off of gas supply (either transmission level or at the household connection level) can be confirmed as the reason for this good outcome.

8.2 Gas Outages

The gas system operator is Saibu Gas Co., Ltd. After the April 16 2016 main shock, nearly all gas customers in the Kumamoto area lost gas supply. The extent of the outages was initially controlled by the closure of shut-of valves in the transmission system as well as at customer's meters; while the duration of the outages was mostly controlled by the large labor effort needed to repair the relatively modest amount of damage to buried gas pipe mains, the large repair effort associated with damage to service laterals and customer-side issues.

The gas supply in Kumamoto Prefecture is divided into seven blocks, covering most of Kumamoto City (blocks 201, 202, 203, 204, 205) and Kikuyo Town in kikuchi (block 207), see Figure 8-1.

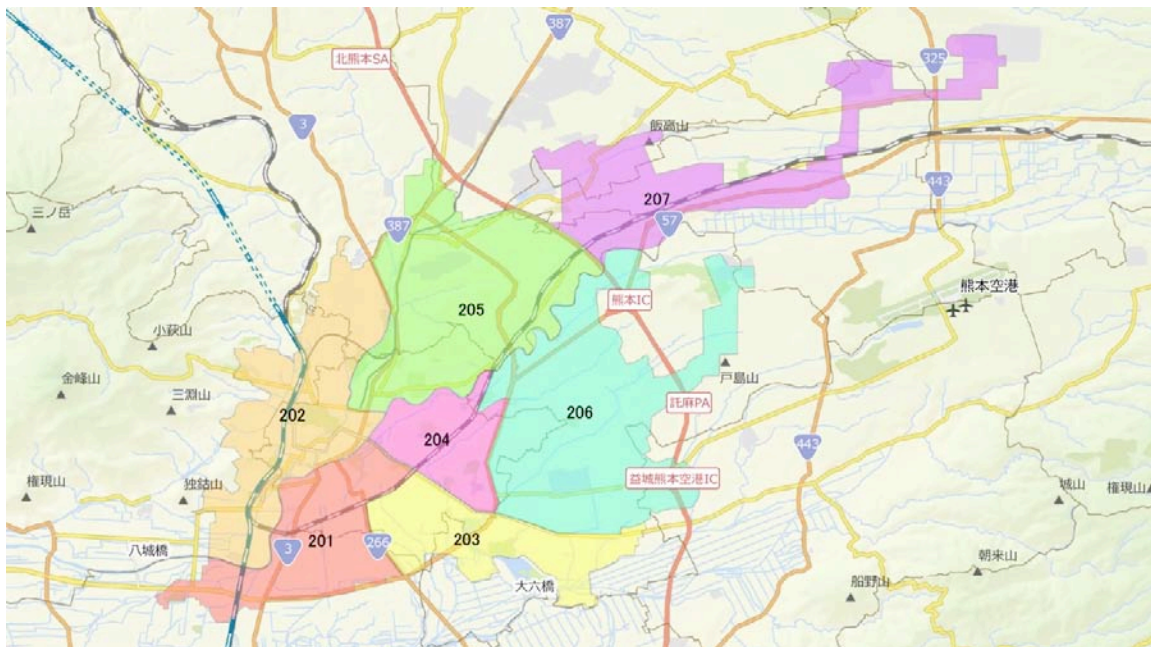


Figure 8-1. Gas Supply Blocks in Kumamoto Prefecture

Underground gas pipes can be vulnerable to earthquake motions, commonly expressed in terms of PGV (cm/sec) or PGD (cm). Older styles of gas pipe construction (such as cast iron pipe, screwed steel pipe) can be extremely vulnerable to locations with PGDs much over 2 cm or so, and somewhat vulnerable to high PGV (much over 60 cm / sec or so). Modern pipe materials often used in gas distribution systems, namely fusion welded medium density polyethylene pipe (MDPE), and been shown to be nearly immune to very high PGVs (60 cm/sec or higher) and moderately high PGDs due to liquefaction (up to 10 to 20 cm or so).

The Japan Gas Association (JGA) developed a map (Figure 8-2) that overlaid the estimated level of PGV (1 cm/sec = 1 kine) and the gas blocks from Figure 8-1.

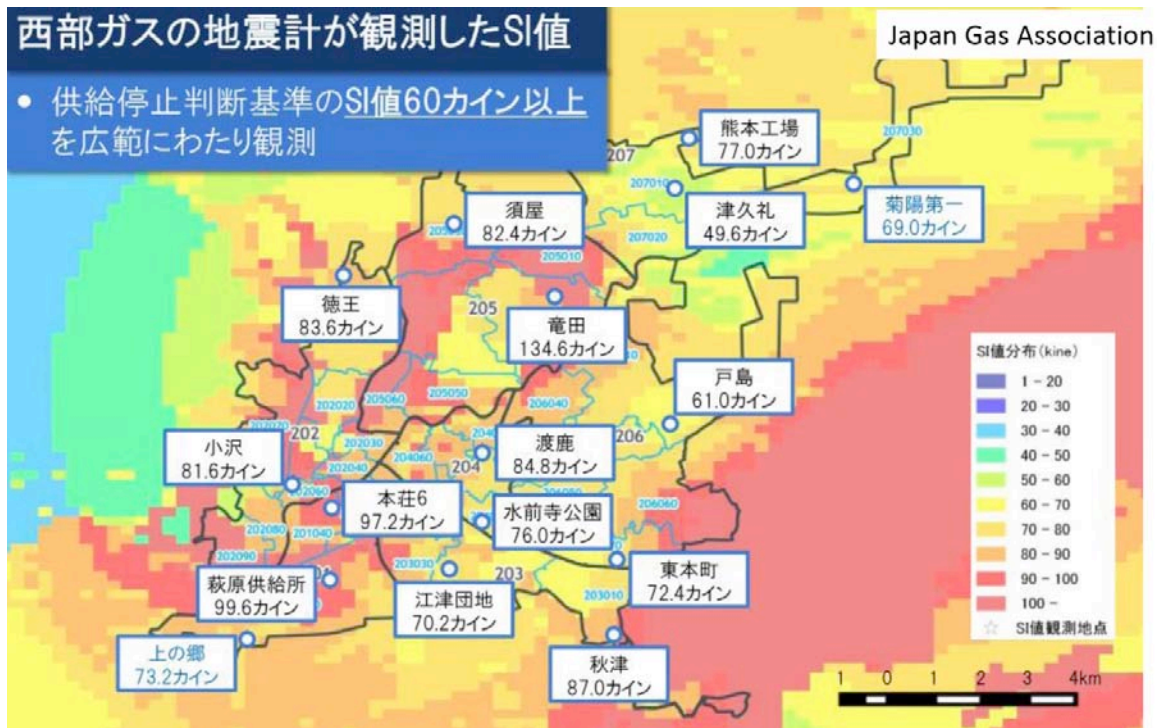


Figure 8-2. Level of Shaking and Gas Supply Blocks in Kumamoto Prefecture

One of the earthquake strategies used in Japan is to automatically shut off the gas supply transmission system to areas that have experienced ground shaking in excess of a prescribed intensity level, using the following formula. This formula integrates the Spectral Velocity response spectrum from an instrument, for 20% damping, from 0.1 to 2.5 seconds, and if the weighted average is over 60 cm/sec (a rather high level of ground shaking), the instrument sends a signal to valves in the high pressure gas pipe system to automatically close. The concept here is to avoid new supply of natural gas into an area where ground deformations may have likely resulted in serious levels of underground gas pipe damage. This strategy is relatively easy to implement, needing only a suitable instrument and logic to convert a felt motion into an integrated spectrum, a process that can be done within a second or so of the end of shaking), and then a signal to suitable pipe valves at suitable locations to close. Of course, it would be better if this strategy relied on PGDs (rather than ground velocities), as well as actual gas pipe damage, but PGDs are nearly impossible to measure within the first seconds after an earthquake, and knowing the exact pattern of gas pipe damage is similarly difficult to assess in the first seconds after an earthquake. It is well recognized that isolation of the gas supply pipes does little to nothing to resolve the residual amount of gas within all the gas pipes, which can be a substantial source of fuel for feeding any fire ignitions, should fire ignitions occur.

$$SI = \frac{1}{2.4} \int_{0.1}^{2.5} S_v^{\xi=0.2}(T) dT \geq 60 \text{ cm/sec}$$

Figure 8-2 shows that the SI values for 16 instruments in the Kumamoto Prefecture area ranged from 49.6 to 134.6 cm/sec, with most between 70 and 100, high enough to trigger isolation. In Figure 8-3, the areas that had gas supply shut-off after the April 16 main shock are plotted in red (about 100,000 households), and the two areas with continuing supply after April 16 are in blue (about 1,500 households).

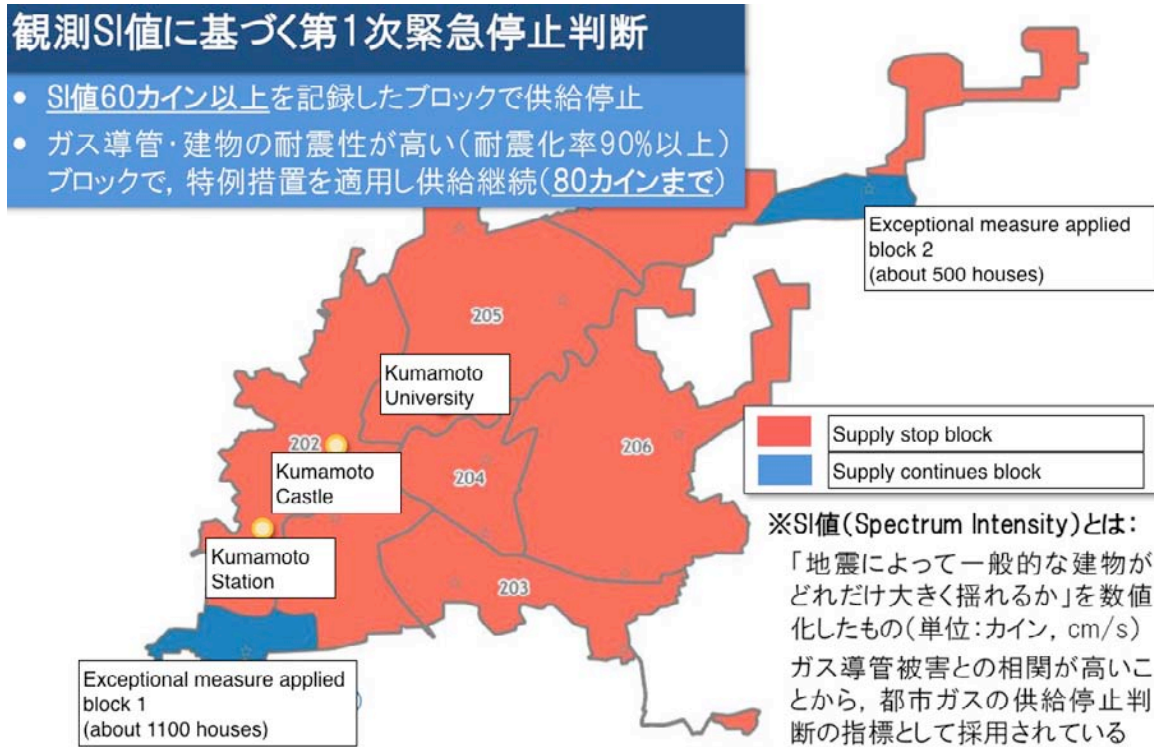


Figure 8-3. Initial Shutoff of Gas Supply on April 16 2016

Figures 8-4 and 8-5 show the number of households with gas disruption as a function of time after the earthquakes. In these figures, "Day 0" refers to April 14 2016, the day of the fore shock. Figure 8-6 provides a spatial set of maps, highlighting the progress of the restoration of gas. The number of households disrupted from gas supply decreased rapidly after April 23. Gas supply was totally recovered at 1:40 pm local time on April 30.

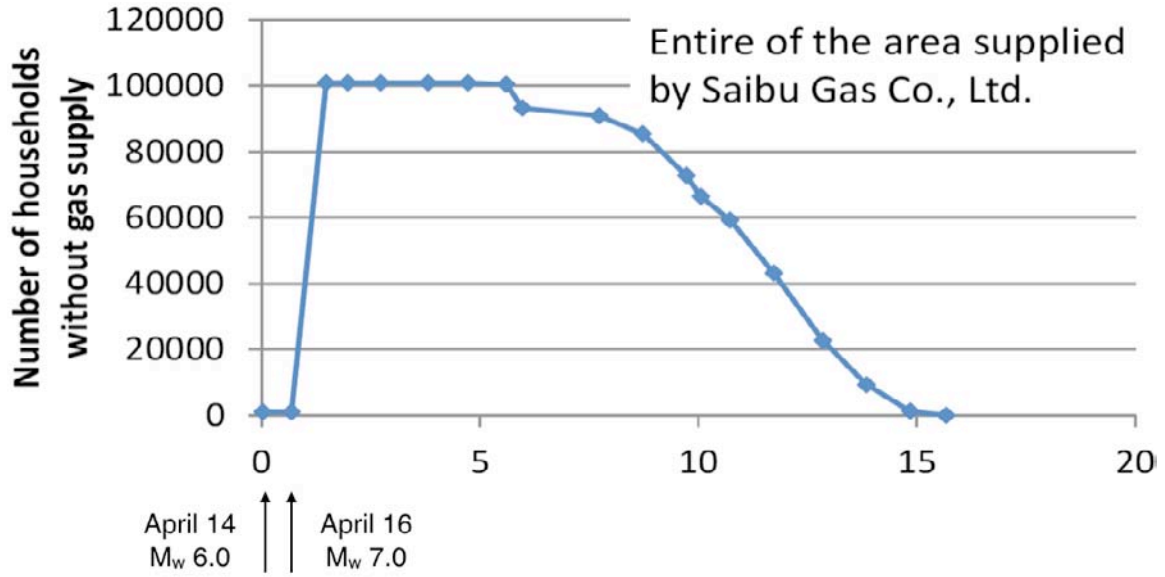


Figure 8-4. Natural Gas Disruptions

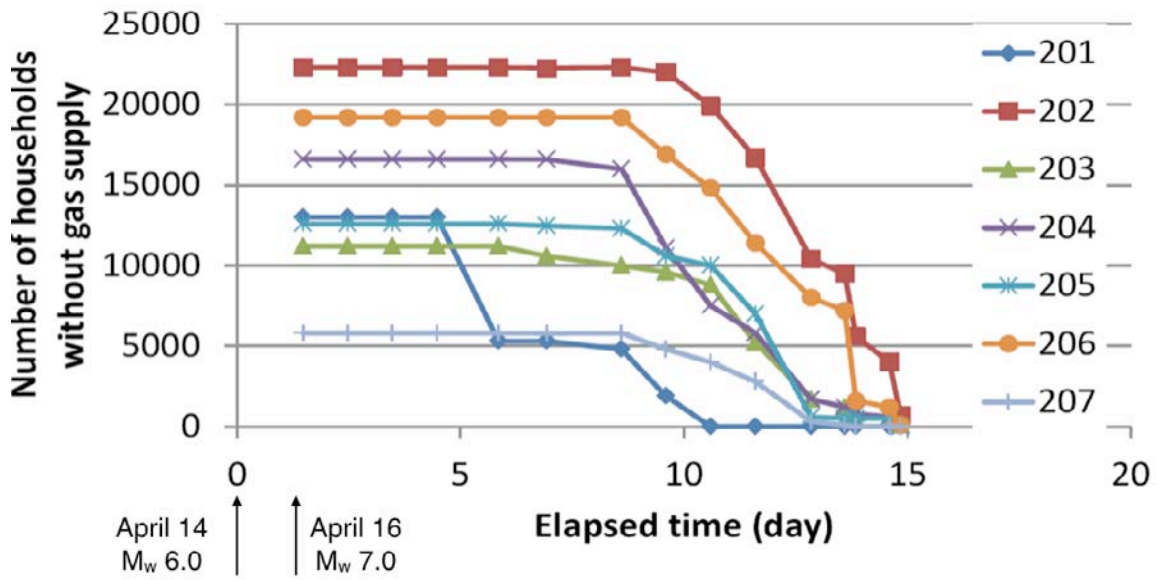


Figure 8-5. Natural Gas Disruptions by Block

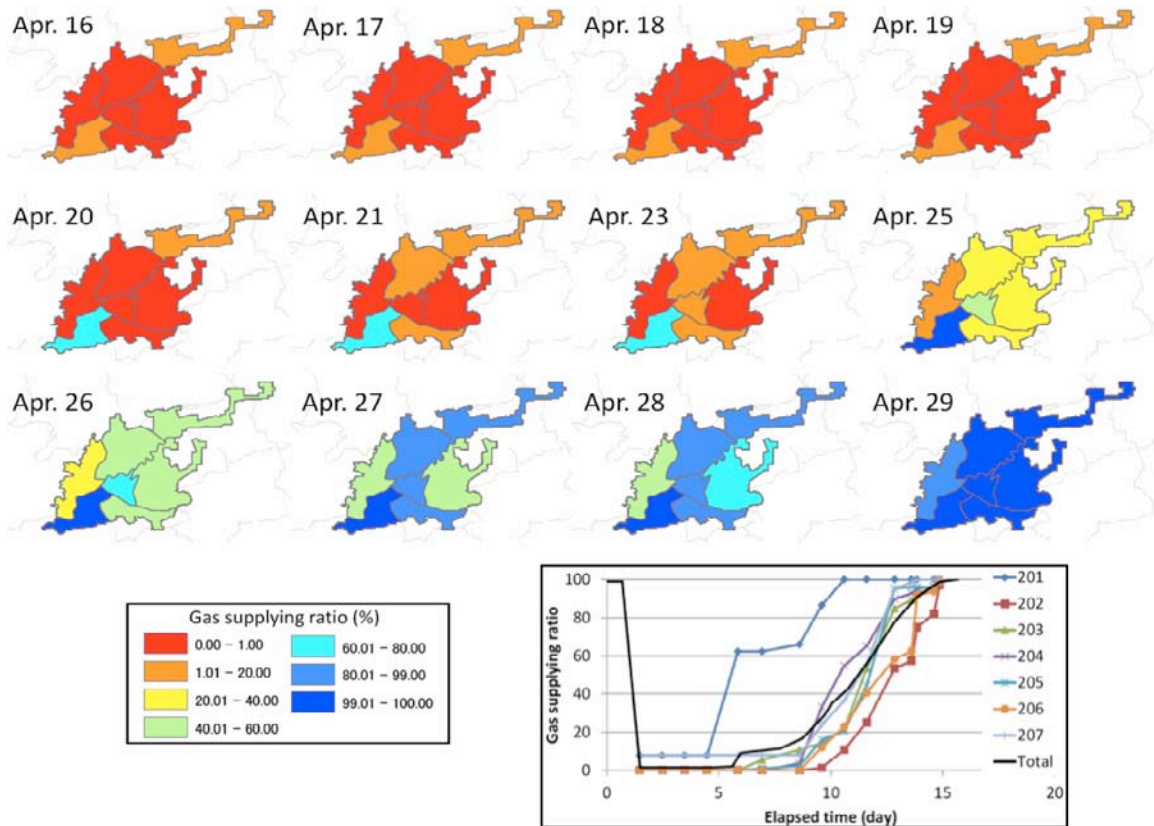


Figure 8-6. Natural Gas Restoration Map

8.3 Gas Facilities

There was no damage to any of the natural gas import or production facilities in Kyushu; all of which are believed to have felt very low levels of shaking.

Some gas holders were exposed to moderately high level of shaking: Figure 8-7 shows a tank using a very light steel rod cross bracing system. The rods show yielding, and the tank's foundation seen in Figure 8-8 at the base of the right column in Figure 8-7 was spalled, confirming that a high level of seismic force occurred; the tank retained its pressure boundary.



Figure 8-7. Gas Holder with Yielding Cross Braces



Figure 8-8. Gas Holder with Yielding Cross Braces

8.4 Gas Pipes

The pipe inventory in the area is about 1,647 km of transmission mains and 12,689 km of distribution mains. About 86% of this inventory was already constructed using seismic

resistant pipes at the time of the earthquake, using welded steel transmission or polyethylene (PE) distribution pipes. There was no damage to any PE pipes in the system.

Figure 8-9 shows the locations of damage to pipe mains.

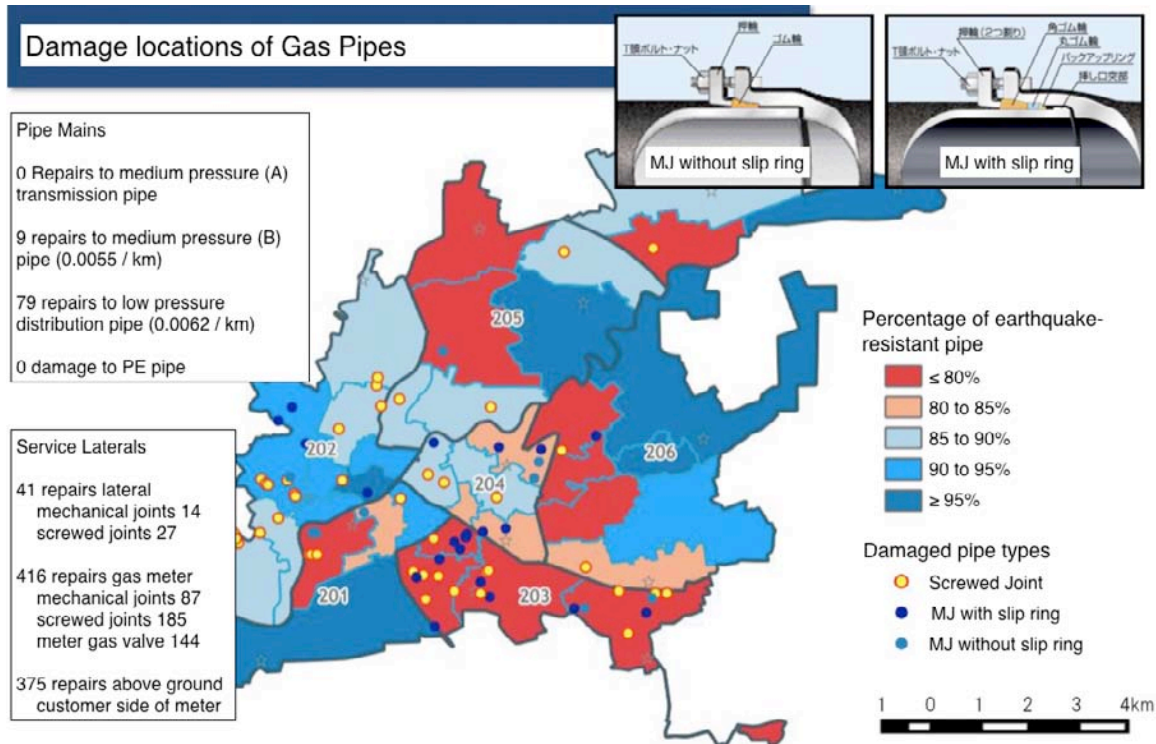


Figure 8-9. Location of Damaged Pipe Mains

The following damage to gas mains occurred:

- 0 repairs to high pressure (also called medium pressure class A) transmission pipes
- 9 repairs for medium pressure (class B) pipe mains (9 / 1,647 km = 0.0055 repairs per km). Damage was at mechanical joints. In each case, the damage can be characterized as a loosening of the joint that resulted in a detectable leak. The typical repair was to excavate the pipe, and tighten the joint, see Figure 8-10.
- 79 repairs to low pressure pipe mains (79 / 12,689 km = 0.0062 repairs per km). This includes damage to mechanical joints at 23 places (needing tightening of the joint, see Figure 8-11), and damage at 46 low pressure galvanized steel pipes that were connected with screwed connections (damage included cracks, breakage of the joint, with repair needed pipe replacement, see Figure 8-12).
- There was no damage to PE (polyethylene) pipe used for either medium pressure class B or low pressure distribution pipe.

There was substantial damage to supply equipment (service laterals), as follows:

- Supply pipe. 41 locations, including mechanical joints (14 locations) and screwed joints on galvanized steel pipe (27 locations), see Figure 8-13.
- 416 locations, buried, with damage at the gas meter, including mechanical joints (87 locations), screwed joints in galvanized steel pipe (185 locations), and meter gas stoppers (144 locations) etc.
- 375 locations, above ground, with damage being on the downstream side of the microcomputer gas meter with earthquake isolation function.
- There was no damage to PE pipe.

Available data at this time do not allow us to provide breakdowns by pipe material, but the trends are as follows:

- In areas where fewer than 80% of all pipes were MDPE (considered to be earthquake resistant), the pipe repair rate for mains was 0.10 repairs per km, correlated to a typical SI of about 80 cm/sec.
- In areas where between 80% to 90% of all pipes were MDPE (considered to be earthquake resistant), the pipe repair rate for mains was 0.05 repairs per km, correlated to a typical SI of about 85 cm/sec.
- In areas where over 90% of all pipes were MDPE (considered to be earthquake resistant), the pipe repair rate for mains was 0.03 repairs per km, correlated to a typical SI of about 80 cm/sec.

This preliminary data shows that the pipe repair rate reduces with the quantity of non-seismic pipe inventory, as would be expected.



Figure 8-10. Repair to Median Pressure Class B Pipe. Repair was to tighten the mechanical joint (typical of 9 locations)



Figure 8-11. Repair to Low Pressure Distribution Pipe. Repair was to tighten the mechanical joint (typical of 23 locations)



Figure 8-12. Damaged at Screwed Joint for Low Pressure Distribution Pipe (typical of 46 locations)



Figure 8-13. Damaged Low Pressure Pipe Customer Service Lateral

8.5 Emergency Response

The repair of all the gas pipes, including re-lights, etc., took a substantial effort. Figure 8-14 shows the number of workers involved with the restoration of the gas system, which peaked at 4,641 workers. Saibu Gas provided 1,965 workers. The Japan Gas Association provided an additional 2,676 workers, with these people coming from 22 other gas companies in Japan.

As part of the emergency response effort, 127 mobile gas generating facilities were used, and 15,022 cassette stoves (portable gas stove) and more than 60,000 cassette gas cylinders were distributed to houses, municipalities, etc.

It was felt that improvements in the management of the emergency response could be possible.

It was felt that the interruption of supply and automatic gas shut off valves at houses reduced (eliminated) secondary impacts, namely gas-fueled fires.

It was felt that since about 85% of all pipe had already been replaced with "seismic resistant pipe", that the overall impacts were greatly reduced. It was felt that a continuing effort to replace vulnerable distribution pipe with seismic resistant pipe is a good practice.

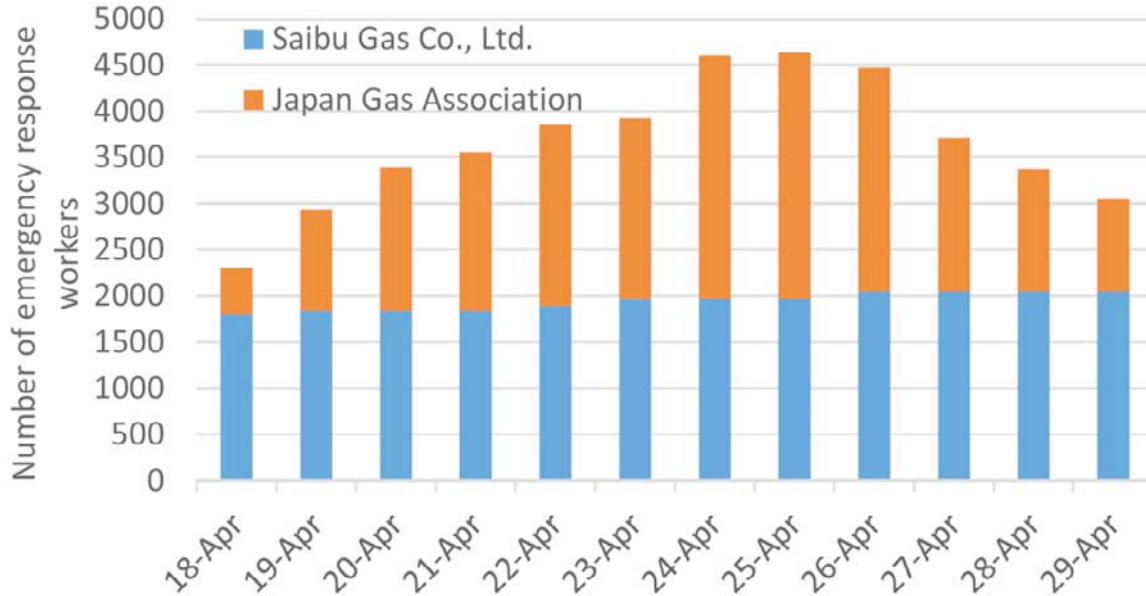


Figure 8-14. Gas Workers in Emergency Response

8.6 Acknowledgements

The description of the piped natural gas system presented in Section 8 is adapted from materials developed originally by Prof. Yoshihisa Maruyama of Chiba University, Prof. Nojima of Gifa University, information from the Japan Gas Association, and information

from Saibu Gas (www.saibugas.com). We especially extend our sincere appreciation to Professor Maruyama for collecting and developing much of the information presented in Chapter 8.

9.0 Transportation

Kyushu (Figure 9-1) is south of Honshu, which is the largest island of Japan. This is the island with the most active volcanoes in Japan. It is also a very popular vacation location. The island consists of seven prefectures – Fukuoka, Kumamoto, Saga, Nagasaki, Kagoshima, Miyazaki, and Oita. All major cities within the prefecture are connected by a road network and railway network, Figure 9-2. Sanyo Shinkansen and bridge connects the island to Honshu. Ferry is also a means of transportation from Kyushu to Honshu.

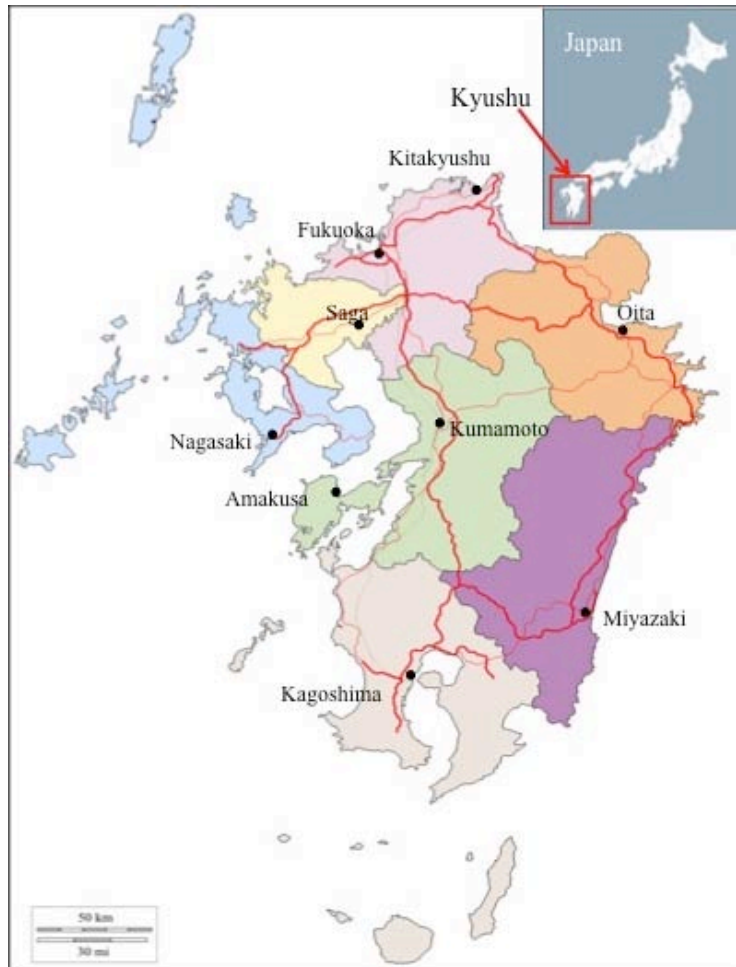


Figure 9-1. Kyushu Expressway and the major cities. (Base map from Reference 1)

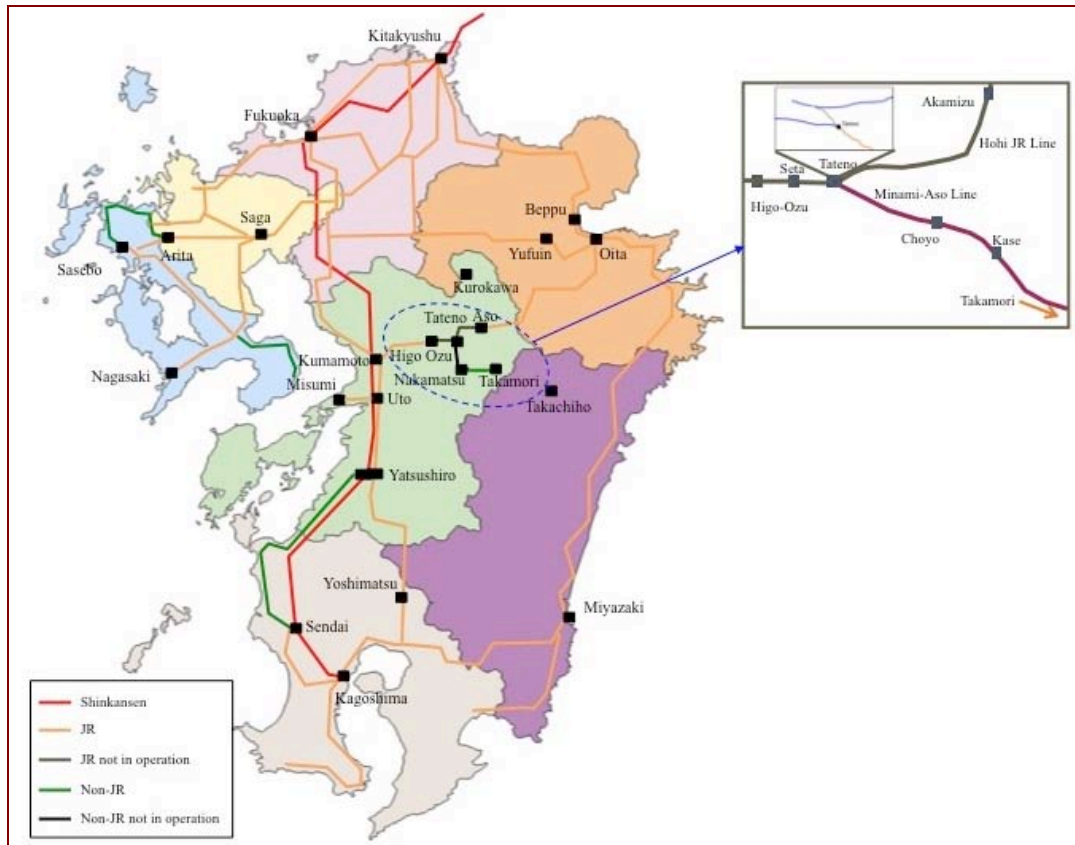


Figure 9-2. Rail Network within Kyushu. (Base map from Reference 1)

All transportation networks that were exposed to JMA intensity 4 or higher sustained various degrees of impact. Landslides caused significant impact to transportation network elements. The collapse of Aso Bridge (Aso Ohashi⁹) became the signature of this earthquake, Figure 9-3. This also caused major transportation problems in Minami Aso region.

Although we arrived on site two months after the earthquake, there were areas in Minami Aso that remained closed to public. MLIT Kyushu was kind enough to provide us with their information and also allowed us to use the photos in our report. Some of the information was provided by Civil Engineering Department of Kumamoto Prefecture Government.

⁹ Ohashi = Big Bridge in Japanese



Figure 9-3. Aerial view of the landslide that caused the collapse of Aso Bridge (Source: Geospatial Information of Japan)

9.1 Transportation Network of Kyushu

The focus of this chapter is to report both road and railway service interruption due to the earthquake.

All major cities within Kyushu are connected by Expressways and paved roads. Many bridges, overpasses and road surfaces were damaged by the strong shaking as well as ground deformations and landslides. There were also many county and village roads damaged in this earthquake. This report covers only a portion of the overall damage to the highways, bridges, tunnels and roadways of the road network, in part as we were unable to gain access to all locations due to closures to hazardous areas where recovery was still taking place during our visit.

There are two high speed (called Shinkansen) rail lines in Kyushu. The Kyushu Shinkansen route going along the west side of the island connects Fukuoka to Kagoshima. The Sanyo Shinkansen connects Fukuoka to Honshu. Local (regular speed) railways also connects all cities in Kyushu. Although there were two incidents where rail cars derailed, most of the railway service interruptions were results of rail tracks covered or destroyed by landslides, or ground deformations.

9.2 Expressway and Bridges

Expressway damage was concentrated just east of Kumamoto City to Minami Aso. The Kyushu Expressway a key transportation route in Kyushu. Figure 9-4 shows the area where there were major traffic disruptions or delays along the Kyushu Expressway caused by damage to road surfaces and overpasses.



Figure 9-4. The four locations with significant impact to Kyushu Expressway are identified in red circles

After the main shock on 16 April 2017, the Kyushu expressway was closed to allow MLIT to inspect the road conditions. Starting from the top section of Figure 9-4, this section was fully opened to traffic on 16 April 0630, the second section from top was fully opened to traffic on 29 April 0900, the third section was fully opened to traffic on 29 April 1500, and the last section was fully opened to traffic on 15 April 1500 (this section was not closed after the main shock, but closed after the foreshock of 14 April).

9.2.1 Kanon Bashi (N32.8335° . E130.7802°)

This bridge was an overpass of Kyushu Expressway at the junction of the Kumamoto exit, Figure 9-5. After the main shock on 16 April, the bridge support columns were

leaning a few degrees but it did not collapse, Figure 9-6. However, after inspection the bridge, MLIT decided to remove it to avoid the possibility that further aftershocks might collapse it. Figures 9-7 to 9-9 show the removal and reopening of the Expressway.



Figure 9-5. Location of Kanonbashi



Figure 9-6. The columns on the west side were tilted, Note the drain pipe on the far side was bent



Figure 9-7. MLIT in the process of removing the bridge



Figure 9-8. Road surface being prepared for reopening after the bridge removal



Figure 9-9. Expressway fully re-opened in both directions

9.2.2 Mashiki Area of Kyushu Expressway (N32.7796°, E130.7941°)

The embankment collapsed after the fore shock of 14 April, Figure 9-10. As this part of the expressway is usually quite busy, the damage caused heavy traffic congestion. A detour was set up to ease the traffic but overall the traffic was slow due to reduced lanes. Figures 9-11 and 9-12 provide more details of this site.

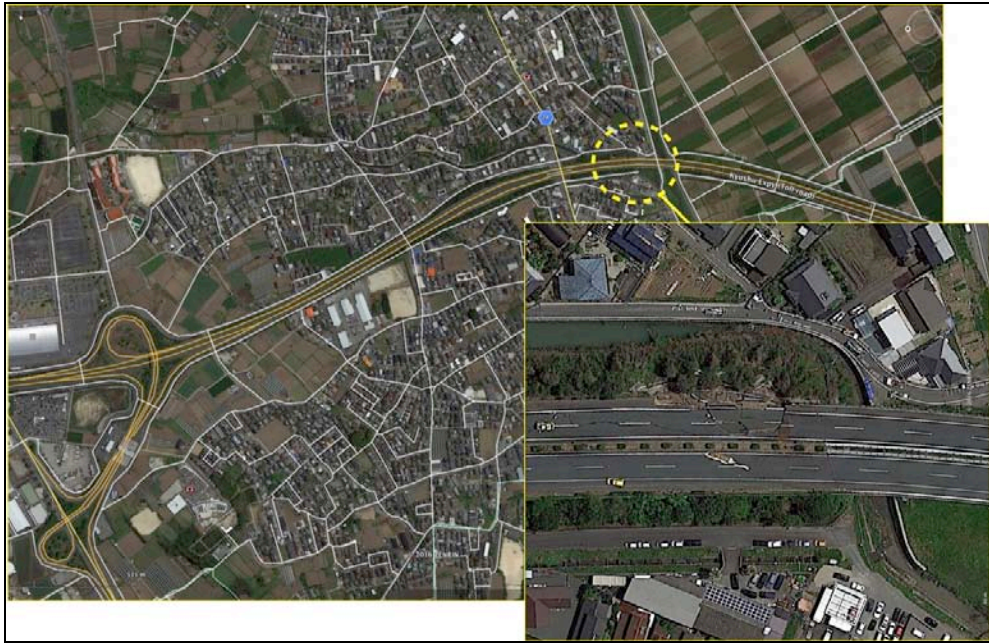


Figure 9-10. The road surface of the north bound lanes embankment collapsed



Figure 9-11. Close up view of the collapsed embankment of Kyushu Expressway



Figure 9-12. Repairs in progress

9.2.3 Kiyamagawa Bridge (N32.7654°, E130.7886°)

This bridge is a part of the Kyushu Expressway that runs across the rice field, Figure 9-13. This is a divided expressway bridge, which sustained damages to most piers that support this bridge after the main shock of 16 April. Shoring supports were constructed to brace the bridge decks, Figures 9-14 to 9-16. Many bearings were unseated, Figure 9-17. There was evidence of deck sections pounding against each other, Figures 9-18 and 9-19. Broken drainpipes provided evidence of movement of the deck with respect to the piers, Figures 9-20 to 9-21. The two tanks (lower part of Figure 9-13) are part of the water system, and in that vicinity, there was widespread differential ground settlements on the order of 10 to 20 cm (see Chapter 5 on water systems for further details of the settlements in this area).



Figure 9-13. Location of the Kiyamagawa Bridge (Source: Google Earth)



Figure 9-14. Additional shoring to support the bridge deck (Tang)



Figure 9-15. Some brace supports were needed to raised the deck to repair the bearings (Tang)



Figure 9-16. This shows another section of the bridge deck with shoring support (Tang)



Figure 9-17. Girder slipped off the bearing pad



Figure 9-18. Pounding damage to side rail at the abutment (Tang)



Figure 9-19. Pounding damage to both concrete side wall and junction plate of the steel girder (Tang)



Figure 9-20. Drainpipe broken and the bearing rocker was pushed and damage the steel girder flange



Figure 9-21. Broken drain pipe due to bridge movement

9.2.4 Furoyo First Bridge (N32.7075°, E130.7556°)

This bridge was damaged after the foreshock on 14 April. Figure 9-22 shows the location of this bridge with respect to the epicenter and Kumamoto City. Part of it collapsed on the Expressway and blocking the north bound lanes, Figures 9-23 and 9-24. Furoyo town is on both sides of the expressway. This is the first bridge that allows traffic to cross the expressway without having to go to interchange junction.

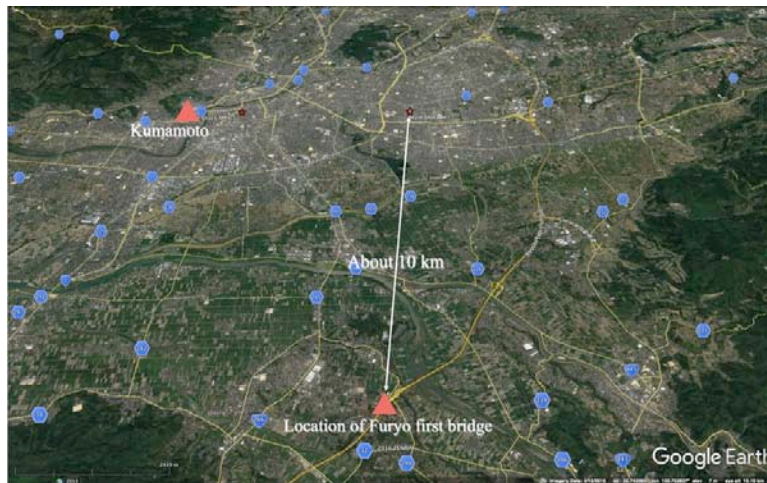


Figure 9-22. Location of Furoyo First Bridge with respect to epicenters. (Source: Google Earth)

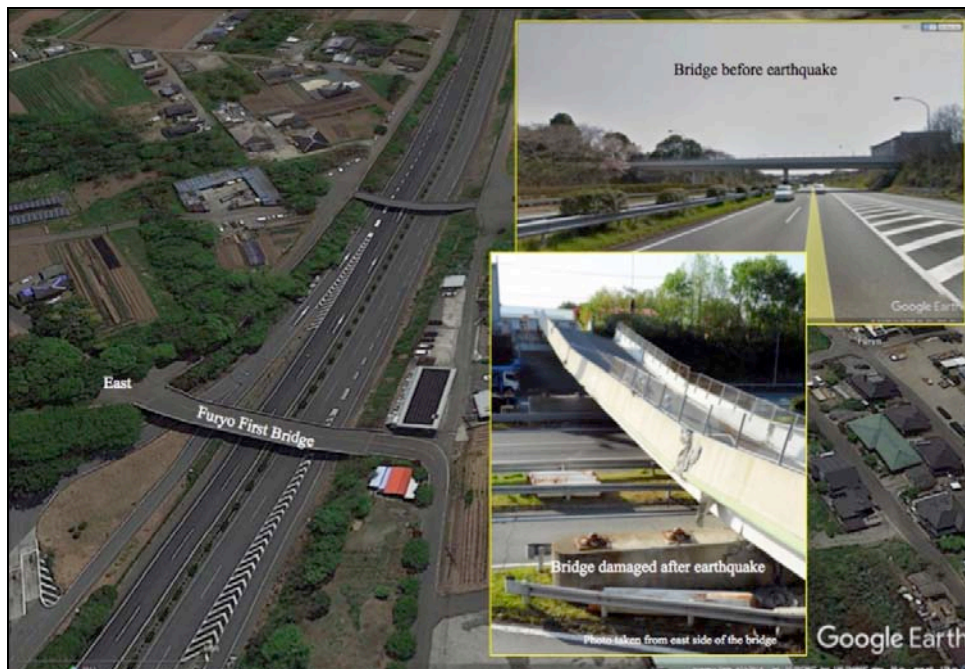


Figure 9-23. This shows the before and after photo of the bridge



Figure 9-24. The collapsed bridge blocked the northbound traffic

Many bridges in the Minami Aso area sustained extensive damage and a few were destroyed. As mentioned above, the destruction of Aso Ohashi created a big transportation problem of access to many towns and villages in the area. That is in addition to railway damages.

9.2.5 Aso Ohashi

This is the location commonly known as the ground zero of this earthquake. It is the shear size of this landslide and its impact to the transportation in Minami Aso region. The landslide was approximately 200 m wide and 700 m high.

Figures 9-25 and 9-26 show the bridge and mountainside before the earthquake. Figures 9-27 and 9-28 show the destruction of the massive landslide to the bridge and the road and railway in its destructive path. See Chapters 2 and 3 for additional images of this large landslide.

Due to the time required to stabilize the Great Aso landslide seen in Figures 1-7, 2-21, 2-22, 2-23, 3-4, 3-46, 3-47 and 9-28, a detour route was established. Figure 9-29 shows the detour established. In early July 2016, remote-controlled bulldozers (Figures 2-23, 9-30) were being used to establish slope control and build a retaining barrier to prevent further landslide and debris flow before starting to repair the Route 57 and Hohi Main Line (JR).



Figure 9-25. Aerial view of Aso Bridge before the Kumamoto earthquake. (Source: Google Earth)

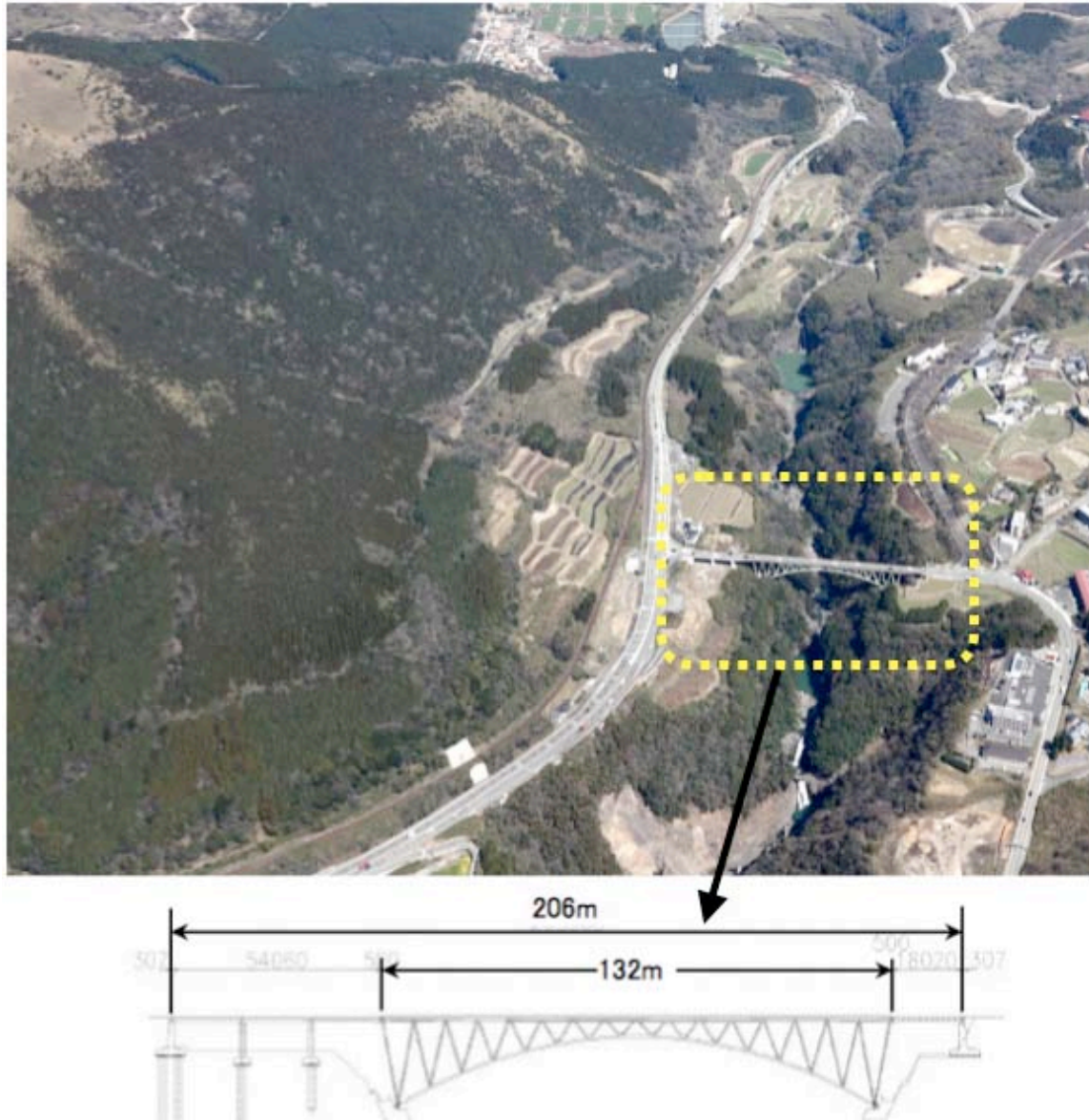


Figure 9-26. View of Aso Bridge and Mountainside before the Kumamoto earthquake



Figure 9-27. The east side of the Aso Bridge after the main shock on 16 April



Figure 9-28. The landslide that destroyed Aso Bridge cut off the railway, and the junction between Route 57 and Route 325

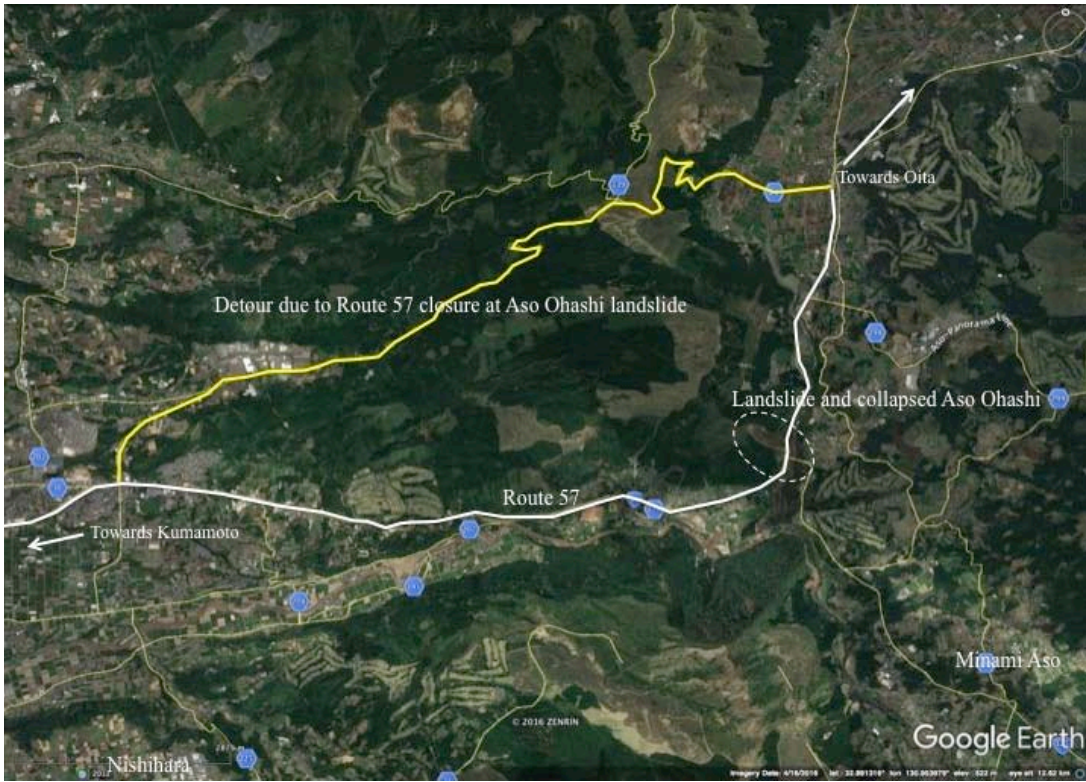


Figure 9-29. The yellow line shows the detour around the great landslide at Aso Ohashi (Source: Google Earth)



Figure 9-30. Remote controlled bulldozers were used to remove landslide material (Tang)

The bridges shown in Figure 9-31 are further described in Sections 9.2.6 to 9.2.9. These bridges are located just south-west of Aso Ohashi. Figure 9-31 shows the locations of Oh Kiri-hata Bridge, Kuwatsuru Bridge, and Tawarayama Bridge.



Figure 9-31 Locations of the three bridges along Route 28. (Source: Google Earth)

9.2.6 Oh Kirihata Ohashi (N32.8425°, E 130.9285°)

This bridge is on Route 28. The bridge sustained damage at both abutments; the landslide under the bridge created unsafe situations. The landslide did cover the by-pass road, which created access problem for this area.

Figure 9-32 shows the aerial view of the bridge before the earthquake, while Figure 9-33 shows an aerial view of the damages around the bridge, as well as the bridge itself.

Figures 9-34 to 9-37 details the damage of structural elements of the bridge.

Access to this part of the road remained closed as of July 4 2016.



Figure 9-32. Aerial view of Oh Kirihata Bridge before the earthquake (Source: Google Earth)



Figure 9-33. The circled areas were the damages observed. The blue color dashed line indicates the bypass road covered by landslide (Source: Google Earth)



Figure 9-34. Relative movement between the deck and the support column demonstrated strong ground motion

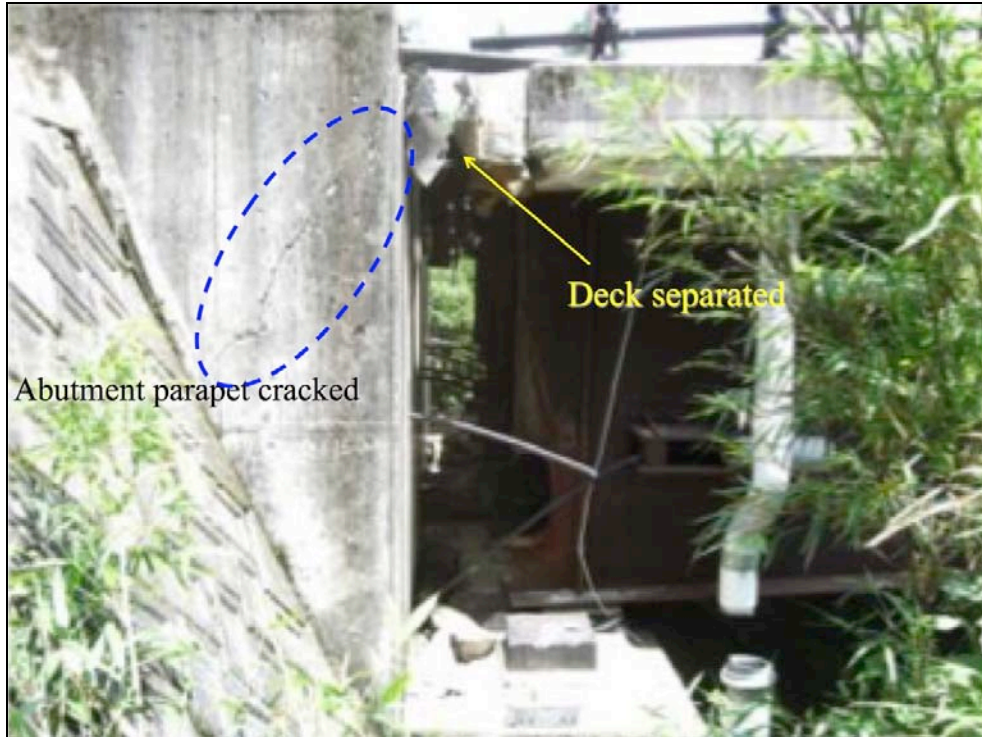


Figure 9-35. Abutment cracked and deck separation from abutment

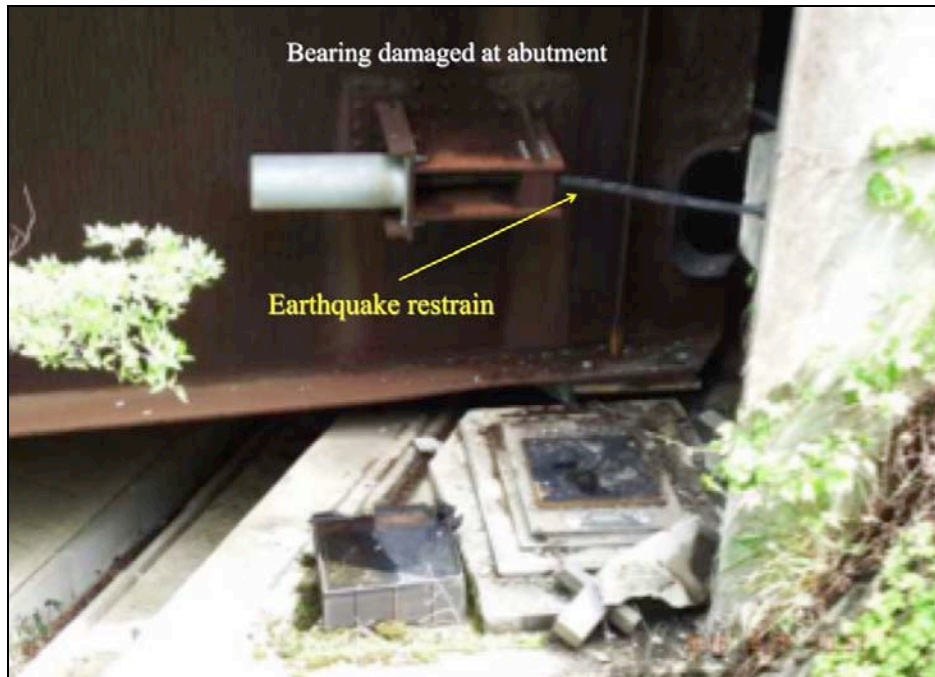


Figure 9-36. Bearing pad damaged the earthquake restraint mechanism restrained the bridge deck



Figure 9-37. The abutment "appears" raised as the bridge deck shifted sideways off its rubber bearings and fell on the abutments

9.2.7 Kuwatsuru Ohashi (N32.8517°, E 130.9455°)

This a cable stay bridge along Route 28. Figure 9-38 is the aerial view of the bridge after the earthquake.

Although surface faulting crossed the southwestern approach of this bridge, the observed damage does not appear to be due to ground deformations. The entire bridge deck as a whole was observed bent downward with its southwestern end touching the curtain wall of the southwestern abutment, while the other end was lifted up from the northeastern abutment as shown in Figure 9-39. The X-shaped central tower has a lateral beam beneath the bridge deck, and the deck was pinned to this beam; but the deck was detached from this lateral beam.



Figure 9-38. The circled area shows the abutment failure. (Source: Google Earth)

Figures 9-39 to 9-41 show the details of damage observed.



Figure 9-39. Close up view of the Northeastern abutment damage



Figure 9-40. Due to pounding the bearing rocker broke off and the abutment concrete was shattered



Figure 9-41. A few cables were loose

9.2.8 Tawarayama Ohashi (N32.8634°, E 130.9608°)

This is the third bridge along Route 28 that was damaged by the earthquake. This bridge sustained damage at the abutments and also on the west side the embankment failed, Figure 9-42. Figures 9-43 to 9-46 show details the observed failures.



Figure 9-42. Aerial view of the failures of Tawarayama bridge. (Source: Google Earth)



Figure 9-43. Close up view of the abutment damage at the expansion joint



Figure 9-44. Ground failure close to the abutment support, the pile was exposed



Figure 9-45. Damage to the abutment concrete and the bearing pad as well as the steel girder



Figure 9-46. The steel girder slipped off the bearing pad

9.2.9 Aso Choyo Ohashi (N32.8754°, E 130.9855°)

The Aso Choyo bridge is along the Tochonomi to Oniike Line village road, south of Aso Ohashi. Figure 9-47 shows the location of this bridge.



Figure 9-47. Locations of Aso Choyo and Toori Bridges, Aso Ohashi (collapsed) was on the top right hand corner

The Aso Choyo bridge is about 276 m long with three support piers, where the middle pier is the tallest. The deck is a continuous box girder. The damage sustained was at the abutments on both ends, Figures 9-48 to 9-49. Pier P3, which is on the east end of the bridge, had concrete spalling close to the base, Figure 9-50.



Figure 9-48. West end of the bridge, damage to the abutment and bridge deck

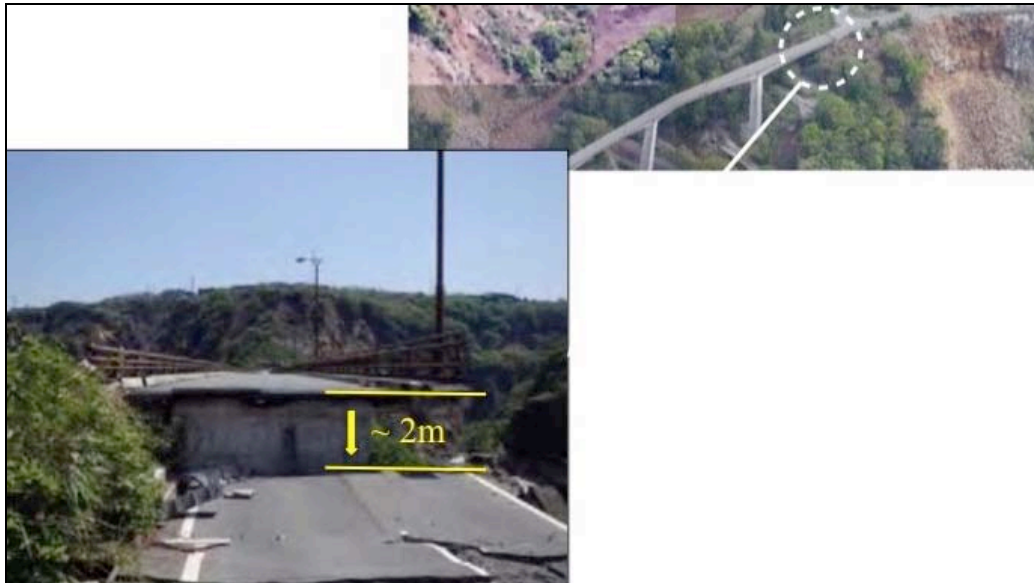


Figure 9-49. East end of the bridge, the abutment subsided about 2 meters



Figure 9-50. P2 pier close to the base showed concrete spalling

9.2.10 Toshita Ohashi (N32.8752°, E 130.9888°)

Figure 9-47 shows the location of the Toshita (Toori) Ohashi bridge. This bridge is about 380 m long of hollow box concrete deck. It was damaged in two locations, Figure 9-51. The site to east (circled location) of the heavy damage was a small break of the deck due to ground deformation and a small landslide.

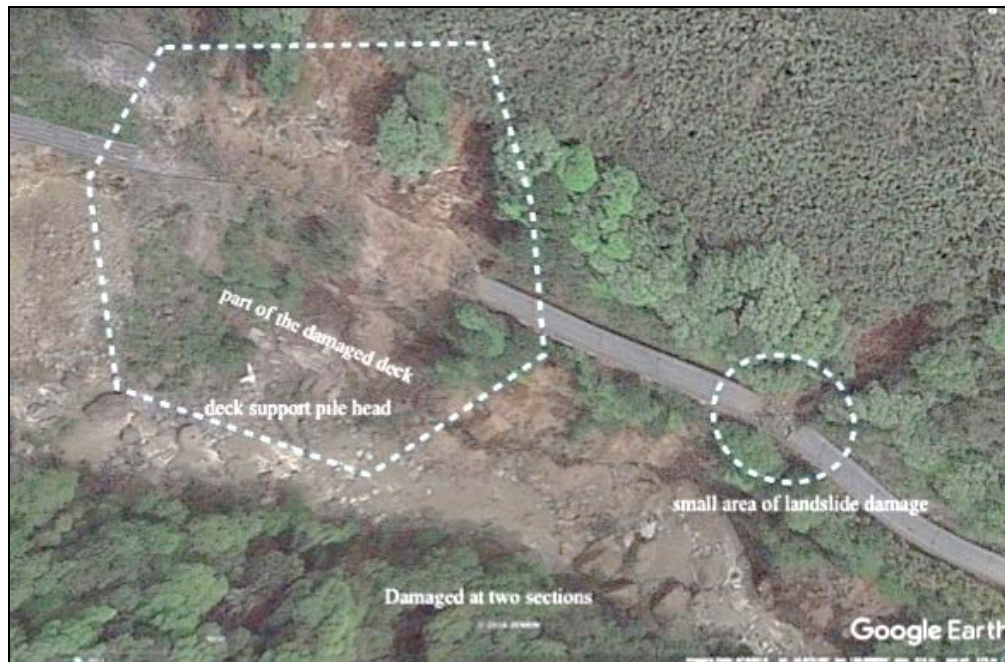


Figure 9-51. The bridge damage on the left hand side was about 60 m. The damage of the deck was small on the right hand side. (Source: Google Earth)

Close ups of observed damage are shown in Figures 9-52 to 9-55.



Figure 9-52. Aerial view (by MLIT drone) of destruction of this section of the bridge



Figure 9-53. A close up view of the landslide



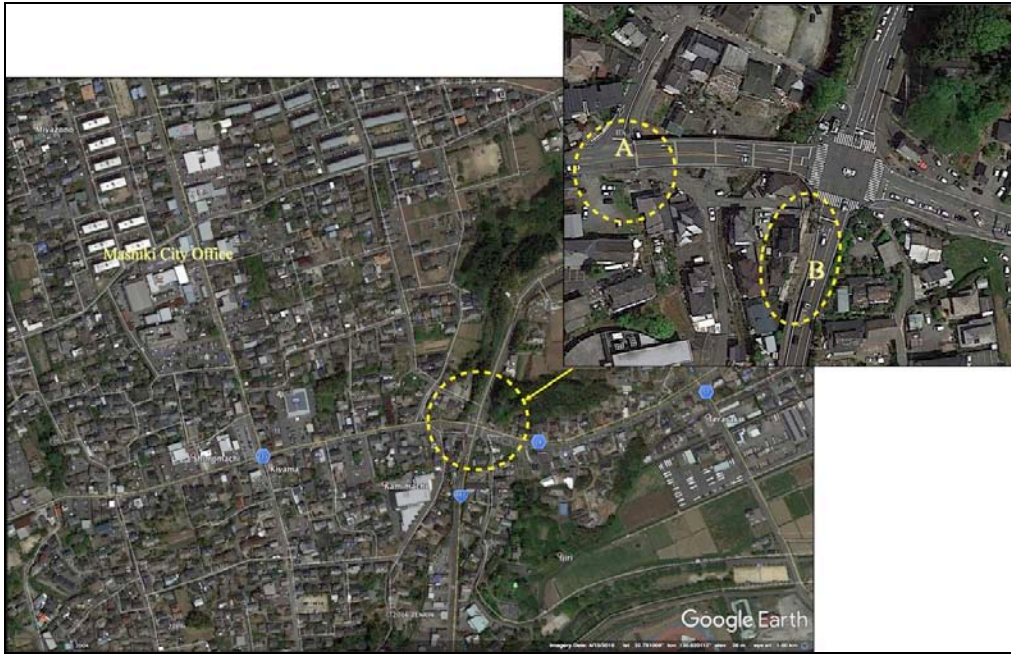
Figure 9-54, Another view showing the landslide that destroyed the bridge deck. Note part of the deck about 100 m down the slope



Figure 9-55. This is under the deck just before the landslide that destroyed 30 m of the bridge

9.2.11 Mashiki area (N32.7902°, E 130.8210°)

At this intersection highlighted by the dashed circle in the center of Figure 9-56, a short bridge sustained impact damage at one abutment (location "B"), while on the other side the road the embankment failed (location "A"). Figures 9-57 to 9-58 details the damage. The road was still useable.



*Figure 9-56. Location of damaged bridge abutment (A) and the embankment failure (B)
(Source: Google Earth)*



Figure 9-57. The embankment failure and temporary fix of (A)

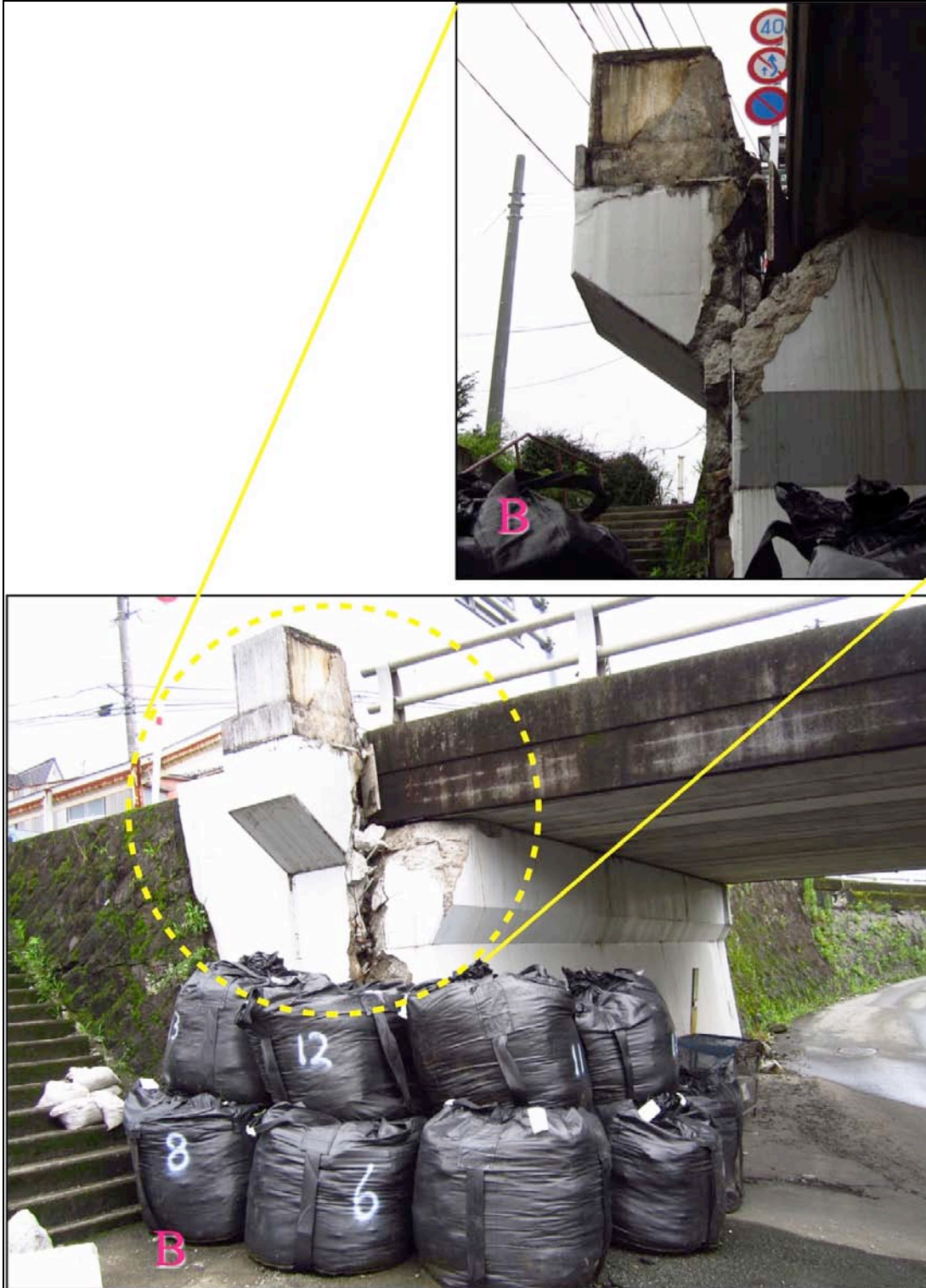


Figure 9-58. The bridge abutment failure at (B) and the temporary fix

9.3 Roads

There were significant impacts to county and village roads in the Minamiaso area. MLIT informed us that there were so many damage locations along these roads that outside resources from other parts of Japan were required to provide temporary fixes and detours to easy transportation demand in the area.

Section 9.3 describes the damage to only a small sample of the county roads. This area (N32.8840°, E130.9915°) is close to the “ground zero” zone. Figure 9-59 shows the aerial view of the area with road damages. Figures 9-60 to 9-64 show the impact of surface faulting and ground deformation to roads. Road surface cracks, abutment lateral spreading, sink holes, subsidence, etc. were observed. Some of the failures observed did impact buried pipes and cables.



Figure 9-59. The circled area was explored by the investigation team. The red rectangle area shows the surface faulting. (Source: Google Earth)



Figure 9-60. Slight road surface damaged. In the background is the major landslide described in Section 2. (Tang)



Figure 9-61. Road surface damaged but local traffic can still go around on this part of the road (Tang)



Figure 9-62. A sinkhole appeared here and it was not filled in when we were there in July (Tang)



Figure 9-63. The cracks were filled with asphalt to allow traffic flow. This section of road was exposed to surface faulting. Note the destroyed surface water drain on the left side of the road has not yet been repaired. (Tang)



Figure 9-64. This part of road was temporarily paved to allow traffic flow (Tang)

On either side of the major landslide in Aso, Route 57 sustained significant road surface damage and ground failure. On the Kumamoto side (N32.8830°, E130.9872°), the landslide destroyed two lanes of road, Figure 9-65. On the Oita side (N32.8889°, E130.98746°), the road surface crack in many places and also covered with debris (such as rocks and mud) from the slope, Figure 9-66.



Figure 9-65. Slope failure took this part of the road (Route 57) down the slope



Figure 9-66. Embankment failure due to lateral spreading damage this part of Route 57

Although we did not develop a complete inventory of the roads in Kumamoto City, we did drive along about 100 km of roads in Kumamoto City. Along these 100 km, in areas not adjacent to water features, we observed very little damage. At bridges that cross over the various rivers, we observed various types of damage including movement of abutments, permanent movement of the expansion joints (sometimes jammed together, sometimes pulled apart), damage to handrails, etc.

9.4 Tawarayama Tunnel (N32.86014°, E130.96466°)

This tunnel is located near Minami Aso. The tunnel sustained some damage, but without collapse. On the Minami Aso village side, about 430 m from the portal, a large piece of ceiling cladding fell, Figures 9-67 and 9-68.



Figure 9-67. Tunnel cladding broke off, these were very large pieces of concrete



Figure 9-68 This photo was taken from the opposite side

On the Nishihara village side, about 100 m from the portal the road surface buckled, Figures 9-69 to 9-70.



Figure 9-69. Some small piece of cladding fell and the road surface buckled



Figure 9-70. The side path concrete surface buckled

9.5 Shinkansen and Local Railways

Kyushu Shinkansen, Japan Rail (JR), and Local Rail all sustained damage to tracks and train derailments. The Shinkansen derailment was not significant event, as the cars were unoccupied and were slowing moving at the time as part of train position after hours (1:26 am). However, the derailment demonstrates a concern that had the earthquake occurred during normal operating times, and the trains operating at speed, any derailment due to high ground shaking would have serious potential life safety consequences.

The damage to the tracks was caused by landslides, rock falls, ground deformation, and debris flows. No railway bridge collapsed due to ground shaking.

The team was not able to access all the location where the tracks were damaged. With the help of Google Earth and knowledge of the approximate locations, many of these sites were identified and are outlined in the following sections.

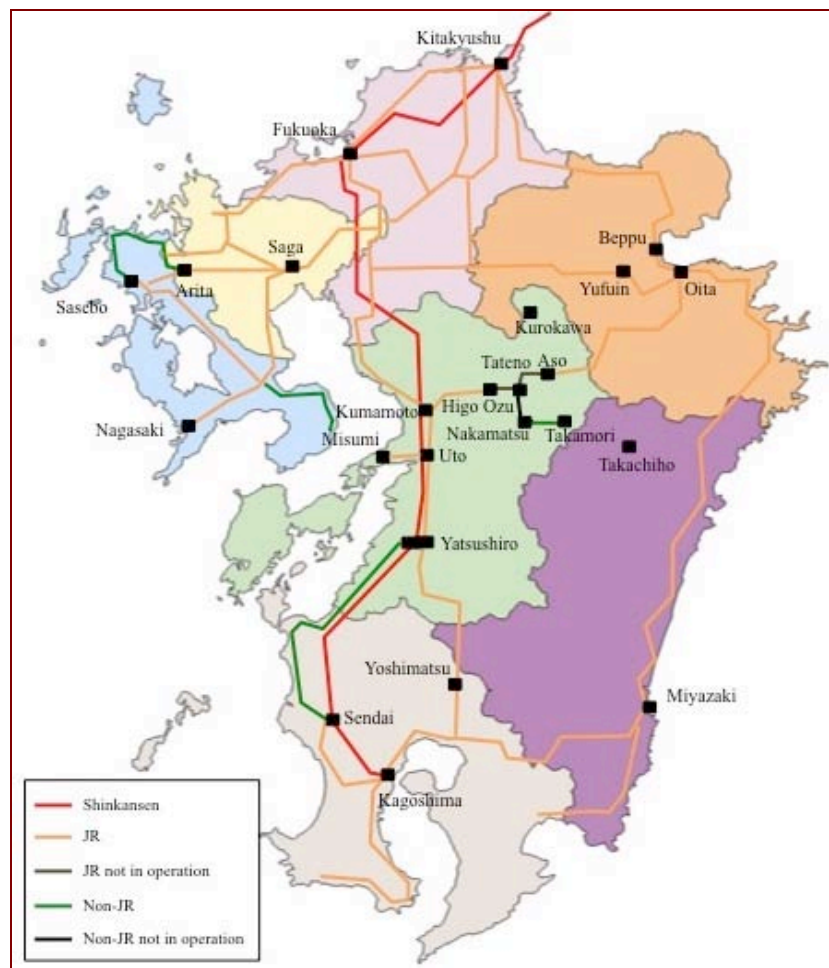


Figure 9-71 Kyushu Railway map (Base map from Reference 1)

9.5.1 Kyushu Shinkansen

The damages to Kyushu Shinkansen in this section occurred after the 14 April 2017 earthquake, which is called the foreshock. The epicenter was located east of Kumamoto Station at a distance of less than 2 km.

As shown in Figure 9-71, the red line that runs north south on the Kyushu Island is the Kyushu Shinkansen. The derailment occurred close to the Kumamoto Station (N32.7805°, E130.68603°), Figure 9-72. There was no injury due to this derailment as this was a deadheading¹⁰ line. This is a six-car train. A close up look at the damage caused by the derailed car is shown in Figure 9-73.



Figure 9-72. Aerial view of the location where the deadheading Shinkansen derailed. Kumamoto Station is about 1 km north of this location

¹⁰ Deadheading = train out of service returning to service depot.

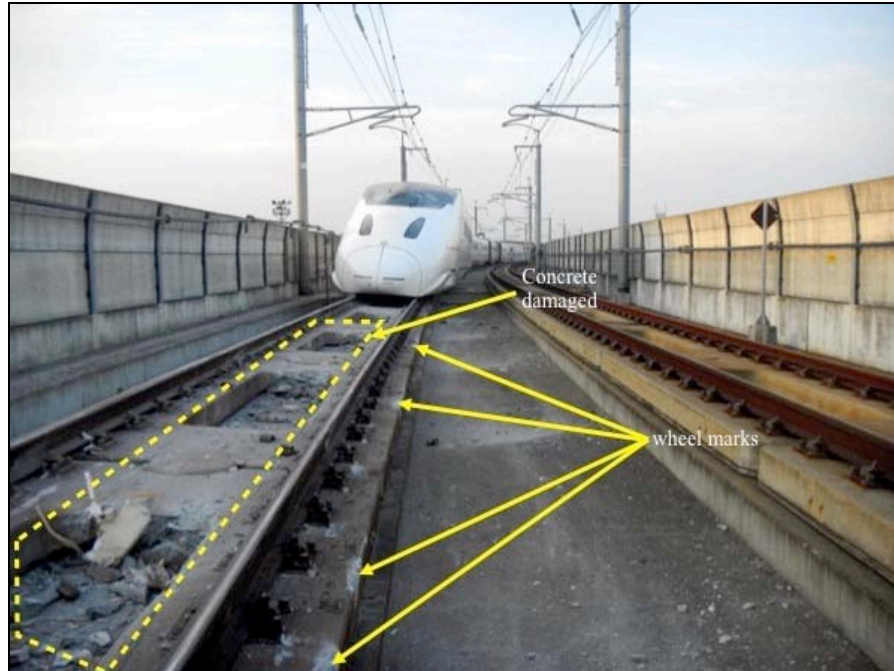


Figure 9-73 This deadheading Kyushu Shinkansen derailed closed to Kumamoto Station after the 14 April 2017 earthquake (the foreshock)

In addition to the derailment, several locations of the Shinkansen track north of Kumamoto Station sustained damage. Along this section of the Shinkansen line, the tracks are on raised platform. Figures 9-74 to 9-76 show the observed damages to the structure of the platform. All these set backs were repairable. The Kyushu Shinkansen returned to service in about 4 days.

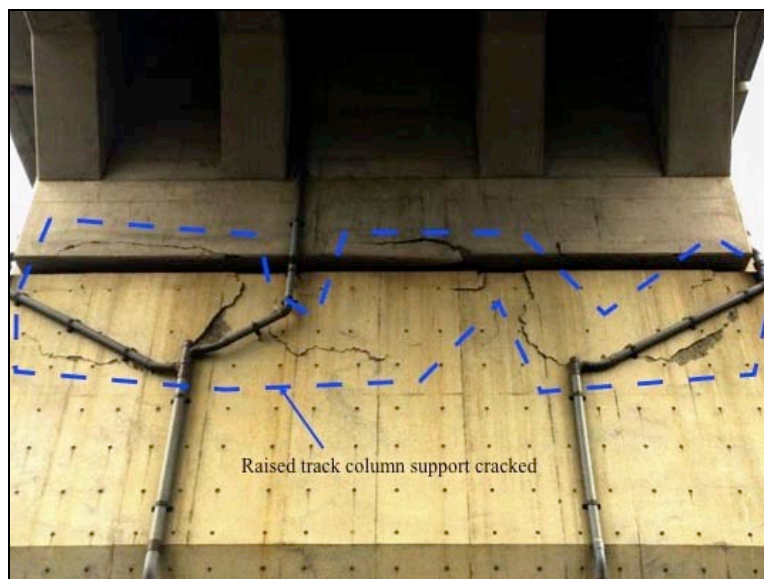


Figure 9-74 Raised track support column cracks

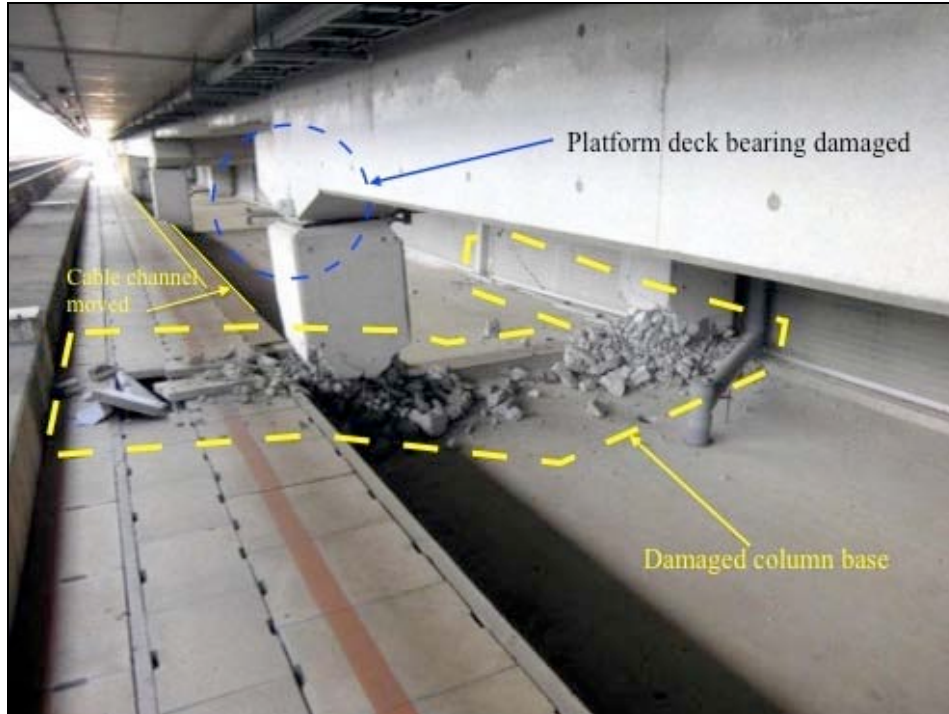


Figure 9-75. Bearing support column was damaged most likely due to the shifted cable duct structure



Figure 9-76. The rail platform shifted and broke the drain pipe. The concrete surface also showed cracks. Note the bearing is very close to the edge of the support

There were several locations where the sound barriers were broken and fell to the ground away from the tracks, Figure 9-77.



Figure 9-77 The sound barrier of the raised track fell to the ground

A chimney also fell on the raised track (N32.80759°, E130.69489°), broke the sound barrier and a part of chimney ended up resting on the track, Figure 9-78. This location is about 2 km from Kumamoto Station. Figure 9-79 shows the chimney before the earthquake. Avoiding having a functional element (in this case, the chimney) that can fall on another functional component (in this case, the railway alignment) is ideal to reduce loss of service of both components. However, it is a challenge to coordinate identification of all such possible sources for a company like JR, as they do not own the adjacent potentially vulnerable components, and in any case, will rarely have access to sufficient design details to make a detailed assessment.



Figure 9-78. The chimney broke apart after falling on the raised track. Luckily it did not damage the rails; only the sound barrier was damaged. (Source: Google Earth and Fukuoka MLIT)



Figure 9-79. This photo shows the tall chimney before the earthquake, on the left side of the service road and the Shinkansen raised tracks

9.5.2 JR and Local Railways

Japan Rail (JR) Kyushu basically runs the majority of the railway network in Kyushu. This earthquake caused service interruption to a JR line and a Local line.

- The JR line that sustained significant damage is the section of Hohi Main Line from Higo Ozu station to Aso station. There was a train derailment close to the Akamizu Station.
- The Local line that sustain significant damage is the Minami Aso Line from Tateno Station to Nakamatsu Station.

Close to the Kumamoto Station, a section of local railway tracks were deformed, Figure 9-80.



Figure 9-80. This section of JR tracks were deformed

The service depot in Kumamoto had the service crane dislocated from the rail along the wall and the crane fell to the ground, Figure 9-81. There was no damage to any equipment within the service depot. It is generally thought that traveling cranes of the type in Figure 9-81 are more vulnerable to derailment and falling if they are supported on rails that in turn are supported atop flexible moment frame buildings, and less vulnerable if they are supported atop stiffer shear wall buildings, reflecting the the failure mode is likely due to out-of-phase movement of the crane rails; coupled possibly with high levels of vertical shaking that allow temporary uplifting of the wheels off the track.



*Figure 9-81. The service crane was dislocated from the track along the sidewall.
(Source: Fukuoka MLIT)*

Hohi JR Main Line

The section of tracks between Higo Ozu Station and Aso Station to the east sustained damage in several locations. The main causes were landslide, rock fall, ground deformation, and debris flows. Some of the damage resulted from rainfalls that followed in the days and weeks after the earthquakes, as the rainfalls initiated more landslides and debris flows; recorded rainfalls in Kumamoto were 10.5 mm, 6.5 mm, 7.0 mm, 3.5 mm and 1.0 mm on April 21, May 3, 10, 16, 28 and 29, respectively; a torrential rainfall of about 500 mm fell on June 20 and 21.

Luckily the derailment (N32.9151°, E130.9928°) did not result in any injury as the train was running slow close to Akamizu Station. One car of the two-car train derailed at the level crossing, Figures 9-82 and 9-83.



Figure 9-82. The train station is on the right this photo.



Figure 9-83. Aerial view of the derailment (Source: MILT Kyushu)

The following shows aerial views of locations of damage to the Hohi Main Line. By July 4 2016, this part of the rail was not in service yet. The train track damage locations start east of Higo Ozu Station and end around just north of Aso Ohashi.

Figures 9-84 to 9-88 are the known locations of track damage after the 16 April main shock.



*Figure 9-84 Landslides damaged the train tracks at two places (N32.8782°, E130.9546°)
(Source: Google Earth)*

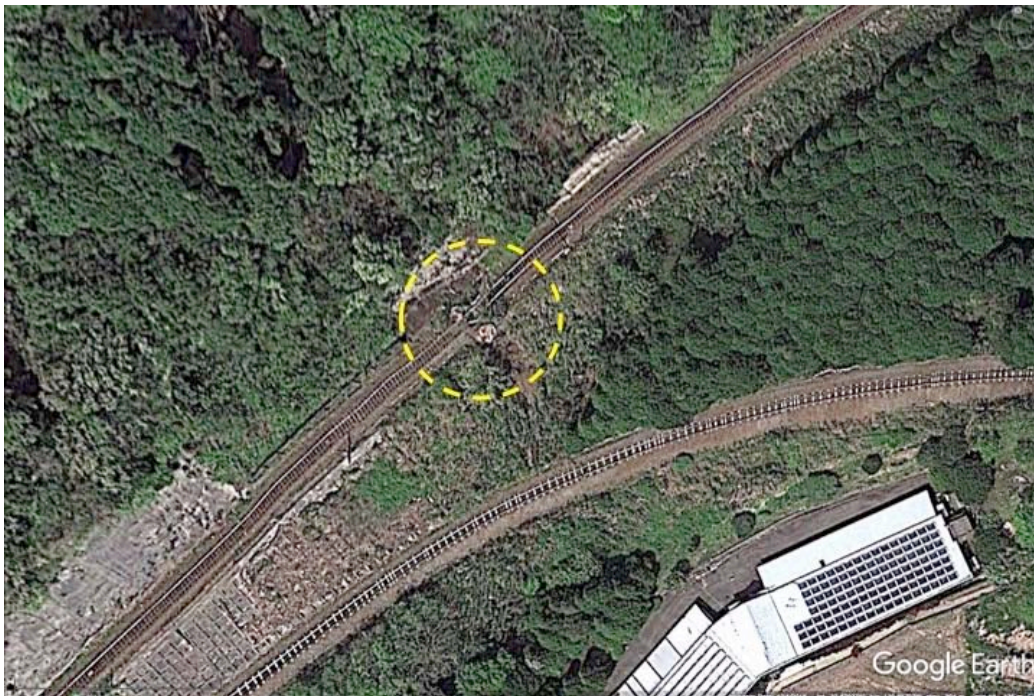


Figure 9-85. Rock fall damaged this section of the train track, located just east of Figure 8.1 (N32.879°, E130.9569°) (Source: Google Earth)



Figure 9-86. Debris flow on to the train track (N32.880°, E130.969°) (Source: Google Earth)



Figure 9-87. A large boulder rested in the center of this part of the train track (N32.880°, E130.973°) (Source: Google Earth)



Figure 9-88. This is the great landslide site, the signature failure of this earthquake. A long section of the Hohi Main Line was damaged and covered under tons of mud and rocks. The insert shows the dislocation of the train tracks to route 57 below it, caused by the landslide. (N32.88387°, N130.98705°)

Figure 9-89 is the landslide (debris flow) onto the railway track due to heavy rainfalls after the main shock.



*Figure 9-89. Heavy rainfalls initiated this landslide that covered the tracks. (N32.87685°
E130.94996°)*

As of early July 2016, there was still no information relating to the full recovery of this section of the Hohi Main Line (JR). Recovery of the track that is parallel to Route 57 entirely depends on the removal of the landslide and slope protection to be developed. Based on MLIT information with respect to the road (Route 57) recovery, one might expect the recovery of the rail line through this landslide zone will take at least 1 to 1.5 years. In the interim time frame, the Hohi Main Line is operating in two sections, one from Kumamoto City to a location west of the major landslide, and the other from Oita City in the east to a location east of the major landslide.

Minami Aso Line (Non-JR)

This railway line between Tateno Station and Takamori Station sustained damage in a couple of locations. Figures 9-90 to 9-92 show the locations of damaged track. The most significant damage was due to a landslide that covered the track shown in Figure 9-90.

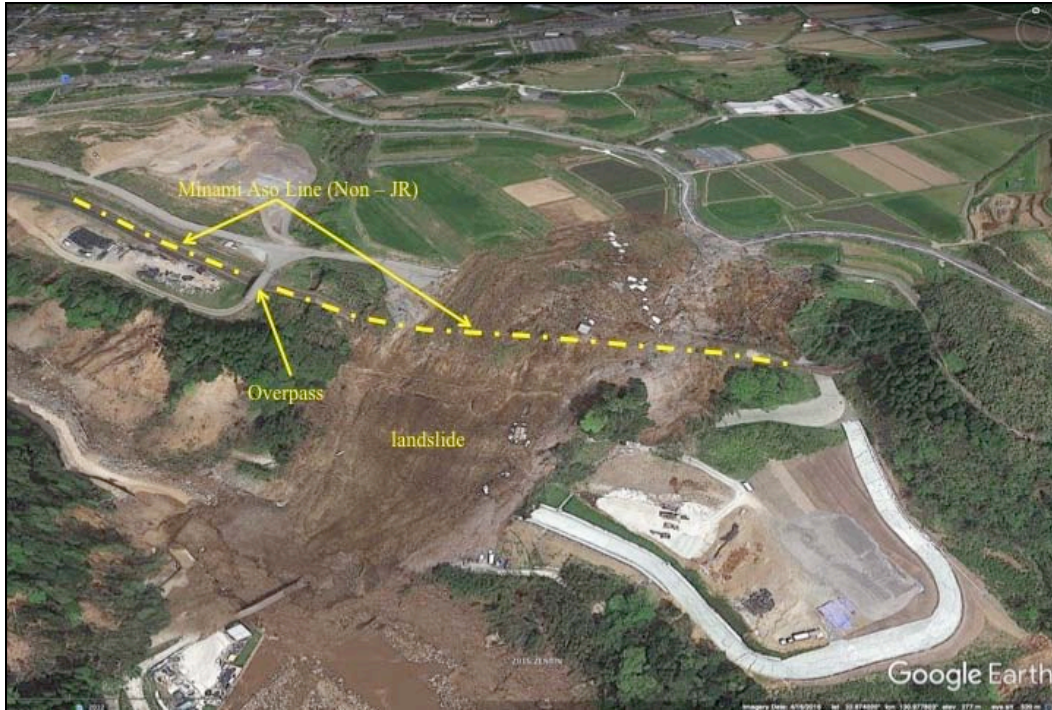


Figure 9-90. The landslide at this location is very large, it covered and damaged the train track as well as the county road below. (N32.87412°, E130.9778°). The landslide also covered a temporary construction office site. (Source: Google Earth)



Figure 9-91. A combination of debris flow and landslide across the river caused the scouring of the ground under the track. (N32.86774°, E130.9909°) (Source: Google Earth)

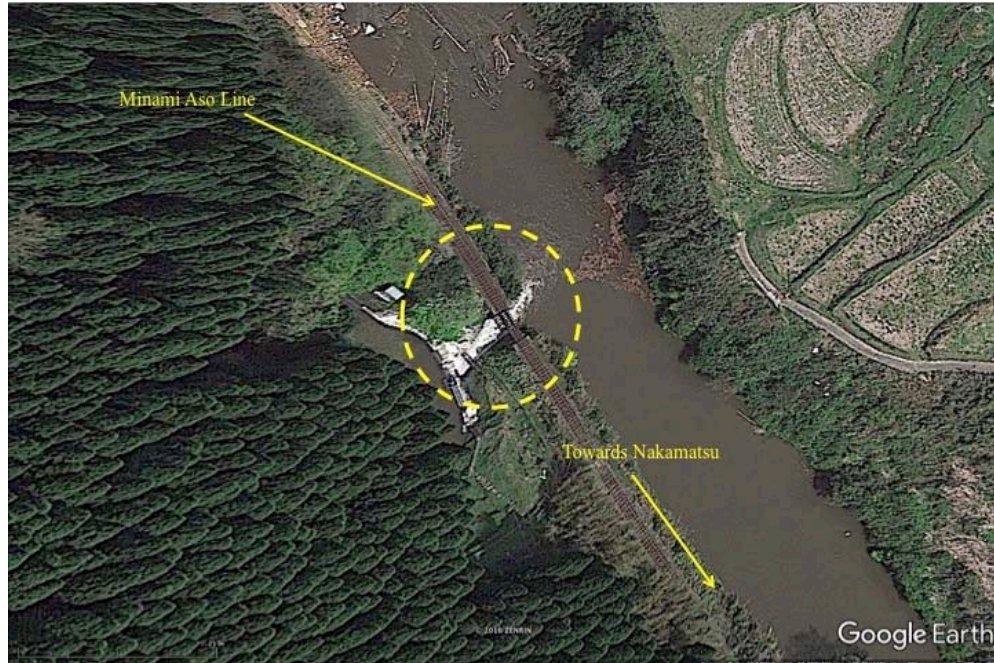


Figure 9-92. Part of the bridge that supported the tracks was damaged (N32.86712°, E130.9914°) (Source: Google Earth)

In addition to the damage outlined in Section 9.1 through 9.5, there were many more locations with damaged roads and bridges, as highlighted by the X-d circles in Figure 9-93.

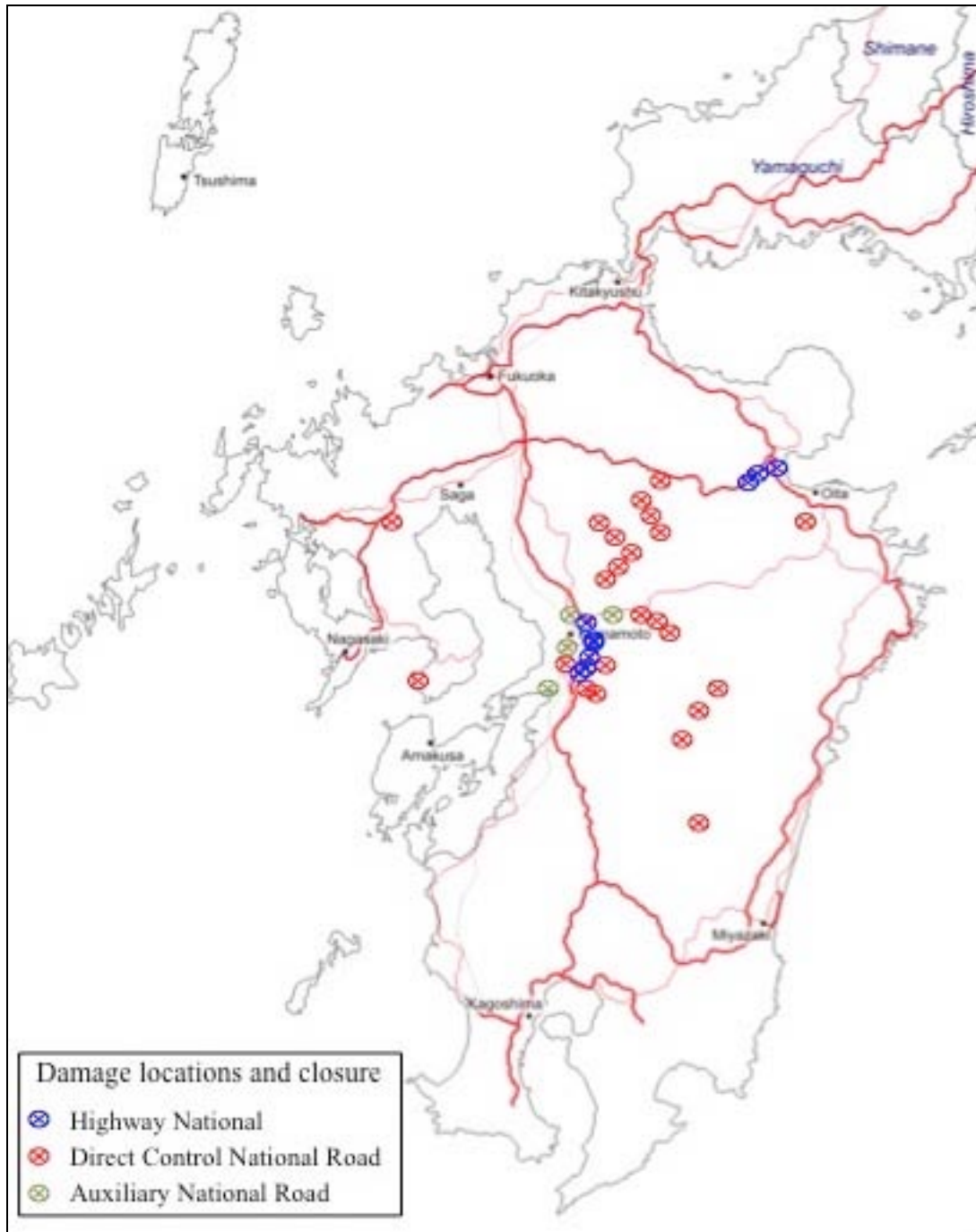


Figure 9-93. Map showing location of roads and bridges damage locations

9.6 Repair and Recovery Effort

TEC-FORCE is a specialized group of individuals from MLIT. The responsibility of this group is managing and executing recovery/repair to damaged roads and bridges. They are equipped with the most up-dated equipment to do their job. Their decision of how (construction process), what (materials, equipment), and when to repair failure to reduce traffic and access problems is the most important part of the whole recovery process. Therefore this group will be on site first and perform their tasks and draft a plan for implementation.

Figure 9-94 shows the TEC-FORCE team inspecting the damage at the Kuwatsuru Ohashi bridge (see Section 9.2.7) prior to drafting a repair plan.



Figure 9-94. TEC-FORCE team at Kuwatsuru Ohashi

Figures 9-95 to 9-96 shows the TEC-FORCE inspecting the damage then the starting repairs. The road in these figures is close to Tokai University Aso, which is in the neighborhood of the large landslide at Aso Ohashi.



Figure 9-95 TEC-FORCE inspecting and recording damage to Prefecture Route 149 (N32.8924°, E130.9918°)



Figure 9-96. Prefecture Route 149 damage repairing in progress

Aso Ohashi Replacement Plan

During our meeting with the Kyushu Regional Development Bureau, MLIT, they presented a plan of replacing the collapsed Aso Ohashi (Bridge). The plan is to construct a bridge from Route 325 across the valley to Route 57, Figure 9-97. The bridge will much longer than the failed Aso Ohashi bridge.

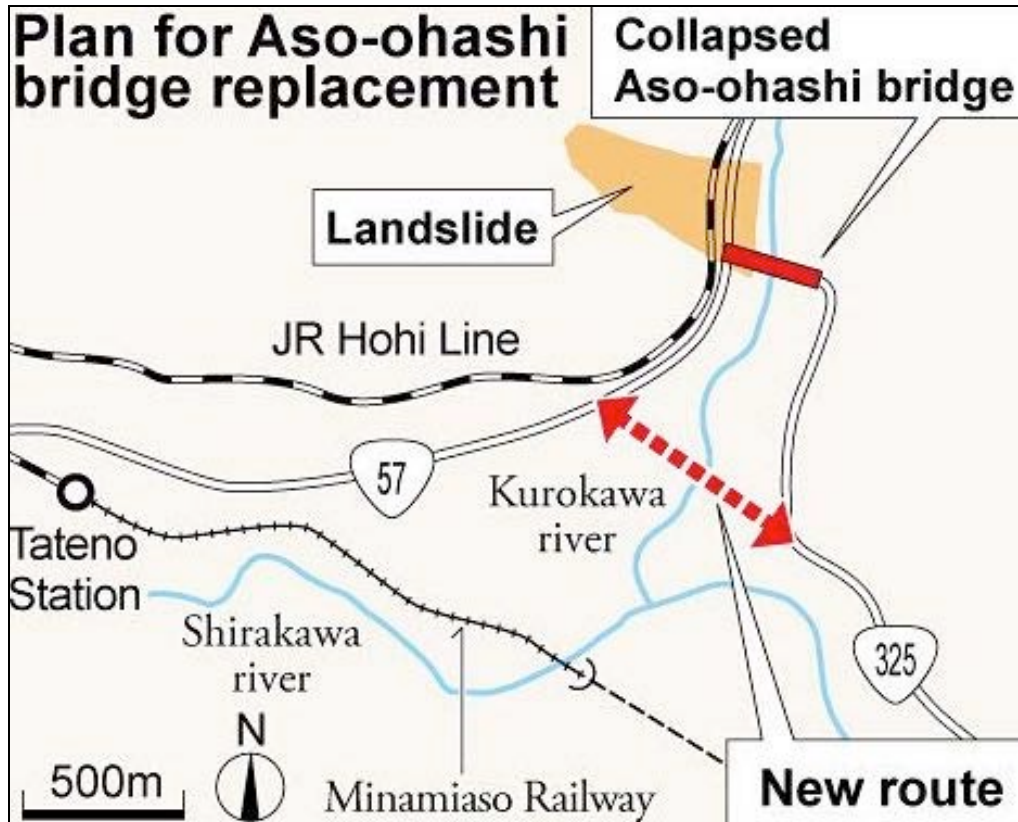


Figure 9-97 Location of the Aso Ohashi replacement connecting National Route 57 to National Route 325

9.7 Major Observations and Recommendations

In this report, we have concentrated on outlined the location and type of damage that occurred. The underlying questions are: why did the damage occur, and how can this damage be mitigated in the future?

To answer these questions, a lot of further investigations are needed. It is relatively straightforward to obtain the level of ground shaking (PGA, response spectra, PGV) at each bridge location, and then compare that level of inertial loading with the underlying original seismic design basis. While technically straightforward, this can still be a time consuming process. Even so, this effort will lend insight as to the efficacy of the seismic inertial design process. Without doubt, one major finding will be that seismic design that relies on probabilistically-computed ground motions will be sorely deficient if a long return period (5,000 year to 15,000 year) $M 7\pm$ crustal earthquake event occurs nearby, as was the case in Kyushu in 2016, and will no doubt be the case at some location in San Francisco or Los Angeles California in the near term, and possibly in the near term (and nearly certainly eventually) in Seattle, Salt Lake City, San Diego and other moderate seismic hazard regions. While there is a case to be made that seismic design motions on the order of $PGA = 0.2g$ to $0.3g$ are "cost effective" when considering long return period earthquakes, one must also recognize that when the earthquakes eventually occur and result in $PGA = 0.5g$ or above, they will cause a lot of damage and suffering. One should

examine closely whether "R" ductility factors between 4 and 6, often presumed in seismic design codes, are in fact the right way to design and operate critical lifelines.

Perhaps a far more challenging issue is to forecast the locations of landslides, and to a lesser extent, surface faulting and liquefaction. In this earthquake, landslides cause the bulk of the damage to the transportation network, and were also a major issue for electric transmission towers. If these zones had been established during the design process, the bridges and roads could have been rerouted away from them, or the landslides could have been mitigated. Even small slope failures at bridge abutments, whether we call them lateral spreads, settlements or landslides, remain a threat to many bridges. We need improved landslide maps and models (also liquefaction and surface faulting) so that we can rationally forecast the hazard locations, triggering processes and resulting permanent ground deformations imposed in these zones, and their impact on the infrastructure (whether bridges, roads, transmission towers, pipelines, etc. Perhaps it might be satisfactory if one road or one rail line are damaged by a landslide in an earthquake; but the simultaneous damage to many roads and railways at the same time in a single event, can destroy any concept of network redundancy, and result in long term economic impacts to the community.

Prior to this 2016 earthquake, the landslide risk in the Mount Aso area was not well understood. For example, the electric power company told us that before the earthquake, they had no specific design requirements so their transmission towers might not fail due to landslides. Since the earthquake, studies are underway to better understand the landslide risk in the area. Already, it has been identified that many of the actual landslide locations in this earthquake had landslides decades ago in the same location; and possibly other landslide zones that have moved in the past did not move in this earthquake. This is based on LiDAR technology scans of the Aso volcano areas¹¹. Overlaying this kind of information to the transportation network (or any spatial lifeline network) will provide a good starting point to mitigate future damage.

It is hoped that these types of studies will be performed, so that lifeline owners will have access to the information needed to improve design, construction, network redundancies, enhance policies and eventually change the standards.

9.8 Acknowledgements

Much of the information in this chapter was collected by the Kyushu Regional Development Bureau, (MLIT, as used throughout this chapter). Many of the photos in Section 9 are courtesy of MLIT, indicated by photos without other attribution in the photo caption.

We are deeply indebted to the MLIT officials who provided us with the information and photos. We appreciate their co-operation and taking the time and effort out of their busy and demanding efforts to meet with us.

¹¹ Conversation with Professor Konagai.

The efforts of Professor Fujio Kurokawa and Professor Eto Haruchi of Nagasaki University were instrumental in setting up meetings with Fukuoka MLIT. We are very grateful of their support. We are also grateful to Professor Alexis Kwasinski of Pittsburg University for his introduction to Professor Fujio Kurokawa and Professor Eto Haruchi of Nagasaki University, as without this beginning there would not have been a happy ending.

Finally, Professor Kazuo Konagai's tireless support of maintaining constant communications with all parties is the center of our success. We don't know if we can ever return his favors for all his own time, efforts and support of his students to accompany us in the field.

9.9 References

Kyushu map from d-maps.com.

MLIT and TEC-FORCE presentations – July 2016.

10.0 Levees

There are a number of rivers, canals and irrigation ditches in the area, with a lot of water used for rice farming. Various agencies constructed these levees over the past several decades. The earthquake damaged many levees and embankments. The common damage modes were slumping and lateral spreading. Typical damage is shown in Figures 10-1 to 10-4.



Figure 10-1. Levee Damage. Yagata River (Masuki-machi)



Figure 10-2. Levee Damage. Kiyamagawa River (Masuki-machi)



Figure 10-3. Levee Damage. Oosakawa River (Yatsushiro River). Masonry seawall collapse



Figure 10-4. Levee Damage. Akitsugawa River (Masuki-cho). Seawall collapse

Figure 10-5 shows a slope failure / lateral spread of a shoreline near a lake.



Figure 10-5. Shoreline Lateral Spread. Suizenji Ezu Lake Park, Kumamoto City

The damage to the levees did not result in unrestricted release of water from the river into the adjacent farmlands. However, had the earthquake occurred a few months later, in the rainy season, the river levels might have been higher, and more catastrophic failures might have occurred.

The short term fix for many of the levees was to place plastic-lined rock-filled bags atop the levee, as for example seen in Figure 2-35. This increases the height of the levee, considering that the liquefaction has resulted in slumping of the crest on the order to 10 cm to 1 meter in places. For adjacent residential areas (like Figure 2-35) to be protected, then the bags were prevalent. As of May 31 2016, Kumamoto Prefecture had placed bags at 66 locations along 34 rivers including the Kurokawa River in the Aso Caldera and the Kiyama River.

Kumamoto Prefecture continued its effort to place bags at 33 more locations to be prepared for the rainy season in June; this is the season for rice planting. However, the torrential rains of June 20 and 21 2016 (500 mm) caused serious flooding (Konagai et al 2017).

10.1 Acknowledgements

The photos in this chapter were kindly provided by the Kumamoto Prefecture Civil Engineering Department.

10.2 References

Konagai, K., Shiga, M., Kiyota T., Ideda T., Ground deformation built up along seismic fault activated in the 2016 Kumamoto Earthquake, accepted for publication in the JSCE Journal, Ser. A1, Vol. 73, No. 4, August 2017.